

Aus der Klinik für Allgemeine, Unfall- und Wiederherstellungschirurgie

Klinikum der Universität München

Direktor: Prof. Dr. med. Wolfgang Böcker

Experimentelle Chirurgie und Regenerative Medizin

Leitung: PD Dr. rer. nat. Attila Aszodi

Chondrogenic differentiation of murine induced pluripotent stem cells generated by a transposon based reprogramming system via embryoid bodies

Dissertation

zum Erwerb des Doktorgrades der Medizin

an der Medizinischen Fakultät der

Ludwig-Maximilians-Universität zu München

vorgelegt von

Nicole Trebesius

Aus

Rosenheim, Deutschland

2020

Mit Genehmigung der Medizinischen Fakultät
der Universität München

Berichterstatter: PD Dr. rer. nat. Attila Aszodi

Mitberichterstatter: Prof. Dr. Peter Müller
PD Dr. Anton Eberharter
Prof. Dr. Ralf Huss

Mitbetreuung durch den

Promovierten Mitarbeiter: Dr. Paolo Alberton

Dekan: Prof. Dr. med. dent. Reinhard Hickel

Tag der Mündlichen Prüfung: 16.01.2020

Meinen Eltern

Table of content

1.	Abstract	13
2.	Zusammenfassung	15
3.	Introduction.....	17
3.1.	Induced pluripotent stem cells	17
3.1.1.	Potency of stem cells	17
3.1.2.	Types of pluripotent stem cells	18
3.1.2.1.	Sources of pluripotent stem cells.....	18
3.1.2.2.	Naïve and primed state of pluripotent stem cells.....	21
3.1.3.	Methods for the generation of induced pluripotent stem cells	22
3.1.3.1.	Transposons	23
3.1.3.2.	Sleeping Beauty transposon system	24
3.1.4.	Mechanisms of reprogramming	26
3.1.4.1.	Early events of the reprogramming process	26
3.1.4.2.	Intermediate events of the reprogramming process.....	27
3.1.4.3.	Late events of the reprogramming process.....	29
3.1.4.4.	Function of the reprogramming factors	30
3.1.4.5.	Roles of the reprogramming factors in reprogramming	31
3.1.5.	Applications of induced pluripotent stem cells	33
3.2.	Articular cartilage	35
3.2.1.	Components of articular cartilage	36
3.2.1.1.	Chondrocytes	36
3.2.1.2.	Extracellular matrix	37
3.2.1.2.1.	Collagens.....	37
3.2.1.2.2.	Aggrecan	38
3.2.1.2.3.	Non-collagenous proteins	39
3.2.1.2.4.	Function of articular cartilage extracellular matrix	40
3.2.1.3.	Integrins	41
3.2.2.	Structure of articular cartilage.....	42

3.2.3.	Articular cartilage development.....	43
3.2.3.1.	Chondrogenesis and endochondral ossification.....	43
3.2.3.2.	Chondrogenic growth and transcription factors	45
3.2.3.2.1.	Chondrogenic growth factors.....	46
3.2.3.2.1.1.	Transforming growth factor β	46
3.2.3.2.1.2.	Bone morphogenetic protein	48
3.2.3.2.2.	Chondrogenic transcription factors.....	49
3.2.3.2.2.1.	Sox9.....	49
3.2.3.2.2.2.	Runx2	50
3.2.4.	Clinical relevance of articular cartilage	51
3.2.4.1.	Focal cartilage lesions and osteoarthritis.....	51
3.2.4.2.	Current treatment options	52
3.2.4.2.1.	Total joint replacement and endoprostheses	53
3.2.4.2.2.	Microfracture and autologous matrix-induced chondrogenesis.....	54
3.2.4.2.3.	Osteochondral autograft transfer and osteochondral allograft transplantation ..	55
3.2.4.2.4.	Autologous chondrocyte injection	56
3.3.	Stem cells for articular cartilage repair	58
3.3.1.	Mesenchymal stem cells for cartilage repair.....	58
3.3.1.1.	Mesenchymal stem cells	58
3.3.1.2.	Chondrogenic differentiation of MSCs	58
3.3.1.3.	Clinical application of MSCs for cartilage regeneration	59
3.3.2.	Induced pluripotent stem cells for cartilage repair	60
3.3.2.1.	Applications of induced pluripotent stem cells in cartilage repair	60
3.3.2.2.	Chondrogenic differentiation of pluripotent stem cells	60
3.3.2.2.1.	Chondrogenic differentiation of PSCs via co-culture and conditioned medium	61
3.3.2.2.2.	Chondrogenic differentiation of PSCs via sequential exposure to growth factors	62
3.3.2.2.3.	Chondrogenic differentiation in a two-step protocol via MSC-like cells	63
3.3.2.2.4.	Chondrogenic differentiation via embryoid bodies	63
4.	Aims and milestones of the thesis	65

5.	Materials and Methods.....	66
5.1.	Sleeping Beauty transposon based reprogramming system	66
5.1.1.	Structure of plasmid vectors.....	66
5.1.2.	Plasmid transformation in competent bacteria and plasmid DNA isolation by MaxiPrep	67
5.2.	Cell culture	69
5.2.1.	Standard cell culture conditions and procedures	69
5.2.1.1.	Culturing primary fibroblasts	69
5.2.1.2.	Culturing mouse ESCs and mouse iPSCs	70
5.2.1.3.	Passaging and counting of cells.....	71
5.2.1.4.	Cryo-conservation of cells.....	72
5.2.1.5.	Thawing of cells	73
5.2.2.	Generation of iPSCs from primary murine fibroblasts.....	73
5.2.2.1.	Isolation of primary murine fibroblasts	73
5.2.2.2.	Isolation of primary mouse embryonic fibroblasts.....	74
5.2.2.3.	Preparation of mitotically inactivated feeder cells	75
5.2.2.4.	Nucleofection of fibroblasts	75
5.2.2.5.	Reprogramming of primary murine fibroblasts.....	77
5.2.2.6.	Picking of colonies and establishment of clonal cell lines	77
5.2.3.	Differentiation of induced pluripotent stem cells	79
5.2.3.1.	Formation of embryoid bodies in hanging drops.....	79
5.2.3.2.	Spontaneous differentiation of mIPSCs in embryoid bodies.....	80
5.2.3.3.	Chondrogenic differentiation of mIPSCs via chondrogenic colonies	81
5.2.3.4.	Chondrogenic differentiation of mIPSCs via embryoid bodies.....	83
5.3.	Cytological analysis	85
5.3.1.	Alkaline phosphatase staining	85
5.3.2.	Immunocytochemistry.....	85
5.4.	mRNA analysis.....	87
5.4.1.	Total RNA isolation	87

5.4.1.1.	Total RNA isolation from cells.....	87
5.4.1.2.	RNA isolation from embryoid bodies, chondrogenic nodules and spheroids	87
5.4.2.	cDNA synthesis	88
5.4.3.	Semi-quantitative reverse transcription PCR.....	89
5.4.4.	Quantitative PCR.....	91
5.4.4.1.	LightCycler SYBR Green method.....	91
5.4.4.2.	Taq-Man probes.....	92
5.5.	Splinkerette PCR	94
5.5.1.	Isolation of genomic DNA	96
5.5.2.	Digestion of gDNA	96
5.5.3.	Ligation of digested gDNA with Splinkerette adapters	97
5.5.4.	PCR amplifications.....	98
5.5.5.	Oligonucleotides used for Splinkerette PCR.....	99
5.6.	Histological analysis	100
5.6.1.	Processing of samples	100
5.6.1.1.	Fixation.....	100
5.6.1.2.	Embedding.....	100
5.6.1.3.	Sectioning	100
5.6.2.	Histochemical staining	101
5.6.2.1.	Safranin Orange staining	101
5.6.2.2.	Toluidine blue staining	101
5.6.3.	Immunohistochemistry	101
5.7.	Chemicals	103
5.8.	Microscopy	103
5.9.	Computer programs and statistics.....	104
6.	Results.....	105
6.1.	Isolation and culture of primary fibroblasts.....	105
6.2.	Nucleofection of primary fibroblasts	106
6.3.	Reprogramming of primary fibroblasts.....	108

6.3.1.	Reprogramming of MEFs, EAR-FBs and TAIL-FBs with the <i>pT2OSKM(L)</i> plasmid.....	108
6.3.1.1.	Reprogramming of MEFs with the <i>pT2OSKM</i> or <i>pT2OSKML</i> plasmid.....	108
6.3.1.2.	Reprogramming of EAR-FBs with the <i>pT2OSKM</i> or <i>pT2OSKML</i> plasmid.....	109
6.3.1.3.	Reprogramming of TAIL-FBs with the <i>pT2OSKM</i> or <i>pT2OSKML</i> plasmid	110
6.3.2.	Reprogramming of EAR-FBs with the <i>RMCE-OSKM(L)-Cherry</i> plasmid ..	112
6.3.3.	Morphological changes during the reprogramming process.....	113
6.4.	Analysis of induced pluripotent stem cells	116
6.4.1.	Morphology and proliferation	116
6.4.2.	Alkaline phosphatase staining	117
6.4.3.	Number of transposon insertion sites	119
6.4.4.	Expression of pluripotency markers.....	120
6.4.4.1.	mRNA analysis of pluripotent stem cell markers.....	120
6.4.4.2.	mRNA analysis of reprogramming factors.....	123
6.4.4.3.	Protein analysis of pluripotency markers by immunocytochemistry	126
6.4.5.	Trilineage differentiation potential during spontaneous differentiation in embryoid bodies	129
6.5.	Chondrogenic differentiation of iPSCs via chondrogenic colonies	131
6.5.1.	Histological analysis of chondrogenic colonies	132
6.5.2.	Gene expression analysis of chondrogenic colonies.....	132
6.5.2.1.	Analysis of pluripotency markers in chondrogenic colonies.....	133
6.5.2.2.	Analysis of chondrogenic markers in chondrogenic colonies	133
6.6.	Chondrogenic differentiation of iPSCs via embryoid bodies.....	135
6.6.1.	Histological analysis of chondrogenic spheroids.....	137
6.6.1.1.	Safranin Orange staining of chondrogenic spheroids.....	137
6.6.1.2.	Toluidine Blue staining of chondrogenic spheroids	137
6.6.1.3.	Immunohistochemistry for aggrecan and type II collagen	139
6.6.2.	Gene expression analysis of chondrogenic spheroids.....	140
6.6.2.1.	Expression of pluripotency markers in chondrogenic spheroids.....	140
6.6.2.2.	Expression of chondrogenic markers in chondrogenic spheroids	141

6.6.2.3.	Expression of hypertrophy markers in chondrogenic spheroids	144
7.	Discussion	145
7.1.	Sleeping Beauty transposon system for reprogramming.....	145
7.1.1.	Integrating viral vectors.....	147
7.1.2.	Non-integrating viral vectors.....	147
7.1.3.	Non-integrating non-viral vectors	148
7.1.4.	Integrating non-viral vectors	149
7.1.5.	Conclusion	152
7.1.6.	Reprogramming of murine fibroblasts with a Sleeping Beauty transposon-based reprogramming system.....	153
7.2.	Significance of iPSCs for cartilage regeneration.....	155
7.2.1.	State of the art of cartilage repair	155
7.2.2.	Mesenchymal stem cells for cartilage repair.....	158
7.2.3.	Induced pluripotent stem cells for cartilage regeneration	159
7.3.	Chondrogenic differentiation of pluripotent stem cells	162
7.3.1.	Chondrogenic differentiation of iPSCs via chondrogenic colonies.....	162
7.3.2.	Chondrogenic differentiation of iPSCs via embryoid body derived chondrogenic spheroids.....	164
7.3.3.	Generation of chondrogenically primed iPSCs by RMCE.....	168
8.	Literature.....	171
9.	List of Figures	186
10.	List of Tables	189
11.	List of Equations	191
12.	List of abbreviations	192
13.	Acknowledgement.....	196
14.	Curriculum Vitae.....	Fehler! Textmarke nicht definiert.

15. Publikationen	197
16. Eidesstattliche Versicherung	198

1. **Abstract**

In 2006 it was first reported by *Takahashi et al* that somatic cells can be reprogrammed to a pluripotent state by four reprogramming factors – Oct3/4, Sox2, Klf4 and c-Myc. These pluripotent stem cells were termed induced pluripotent stem cells (IPSCs). They offer promising possibilities for regenerative medicine and tissue engineering due to their unlimited proliferation and differentiation potential while facing less ethical concerns than embryonic stem cells (ESCs). Many different cell types and reprogramming strategies have been described since then. Transposon-based reprogramming systems like the Sleeping Beauty system combine the higher efficiency of integrating vectors with the enhanced safety profile of non-viral vectors, and are therefore an interesting option for the generation of IPSCs both for research and clinical applications.

Articular cartilage is a highly specialized connective tissue that covers the surfaces of diarthrodial joints. Due to its limited intrinsic regeneration potential, lesions of articular cartilage progress into osteoarthritis that can only be efficiently treated with total joint replacement by endoprotheses at the moment. Repair strategies for chondral lesions lead to formation of biomechanically inferior fibrocartilage or require invasive harvesting and destruction of healthy articular cartilage. Patient-derived autologous or HLA (human leucocyte antigen)-matched allogenic IPSCs might overcome these limitations and become an attractive alternative for cartilage repair. However, there is still no optimal protocol for chondrogenic differentiation of IPSC available.

In this thesis we generated IPSCs from primary murine fibroblasts and established an efficient and reliable protocol for their chondrogenic differentiation.

Embryonic and adult murine fibroblasts were successfully reprogrammed to IPSCs using the Sleeping Beauty reprogramming system for delivery of the reprogramming factors. Several clonal IPS cell lines were established and assessed for pluripotency traits and expression of pluripotency-related genes as well as for their tree-lineage differentiation potential. Transposon copy number analysis by Splinkerette PCR revealed two single integration clones.

Efficient and reliable chondrogenic differentiation was achieved in one of these single-integration clones by culturing embryoid bodies (EBs) in chondrogenic medium in a free-floating culture system. When stimulated by the chondrogenic growth factors BMP2 and

TGF β 1 the developing chondrogenic spheroids expressed chondrogenic markers like *Sox9*, *Integrin α 10* and showed deposition of aggrecan and type II collagen in their extracellular matrix (ECM). Expression of pluripotency markers was downregulated yet still detectable.

In conclusion, we have not only generated and assessed more than 20 IPS cell lines from primary murine fibroblasts reprogrammed by the Sleeping Beauty transposon system, but we have also developed an efficient and scalable protocol for their chondrogenic differentiation. More research is required to assess the impact of more elaborate growth factor substitution during chondrogenic differentiation on the resulting spheroids as well as their potential to repair osteochondral defects in vitro and in vivo. Furthermore, removal of the reprogramming factor cassette or its replacement by chondrogenic factors by recombinase mediated cassette exchange (RMCE) facilitated by heterospecific *loxP* sites incorporated in the Sleeping Beauty transposon would allow formation of chondrogenically primed iPSCs. It remains to be elucidated whether this would lead to improved chondrogenic differentiation and cartilage repair.

2. Zusammenfassung

Im Jahre 2006 wurde erstmalig von *Takahashi et al.* beschrieben, dass somatische Zellen durch die vier Reprogrammierungsfaktoren – Oct3/4, Sox2, Klf4 und c-Myc – in einen pluripotenten Zustand reprogrammiert werden können. Diese pluripotenten Stammzellen wurden induzierte pluripotente Stammzellen genannt. Aufgrund ihres unbegrenzten Proliferations- und Differenzierungspotentials bieten sie vielversprechende Möglichkeiten für die Zukunft der regenerativen Medizin und der Gewebetechnologie, wobei ihnen weniger ethische Bedenken als embryonalen Stammzellen entgegengebracht werden. Die Reprogrammierung verschiedener Zellarten sowie die Verwendung verschiedener Reprogrammierungsstrategien wurden in den letzten Jahren beschrieben. Transposon-basierte Reprogrammierungs-Systeme, wie zum Beispiel das Sleeping-Beauty Transposon System, vereinen die hohe Effektivität integrativer Vektoren mit dem besseren Sicherheitsprofil nicht-viraler Vektoren und stellen daher eine interessante Option für die Herstellung induzierter pluripotenter Stammzellen sowohl für Forschungs- als auch für klinische Anwendungen dar.

Gelenkknorpel ist ein hoch spezialisiertes Bindegewebe, das die Oberflächen diarthrodialer Gelenke bedeckt. Aufgrund seines limitierten intrinsischen Regenerationspotentials führen Verletzungen des Gelenkknorpels zu Arthrose, die gegenwärtig nur durch Gelenkersatz mit Totalendoprothesen effektiv behandelt werden kann. Reparaturstrategien für Verletzungen des Gelenkknorpels führen zur Bildung von biomechanisch minderwertigem Faserknorpel oder erfordern invasive Gewinnung und Zerstörung von intaktem Gelenkknorpel. Autologe, vom Patienten abstammende oder HLA-gematchte, allogene induzierte pluripotente Stammzellen könnten diese Einschränkungen überwinden und sich zu einer attraktiven Alternative für die Knorpelregenerierung entwickeln. Allerdings gibt es bislang kein optimales chondrogenes Differenzierungsprotokoll für induzierte pluripotente Stammzellen.

In dieser Doktorarbeit haben wir induzierte pluripotente Stammzellen ausgehend von primären murinen Fibroblasten hergestellt und ein effizientes und verlässliches Protokoll für deren chondrogene Differenzierung entwickelt.

Murine embryonale und adulte Fibroblasten wurden erfolgreich zu induzierten pluripotenten Stammzellen reprogrammiert, wobei das Sleeping Beauty Reprogrammierungssystem für die Übertragung der Reprogrammierungsfaktoren verwendet wurde. Mehrere klonale induzierte

pluripotente Stammzelllinien wurden etabliert und bezüglich pluripotenter Merkmale und der Expression pluripotenter Marker sowie ihres Differenzierungspotentials in Derivate aller drei embryonalen Keimblätter untersucht. Analyse der Anzahl genomischer Insertionsstellen des Transposons mittels Splinkerette PCR zeigte zwei Klone mit einer einzelnen Integration.

Zur effizienten und verlässlichen chondrogenen Differenzierung eines dieser Klone mit einer einzelnen Integrationsstelle wurden zunächst embryoide Körperchen im hängenden Tropfen gebildet, die anschließend im chondrogenen Medium frei-schwimmend kultiviert wurden. Durch Stimulierung dieser chondrogenen Spheroide mit den chondrogenen Wachstumsfaktoren BMP2 und TGF β 1 wurde die Expressierung chondrogener Marker, wie z.B. *Sox9* und *Integrin α 10* induziert und die Ablagerung von Aggrecan und Typ II Collagen in der extrazellulären Matrix erreicht. Die Expressierung pluripotenter Marker war reduziert aber dennoch nachweisbar.

Zusammenfassend haben wir nicht nur erfolgreich mehr als 20 induzierte pluripotente Stammzelllinien mit dem Sleeping Beauty Reprogrammierungssystem etabliert und getestet, sondern auch ein effizientes und anpassbares Protokoll für deren chondrogene Differenzierung entwickelt. Weitere Forschungsarbeiten sind notwendig, um die Auswirkung ausgeklügelterer Wachstumsfaktorsubstitutionsschemata auf die chondrogene Differenzierung der Spheroide sowie deren Potential osteochondrale Defekte in vivo und in vitro zu reparieren zu untersuchen. Zudem würde der Austausch der Reprogrammierungsfaktorexpressionskassette gegen chondrogene Differenzierungsfaktoren mittels Rekombinase-vermitteltem Kassettenaustausch über heterospezifische *loxP* Stellen, die im Sleeping Beauty Reprogrammierungssystem enthalten sind, die Herstellung chondrogen-geprimter induzierter pluripotenter Stammzellen ermöglichen. Es muss weiter untersucht werden, ob dies zu verbesserter chondrogener Differenzierung und Knorpelreparatur beitragen könnte.

3. Introduction

3.1. Induced pluripotent stem cells

3.1.1. Potency of stem cells

Stem cells are undifferentiated cells that are capable of self-renewal and differentiation into more specialized cell types [1, 2]. Self-renewal refers to the ability to undergo multiple divisions while maintaining an undifferentiated state [3]. According to their differentiation potential stem cells can be classified as totipotent, pluripotent, multipotent or unipotent (Figure 1) [2].

Totipotent stem cells can give rise to all embryonic and extraembryonic tissues, thus they can form a complete embryo and the placenta [2]. Traditionally only a fertilized oocyte up to the 8-cell stage of the morula is considered totipotent [1].

Pluripotent stem cells are able to differentiate into all cell types of the three embryonic germ layers – ectoderm, endoderm and mesoderm [2]. They can form a complete embryo but cannot give rise to extraembryonic tissues like the placenta [4]. There are many different types of pluripotent stem cells that will be discussed in detail in 3.1.2. *Types of pluripotent stem cells*.

Multipotent stem cells can differentiate into several cell types from a single germ layer [2]. Mesenchymal stem cells *e.g.* can give rise to various mesodermal tissues like adipose tissue, bone or cartilage [2]. Unipotent stem cells produce only one specific cell type [4]. Muscle stem cells *for example* can develop only into mature muscle cells [2].

By the traditional developmental dogma, totipotent stem cells differentiate via a pluripotent and multipotent intermediate state to unipotent stem cells that finally give rise to fully differentiated, mature cells [4]. During this process, their self-renewal capacity and differentiation potential gradually decreases [4]. However, the discovery of reprogramming methods like somatic cell nuclear transfer (SCNT) and induced pluripotent stem cells (iPSCs) by which fully differentiated cells can return to a pluripotent state reversed this hierarchy [4].

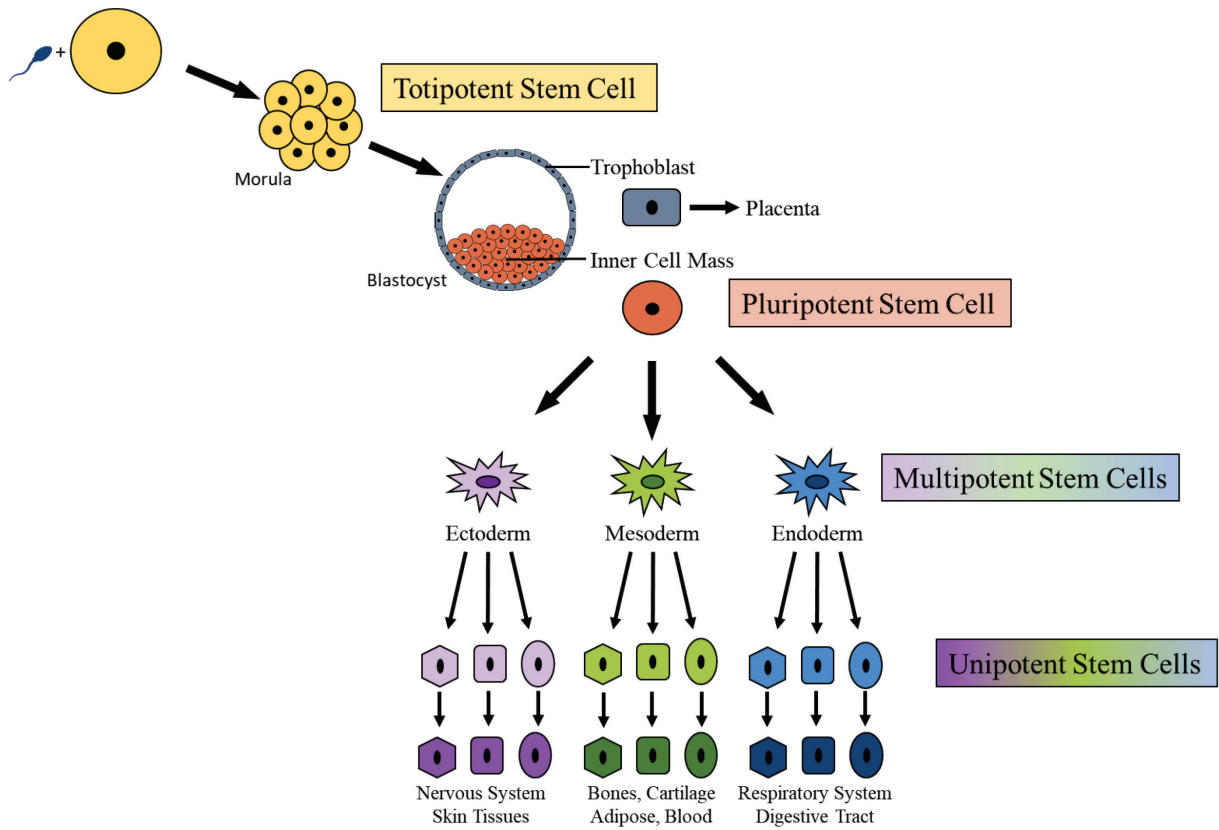


Figure 1: Potency of stem cells (self-designed).

Totipotent stem cells are present up to the morula stage of embryonic development and can differentiate into all embryonic and extraembryonic cell types. The blastocyst is composed of the surrounding trophoblast that gives rise to the placenta and the inner cell mass (ICM) that contains pluripotent embryonic stem cells (ESCs). These develop in vivo to the embryo and have the potential to give rise to cell types of all three germ layers – ectoderm, mesoderm and endoderm. Multipotent stem cells can differentiate into several cell types of their respective lineage, whereas unipotent stem cells can give rise to only one single cell type.

3.1.2. Types of pluripotent stem cells

3.1.2.1. Sources of pluripotent stem cells

Many types of pluripotent stem cells have been described including embryonic carcinoma cells (ECCs) derived from teratocarcinomas [5], embryonic germ cells (EGCs) derived from primary germ cells (PGCs) of the embryo or germ stem cells (GSCs) derived from neonatal and adult spermatogonial cells [4]. However, the most important types of pluripotent stem cells are embryonic stem cells (ESCs), somatic cell nuclear transfer-derived stem cells (NT-SCs) and induced pluripotent stem cells (iPSCs) (Figure 2) [4].

Embryonic stem cells (ESCs) can be isolated from the inner cell mass of a preimplantation blastocyst. The blastocyst consists of the inner cell mass (ICM) that will form the embryo, a fluid filled cavity, the blastocoele, and the outer cell mass, the trophoblast, that gives rise to the placenta [1, 2]. ESCs have first been isolated in mouse by *Evans and Kaufman* in 1981 [6]. In 1998 *Thomson et al.* reported the isolation of ESCs from human blastocysts [7]. ESCs show unlimited proliferation capacity in vitro and can differentiate into cells from all germ layers in vivo and in vitro [4]. However, their use in regenerative medicine is limited due to ethical concerns and the risk of immune rejection after allogenic transplantation [1, 8].

In rodents, pluripotent stem cells can also be isolated from the epiblast layer of post-implantation blastocysts [9]. These cells are termed epiblast stem cells (EpiSCs) [9]. In humans, an equivalent stem cell population has not been isolated due to ethical restrictions regarding the destruction of post-implantation embryos [4].

Over the last decades two reprogramming techniques which reverse the differentiation process of somatic cells and return the cells into a pluripotent state have been described.

During somatic cell nuclear transfer (SCNT), the nucleus of a somatic cell is transferred into the cytoplasm of an enucleated oocyte [10]. Unknown factors in the oocyte cytoplasm then reprogram the somatic nucleus to a totipotent state by erasing epigenetic marks. This process is comparable to the reprogramming of the sperm genome after fertilization [11]. Following activation, the oocyte starts to divide and develops into an artificial embryo carrying the same genetic information as the donor nucleus [10]. This embryo can be transferred into the uterus of a recipient animal via in vitro fertilization resulting in development of a clone like the sheep “Dolly” in 1997 [12]. Furthermore, pluripotent stem cells can be isolated from the inner cell mass of the developing blastocyst [13, 14]. These nuclear transfer derived stem cells are comparable to ESCs in terms of morphology, gene expression pattern and differentiation potential [13, 14]. Despite their potential to produce isogeneic pluripotent stem cells, the utility of SCNT in regenerative medicine and tissue engineering is limited due to ethical concerns regarding need for human oocytes and destruction of human embryos [1, 11]. Furthermore, complete reprogramming is achieved only in a very small portion of cells, whereas many SCNT-derived embryos show epigenetic abnormalities [11].

Induced pluripotent stem cells (IPSCs) were first described by *Takahashi and Yamanaka* in 2006 [15]. They screened 24 candidate genes known to play important roles for the maintenance of pluripotency or to contribute to carcinogenesis for their ability to induce reexpression of *Fbx15*, a gene that is expressed in mouse ESCs but dispensable for the maintenance of pluripotency [15]. Thereby they showed that four factors, namely *octamer-binding transcription factor 3/4* (Oct3/4), *SRY (Sex determining region of Y)-box2* (Sox2), *kruppel-like factor 4* (Klf4) and *avian myelocytomatosis viral oncogene homolog* (c-Myc), were sufficient to reprogram mouse embryonic and adult fibroblasts to an embryonic stem cell-like state [15]. These factors were therefore termed reprogramming factors [15, 16].

The reprogrammed cells were similar to ESCs in terms of morphology, proliferation, gene expression and epigenetic status [15]. Furthermore, they formed teratomas containing tissues from all three germ layers after subcutaneous injection into nude mice [15]. Therefore, these cells represent an additional type of pluripotent stem cells and are designated induced pluripotent stem cells [15].

Although these IPSCs contributed to embryonic development after injection into blastomeres, no live-born chimeras could be obtained from the *Fbx15*-IPSCs [15]. By selection for reexpression of *Nanog* or endogenous *Oct3/4*, however, adult chimeras could be obtained from IPSCs [17, 18]. Furthermore, these IPSCs could be transmitted through the germ line and were able to produce “all IPSC embryos” after injection into tetraploid (4N) blastocysts [17, 18].

In 2007 the first human IPSCs were generated from human dermal fibroblasts by retroviral transduction of the same set of factors (Oct3/4, Sox2, Klf4 and c-Myc) [19]. *Yu et al.* showed that a different combination of reprogramming factors, namely Oct3/4, Sox2, Nanog and Lin28, was also sufficient to reprogram human somatic cells [20].

As IPSCs represent a potential source of personalized, patient specific pluripotent stem cells omitting the ethical concerns associated with ESCs and NT-SCs they offer promising possibilities for the future of stem cell research and regenerative medicine. Therefore S. Yamanaka was awarded the Nobel Prize in medicine for the discovery of induced pluripotent stem cells in 2012 [21].

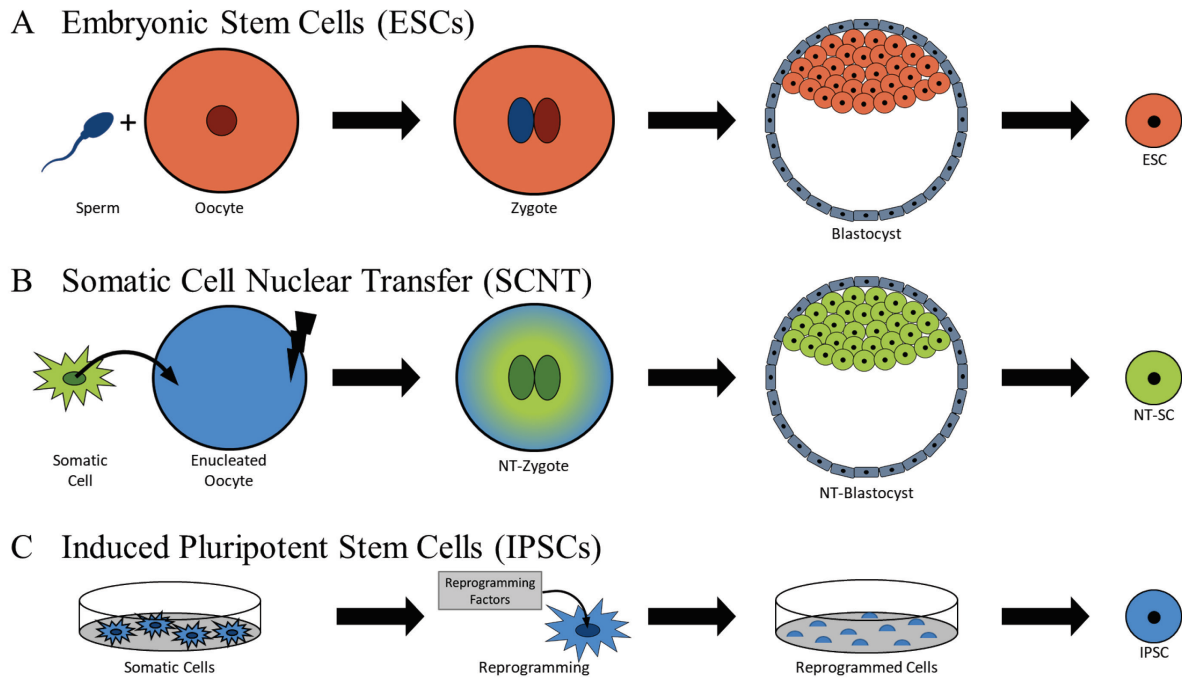


Figure 2: Types of pluripotent stem cells (self-designed).

(A) Embryonic stem cells (ESCs) are derived from the inner cell mass of a blastocyst that is generated by the fertilization of an oocyte by a sperm cell. (B) During somatic cell nuclear transfer (SCNT), the nucleus of a somatic cell is transferred into an enucleated oocyte. After activation the oocyte now carrying the somatic cell's genetic material starts to develop into a blastocyst from which pluripotent stem cells can be isolated. (C) Induced pluripotent stem cells (IPSCs) are derived from somatic cells by expression of reprogramming factors. After successful reprogramming IPSC colonies can be picked and clonal IPS cell lines can be established.

3.1.2.2. Naïve and primed state of pluripotent stem cells

Comparison of the various types of pluripotent stem cells showed that pluripotency is rather dynamic, and that there are multiple pluripotent states [4, 22]. Two main different states of pluripotency can be distinguished: naïve and primed [22].

Mouse ESCs obtained from preimplantation blastocysts represent the naïve or ground state of pluripotency [22]. These cells form compact, dome shaped colonies and proliferate rapidly in vitro [23]. As a characteristic epigenetic feature, female naïve embryonic stem cells show two active X-chromosomes (XaXa) [22, 24]. Furthermore, they readily form chimeras after injection into blastocysts [4]. Mouse IPSCs have been shown to reach the naïve state of pluripotency [24, 25].

Human ESCs and iPSCs, however, show a primed state of pluripotency comparable to mouse EpiSCs [22, 24]. These cells form flatter colonies and proliferate slower in vitro [23]. They represent a developmentally more advanced state of pluripotency [24]. Female cells contain an epigenetically silenced X-chromosome (XaXi) [22, 24]. Mouse epiblast stem cells fail to contribute to chimeras, however due to ethical reasons this assay is not applicable to human stem cells [22].

However, both, naïve and primed pluripotent stem cells, show three-lineage differentiation potential in vitro and form teratomas when implanted into immunodeficient mice [4, 22]. How different states of pluripotency affect their utility for tissue engineering and regenerative medicine applications needs to be further elucidated.

3.1.3. Methods for the generation of induced pluripotent stem cells

Since their discovery, successful generation of iPSCs has been reported in a broad range of species including not only human [19, 20] and mice [15, 17] but also *for example* rat [26, 27], rabbit [28], pig [29, 30], horse [31], cattle [32] and monkey [33, 34]. Various somatic cell types including *e.g.* fibroblasts [15, 19], adipose-derived cells [35], blood cells [36], keratinocytes [37], neural progenitor cells [38], hepatocytes [39] or pancreatic beta islet cells [40] have been used as starting cell population for reprogramming [41].

Furthermore, different gene delivery methods have been applied for the induction of pluripotency. Whereas integrating viral vectors like retroviruses or lentiviruses provide stable transgene expression over a prolonged time allowing high reprogramming efficiencies, they bear the risk of insertional mutagenesis [15, 19, 42]. Non-integrating viral vectors, however, are considered safer but suffer from lower reprogramming efficiencies due to limited duration of transgene-expression [43]. Adenoviral vectors have been successfully used for reprogramming [44]. As they do not integrate their cargo into the host genome, multiple transfections are required and reprogramming efficiency remains low [41]. The non-integrating RNA Sendai virus offers efficient and safe reprogramming as it does not bear the risk of insertional mutagenesis [3, 45]. However, Sendai viruses are difficult to handle and not suitable for clinical applications yet [3, 41].

The reprogramming factors can also be delivered non-virally as plasmids, minicircles or episomal plasmids [46-48]. Although these DNA-based vectors are easy to produce, they suffer from low reprogramming efficiencies [3, 41, 42]. Delivery of the reprogramming factors as mRNA or proteins has also been reported [49, 50]. These methods do not bear the risk of insertional mutagenesis. However, mRNA is unstable and multiple transfections are required [3], whereas proteins are difficult to synthesize in an appropriate quality and offer only low reprogramming efficiencies [3, 41].

3.1.3.1. Transposons

Transposons are integrating, non-viral vectors which combine the advantages of integrating viral vectors (*i.e.* efficient reprogramming due to long-term transgene expression due to stable genomic integration) with the advantages of non-viral delivery systems (*i.e.* safer integration profile, cost effective production, no requirement for a specialized biohazard containment facility) [42, 51]. Therefore, transposons represent a promising gene vector for the generation of induced pluripotent stem cells for various applications.

Transposons are mobile genetic elements with the ability to change their position within the genome by a cut-and-paste mechanism called transposition [43]. Wild-type transposons consist of a transposase gene flanked by terminal inverted repeats (TIRs) that carry the transposase binding sites (Figure 3A) [42]. These two components can be separated from each other to use transposons as DNA delivery vehicles [42]. The gene of interest is placed between the transposon TIRs, whereas the transposase is supplemented from an alternative source (Figure 3B) [43]. Although, there are no known active wild-type transposons in mammals, many transposon systems have been genetically engineered during the last decades [52]. Of these, the Sleeping Beauty (SB) and the PiggyBac (PB) transposon systems have been used successfully for the generation of iPSCs [53-55]. Reprogramming efficiencies with the SB system are comparable to those achieved with integrating viral vectors [53].

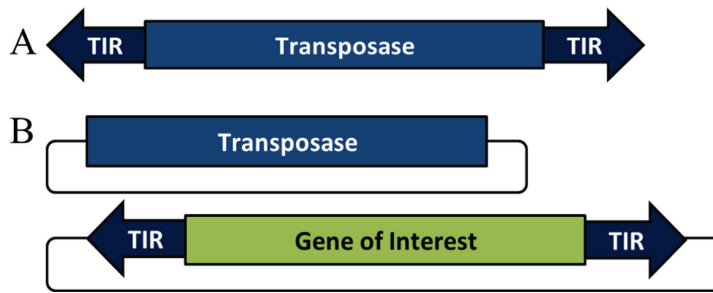


Figure 3: Transposons. Modified from Ivics *et al.* [43].

(A) Wild-type transposons are composed of the transposase gene flanked by the terminal inverted repeats (TIRs) that act as transposase binding sites. (B) Transposon gene delivery system. A gene of interest is placed between the transposons TIRs and the transposase is provided from an alternative source, most conveniently as a second plasmid.

3.1.3.2. Sleeping Beauty transposon system

The SB transposon system was reawakened from inactive transposons of the Tc1/mariner family found in fish in 1997 [56]. It was the first known transposon system to be active in vertebrate cells [43]. The TIRs of SB are about 230 bp long and contain two direct repeats (DRs) of about 32 bp length each [57]. These direct repeats act as transposase binding sites during transposition [57]. By screening amino acid replacements for more active variants of the transposase, the hyperactive transposase SB100X was developed [58]. Thereby the SB transposon system was the first non-viral gene delivery system with gene delivery efficiency rates comparable to viral vectors [59]. Optimization of the TIRs and insertion of a multi-cloning site between the TIRs led to the pT2 SB transposon vector [42].

After its delivery into a host cell, four transposase molecules bind the DRs within the TIRs flanking the gene of interest [57]. This leads to the formation of the so-called synaptic complex in which the ends of the element are brought close together [60]. Then the transposase catalyzes the excision of the transposon and its integration into a TA dinucleotide which is duplicated upon insertion [61]. Thereby SB transposition leaves a characteristic footprint within the genome (Figure 4) [61].

The transposase can be provided on the same plasmid as the transposon, on a second plasmid or as mRNA [57]. A second plasmid, however, is the most convenient source as it is easy to produce and handle, and allows adjusting of the transposase : transposon ratio. Too high levels of transposase inhibit transposition efficiency by a mechanism called overproduction inhibition

[52, 62]. For the SB100X transposase the optimal transposase : transposon ratio was shown to be 1 : 10 [63].

On the primary DNA sequence level SB integrations occur only at TA dinucleotides located within a bendable DNA structure composed of AT-rich palindromes [56, 64]. On a genome wide level, the integration profile of SB is fairly random with no overt bias for integration into genes or transcriptional regulatory regions [59, 65]. Its favorable integration profile renders Sleeping Beauty a safer gene delivery vehicle than other transposons like *e.g.* PiggyBac or viral vectors that show a considerable potential for genotoxicity [42, 65].

Taken together, the Sleeping Beauty transposon system is an easy to use and comparably safe gene delivery system that provides high reprogramming efficiencies in mouse and human [53, 54]. Therefore, we decided to use a Sleeping Beauty based reprogramming system for the generation of iPSCs in this thesis.

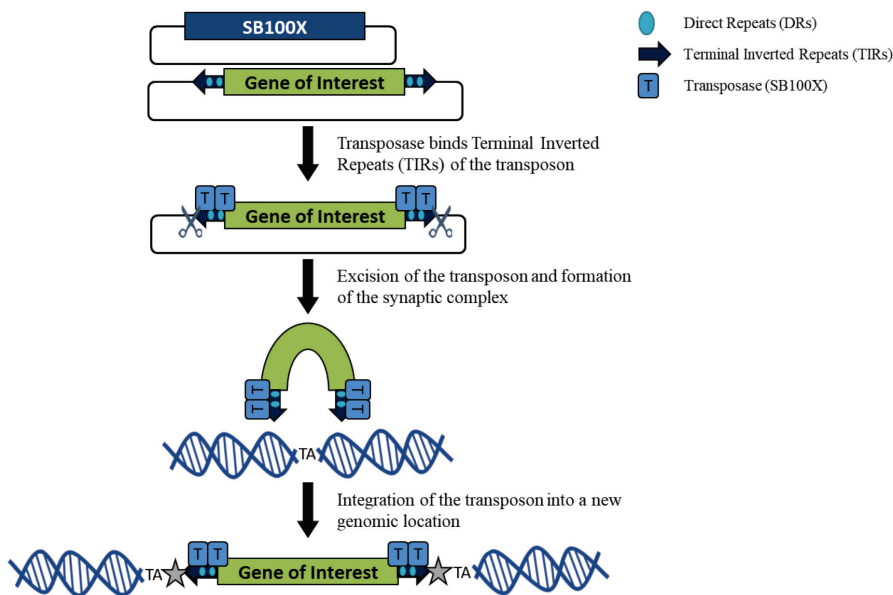


Figure 4: Sleeping Beauty transposition. Modified from Liu et al [57].

After delivery of the transposase (SB100X) and the transposon plasmid to the nucleus the transposase gene is transcribed, and transposase enzyme is produced. This enzyme binds the direct repeats (DRs) within the transposon's terminal inverted repeats (TIRs) flanking the gene of interest and catalyzes excision of the transposon followed by formation of the synaptic complex. This complex mediates integration of the transposon into a TA-dinucleotide that is duplicated upon integration.

3.1.4. Mechanisms of reprogramming

Despite the successful generation of iPSCs from a broad range of species and a wide variety of cell types, the molecular and epigenetic mechanisms behind induction of pluripotency by reprogramming factors are still not completely understood.

Most studies of the reprogramming process have been carried out in mouse embryonic fibroblasts (MEFs) [66-69]. It remains yet to be elucidated whether the mechanisms described in this population also account for other starting cell types or human cells [66, 70]. Reprogramming of MEFs takes at least one to two weeks and occurs at low frequencies rendering studies of the reprogramming process difficult [24, 70]. Dissecting the molecular and epigenetic mechanisms behind reprogramming relies on population wide analysis [67, 68] or on tracing back successful reprogramming events [66, 69] carried out in inducible secondary reprogramming systems [66-68, 71].

Overall, the reprogramming process is considered a stochastic event [71]. Yet, recent studies have identified key intermediate steps that are reached by fewer and fewer cells during the reprogramming process [24]. Based on transcriptional profiling *Samavarchi-Tehrani et al.* described three phases of reprogramming: initiation, maturation and stabilization [68, 70]. *Polo et al.* reported that transcriptional changes during the reprogramming process occur in two major waves separated by a phase of more gradual changes by analysis of intermediately reprogrammed populations (Figure 5) [67, 70].

3.1.4.1. Early events of the reprogramming process

At the beginning of the reprogramming process each cell undergoes certain transcriptional and morphological changes [67, 68, 70]. During this initiation phase of reprogramming the original cell identity is erased [72]. Furthermore, cells increase their proliferation to an ESC-like rate and become resistant to apoptosis and senescence during the initiation phase [69, 70].

One of the first obvious signs of ongoing reprogramming in murine fibroblasts is a change in morphology [69, 73]. The cells start to aggregate in tightly packed clusters of small rounded cells exhibiting an epithelial phenotype [69, 73]. This mesenchymal to epithelial transition

(MET) is a critical step during early reprogramming [68, 73]. On the molecular level MET is marked by the upregulation of epithelial markers like *E-Cadherin* and by the downregulation of mesenchymal markers like *Snail* [68, 73]. These transcriptional changes account for the first wave of transcriptional changes revealed by gene expression profiling [67, 68].

Reprogramming of epithelial cells like keratinocytes or hepatocytes is more effective than reprogramming of cells of a mesenchymal origin likely due to skipping the MET step [24, 74, 75]. It remains to be elucidated whether the remaining steps of reprogramming are the same for cells of different origins or whether they take different pathways to pluripotency.

At the epigenetic level, mostly changes of histone modifications occur during early reprogramming, whereas DNA methylation changes take place later in the process [67, 70]. Gain of activating H3K4 methylation marks at the promoters and enhancers of pluripotency associated genes occurs during the initiation phase prior to their transcriptional activation [24, 76]. Remaining repressive H3K27 marks and DNA methylation that are lost only towards the end of the reprogramming process likely prevent expression of these genes [67, 77]. Loss of the activating H3K4 methylation at somatic genes, however, is followed by their downregulation [24, 76]. Correspondingly, transcriptional changes are limited to pre-existing accessible chromatin that can be targeted directly by the reprogramming factors leading to the observed activation of proliferation-associated genes and silencing of somatic genes [24, 76]

Despite deciphering certain key events occurring during the initiation phase, no clear sequence of events has been described so far [70]. The significant variation of gene expression profiles between single cells during the initiation phase indicates that changes in gene expression occur in a stochastic manner [66]. Yet – as long as all steps associated with the initiation phase are acquired – cells may proceed in the reprogramming process no matter in which order the key events have been reached [66, 70].

3.1.4.2. Intermediate events of the reprogramming process

Transition from the initiation phase to the maturation phase is marked by appearance of the first pluripotent surface markers SSEA1 (stage specific embryonic antigen 1) and alkaline

phosphatase (AP) [68, 70]. This transition is one of the major bottlenecks in the reprogramming process [68, 70].

During this phase, pluripotency associated genes are activated and the pluripotency network is gradually established [70]. These changes in the transcriptional profile account for the second wave of transcriptional changes described by *Polo et al.* [67].

Single cell gene expression analyses have revealed that pluripotency-associated markers are activated in a sequential manner during reprogramming [66, 67, 70]. First, the markers *Fbx15*, *Sall4* and endogenous *Oct3/4* can be detected, followed by upregulation of *Nanog* and *Rex1* [66-68, 70]. Finally, expression of endogenous *Sox2* and *Dppa4* appears towards the end of the maturation phase [66, 67, 70]. Although these markers are good indicators of successful reprogramming, their acquisition does not guarantee complete reprogramming of cells [66, 67, 70].

On the epigenetic level, changes in DNA methylation take place during the late maturation phase [67, 70]. Methylation of cytosine (C) residues of CG dinucleotides in promoter regions leads to stable silencing of the corresponding genes [11]. Methylation of somatic genes and demethylation of pluripotency associated genes “locks” the acquired pluripotency [67, 72]. Thereby, the cells reach a stably reprogrammed state that marks the transition to the stabilization phase [70]. Whereas methylation is carried out by DNA-methyltransferases, it remains unclear, if methylation marks at pluripotency associated genes are passively lost during repeated cell divisions, or whether they are actively removed by still unknown mechanisms [24, 67].

Overall, the maturation phase represents a slow, hierarchical process [66, 70]. Only few SSEA1 positive cells completely activate the pluripotency network and successfully complete the reprogramming process [24, 78]. The exact mechanisms of how exogenous Oct3/4, Sox2, Klf4 and c-Myc activate the pluripotency network are still not completely understood.

3.1.4.3. Late events of the reprogramming process

Once the pluripotency network is stably established, the freshly reprogrammed cells can maintain their pluripotency independently from the exogenous reprogramming factors [24, 70]. Therefore, transgene silencing marks the transition from the maturation phase towards the stabilization phase [68, 70]. During this phase, clonal IPS cell lines are usually established and analyzed [70].

Despite being already successfully reprogrammed to a pluripotent state, epigenetic changes continue [70]. Although expression of somatic genes is downregulated early during reprogramming, methylation of their promoters occurs only at the end of the reprogramming process [24, 76]. Low passage induced pluripotent stem cells show residual DNA methylation signatures characteristic of the cell type of origin [24, 79, 80]. This “epigenetic memory” affects their differentiation potential as it favors differentiation along the original lineage [24, 79, 80]. By continuous passaging these remaining epigenetic marks can be removed [24, 80]. This resetting of the epigenetic memory occurs during the stabilization phase [70, 78].

EARLY	INTERMEDIATE	LATE
Transgene Dependent		Transgene Independent
<ul style="list-style-type: none"> • Mesenchymal to Epithelial Transition <ul style="list-style-type: none"> - Somatic genes ↓ - Epithelial markers ↑ - Morphological changes (smaller, round cells) • Increase of proliferation rate • Resistance to apoptosis/ senescence • Histone modifications 	<ul style="list-style-type: none"> • Expression of first pluripotency markers and step-wise establishment of the pluripotency network • Histone modifications and changes in DNA methylation 	<ul style="list-style-type: none"> • Pluripotency • Transgene silencing • Changes in DNA methylation • Loss of epigenetic memory
-Snail +ECad	+SSEA1 +AP	+Oct3/4 +Nanog +Sox2

Figure 5: Phases of the reprogramming process. Adapted from *David et al.* [70] and *Plath et al.* [24].

Hallmark events and markers of the early, intermediate and late phase of reprogramming are indicated.

3.1.4.4. Function of the reprogramming factors

Oct3/4, also known as Pou5f1, is a member of the POU homeodomain transcription factors [81]. It is an essential part of the pluripotency network in ESCs involved in the maintenance of pluripotency [24, 82]. Oct3/4 is a crucial reprogramming factor and fundamentally required in most reprogramming experiments [83]. It cooperates with many other factors to induce the expression of pluripotency associated transcriptional regulators including its own and to repress expression of lineage specific genes during reprogramming [81, 84]. Activation of endogenous Oct3/4 during reprogramming marks the transition of partially reprogrammed cells to fully reprogrammed induced pluripotent stem cells [24, 85].

Sox2 is a member of the sex determining region of Y (SRY)-related, high-mobility group box transcription factors [81]. It is one of the core transcription factors of the pluripotency network in ESCs, however, it is also expressed at high levels in a variety of other cell types like *e.g.* neural progenitor cells [24, 38]. In ESCs, it forms heterodimers with Oct3/4 and enhances expression of genes that are required for the maintenance of pluripotency including its own [84, 86]. Sox2 is an essential reprogramming factor, however, in cells with high endogenous levels of Sox2 reprogramming can be achieved with Oct3/4 alone [38, 84]. In MEFs endogenous Sox2 is reactivated late during the reprogramming process and marks the transition to the stabilization phase of reprogramming [68, 70].

Klf4 (Krüppel-like factor 4) is a zinc finger transcription factor that belongs to the family of Sp1-like transcription factors [81, 87]. It is part of the pluripotency network in ESCs but is also highly expressed in adult epithelial tissues with high turnover like gut or skin [81, 87]. It plays important roles in many physiological processes such as cell cycle control, DNA repair, apoptosis and differentiation [87]. It can act as a tumor-suppressor or exhibit oncogenic activity in a context-specific manner [87]. During the reprogramming process Klf4 induces epithelial genes during mesenchymal to epithelial transition and later acts as a cofactor of Oct3/4 and Sox2 in establishing the pluripotency network [73, 86].

c-Myc is known as an oncogene associated with many types of cancer including *e.g.* Burkitt lymphoma [81, 88]. Although it is not absolutely required during reprogramming, it greatly enhances efficiency and kinetics of the reprogramming process [81, 83]. Expression of c-Myc upregulates cell cycle promoters and increases cell proliferation and metabolism to an ESC-like

state during the initiation phase of reprogramming [24, 83]. By interacting with chromatin remodelers, it creates a permissive cellular state that facilitates the activation of the pluripotency network by the other transcription factors despite not being directly involved in the upregulation of the network itself [81, 83]. Re-expression of genomically integrated c-Myc can lead to tumor formation upon differentiation of iPSCs hampering clinical applicability of these cells [81, 89].

The potentially oncogenic factors Klf4 and c-Myc are not absolutely required for reprogramming as they can be replaced *e.g.* by Nanog and Lin28 [20].

Nanog is a core member of the pluripotency network that co-occupies more than 300 target genes together with Oct3/4 and Sox2 in ESCs [24, 25]. Its upregulation is essential for the generation of iPSCs and marks the transition from an intermediate to the fully reprogrammed state during the maturation phase of reprogramming [24, 70].

Lin28 is an ESC-specific RNA binding protein that is induced by c-Myc [81, 84]. By degrading let-7 miRNAs that are expressed ubiquitously in somatic cells but repressed in pluripotent stem cells, it accelerates the reprogramming process [81, 84].

3.1.4.5. Roles of the reprogramming factors in reprogramming

In ESCs, an autoregulatory network of transcription factors is responsible for maintenance of pluripotency [90, 91]. This pluripotency network needs to be established in somatic cells during the reprogramming process.

Repressive chromatin at pluripotency associated genes is one of the major barriers that has to be overcome during reprogramming [24]. Pioneer factors are transcription factors that can engage target genes in closed, inactive chromatin and thereby enable other transcription factors and chromatin remodelers to access and activate these sites finally leading to acquisition of an active chromatin state and expression of the target genes [92]. Oct3/4, Sox2 and Klf4 have been shown to act as pioneer factors during establishment of the pluripotency network, whereas c-Myc only enhances their binding without having pioneer activity itself [93].

Genome wide analysis of the binding patterns of Oct3/4, Sox2, Klf4 and c-Myc during the reprogramming process gave further insight to the different roles of the reprogramming factors

during the reprogramming process [85, 93]. Whereas the binding patterns of the factors are comparable between fully reprogrammed iPSCs and ESCs, the binding patterns at the initiation of reprogramming and in partially reprogrammed iPSCs are markedly different [85, 93].

After 48h of expression in fibroblasts, Oct3/4, Sox2, Klf4 and c-Myc (OSKM)-binding sites show only partial overlap with their binding pattern in ESCs [93]. The factors bind together at genes with pre-existing active chromatin marks inducing the early transcriptional changes associated *e.g.* with mesenchymal to epithelial transition [24, 76, 93]. They also activate apoptosis-related genes likely presenting a protective mechanism to eliminate cells in which aberrant transcription factor expression has occurred [93]. Other than that, OSKM binding occurs mostly at enhancers of genes that will become activated later during the reprogramming process [93]. Still unknown events are required for the factors to engage with promoters and activate transcription during the reprogramming process [72, 93].

In partially reprogrammed pre-iPSCs, Oct3/4, Sox2 and Klf4 show a different binding pattern than c-Myc indicating their different roles in establishing the pluripotency network [85]. Partially reprogrammed cells constitute a stable intermediate cell population in which cells have already acquired the proliferative and biosynthetic properties of iPSCs but the endogenous pluripotency network has not been activated yet [24]. At this pre-iPSC stage, c-Myc has already bound most of its final targets [85]. These are mostly genes associated with proliferation and metabolism indicating that c-Myc is not directly involved in the upregulation of the pluripotency network [85].

In fully reprogrammed iPSCs, Oct3/4 and Sox2 together with Klf4 and other factors like Nanog co-occupy promoters of highly expressed pluripotency associated genes including their own [24]. Thereby these factors are core elements of the pluripotency network [90, 91]. However, Oct3/4, Sox2 and Klf4 only bind about 1/3 of their targets at the pre-iPSC state [85]. In accordance partially reprogrammed cells have not upregulated endogenous pluripotency markers yet [24]. The different binding patterns might result from repressive epigenetic modifications at the pluripotency associated genes or lack of cofactors like *e.g.* Nanog in pre-iPSCs [24, 85]. Stochastic events are required to overcome these barriers that represent one of the major hurdles in reprogramming [24, 70].

3.1.5. Applications of induced pluripotent stem cells

IPSCs, as a somatic-cell derived cell source with unlimited proliferation and differentiation potential, offer promising possibilities for regenerative medicine. Currently, there are three major applications for IPSCs: basic research, disease modeling and drug discovery, and finally replacement of diseased or injured tissues and organs by autologous transplants (Figure 6) [23].

The reprogramming process itself is an intensively studied topic in basic research. Deciphering the mechanisms of reprogramming offers valuable insights into the pluripotency network that plays important roles in embryogenesis and early development [23, 72, 86].

Furthermore, as carcinogenesis and reprogramming are closely related processes IPSCs are now broadly applied in cancer studies [23, 94]. Cancer cells share many features with IPSCs like *for example* their unlimited proliferation potential, their ability to self-renew, their metabolic state and, to a certain extent, their gene expression pattern and epigenetic status [94]. The reprogramming factors Klf4 and c-Myc are known oncogenes, whereas Oct3/4 and Sox2 exhibit high expression in certain types of cancer [94]. Reprogramming of cancer-derived cells to so-called induced cancer stem cells (ICSCs) offers insights into cancer development and progression, therapy resistance and relapse and may contribute to the development of novel anti-cancer therapies [94].

IPSCs offer new ways to study genetic diseases and provide a platform for drug discovery and toxicity screening [95]. Conventional disease models rely on immortalized cell lines or on transgenic animal models [95, 96]. However, animal models often show significant differences from human pathophysiology and certain tissue samples like *e.g.* cardiac or neuronal tissue are difficult or impossible to access from patients [95, 96]. IPSCs can be generated from patients suffering from a known genetic disease and differentiated into disease-relevant cell types [95]. This “patient-in-a-dish” can be used to study the pathophysiology of the disease as these patient-derived IPSCs exhibit a diseased phenotype [23, 97]. Patient-specific IPSCs have been established from a broad range of neurologic disorders including *e.g.* amyotrophic lateral sclerosis [98] or Parkinson’s disease [99], heart diseases like hypertrophic or dilatative cardiomyopathy [100, 101] and other genetic diseases like familial hypercholesterinemia [102] or juvenile diabetes [103]. The main limitation for the application of IPSCs to study disease mechanisms is, however, the lack of efficient and reliable differentiation protocols into disease-

relevant cell types [104]. Furthermore, these patient-derived iPSCs could be used for high-throughput drug testing and toxicity screening [95, 96]. *For example*, human iPSC-derived cardiomyocytes could become an important alternative to cardiotoxicity screening in animal models or on cell lines [95].

Patient-derived iPSCs could open the road to individual precision medicine in which the right drug is provided for the right patient in the right dosage [95]. Every patient has a different genetic background and will therefore react differently to medication. iPSCs based drug screening for an individual patient could contribute to find the ideal therapeutic option for every single patient [95]. On the other hand, iPSCs derived from cohorts of patients could be used for high-throughput drug and toxicity screening in a “clinical trial in a dish” set-up [95]. Thereby a large number of compounds can be easily screened, and potential responders and non-responders could be identified prior to testing the drug in an actual patient [95, 105]. Many iPSC-based drug screenings are currently performed on various genetic disorders and first clinical trials using iPSC-discovered compounds are ongoing [96, 106].

Organ transplantation is limited by lack of donor organs and immunorejection of allogenic tissues [95]. iPSCs could provide a source of autologous cells that can be differentiated into any cell type needed [95, 97]. iPSCs derived cells and tissues could be transplanted back into the patient without the risk of rejection and thus without need for immunosuppressive drugs [95]. Unlike ESCs, patient-derived iPSCs face less ethical concerns and immune barriers [95]. The potential of iPSCs to replace diseased tissues has been shown in many animal models including models of liver failure [107, 108], spinal cord injury [109] or hematological disorders [110, 111]. First clinical trials using patient-derived iPSCs are on their way [112]. However, there is still a lack of efficient and reliable differentiation protocols for many desired cell types [97]. Furthermore, iPSCs still face many safety concerns. Transplantation of residual pluripotent stem cells imposes the risk of teratoma formation [97]. Incomplete reprogramming and genetic mutations occurring during reprogramming might render even patient-derived IPS cell lines immunogenetic [97]. Lastly, efficiency of reprogramming is still low and generating patient derived iPSCs under good manufacturing practice (GMP) conditions is a time consuming and costly process [16]. Therefore, the generation of a human iPSC-bank from patients with common HLA types has been proposed [113, 114].

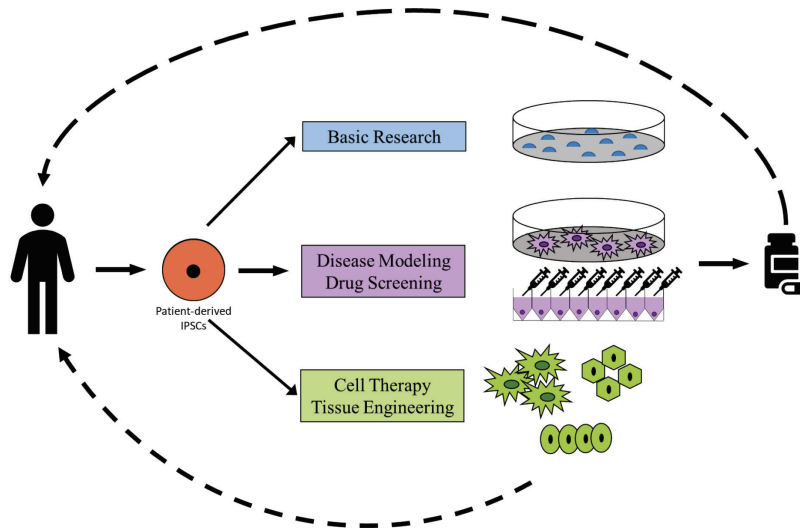


Figure 6: Applications of induced pluripotent stem cells (self-designed).

Patient-derived iPSCs can be used for basic research purposes including deciphering of the reprogramming mechanism itself or cancer studies. Furthermore, patient-derived iPSCs can be differentiated to disease-relevant cell types and used as a model to study the pathomechanisms of the disease or discover new possible drug targets in high-throughput screenings. Finally, iPSCs can serve as an autologous cell source for cell therapy or tissue transplants.

3.2. Articular cartilage

Cartilage is a highly specialized connective tissue. There are three kinds of cartilage within the human body: hyaline cartilage, fibrocartilage and elastic cartilage [115]. Hyaline cartilage is present *e.g.* in diarthrodial joints and in the trachea [115]. Fibrocartilage contains more collagen fibers in the extracellular matrix (ECM) and can be found *e.g.* in the intervertebral discs or knee menisci [115, 116]. Elastic cartilage contains elastin in the ECM and forms parts of ear and nose [116].

Articular cartilage is a specialized hyaline cartilage that covers the surfaces of diarthroidal joints [115]. The mean thickness of articular cartilage in human is 3 - 4 mm but it can reach up to 6 - 8 mm *e.g.* at the patellar articular surface [117]. Together with the synovial fluid, articular cartilage provides almost frictionless articulation in the joint [118]. The viscoelastic properties of the ECM endow articular cartilage with high resistance to mechanical stress and help to distribute joint loads [115, 119]. As articular cartilage is devoid of blood and lymphatic vessels, nutrition is provided only via diffusion from the synovial fluid [117, 119]. This together with the limited proliferation capacity of chondrocytes accounts for the low intrinsic regenerative potential of articular cartilage [115].

3.2.1. Components of articular cartilage

Generally, articular cartilage is composed of a solid and a liquid phase [115]. 60 - 80% of the wet weight of articular cartilage consist of water and electrolytes (fluid phase), whereas cells and ECM make up about 20 - 40% of the wet weight (solid phase) [115].

The cells, so called chondrocytes, are embedded in an extensive ECM [117]. The ECM of articular cartilage is made up of a meshwork of collagen fibrils, proteoglycans and other non-collagenous proteins and is responsible for articular cartilage's unique mechanical properties [117].

3.2.1.1. Chondrocytes

Chondrocytes are the only cell type found in healthy articular cartilage [115]. They make up only about 1-3% of the tissue volume [120]. These specialized cells synthesize and maintain the ECM [115]. Chondrocytes have cilia that extend into the ECM and allow the cells to sense and respond to mechanical stimuli from joint loading [116].

Chondrocytes originate from mesenchymal stem cells (MSCs) in a process called chondrogenesis [116, 121]. This is discussed in detail in *3.2.3.1. Chondrogenesis and endochondral ossification*. At birth, articular cartilage is highly cellular and composed of small cells in scanty matrix [116]. Postnatally, articular cartilage expands vertically and laterally by chondrocyte proliferation, chondrocyte hypertrophy and matrix accumulation [116]. As mature chondrocytes are completely encapsulated by dense ECM, they are not able to migrate or proliferate significantly [115, 116]. This in addition to the lack of vascular, lymphatic and neuronal networks hampers the regenerative potential of articular cartilage [115].

3.2.1.2. Extracellular matrix

3.2.1.2.1. Collagens

The ECM of articular cartilage is composed of collagen fibrils that form an extensive network and account for about 50 - 75% of the dry weight of articular cartilage [115, 118].

Collagens are the main structural proteins of tissues providing resistance to tensile stress [122]. Collagens consist of three α chains that contain glycine as every third amino-acid and have a high proline and hydroxyproline-content, and therefore form triple helices, the characteristic structural feature of all collagen molecules [123]. Collagens can be divided into fibril-forming collagens (Types I, II, III, V, XI), network forming collagens (Types IV, VIII, X), fibril-associated collagens (Types IX, XII, XIV) and transmembrane proteins (Types XIII, XVII) [122].

Fibril-forming collagens are synthesized as procollagen molecules containing an amino-terminal propeptide followed by a N-telopeptide, a central triple helix, a C-telopeptide and a carboxy-terminal propeptide [123]. Proteolytic cleavage of both propeptides by procollagen N- and C-proteinases results into mature collagen molecules which then spontaneously assemble into fibrils [122]. The telopeptides contain lysine residues that form intra- and intermolecular cross links, which stabilize collagen fibrils and networks [118, 123].

The ECM of articular cartilage contains collagen types II, VI, IX, X and XI [115]. With over 90% type II collagen is the dominant type of collagen in articular cartilage [118]. Type II collagen fibrils consist of three identical $\alpha_1(\text{II})$ -chains (Col2a1) and form an extensive network in the extracellular matrix of articular cartilage [118]. Evidence of *Col2a1* expression during chondrogenic differentiation of mesenchymal stem cells (MSCs) [124, 125] or pluripotent stem cells (PSCs) [126, 127] is widely accepted as a marker for successful chondrogenesis. There are two isoforms of type II procollagen, named procollagen IIA and procollagen IIB that are generated by alternative splicing of exon 2 [128]. The type IIA isoform contains exon 2 and is produced mainly by chondroprogenitor cells during chondrogenesis. It can furthermore be found in non-cartilaginous tissues like retina, heart or tendons, too [128, 129]. The type IIB isoform, however, is devoid of exon 2 and found predominantly in differentiated cartilage [128, 129]. Both isoforms are reliable markers of chondrogenic differentiation [128]. Whereas type

IIA procollagen expression is characteristic for chondroprogenitor cells, type IIB procollagen expression identifies differentiated chondrocytes [128].

Type IX and type XI collagens crosslink with type II collagen fibrils, regulate fibril assembly, modify fibril diameters and stabilize the collagen network [115, 118]. Type VI collagen forms beaded filaments that intertwine to a highly branched filamentous network at pericellular sites and mediate cell-collagen-interactions via mechanotransduction [115, 118, 123].

Type X collagen is expressed in the calcified cartilage layer and in hypertrophic cartilage during endochondral ossification [118, 123]. Expression of type X collagen during in vitro chondrogenesis is therefore a marker of hypertrophic cartilage [130].

Articular cartilage as a type of hyaline cartilage is per definition devoid of type I collagen [118]. This collagen type is present in fibrocartilage tissue like meniscal cartilage [118]. Its occurrence during in vitro chondrogenesis indicates fibrocartilaginous dedifferentiation of chondrocytes [130].

3.2.1.2.2. Aggrecan

Aggrecan (Acan) is the main proteoglycan of cartilage ECM accounting for about 5% of the wet weight of articular cartilage [131]. Proteoglycans consist of glycosaminoglycan (GAG)-chains attached to a protein core [117]. The GAGs are long polysaccharide chains made up of repeating disaccharides that contain many negatively charged sulfate- and carboxyl-groups [117]. Aggrecan consists of a core protein and some keratan sulfate (KS) and many chondroitin sulfate (CS) chains that spread out from the core protein like tubular brushes [115, 132].

Aggrecan forms large aggregates in the ECM of articular cartilage (Figure 7) [131]. Up to 100 aggrecan molecules are attached to a long hyaluronan filament [132]. Hyaluronan is a non-sulfated GAG that is characterized by its large length and its synthesis by hyaluronan-synthases (HAS) at the plasma membrane of cells [132]. The so called link protein (LP) can bind hyaluronan and aggrecan and stabilizes the proteoglycan aggregates [132].

As described in 3.2.1.2.4. *Function of articular cartilage extracellular matrix* aggrecan is responsible for the unique viscoelastic properties of articular cartilage. Furthermore, it is an important marker for successful chondrogenic differentiation of MSCs [130, 133] and PSCs [134, 135].

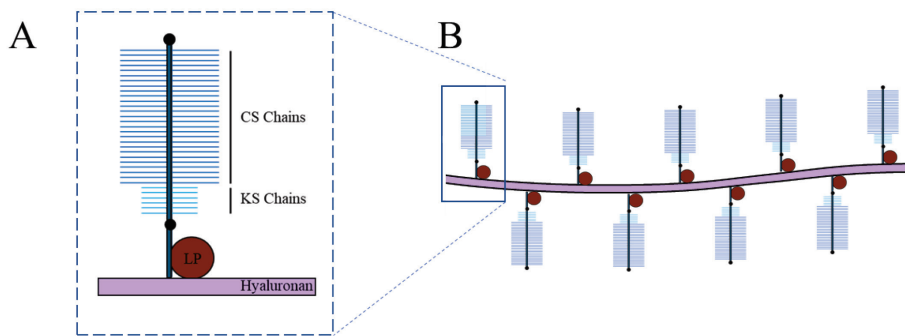


Figure 7: Structure of aggrecan. Adapted from Brody *et al.* [117].

(A) Aggrecan is composed of a core protein to which chondroitin sulfate (CS) and keratan sulfate (KS) chains are attached. Link protein (LP) connects aggrecan monomers and hyaluronan filaments. (B) Several aggrecan molecules bind to long hyaluronan chains the ECM of articular cartilage forming large aggregates.

3.2.1.2.3. Non-collagenous proteins

Besides collagens and aggrecan there are many other proteins in the ECM of articular cartilage.

Small leucin rich repeat proteins (SLRPs) like *e.g.* biglycan, decorin, fibromodulin and lumican are a group of proteins characterized by repeats of a leucin rich motif flanked by disulfide loop structures [131, 132]. These proteins bind collagen fibers and thereby modify fiber formation, and promote cross linking of collagen fibers to an extensive collagen network [131]. Furthermore, they can act as binding sites for growth factors and cytokines in the extracellular matrix or provide cell-matrix interactions [131].

The cartilage oligomeric matrix protein (COMP) can bind five collagen molecules and by bringing these molecules in close proximity it enhances collagen fibril formation [131]. Furthermore, it stabilizes the collagen network in adult cartilage [131].

3.2.1.2.4. Function of articular cartilage extracellular matrix

Interaction of the matrix components provides articular cartilage with viscoelastic properties that are important for its ability to dissipate compressive loads, redistribute loading forces and lower joint friction (Figure 8) [115].

The negatively charged sulfate- and carboxyl-groups of keratan sulfate and chondroitin sulfate bound to aggrecan provide an extreme anionic charge density in the ECM of articular cartilage [117, 131]. Since the network of collagen fibers entraps aggrecan and prevents it from escaping the tissue, the fixed negative charges attract mobile cations [115, 132]. The high density of ions within the tissue creates an osmotic gradient attracting water and causes cartilage to swell [115]. The tendency to swell is restricted by the tensile properties of the collagen fibers [118, 131].

During compression, interstitial fluid flows out of the porous collagen-proteoglycan matrix until the frictional drag that increases with tissue condensation counterbalances the compressive force [115, 136]. The fluid exudation from the tissue also provides lubrication of the joint [115]. With decompression, the swelling pressure of the proteoglycans causes the tissue to expand again and drags water back into the tissue [118, 136]. Alteration between compression and decompression of articular cartilage during motion enhances the flow of interstitial fluid what aids to provide nutrition to the avascular tissue [136].

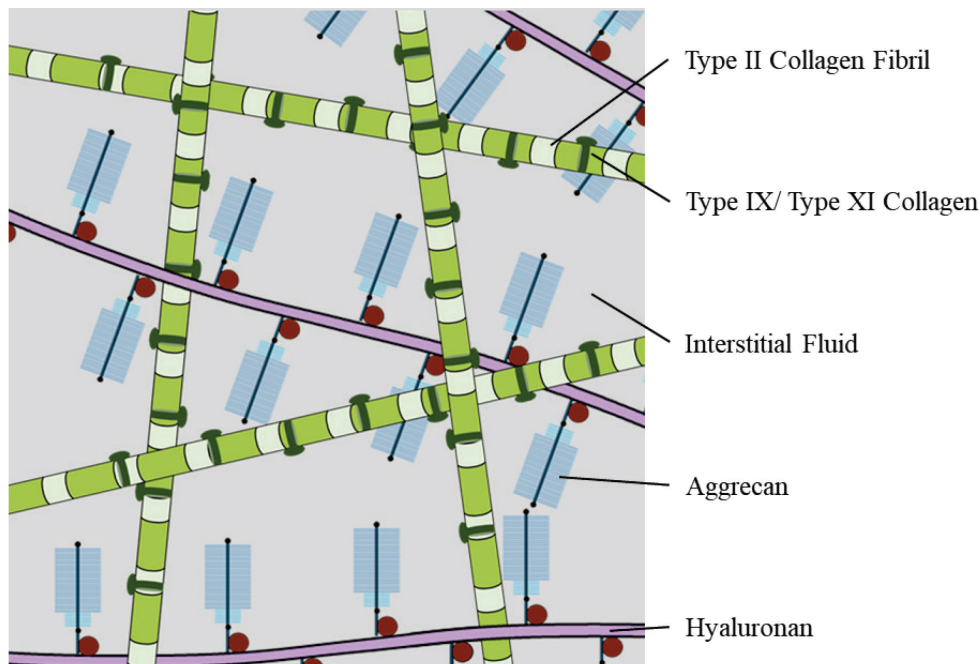


Figure 8: Extracellular matrix of articular cartilage. Adapted from Brody *et al* [117] and Poole *et al.* [118].

Type II collagen fibrils form an extensive network in the ECM of articular cartilage. Type IX and type XI collagens bind type II collagen fibrils. Aggrecan forms large aggregates with hyaluronan filaments that intertwine with the collagen meshwork. The negatively charged GAG-chains attached to aggrecan attract mobile cations and water causing the tissue to swell. The tendency to swell is restricted by the collagen meshwork leading to articular cartilages unique viscoelastic properties.

3.2.1.3. Integrins

Integrins are heterodimeric transmembrane proteins composed of α and β subunits [137]. Today, at least 24 different integrin heterodimers formed by the combination of 8 types of β subunits and 18 types of α subunits have been described [137].

Integrins are cell surface receptors and have large extracellular domains that bind components of the ECM, and short cytoplasmatic domains that bind cytoskeletal structures. By connecting ECM and cytoskeleton, integrins serve as transducers of chemical and mechanical signals [137]. Additionally, integrins can indirectly activate various intracellular signaling pathways and take part in the regulation of cell proliferation, migration, differentiation and survival [137, 138].

Integrins $\alpha 1\beta 1$, $\alpha 2\beta 1$, $\alpha 10\beta 1$ and $\alpha 11\beta 1$ constitute a subset of the integrin family with affinity for collagens and are therefore referred to as collagen-binding integrins [137, 138].

Articular cartilage chondrocytes express many types of integrins including $\alpha1\beta1$, $\alpha3\beta1$, $\alpha5\beta1$, $\alpha10\beta1$, $\alpha V\beta1$, $\alpha V\beta3$, and $\alpha V\beta5$ [137]. Integrin $\alpha10\beta1$ is the most abundant collagen-binding integrin in cartilage and shows high affinity for type II collagen [137, 139]. It was first identified in 1998 by *Camper et al* [140]. Mice deficient of integrin $\alpha10\beta1$ develop a mild chondrodysplasia due to a disorganized growth plate [141]. It serves as an important mediator of cell-matrix interactions during endochondral ossification [139, 141]. As integrin $\alpha10\beta1$ is a unique marker of chondrocytes, upregulation of *$\alpha10$ -integrin (*Itga10*)* mRNA during in vitro chondrogenesis is considered as a sign of successful chondrogenic differentiation [139, 142].

3.2.2. Structure of articular cartilage

Due to differences in cell morphology and matrix composition, articular cartilage can be divided into four different layers [115, 117]. These are termed superficial, middle, deep and calcified zone [115].

The superficial or tangential zone is the outermost zone, making up about 10 - 20% of the total articular cartilage thickness [115]. It is designed to resist shear forces that occur during joint movements [117]. The chondrocytes here are flattened and aligned parallel to the surface and the direction of shear stress [115, 118]. Cell density is the highest in this zone [117]. The ECM is composed of thin collagen fibers that are densely packed and orientated tangential to the articular surface forming the lamina splendens [115]. Proteoglycan content is the lowest in this layer [118].

The lower layers with vertical fiber orientation and higher proteoglycan content are designed to resist compressive forces and distribute joint loads [117]. The middle or tangential zone accounts for 40 - 60% of articular cartilage thickness [115, 117]. Cell density in this layer is lower and chondrocytes exhibit a round morphology [117, 118]. Collagen fibers are orientated more randomly as they change their direction from a tangential orientation in the superficial zone to an orientation vertical to the surface in the deep zone [115]. Furthermore, the fiber diameter gradually increases [115]. The matrix in this layer has the highest proteoglycan content [118]. The remaining 20 - 30% of articular cartilage thickness are termed deep or radial zone [115, 117]. Chondrocytes are orientated perpendicular to the subchondral bone and form

columns [115, 117]. Thick collagen fibers are orientated parallel to the chondrocyte columns [117]. These fibers are inserted across the tidemark in the underlying calcified layer and help to anchor the cartilage layer to the subchondral bone [115].

The tidemark is a basophilic line in histological samples that separates deep and calcified zone [115]. It also marks the boarder of nutritional supply in adult articular cartilage [117]. Above the tide mark nutritional supply is provided via diffusion from the synovial fluid, whereas the calcified cartilage layer below the tidemark is supplied from the subchondral bone [117].

The calcified zone is the transitional zone between articular cartilage and subchondral bone with intermediate mechanical properties [115, 118]. Chondrocytes in the calcified zone exhibit a hypertrophic phenotype, express type X collagen and are able to calcify the surrounding ECM [118].

3.2.3. Articular cartilage development

3.2.3.1. Chondrogenesis and endochondral ossification

The formation of cartilage from mesenchymal stem cells during embryonic development is termed chondrogenesis [121]. Osseous tissues are formed via two distinct processes: intramembraneous and endochondral ossification [143]. During intramembraneous ossification mesenchymal stem cells directly differentiate into osteoblasts, whereas during endochondral ossification first a cartilage template, the so-called cartilage anlage, of the respective bone is formed and then gradually replaced by osseous tissue (Figure 9) [143, 144].

During the process of gastrulation in early embryonic development the primitive streak as a mesoendodermal intermediate leads to the development of the three embryonic germ layers, ectoderm, mesoderm and endoderm [145]. The mesodermal layer gives rise to a variety of tissues, including heart and vascular tissues, muscles as well as cartilage and bone [145, 146]. Cartilaginous and osseous tissues of the limbs arise from the paraxial mesoderm that further differentiates into the lateral plate mesoderm during the outgrowth of limb buds [146].

The first step in chondrogenesis or endochondral ossification, is a condensation of mesenchymal stem cells in these limb buds [143]. These cells then differentiate into chondroprogenitors that start to produce a matrix rich in type II collagen and aggrecan forming the cartilage anlage of the skeletal element and finally develop into chondrocytes [121, 143]. The cells at the periphery of the condensations from the perichondrium that demarks the developing bone from the surrounding mesenchyme [143].

The chondrocytes in the cartilage anlage form two different subpopulations: round, low proliferating chondrocytes at the distal ends of the condensation (round proliferating (RP) chondrocytes) and high proliferating chondrocytes that are aligned in columns at the center of the condensation (columnar proliferating (CP) chondrocytes) [144]. The high proliferating chondrocytes then exit the cell cycle and differentiate into prehypertrophic and hypertrophic chondrocytes [144]. These cells start to produce type X collagen and mineralize their ECM [143, 144]. Furthermore, the hypertrophic chondrocytes produce VEGF (vascular endothelial growth factor), that attracts blood vessels from the perichondrium [121]. In parallel, cells of the perichondrium differentiate into osteoblasts that produce a bone collar around the diaphysis of the skeletal element and the perichondrium becomes the periosteum [143, 144]. Together with blood vessels, osteoblast and osteoclasts from the bone collar migrate into the mineralized cartilage, which is thereby replaced by bone forming the primary spongiosa of the primary ossification center [143, 144].

During postnatal development secondary ossification centers are established in the epiphyseal regions of bones [144]. Whereas cartilage at the epiphyseal surfaces develops into articular cartilage, cartilage between the ossification centers forms the growth plate that is essential for longitudinal bone growth [121, 144].

The growth plate is marked by distinct zones of proliferating cartilage, hypertrophic cartilage and bone formation from epiphysis to diaphysis of the skeletal element [143]. Proliferation of the less mature chondrocytes at the epiphysis, followed by their hypertrophy and replacement by trabecular bone results in a distal replacement of the growth plate by osseous tissue and in longitudinal growth of the skeletal element [143].

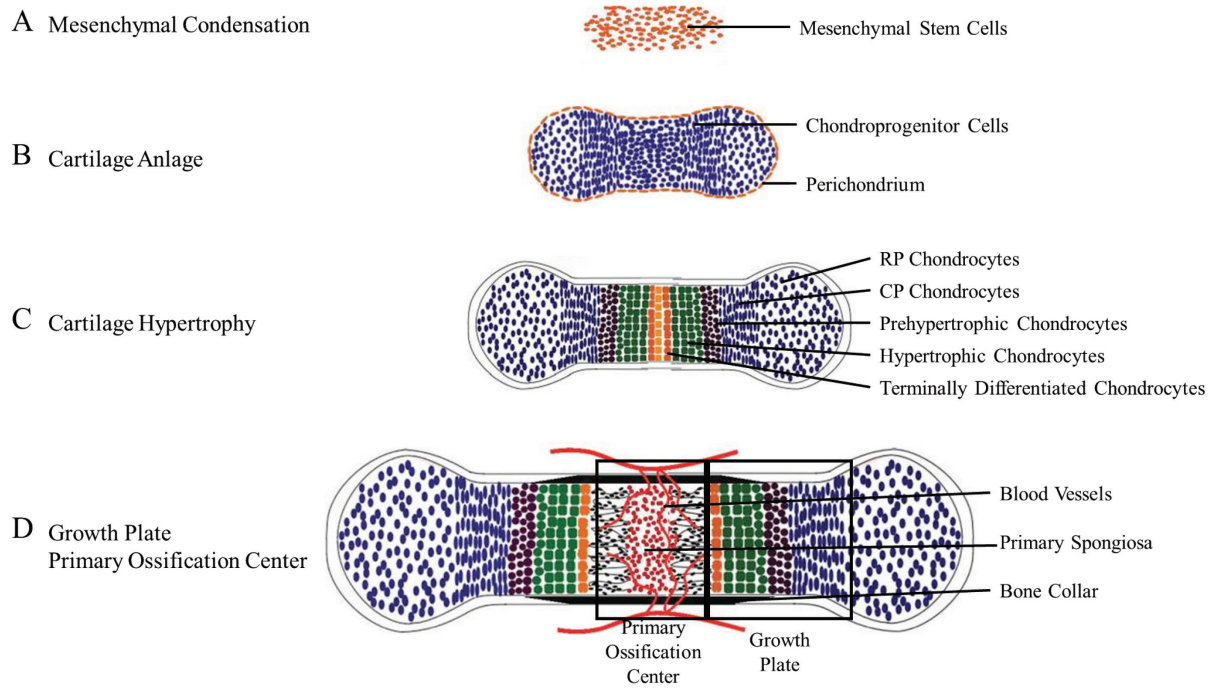


Figure 9: Endochondral ossification. Adapted from Long et al. [143].

(A) Mesenchymal stem cells condense and (B) differentiate into chondroprogenitors that deposit type II collagen and aggrecan in their extracellular matrix forming the cartilage anlage of the bone. The cells at the border form the perichondrium. (C) Upon differentiation the chondrocytes form distinct subpopulations. Round proliferating (RP) chondrocytes are located at the distal ends whereas high proliferating chondrocytes form columns towards the center of the developing bone (columnar proliferating (CP) chondrocytes). These cells exit the cell cycle and become prehypertrophic and hypertrophic chondrocytes that mineralize their surrounding matrix and finally develop into terminally differentiated chondrocytes. (D) Blood vessels together with osteoblasts and osteoclasts invade the hypertrophic cartilage and form a primary ossification center surrounded by a bone collar. The cartilage at the ends of the primary ossification center forms the growth plate that is essential for longitudinal bone growth.

3.2.3.2. Chondrogenic growth and transcription factors

Many growth factors and transcription factors are involved in regulation of chondrogenesis, chondrocyte hypertrophy and endochondral ossification during embryonic development. In tissue engineering for cartilage regeneration, they can either be used to induce *in vitro* chondrogenesis, or serve as markers for successful chondrogenic differentiation.

3.2.3.2.1. Chondrogenic growth factors

Growth factors are extracellular proteins or peptides that bind to cell surface receptors activating downstream signal cascades that stimulate proliferation or differentiation of the cell.

Development of cartilage is orchestrated by a complex signaling network including fibroblast growth factors (FGFs), insulin-like growth factors (IGFs), members of the wingless family (Wnt), indian hedgehog (Ihh) as well as bone morphogenetic proteins (BMPs) and transforming growth factors (TGF β) [143, 147]. Especially BMPs and TGF β s have great potential at inducing in vitro chondrogenic differentiation of mesenchymal stem cells (MSCs) and pluripotent stem cells (PSCs) [115].

3.2.3.2.1.1. Transforming growth factor β

The transforming growth factor β superfamily consists of bone morphogenetic proteins (BMPs), transforming growth factors β (TGF β) and other proteins like growth and differentiation factors (GDFs), activins, inhibins and Mullerian inhibitory factor (MIF) [148, 149]. TGF β signaling regulates cell proliferation, differentiation and death, and plays important roles in skeletal development and regeneration [149, 150].

TGF β receptors (TGFBR) are transmembrane serine/threonine kinases [148, 150]. There are two types of TGF β receptors, TGFBR-type I and TGFBR-type II, each with several subtypes [147, 148]. Upon ligand binding, a heterotetramer, consisting of two TGFBR-type I and two TGFBR-type II subunits, is formed. The TGFBR-type II subunit now phosphorylates and activates the TGFBR-type I subunit [147, 150]. The TGFBR-type I subunit in turn phosphorylates and activates the receptor-regulated Smads (R-SMADs) 2 and 3, which form a heterotrimer with the common-mediator Smad (CoSMAD) 4 [147, 149]. This complex translocates into the nucleus where it – by interaction with other transcription factors, co-activators and co-repressors – regulates TGF β induced changes in gene expression (Figure 10) [147, 148].

TGF β signaling is also mediated by Smad-independent pathways [148]. TGF β signaling activates mitogen activated protein kinases (MAPKs) including extracellular signal regulated kinases (Erk), C-Jun-N-terminal kinases (JNK) and p38/MAPK [148, 149, 151]. Interactions

between Smads and MAPKs generate a complex network of intracellular signals leading to cell type and developmental stage specific cellular responses to TGF β signaling [148, 149]. Many other signaling pathways, including the phosphatidylinositol-3-kinase (PI3K)/Akt-pathway, Rho-like-GTPases and proteinphosphatase2A (PP2A) have also been shown to interact with TGF β signaling [148, 149].

TGF β 1 is one of the key transcription factors in cartilage and bone formation, and is required for the formation of articular cartilage [147]. Furthermore, during joint development TGF β 1 signaling plays a significant role in the control of chondrocyte hypertrophy and prevents premature degeneration of articular cartilage [147]. TGF β 1 is therefore commonly used to induce chondrogenic differentiation of mesenchymal stem cells (MSCs) [152-154], and pluripotent stem cells (PSCs) [126, 127] in vitro.

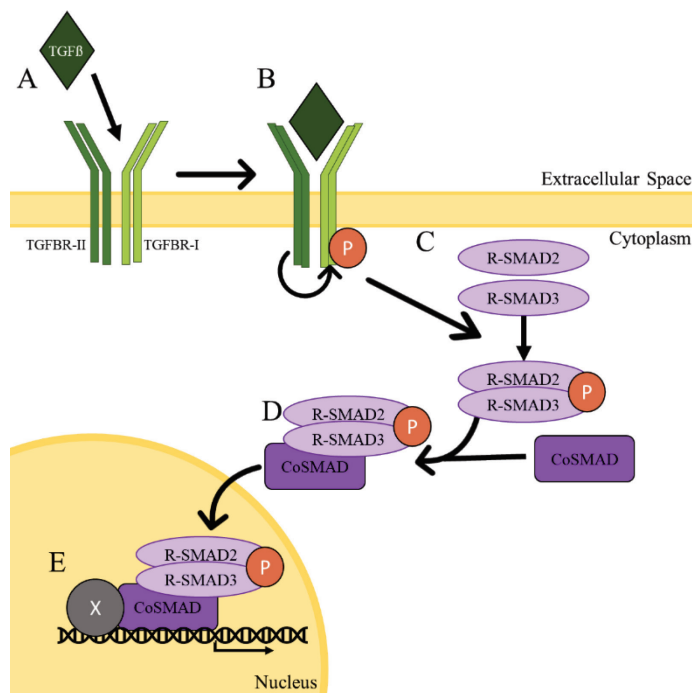


Figure 10: TGF β signaling pathway.
Adapted from *Derynck et al.* [148].

(A) TGF β binds its receptor that is composed of a heterotetramer of two TGFBR-type I and two TGFBR-type II molecules. (B) TGFBR-II phosphorylates and activates TGFBR-I. (C) The active receptor complex phosphorylates and activates R-SMADs 2 and 3. (D) Active R-SMADs 2 and 3 form a complex with the CoSMAD4. (E) This SMAD complex translocates into the nucleus and modulates gene expression of target genes together with other transcription factors.

3.2.3.2.1.2. Bone morphogenetic protein

Bone morphogenetic proteins (BMP) belong to the transforming growth factor β (TGF β) superfamily of growth factors [143]. At least 20 BMP family members have been identified and characterized [155]. BMPs play a crucial role in chondrogenesis, chondrocyte hypertrophy and endochondral ossification but are also involved in non-osteogenic developmental processes including neural development [155, 156].

BMPs bind to cell surface receptors that act as serine/threonine kinases [151, 155]. These receptors are composed of BMP receptor type I (BMPR-I) and type II (BMPR-II) subunits [155]. BMPs bind primarily to BMPR-I, but heteromeric complexes of BMPR-I and BMPR-II subunits show higher affinity to the ligands [148]. Ligand binding induces autophosphorylation of the receptor starting an intracellular signaling cascade [143, 151]. The activated BMP receptor phosphorylates and activates the receptor-regulated Smads (R-SMADs) 1, 5 and 8 [143, 149]. These R-SMADs form a complex with the common-mediator Smad (CoSMAD) 4 that enters the nucleus and regulates gene expression (Figure 11) [143, 151].

BMP2 is one of the main chondrogenic growth factors [156]. It promotes MSCs condensation, chondrogenic differentiation and chondrocyte proliferation by inducing the expression of *Sox9* (*sex determining region of Y box 9*) [156, 157]. Therefore, BMP2 is widely used to induce and enhance chondrogenic differentiation of mesenchymal stem cells (MSCs) [156, 158] and pluripotent stem cells (PSCs) [159-161] in in vitro culture systems.

However, BMP2 also stimulates chondrocyte hypertrophy, osteogenic differentiation and endochondral ossification as it upregulates *Runx2* (*Runt-related transcription factor*) [156].

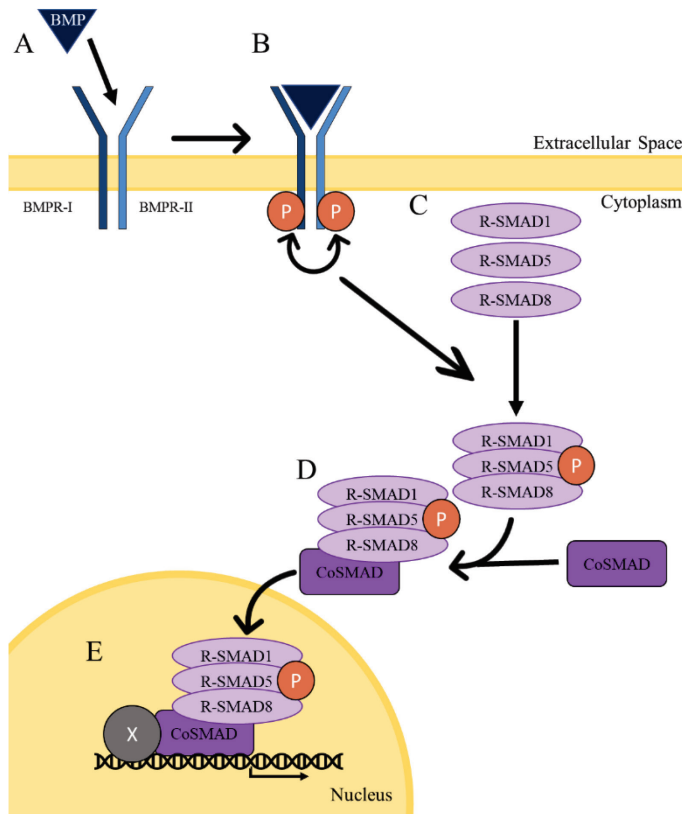


Figure 11: BMP signaling pathway.

Adapted from Derynck et al. [148].

(A) BMP binds its receptor that is composed of a type I (BMPR-I) and type II (BMPR-II) subunit. (B) The subunits autophosphorylate and activate themselves. (C) The active receptor complex phosphorylates and activates R-SMADs 1, 5 and 8. (D) Active R-SMADs 1, 5 and 8 form a complex with CoSMAD4. (E) This SMAD complex translocates into the nucleus and modulates gene expression of target genes together with other transcription factors.

3.2.3.2.2. Chondrogenic transcription factors

Transcription factors are intracellular proteins that bind genomic DNA and regulate transcription rate and expression of genes. Many transcription factors are involved in chondrogenesis and osteogenesis with Sox9 (Sex determining region of Y box 9) and Runx2 (Runt-related transcription factor) being the principal regulators, respectively [151].

3.2.3.2.2.1. Sox9

Sox9 belongs to the SRY family that is encoded by the sex determining region of the Y chromosome [162]. Sox9 is an essential transcription factor in chondrogenesis as it is critical during mesenchymal condensation and differentiation of mesenchymal stem cells into chondrocytes [163, 164]. Later in chondrogenesis, Sox9 inhibits chondrocyte maturation and prevents chondrocyte hypertrophy [163, 164].

Together with Sox5 and Sox6, Sox9 forms the so-called Sox-trio [162]. Sox9 induces the expression of *Sox5* and *Sox6* [164]. While Sox9 is required to activate gene expression of cartilage specific genes like *Col2a1* or *Acan*, Sox5 and Sox6 increase the binding efficiency of Sox9 to cartilage-specific enhancers [162]. So in absence of Sox5 or Sox6, the expression of *Col2a1* and *Acan* is significantly reduced leading to severe impairment of chondrogenesis [162]. In *Sox9* knock-out mice, however, no chondrogenesis occurs at all [156, 163].

Furthermore, Sox9 prevents chondrocyte hypertrophy and osteogenic differentiation by repressing Runx2 expression and activity, and by inhibiting WNT/ β -catenin signaling [157, 162]

During in vitro chondrogenesis, Sox9 is one of the earliest markers indicating successful chondrogenic differentiation [156]. Upregulation of *Sox9* gene expression is therefore commonly assessed during in vitro chondrogenesis of MSCs [130, 156] and PSCs [126, 127, 162].

3.2.3.2.2.2. Runx2

Runx2 belongs to the Runx family (Runt-related transcription factor) of transcription factors, and is one of the key transcription factors during osteoblast differentiation and bone formation [164, 165]. Furthermore, Runx2 is expressed in prehypertrophic and hypertrophic chondrocytes, and induces chondrocyte hypertrophy at the later stages of endochondral ossification [164, 165].

In vitro, Runx2 has been shown to mediate BMP2-induced osteogenic differentiation of MSCs [156, 157]. Runx2 upregulation during in vitro chondrogenesis, however, is considered as a marker of hypertrophic dedifferentiation [165].

3.2.4. Clinical relevance of articular cartilage

Articular cartilage is an avascular tissue in which nutrition is provided only by diffusion from the synovial fluid or the subchondral bone [117]. Furthermore, chondrocytes are embedded in a dense ECM that hampers their proliferation and migration [115, 116]. Cartilage lesions and degradation cause pain and immobility making efficient strategies for cartilage repair necessary.

3.2.4.1. Focal cartilage lesions and osteoarthritis

Focal cartilage lesions are often of traumatic origin [166]. Recent publications have stated that chondral lesions can be found during 57 - 66% of knee-arthroscopies [166, 167]. Furthermore, patients with focal chondral lesions report reduced quality of life to the same extent as patients with severe osteoarthritis scheduled for total joint replacement [168]. Partial thickness lesions do not reach the subchondral bone, so that the defect area is inaccessible for blood or progenitor cells from the bone marrow [115, 116]. Despite an increase in proliferation and metabolic activity of nearby chondrocytes, these defects usually fail to be filled up and represent predilection sites for tissue degeneration [115, 116]. Full thickness lesions, however, reach through the complete articular cartilage layer and penetrate the subchondral bone. They are referred to as osteochondral lesions [115, 116]. These defects are filled up with a fibrin clot which is invaded by progenitor cells from the bone marrow [115, 116]. These cells differentiate into chondrocytes and over time fill the defect with fibrocartilage that is, however, more prone to degeneration than healthy articular cartilage [115, 116]. So, untreated focal cartilage lesions over time progress into osteoarthritis [169].

Osteoarthritis is the most common form of arthritis and leading cause of mobility disability in the world resulting in a large socioeconomic burden [170, 171]. Osteoarthritis is a complex, multifactorial disease that finally leads to irreversible degradation and loss of articular cartilage causing pain, joint stiffness, crepitus, effusion and restricted range of motion [119, 172]. These symptoms together with the typical radiological changes (narrowing of the joint space width, osteophyte formation, development of subchondral sclerosis and cysts) allow the clinical diagnosis of osteoarthritis (Figure 12) [171]. Age, obesity, female gender and genetic predisposition along with traumatic joint lesions and congenital abnormalities like hip dysplasia

or limb malalignment have been described as the main risk factors for developing osteoarthritis in human [170, 171].

Recent research has led to a better understanding of the pathogenesis of osteoarthritis. Activation of chondrocytes, subchondral osteoblasts and synoviocytes by proinflammatory and mechanical stimuli provokes an inflammatory response. The cells release cytokines like interleukin 6 (IL-6) and tumor necrosis factor α (TNF α) that maintain the inflammatory response. Furthermore, the ECM is destroyed by matrix degrading enzymes. Metalloproteases (mostly MMP-1, MMP-3, MMP-13) degrade the collagen II-backbone of the ECM, whereas ADAMTS-4 and ADAMTS-5 (a disintegrin and metalloproteinase with thrombospondin-like motifs) mediate aggrecan degradation [170, 171].

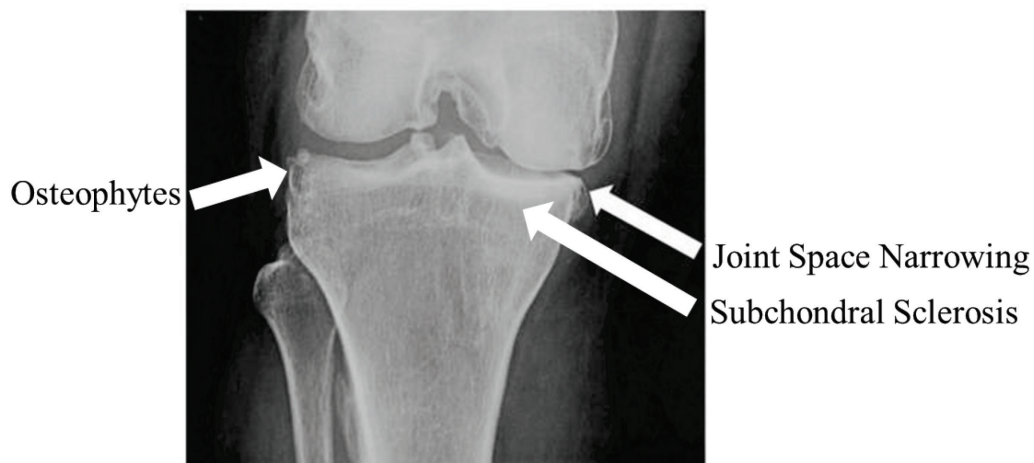


Figure 12: X-Ray Image of an osteoarthritic knee joint. Modified from Braun et al. [173].

Some of the typical radiological signs of osteoarthritis, namely osteophyte formation, joint space narrowing and subchondral sclerosis are clearly visible.

3.2.4.2. Current treatment options

Despite the increasing knowledge of the pathomechanisms of osteoarthritis and advances in MRI technology allowing detection of early osteoarthritic changes, no targeted treatment for early osteoarthritis is available yet [170, 171]. Current treatment options can be divided in conservative and surgical methods. Conservative management includes reduction of risk factors, physiotherapy and symptomatic treatment with pain killers and non-steroidal anti-

inflammatory drugs [119, 171]. Surgical correction of predisposing conditions like hip dysplasia or limb malalignment by osteotomies can delay or prevent the onset of osteoarthritis effectively [174]. The definite treatment for end stage osteoarthritis remains joint replacement by endoprostheses [174].

There is broad consent, that – especially in younger patients – focal cartilage lesions should be treated to delay onset of osteoarthritis and need for joint replacement [175, 176]. Treatment options for focal chondral lesions can be divided into palliative (lavage, debridement), restorative (microfracture) and reparative (osteochondral allograft transfer (OAT) and autologous chondrocyte injection (ACI)) methods [119, 177].

3.2.4.2.1. Total joint replacement and endoprostheses

Total joint replacement with endoprostheses is the maximal invasive definitive treatment for end stage osteoarthritis, severe joint injuries or after tumor resections [115, 174]. The damaged joint is resected and replaced by an artificial implant typically composed of a combination of metal, polyethylene or ceramic (Figure 13) [115, 178]. Due to the increasing incidence of osteoarthritis the number of joint replacement surgeries steadily increases [179].



Figure 13: Total joint replacement of the knee with an endoprosthesis. From *de l'Escalopier et al.* [174]

3.2.4.2.2. Microfracture and autologous matrix-induced chondrogenesis

The microfracture technique was first introduced by *Steadman et al* in the 1990s [180]. Following arthroscopic debridement of the cartilage lesion small holes are made in the subchondral bone. Blood and fat emerging from the bone marrow form a clot rich in bone marrow mesenchymal stem cells (BM-MSCs) that over time differentiate into chondrocytes (Figure 14) [181, 182]. Histological examination revealed that microfracture often leads to biomechanically inferior fibrocartilage [183]. Although most patients initially report clinical improvement, deterioration often occurs after two to four years [181, 183, 184].

Being a minimally invasive, single stage procedure with minimal morbidity [181, 185], microfracture is still the gold standard for treatment of small cartilage defects (< 2cm²) [186].

Recently, application of a collagen I/III-membrane (*Chondro-Gide*®, Geistlich Pharma AG, Wolhusen, Switzerland) to stabilize the clot formed by microfracture was described as autologous matrix-induced chondrogenesis (AMIC) [187]. Although clinical and functional improvement remained stable over more than five years [188, 189], histological examination revealed mostly fibrocartilaginous repair tissue [189].

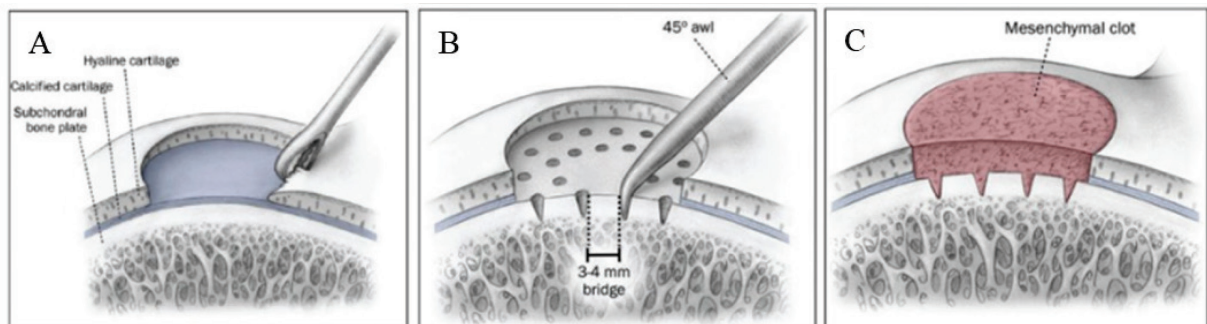


Figure 14: Microfracture. Modified from Mithoefer et al. [190].

(A) Initial debridement of the cartilage lesion to create a stable cartilage margin. (B) Generation of small holes in the exposed subchondral bone with an awl. (C) Blood and fat emerging from the subchondral bone marrow form an clot rich in mesenchymal stem cells that fills the lesion.

3.2.4.2.3. Osteochondral autograft transfer and osteochondral allograft transplantation

Osteochondral autograft transfer (OAT) is a single stage procedure that immediately fills cartilage defects with mature, hyaline cartilage [191, 192]. The use of a single large autograft, like *e.g.* the lateral patellar facet, results in a considerable donor site defect. This likely causes donor site morbidity and surface incongruity at the recipient site, that permanently alters the biomechanics of the joint and might increase risk of developing osteoarthritis in the long term [115, 191, 193]. These limitations can be overcome by mosaic-like transplantation of multiple small grafts, therefore this technique is also referred to as mosaicplasty [193]. These osteochondral cylinders are harvested from a low weight bearing area of the joint – *e.g.* the medial and lateral femoral condyle periphery – reducing donor site morbidity [194, 195]. Perpendicular insertion of multiple small grafts permits progressive contouring of the surface leading to a more congruent resurfaced area (Figure 15) [196].

OAT leads to significant clinical improvement that is stable also in long term follow up [167, 196]. Histological analysis revealed good survival of the transplanted hyaline cartilage and good integration of the cylinders, whereas the donor sites were filled with fibrocartilage [194]. But, OAT is limited to defects smaller than 4 cm² due to limited availability of donor sites [193].

As a salvage procedure for larger defects, MEGA-OAT – *i.e.* transfer of the posterior femoral condyle – might be considered [175, 197]. Osteochondral allograft transplantation (OCAT) of cartilage and subchondral bone cylinders harvested from post-mortal donors is another salvage option for large chondral and osteochondral defects [198]. Although the clinical results are good to excellent, limited availability of allografts and storage facilities along with the risk of immune rejection and infectious disease transmission hamper wide spread clinical use of this approach [115, 198].

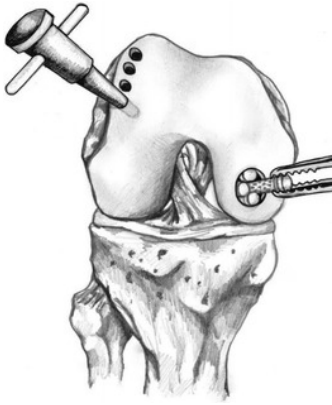


Figure 15: Osteochondral autograft transfer (OAT). From *Winthrop et al.* [199].

Small osteochondral cylinders are harvested from a non-weight bearing area of the joint and transplanted in a mosaic-like fashion into the defect area. Therefore, this technique is also referred to as mosaicplasty.

3.2.4.2.4. Autologous chondrocyte injection

Autologous Chondrocyte Injection (ACI) as the first cell-based cartilage repair technique was described by *Brittberg et al* in 1994 [200]. Shortly, in a first surgery cartilage is harvested from a non-weightbearing area of the joint and subjected to enzymatic digestion to release the chondrocytes. Since cartilage consists mostly of ECM, the number of isolated chondrocytes usually is too small to fill up the defect immediately [115, 172]. Therefore in vitro expansion is necessary before the isolated chondrocytes are inserted into the defect during a second surgery (Figure 16) [200].

However, during expansion in monolayer culture dedifferentiation of chondrocytes occurs, and injection of these dedifferentiated cells leads to formation of fibrocartilage [201, 202]. Initially, the in vitro expanded chondrocytes were injected either under a periosteal flap or under synthetic membranes consisting of collagen I/III (*Bio-Gide*® from Geistlich Biomaterials, Wolhusen, Switzerland) [200, 203]. These membranes evolved into nowadays used matrix assisted ACI (MACI) [176]. Here, chondrocytes are cultured in hydrogels like *CaReS*® from ArthroKinetics, Esslingen, Germany [204] or *BioSeed-C*® from BioTissue, Zürich, Switzerland [205] which prevent chondrocyte dedifferentiation and provide easier surgical handling [186, 205].

ACI is indicated for full-thickness osteochondral defects with a size of 2 cm² up to 12 cm² [177, 186], or in patients where microfracture has failed [115, 177]. Currently reported results show

significant improvements in clinical scores and better outcomes compared to microfracture or mosaicplasty [177, 186]. However, ACI still remains an invasive procedure. Harvesting of healthy cartilage can cause not only pain but also degeneration at the harvesting site (donor-site morbidity) [16]. Furthermore, traditional ACI requires at least two surgeries and a long recovering period [115, 177]. Therefore, single stage procedures using alternative cell sources like mesenchymal stem cells (MSCs) or pluripotent stem cells (PSCs) would be favorable [176, 206].

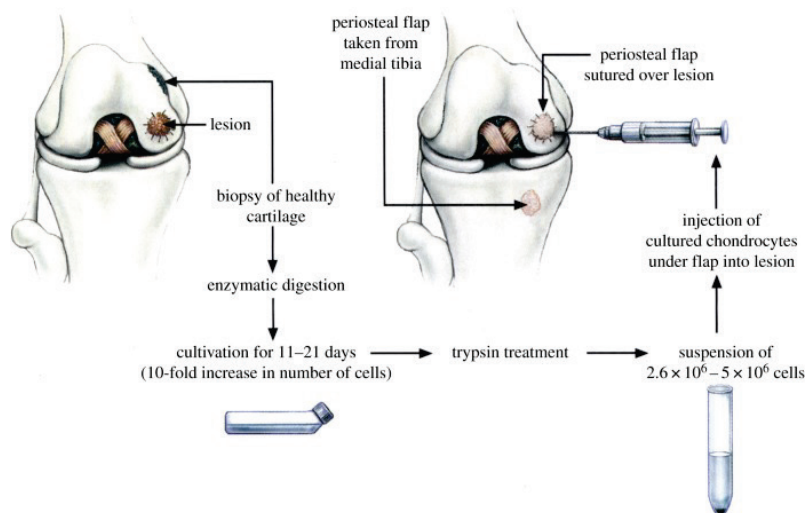


Figure 16: Autologous chondrocyte injection (ACI). From *Brittberg et al.* [200].

Biopsies of healthy cartilage are taken from non-weight bearing areas of the joint and chondrocytes are extracted and propagated in vitro before they are injected into the defect areal during a second surgery. Here the original protocol of *Brittberg et al.* using a periosteal flap to seal the lesion is depicted [200].

3.3. Stem cells for articular cartilage repair

3.3.1. Mesenchymal stem cells for cartilage repair

3.3.1.1. Mesenchymal stem cells

Mesenchymal stem cells (MSCs), also known as mesenchymal stromal cells, are adult, multipotent stem cells that can be found in various mesenchymal tissues and have multilineage differentiation potential [125, 130]. They were first described by *Friedenstein et al* as bone marrow derived cells capable of osteogenesis [207, 208].

According to the International Society for Cellular Therapy (ISCT) cells must fulfill the following three criteria to be classified as mesenchymal stem cells [209]:

1. *Cells must be plastic adherent, when maintained in standard culture conditions.*
2. *Cells must show a specific antigen expression pattern in flow cytometry.*
3. *Cells must have the capacity of trilineage mesenchymal differentiation, thus differentiating to osteoblasts, adipocytes and chondroblasts in standard in vitro conditions.*

MSCs have been successfully isolated from various tissues including bone marrow, adipose tissue, synovial membrane, periosteum, trabecular bone, skeletal muscle, dermis, peripheral blood, umbilical cord blood, umbilical cord stroma and placenta [172, 206, 207]. However, bone marrow derived MSCs (BM-MSCs) and adipose tissue derived stem cells (ADSCs) are the most commonly used sources of MSCs in cartilage tissue engineering [115, 119, 206].

3.3.1.2. Chondrogenic differentiation of MSCs

Induction of chondrogenesis in MSCs requires high cell density mimicking the condensation step of cartilage formation during embryonic development [115, 133, 172]. The standard culture condition for chondrogenic differentiation of MSCs is a high-density pellet culture achieved by centrifugation of cells in a tube with a conical shaped bottom [124]. However, many other culture systems including high-density micromass, scaffold-free and scaffold-based systems have been successfully used for chondrogenic differentiation of MSCs [130, 133, 210]. Furthermore, supplementation of growth factors from the bone morphogenetic protein family,

mostly BMP2 and BMP6, from the transforming growth factor family, mostly TGF β 1 and TGF β 3, or of fibroblast growth factor (FGF2) in different combinations and concentrations is known to enhance chondrogenesis [115]. As different types of MSCs vary in their responsiveness to each growth factor, the optimal combination of growth factors must be amended for each MSC-type [133].

3.3.1.3. Clinical application of MSCs for cartilage regeneration

Their ability to differentiate into cartilaginous tissue makes MSCs an interesting cell source for treatment of osteoarthritis and focal cartilage lesions. Injection of autologous bone marrow-derived MSCs (BM-MSCs) into cartilage defects has resulted in significant clinical improvement comparable to injection of autologous chondrocytes [211]. In contrast to autologous chondrocytes, harvesting of BM-MSCs is less invasive and does not require the destruction of healthy articular cartilage [211]. The use of allogeneic MSCs would further reduce the invasiveness of the harvesting procedure and heterogeneity of the cell population [212]. Due to their hypoimmunogenicity and immunomodulatory features together with the immune privileged character of articular cartilage, the risk of rejection is low [206, 212]. Recently, a first-in human trial has shown a durable clinical improvement as well as an acceptable safety profile after injection of allogeneic umbilical cord blood derived MSCs in osteoarthritic knees [212].

Despite their successful application in clinical trials, many challenges remain for MSCs in cartilage tissue engineering. These include *for example* their invasive harvesting, their propensity to form hypertrophic cartilage, and their age-related decline in *in vivo* frequency and *in vitro* proliferation potential [172, 213]. iPSCs could overcome these limitations and become a promising alternative to MSCs.

3.3.2. Induced pluripotent stem cells for cartilage repair

3.3.2.1. Applications of induced pluripotent stem cells in cartilage repair

As described in 3.1.5. *Applications of induced pluripotent stem cells*, patient-specific iPSCs can be used as disease models for genetic diseases. iPSCs have been successfully generated from patients suffering from various conditions affecting cartilage like *e.g.* familial osteochondritis dissecans [214] or osteoarthritis [215]. These patient-derived iPSCs could provide valuable tools to study the pathomechanisms of these diseases in iPSC-derived chondrocytes or cartilaginous tissues especially as primary chondrocytes require invasive harvesting and are difficult to culture in vitro [202, 216].

However, the most promising application of iPSCs is to use them as a source for autologous tissue grafts. Theoretically, it would be possible to generate iPSCs from a small skin biopsy or even a blood sample of a patient suffering from a symptomatic chondral lesion [19, 36, 37]. These iPSCs could be differentiated into chondrocytes or small cartilage particles in vitro, which could then be used to fill the chondral lesion [127].

Before iPSCs can be used in a clinical setting to treat cartilage lesions many challenges still need to be overcome. This includes, first of all, establishment of an efficient, safe and reliable differentiation protocol for iPSCs into cartilaginous tissue.

3.3.2.2. Chondrogenic differentiation of pluripotent stem cells

There are four main strategies for the differentiation of pluripotent stem cells (PSCs) into cartilaginous tissue (Figure 17): first, co-culture of PSCs with mature chondrocytes [134, 217, 218]; second, culture of PSCs under the influence of growth factors mimicking physiological chondrogenic development during embryogenesis [127, 135, 219]; third, two-step differentiation via MSC-like cells as an intermediate [220-222]; and finally, formation of embryoid bodies (EBs) allowing spontaneous differentiation of PSCs and subsequent selection of a chondrogenically primed subpopulation and its direction towards the chondrogenic lineage [126, 223, 224]. Although ESCs and iPSCs have both been differentiated successfully by all these methods their differentiation pathways are not exactly the same [225].

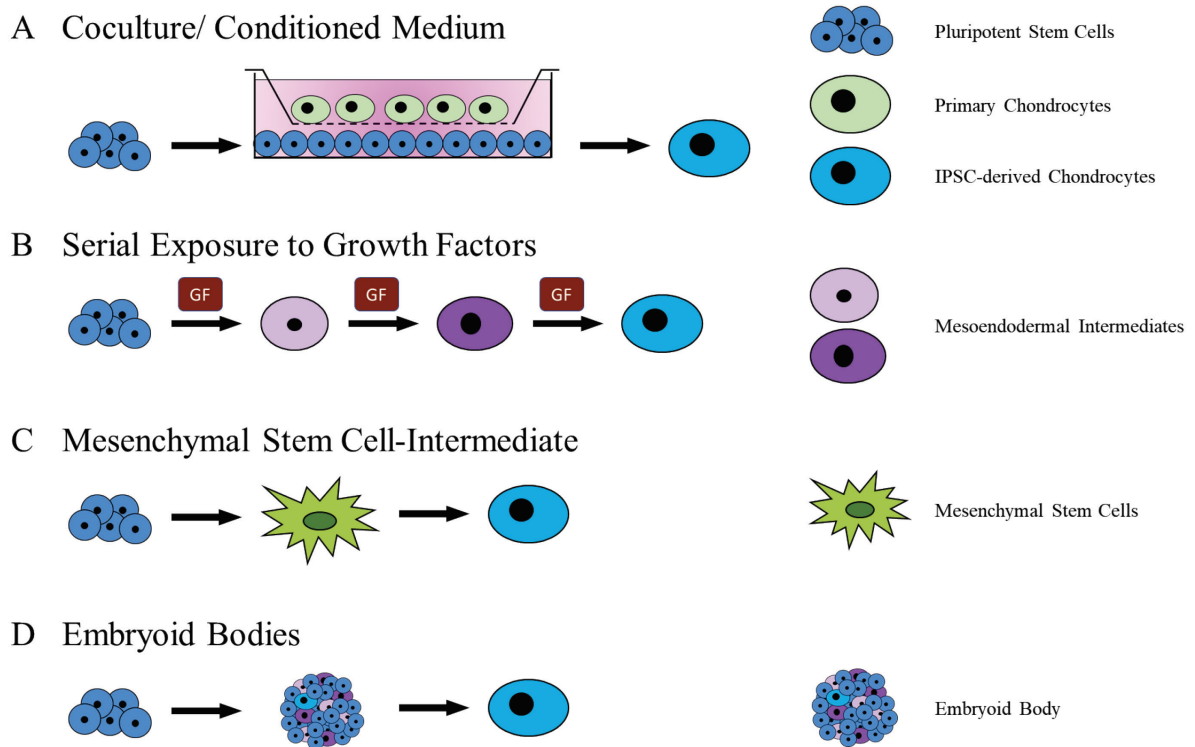


Figure 17: Methods for the chondrogenic differentiation of pluripotent stem cells. Adapted from *Driessen et al.* [225].

(A) Chondrogenic differentiation of PSCs can be achieved by co-culture with primary chondrocytes. (B) By serial exposure to a set of defined growth factors, PSCs can differentiate into chondrocytes via mesoendodermal intermediates. (C) In a two-step differentiation protocol PSCs are first differentiated into mesenchymal stem cells which then are subjected to standard chondrogenic differentiation protocols. (D) Isolation chondrogenically primed cells from spontaneous differentiation in embryoid bodies.

3.3.2.2.1. Chondrogenic differentiation of PSCs via co-culture and conditioned medium

It is possible to induce chondrogenesis of ESCs by culturing the cells together with articular chondrocytes in a direct co-culture system [217]. However, to avoid contamination of the final product with mature chondrocytes, a separation step is necessary [217]. Despite lack of direct cell-cell interactions indirect co-culture using transwell inserts covered with bovine chondrocytes is sufficient driving ESCs and iPSCs towards the chondrogenic lineage [134, 218]. Successful chondrogenic differentiation can furthermore be achieved by exposure of iPSCs towards a medium conditioned by mature chondrocytes, therefore omitting the need of complex co-culture systems completely [162, 165]. Here growth factors and cytokines secreted by mature chondrocytes are driving PSCs towards the chondrogenic lineage. This might even be more effective at inducing chondrogenesis than supplementing the culture medium with

single growth factors [162, 165]. However, batch to batch variation of primary chondrocytes and the need for either human chondrocytes which require invasive harvesting or the use of xenogeneic material like bovine chondrocytes hamper the clinical applicability of these methods [134, 172, 217].

3.3.2.2.2. Chondrogenic differentiation of PSCs via sequential exposure to growth factors

As described in 3.2.3. *Articular cartilage development*, cartilage tissue originates from primitive streak mesendoderm via a paraxial mesoderm intermediate state [146]. During embryonic development chondrogenesis is achieved through the direction of different growth factors including members of the bone morphogenetic protein (BMP), transforming growth factor β (TGF β) and wingless (Wnt) families [143, 147].

By exposing monolayer cultures of ESCs or iPSCs to sequential combinations of growth factors at defined concentrations for each time point, stepwise chondrogenic differentiation via mesoendodermal and mesodermal intermediates can be achieved by mimicking physiological embryonic development [135, 219]. The PSC-derived chondrocytes form tissue grafts that can be implanted into osteochondral defects in in-vivo mouse models [135].

When intact iPSC-colonies were cultured under the influence of defined combinations of growth factors, inducing first mesoendodermal pre-differentiation then chondrogenic differentiation of the cells, the colonies condensed to chondrogenic nodules that could be maintained in suspension culture [127]. These nodules resembled chondrogenic pellets and improved cartilage repair when implanted into osteochondral defects in rats and mini-pigs [127].

Taken together, exposure of PSCs to growth factors is effective at inducing chondrogenic differentiation. However, formation of teratomas, likely originating from remaining undifferentiated cells, was reported after implantation of PSC-chondrocyte derived grafts into in vivo osteochondral defect models [135]. Therefore, a separation step to prevent the contamination of the final product with an undifferentiated cell population would be favorable to increase the safety profile of the PSC-derived chondrocytes before their use in patients is considered.

3.3.2.2.3. Chondrogenic differentiation in a two-step protocol via MSC-like cells

As described in 3.3.1.2. *Chondrogenic differentiation of MSCs*, mesenchymal stem cells can be easily differentiated into cartilaginous tissue. But since MSCs suffer from the need of invasive harvesting procedures providing only limited cell numbers as well as age and donor related variations in their chondrogenic differentiation potential, iPSC-derived MSCs would be an attractive alternative to primary MSCs [225].

MSC-like cells can be derived from iPSCs via repeated passaging of iPSCs in MSC-medium on polystyrene dishes by selecting a rapidly cycling, plastic adherent cell population [222, 226]. Successful differentiation can be confirmed by fluorescence activated cell sorting (FACS) for MSC-markers as well as standard osteogenic, adipogenic and chondrogenic differentiation protocols [222, 226]. Chondrogenic differentiation of these iPSC-derived MSC-like cells can be achieved in standard culture systems like micromass or pellet culture [221, 227]. No teratomas were observed and improved cartilage repair was reported after implantation of those pellets into osteochondral defects in rat knee joints [227].

Recently, neural crest cells (NCCs), which during embryonic development give rise to many cranial tissues including bone and cartilage, have been described as a suitable intermediate to differentiate iPSCs towards MSCs [228]. These iPSC-derived MSCs readily differentiate into chondrocytes in a standard pellet culture system [220].

In summary, performing chondrogenic differentiation of iPSCs via an MSC-intermediate as a two-step approach is effective and might provide an attractive alternative to primary MSCs. Nevertheless, the need for an extensive cell culture period and repeated passaging might hamper clinical applicability [222, 226].

3.3.2.2.4. Chondrogenic differentiation via embryoid bodies

When subjected to suspension culture without supplements that prevent differentiation, pluripotent stem cells form spherical cell aggregates called embryoid bodies (EBs) and start to differentiate into various cell types [229].

By allowing EBs to adhere to gelatin coated plates and culturing the outgrowing cells in chondrogenic medium supplemented with chondrogenic growth factors like BMP2 and TGF β 1, cells that are primed for chondrogenesis, *i.e.* cells that spontaneously differentiated towards the mesodermal lineage, start to proliferate and differentiate into chondrocytes [126, 160].

In order to form an implantable graft, it is possible to use intermediate cells from the outgrowth or directly from dissociated EBs to produce chondrogenic pellets [230, 231].

As a variation of the two-step approach described in 3.3.2.2.3. *Chondrogenic differentiation in a two-step protocol via MSC-like cells*, MSC-like cells can also be derived from EBs. By exposing intact EBs or EB-outgrow cultures to defined media, an MSC-like population can be selected and expanded [213, 224]. Standard micromass and pellet culture systems allow chondrogenic differentiation of this cell population [224].

Taken together, a chondrogenically primed cell population emerged spontaneously in embryoid bodies can be selected and expanded under prechondrogenic culture conditions. Chondrogenic differentiation can be achieved by disrupting the EBs or their outgrowth into a single cell suspension, and subjecting the collected cells to standard chondrogenic protocols like micromass or pellet culture.

Chondrogenic differentiation of EBs formed in microcavities of a hydrogel can also be achieved by exposing the intact EBs to a series of different growth factors inducing chondrogenic differentiation via mesodermal intermediates similar to the protocols described in 3.3.2.2.2. *Chondrogenic differentiation of PSCs via sequential exposure to growth factors* [219, 223]. Finally, the hydrogel matrix can be removed completely leading to a scaffold-free implantable chondrogenic graft [223].

So, suggesting that disruption of EBs into a single cell suspension is not necessary for inducing chondrogenesis, maintenance of intact EBs under chondrogenic conditions could be a simple one-step method for chondrogenic differentiation of PSCs.

4. **Aims and milestones of the thesis**

Due to their unlimited proliferation and differentiation potential as well as their somatic origin overcoming ethical issues associated with ESCs and NT-SCs, iPSCs offer promising possibilities for the future of tissue engineering and regenerative medicine. Especially for cartilage regeneration, where currently available methods are either highly invasive or lead to insufficient repair tissue, iPSCs could provide an attractive alternative cell source for autologous and allogenic tissue grafts. However, there is still a lack of efficient and scalable chondrogenic differentiation protocols hampering clinical application of iPSCs.

The aim of this thesis was therefore, first to find a reliable reprogramming protocol for primary murine fibroblasts using the Sleeping Beauty reprogramming system, and to establish an assessment panel for the generated iPSCs. Secondly, we aimed at finding an efficient and reliable protocol for the chondrogenic differentiation of these iPSCs.

The following milestones were achieved in this thesis

1. Successful reprogramming of primary murine embryonic fibroblasts, primary murine ear fibroblasts and primary murine tail fibroblasts to iPSCs using a Sleeping Beauty transposon-based reprogramming system, and establishment of more than 250 clonal IPS cell lines.
2. Assessment of 22 IPS cell lines for successful induction of pluripotency by morphology, alkaline phosphatase staining, expression of pluripotency markers on mRNA and protein level as well as for three-lineage differentiation potential in spontaneously formed embryoid bodies.
3. Establishment of a Splinkerette PCR protocol to determine the number of genomically integrated transposon copies, and identification of two single integration clones (ETA04 and ETAC41) for subsequent chondrogenic differentiation.
4. Successful establishment of an efficient and reliable chondrogenic differentiation protocol for the generated iPSCs by free floating culture of spontaneously formed embryoid bodies under chondrogenic conditions.

5. Materials and Methods

5.1. Sleeping Beauty transposon based reprogramming system

5.1.1. Structure of plasmid vectors

The Sleeping Beauty transposon reprogramming system consists of two plasmids (Figure 18) [56]. The *pCMV(CAT)T7-SB100X (SB100X)* plasmid contains the cDNA of the hyperactive *SB100X* transposase under the control of a continuously active CMV (cytomegalovirus) promoter [58]. Once expressed in the target cell, the SB100X transposase enzyme catalyzes excision and integration of the sleeping beauty transposon.

In this study we used four different transposon plasmids.

The *pT2OSKM* and *pT2OSKML* plasmids contain the reprogramming factor cassette and a *Puro Δ TK*-selection marker flanked by the SB transposon TIRs, the binding sites for the SB100X transposase [53, 232]. The cDNAs of the reprogramming factors *Oct3/4*, *Sox2*, *Klf4* and *c-Myc* with or without *Lin28* (*pT2OSKM* and *pT2OSKML*) were cloned into a single polycistronic vector separated by self-cleaving 2A peptides allowing their expression for a single CAG promoter [233]. The *puro Δ TK*-selection marker allows for both positive and negative selection. Cells become resistant to puromycin by expressing the puromycin N-acetyltransferase (*puro*) and sensitive to 1-(2-deoxy-fluoro-1-beta-darabino-furanosyl)-5-iodouracil (FIAU) by expression of a truncated version of herpes simplex virus type 1 thymidine kinase (*DeltaTk*) [232].

The *RMCE-OSKM-Cherry* and *RMCE-OSKML-Cherry* plasmids contain – in addition to the corresponding pT2 plasmids – the *EOS(3+)mCherry* pluripotency reporting cassette which consists of the fluorescence reporter gene *mCherry* under the control of the EOS(3+) promoter-enhancer fragment (*ETn* (early transposon) *LTR* (long terminal repeat) coupled with a trimer of the Oct4 enhancer motif), as well as heterospecific *loxP* (*loxP* and *loxP257*) sites which would allow modification of the genomically integrated transposon by recombinase mediated cassette exchange (RMCE) [53].

All plasmids were kindly provided by Dr. Zoltán Ivics (Paul Ehrlich Institute, Federal Institute for Vaccines and Biomedicines, Langen, Germany) whose generosity we wish to acknowledge.

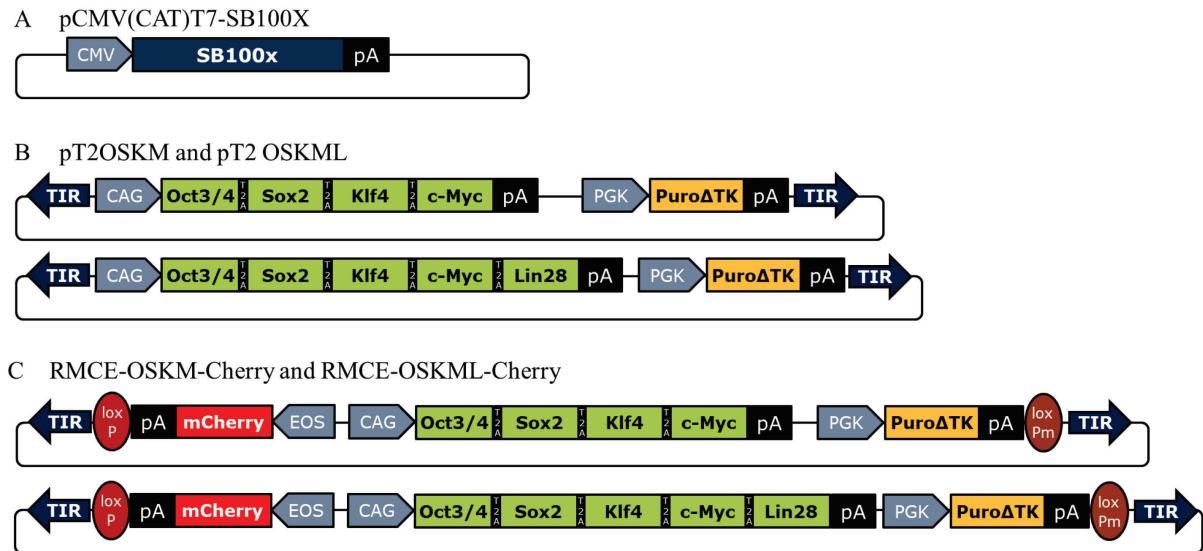


Figure 18: Plasmids of the Sleeping Beauty reprogramming system. Modified from Grabundjiza et al. [53].

(A) The *pCMV(CAT)T7-SB100X* plasmid contains the cDNA of the *SB100X* transposase under the control of a CMV promoter. (B) The *pT2OSKM* and *pT2OSKML* plasmids contain the cDNAs of the reprogramming factors *Oct3/4*, *Sox2*, *Klf4*, *c-Myc* and *Lin28* in a polycistronic expression cassette separated by self-cleaving 2A-peptide sequences under the control of a CAG promoter, and a *puroΔTK* sequence allowing both positive and negative selection. These sequences are flanked by the Sleeping Beauty transposon TIRs. (C) The *RMCE-OSKM-Cherry* and *RMCE-OSKML-Cherry* plasmids additionally contain a *mCherry* gene under the control of the EOS(3+) promoter-enhancer motif. Furthermore, there are heterospecific *loxP* sites (*loxP* and *loxP257*) flanking the transgenes allowing later modification of the genomically integrated transgene by recombinase mediated cassette exchange (RMCE).

pA: polyadenylation signal, TIR: terminal inverted repeats, T2A: self-cleaving 2A peptide, EOS: ETn (early transposon) LTR (long terminal repeat) coupled with a trimer of the Oct4 enhancer motif

5.1.2. Plasmid transformation in competent bacteria and plasmid DNA isolation by MaxiPrep

Prior to their delivery into cells, the provided plasmids were propagated in chemically competent *Escherichia coli* (*E. Coli*, BL21(DE3)) (Invitrogen), and were isolated by the plasmid MaxiPrep kit (Qiagen, Hilden, Germany).

Briefly, bacteria were thawed on ice before approximately 2μg of plasmid-DNA were added, followed by 30 min incubation on ice. Transformation was achieved by a heat shock for 60 sec at 42°. After a 2 min relaxation on ice, bacteria were incubated in SOC medium (Invitrogen) at 37°C with continuous shaking (225 rpm) for 1h. To select transformed clones 50 μl of transformed bacteria solution were plated on LB agar plates consisting of 1% Tryptone, 0,5% Yeast Extract, 1% NaCl, and 1,5% Agar (all Becton Dickinson, Franklin Lakes, New Jersey,

USA) in dH₂O, pH 7.0 supplemented either with 100 µg/ml ampicillin (Carl Roth, Karlsruhe, Germany) for the *pT2OSKM*, *pT2OSKML*, *RMCE-OSKM-Cherry* and *RMCE-OSKML-Cherry* plasmids, or 150 µg/ml chloramphenicol (Sigma-Aldrich) for the *pCMV(CAT)T7-SB100x* plasmid, and cultured overnight at 37°C. The next day single colonies were picked and transferred to 100 ml liquid LB medium supplemented with 100 µg/ml ampicillin or 150 µg/ml chloramphenicol, and cultured overnight at 37°C with continuous shaking at 280 rpm.

Plasmid DNA was extracted with the Qiagen Plasmid Maxi Kit (Qiagen) following the manufacturer's instruction. Shortly, bacteria were pelleted by centrifugation with 6000 g for 10 min at 4°C. Then bacteria were lysed, and DNA was precipitated by the provided buffers. Plasmid DNA was purified by centrifugation and filtration through Qiagen Tips and eluted in a 50 ml Falcon tube (Sarstedt, Nümbrecht, Germany). Finally, plasmid DNA was precipitated by isopropanol (Merck), washed with 70% ethanol (Merck) and resuspended in the provided Tris-EDTA (TE) buffer (Qiagen). DNA concentration and purity were determined spectrometrically at A₂₆₀ and A_{260/280}, respectively, using a Nanodrop 2000 spectrophotometer (ThermoFisher Scientific).

5.2. Cell culture

5.2.1. Standard cell culture conditions and procedures

All cells were cultured at 37° C and 5% CO₂ in a humidified incubator (Hera cell 240, ThermoFisher Scientific). For the in vitro experiments T-25, T-75 and T-225 cell culture flasks (Nunc, ThermoFisher Scientific), 6-well, 24-well and 48-well cell culture plates (Nunc, ThermoFisher Scientific), 96-V-bottom non-treated microplates (Costar, Corning, New York, USA), and 6 cm- and 10 cm-cell culture as well as 6 cm- and 10 cm-Petri dishes (Costar, Corning, New York, USA) were used. All cell-based experiments were carried out under sterile conditions in a laminar flow hood.

5.2.1.1. Culturing primary fibroblasts

Primary murine fibroblasts (Mouse embryonic fibroblasts, MEFs; and adult fibroblasts, FBs) were cultured in monolayer in mouse embryonic feeder (EF) medium consisting of Dulbecco's Modified Eagle's medium (DMEM, Invitrogen) supplemented with 10% Fetal Bovine Serum (FBS, Invitrogen) and 1% Penicillin-Streptomycin (Invitrogen) (Table 1). Medium was changed twice a week unless otherwise indicated.

Table 1: Mouse EF medium

Supplement	Concentration	Volume	Distributor
Dulbecco's Modified Eagle's medium (DMEM) <i>modified with high glucose, sodium pyruvate, GlutaMAXTM and phenol red</i>	90%	500 ml	Invitrogen
Fetal Bovine Serum (FBS)	10%	50 ml	Invitrogen
Penicillin-Streptomycin (5000 U/ml)	1%	5 ml	Invitrogen

5.2.1.2. Culturing mouse ESCs and mouse iPSCs

Pluripotent stem cells require specific culture conditions. Mouse ESCs (mESCs) and mouse iPSCs (mIPSCs) during and after successful reprogramming were maintained in mouse IPSC medium consisting of DMEM (Invitrogen), 20% FBS (Invitrogen) and 1% Penicillin-Streptomycin (Invitrogen) supplemented with 1% non-essential amino acids (Invitrogen), 25 µg/ml L-ascorbic acid (Sigma-Aldrich) and 0.1 mM β-mercaptoethanol (Sigma-Aldrich) (Table 2). Furthermore, Leukemia Inhibitory Factor (LIF, generously provided by Markus Moser, Max Plank Institute for Biochemistry, Martinsried, Germany) was added to prevent uncontrolled differentiation of the pluripotent stem cells [234]. Medium was changed every second day unless otherwise indicated.

Furthermore, mESCs and mIPSCs were cultured either on feeder cells or on Geltrex (ThermoFisher Scientific)-coated plates or flasks. Feeder cells are mitotically inactivated MEFs generated by exposure to Mitomycin C (Sigma-Aldrich) as described in 5.2.2.3. *Preparation of mitotically inactivated feeder cells*. One day before thawing or passaging of stem cells, feeder cells were seeded into the desired cell culture vessel and incubated overnight under standard fibroblast culture conditions to allow the feeder cells to attach and spread properly. Then mouse EF medium was removed, and the feeder layer was washed with sterile Phosphate Buffered Saline (PBS) without Ca²⁺ and Mg²⁺ (Merck) to remove any feeder cells that did not survive the freezing and thawing procedure. Next the cell culture vessel was filled with an appropriate volume of mIPSC medium before pluripotent stem cells were seeded onto it.

Geltrex is a mixture of extracellular matrix proteins that coats vessels with a basal membrane-like matrix allowing feeder-free culture of pluripotent stem cells [53]. For the coating of plates and flasks, an appropriate volume of cold (T = 4°C) Geltrex was transferred to the cell culture vessel and incubated for 60 min at 37°C to allow formation of the matrix. The remaining supernatant was sucked off and medium containing feeder-free stem cells was transferred to the dish.

To separate mESCs and mIPSCs from feeder cells, all cells were harvested using the procedure described below in 5.2.1.3. *Passaging and counting of cells*. The cell suspension was reseeded onto 10 cm-cell culture dishes and incubated for 30 – 45 min at 37°C. During that time, the feeder cells have already adhered to the culture dish whereas the mESCs of mIPSCs still float

in the medium. The supernatant containing the floating stem cells was carefully collected and centrifuged at 500 g for 5 min, and the cell pellet was resuspended in the medium or solution needed for downstream experiments.

For formation of embryoid bodies (EBs) and chondrogenic differentiation cells were cultured under special conditions and in special media as described below in 5.2.3. *Differentiation of induced pluripotent stem cells.*

Table 2: Mouse iPSC medium

Supplement	Concentration	Volume	Distributor
Dulbeco's Modified Eagle's medium (DMEM) <i>modified with high glucose, sodium pyruvate, GlutaMAXTM and phenol red</i>	78%	400 ml	Invitrogen
Fetal Bovine Serum (FBS)	20%	100 ml	Invitrogen
Penicillin-Streptomycin (5000 U/ml)	1%	5 ml	Invitrogen
Non-essential amino acids (100x)	1%	5 ml	Invitrogen
L-Ascorbic acid (12.5 mg/ml)	0.1%	1 ml	Sigma
Leukemia Inhibitory Factor (LIF) (100000 U/ml)	0.1%	1 ml	Max Plank Institute
β -mercaptoethanol	0.1 mM	3.2 μ l	Sigma

5.2.1.3. Passaging and counting of cells

When fibroblasts reached 80 - 90% confluence, or mESC and mIPSC colonies reached medium size and started to flatten at the edges, cells were passaged.

Therefore, the culture medium was aspirated, and the cell layer was washed with sterile PBS (Merck) to remove any remaining medium. Then the cell layer was covered with prewarmed Trypsin-EDTA (Sigma-Aldrich) and incubated at 37° C for 5 - 10 min. When most cells had become detached, the surface was flushed repeatedly with fresh medium at double the volume of trypsin, and the cell suspension was transferred into a 15 ml or 50 ml Falcon tube (Sarstedt). 10 μ l of the suspension were removed for cell counting and injected into a Neubauer chamber

(Brand, Grafrath, Germany). This chamber consists of four quadrants (A, B, C, D). Cells in the quadrants were counted and the total cell count (n) was estimated by the following formulas:

Equation 1: number of cells/ml (CC) = $[(A+B+C+D)/4] \times 10^4$

Equation 2: total cell count (n) = number of cells/ml (CC) x total cell suspension volume (V)

The remaining cell suspension was centrifuged at 500 g for 5 min to collect the cells at the bottom of the tube. Then the supernatant was aspirated, and the cell pellet was resuspended in prewarmed culture medium and reseeded in an appropriate cell culture vessel.

For expansion, MEFs and adult FBs were seeded at a density of about 5000 cells/cm². MESCs and mIPSCs were splitted at a ratio of 1 : 5 – 1 : 10 and seeded at a density of approximately 4×10^5 cells/cm² on feeder cells or on Geltrex-coated vessels.

5.2.1.4. Cryo-conservation of cells

As soon as an appropriate cell number was reached, cells were cryo-conserved until needed. Cells were harvested according to the standard procedure described in 5.2.1.3. *Passaging and counting of cells*. After the centrifugation step, the cell pellet was resuspended in ice cold freezing medium consisting of DMEM (Invitrogen), 20% FBS (Invitrogen) and 1% Dimethylsulfoxid (DMSO, AppliChem, Darmstadt, Germany) (Table 3).

Aliquots were prepared and stored on dry ice until frozen completely. Then the cryovials (Nalgene, Thermo Fisher Scientific) were placed in a -80°C freezer for maximum one week, before the vials were transferred into liquid nitrogen for long-term storage.

Fibroblasts were frozen at a density of 5×10^5 cells/ml (adult FBs) or 1×10^6 cells/ml (MEFs), respectively. MESCs and mIPSCs were frozen at a density of approximately 5×10^6 cells/ml (to be reseeded into a 6-well plate) or 4×10^7 cells/ml (to be reseeded into a 75 cm² flask).

Table 3: Freezing medium

Supplement	Concentration	Volume	Distributor
Dulbecco's Modified Eagle's medium (DMEM) <i>modified with high glucose, sodium pyruvate, GlutaMAXTM and phenol red</i>	79%	400 ml	Invitrogen
Fetal Bovine Serum (FBS)	20%	100 ml	Invitrogen
Dimethylsulfoxid (DMSO)	1%	5 ml	AppliChem

5.2.1.5. Thawing of cells

The frozen cryovials were placed into a water bath at 37°C until the frozen cell suspension had melted completely. Then the cell suspension and 5 ml of mouse EF medium or mouse IPSC medium per vial were transferred into an appropriate Falcon tube and centrifuged at 500 g for 5 min. The supernatant was removed, and the cell pellet was resuspended in prewarmed medium. Then cells were seeded in the desired cell culture vial and incubated at 37°C and 5% CO₂ overnight. The next day, medium was changed to remove any cells that had not survived the freezing and thawing procedure.

5.2.2. Generation of iPSCs from primary murine fibroblasts

5.2.2.1. Isolation of primary murine fibroblasts

Mouse ear fibroblasts (EAR FBs) were isolated from the ear of a four month old wild type C57B1/6 mouse, and mouse tail fibroblasts (TAIL FBs) were derived from the tail tip of the same animal. The sacrificed mouse was placed under a laminar flow hood. The biopsy sites were sprayed twice with 70% ethanol before small (0.5 – 1.0 cm²) tissue pieces were cut from ear and tail tip, and rinsed twice with sterile PBS containing 1% Penicillin-Streptomycin. On a 6 cm-cell culture dish, the biopsies were placed into a drop of Collagenase-Dispase-medium consisting of 4 mg/ml collagenase (Worthington Biochemical Corp., New Jersey, USA) and 4 mg/ml dispase (Sigma-Aldrich) dissolved in DMEM supplemented with 1% Penicillin-Streptomycin (Table 4). The tissue samples were minced with sterile scalpel and forceps. Then,

fresh Collagenase-Dispase medium was added, and the tissue chunks were incubated for 30min at 37°C. Then the dish was filled with 6 ml of mouse EF medium and incubated overnight at 37°C allowing the cells to spread out of the tissue chunks and attach to the plate (passage 0). The following day remaining large pieces of tissue were further dissociated by pipetting up and down to increase the cell harvest. As soon as the outgrowing fibroblasts reached 80-90% confluence, the cells were trypsinized and passaged into a 75 cm² flask (passage 1) as described above in 5.2.1.3. *Passaging and counting of cells.*

Table 4: Collagenase-Dispase medium

Supplement	Concentration	Volume	Distributor
Dulbecco's Modified Eagle's medium (DMEM) <i>modified with high glucose, sodium pyruvate, GlutaMAXTM and phenol red</i>	99%	1.5 ml	Invitrogen
Penicillin-Streptomycin (5000 U/ml)	1%	1.5 µl	Invitrogen
Collagenase	4 mg/ml	6 mg	Worthington
Dispase	4 mg/ml	6 mg	Sigma

5.2.2.2. Isolation of primary mouse embryonic fibroblasts

Mouse embryonic fibroblasts were prepared from mouse embryos at 12.5 dpc to 13.5 dpc. After dissecting the uterus, the embryos were placed in a Petri dish under a laminar flow hood and rinsed with sterile PBS. Head and inner organs were removed using sterile scissors and forceps. Next, the remaining carcasses were minced into a 50 ml Falcon tube containing 1ml Trypsin EDTA per embryo. This suspension was incubated at 37°C for 10 min to digest the tissue. Remaining tissue chunks were mechanically disrupted by pipetting before 3 ml of mouse EF medium per embryo were added to stop the digestion. Next, the suspension was incubated at room temperature for 10 min to let larger pieces of tissue sink down to the bottom of the Falcon tube. The supernatant was carefully transferred into a 50 ml Falcon tube without disturbing the tissue chunks at the bottom, and centrifuged at 500 g for 5 min. The cell pellet was resuspended in mouse EF medium, and the cells were seeded into 75 cm² flasks (passage 0). After two days, supposedly only the embryonic fibroblasts have survived and adhered to the bottom of the flask.

Dead cells and other cell types were removed by sucking off the medium and rinsing the flask twice with sterile PBS before the MEFs were trypsinized and passaged using the standard techniques described above in 5.2.1.3. *Passaging and counting of cells.*

5.2.2.3. Preparation of mitotically inactivated feeder cells

Before MEFs can be used as feeders for stem cell culture, they need to be mitotically inactivated in order not to overgrow the stem cells. Therefore, MEFs at passage 3 – 8 were cultured in 225 cm² flasks under normal conditions until they nearly reached confluence. Then, medium was replaced by mouse EF medium supplemented with 10 µl/ml Mitomycin C (Sigma-Aldrich) and the cells were incubated for 2.5 - 3 hours at 37°C under 5% CO₂. The monolayer was washed twice with sterile PBS to remove any remnants of Mitomycin C before aliquots of approximately 5 x 10⁵ cells/ml were frozen and stored using the standard procedure described in 5.2.1.4. *Cryo-conservation of cells.*

5.2.2.4. Nucleofection of fibroblasts

Nucleofection is an electroporation-based method for delivery of plasmids into the nuclei of target cells. For nucleofection of MEFs we used the P3 Primary Cell 4D-Nucleofector® X Kit (Lonza, Basel, Switzerland), whereas for nucleofection of adult FBs we used the P2 Primary Cell 4D-Nucleofector® X Kit (Lonza). All experiments were carried out in a 4D-Nucleofector™ X Unit (Lonza).

To estimate and optimize efficiency of gene delivery via nucleofection, we first nucleofected fibroblasts with the *pmaxGFP* (green fluorescent protein) vector provided with the nucleofection kit. The cells were cultured, harvested and counted using standard techniques described above. Next, an appropriate number of cells was centrifuged at 200 g for 10 min before 100.000 cells per reaction were resuspended in 16.4 µl nucleofector solution of the respective kit supplemented with 3.6 µl supplement solution and 1 µg of the *pmaxGFP* vector provided by the manufacturer (Table 5). This suspension was transferred into one well of the 16-well Nucleocuvette Strip (Lonza). Nucleofection was carried out testing different programs

as recommended by the manufacturer. After the run, the Nucleocuvette Strip was incubated at room temperature for 10 min before 80 µl of prewarmed mouse EF medium were added. The cell suspension was transferred into one well of a 24-well-plate and incubated overnight. 24 hours after nucleofection survival rate and efficiency were analyzed. To estimate the survival rate, dead cells floating in the medium were counted using the Neubauer chamber as described in 5.2.1.3. *Passaging and counting of cells* and the survival rate was determined as follows:

Equation 3: Survival rate (%) = $(1 - \text{mean dead cell count}/100\ 000) \times 100$.

To determine the efficiency, we screened the cells for expression of GFP. Representative photomicrographs were taken by an AxioCam MRm camera (Carl Zeiss, Oberkochen, Germany) mounted on an Axio Observer.Z1 microscope (Carl Zeiss). GFP+ cells per viewing field (pvf) and total cell number per viewing field were counted and efficiency rate was determined as follows:

Equation 4: Efficiency rate (%) = $(\text{fluorescent cells pvf}/\text{total cell number pvf}) \times 100$.

To initiate the reprogramming process, the *pCMV(CAT)T7-SB100x* transposase plasmid together with either the *pT2OSKM*, *pT2OSKML*, *RMCE-OSKM-Cherry* or *RMCE-OSKML-Cherry* reprogramming factor plasmid were delivered into the cells by Nucleofection.

Fibroblasts were harvested, counted and centrifuged as described above. For one reaction 400 000 cells were resuspended in 82 µl nucleofector solution of the respective kit and 18 µl supplement solution. Then, 1 µg, 2 µg or 5 µg of the respective reprogramming factor plasmid and 0.1 µg, 0.2 µg or 0.5 µg of the transposase plasmid were added (Table 5) before the cell-DNA-mix was transferred into a Single Nucleocuvette (Lonza), and cells were nucleofected with the program EH-198. After the run, the Nucleocuvette was incubated for 10 min at room temperature. Then 500 µl of prewarmed mouse IPS medium were added and the cell suspension was transferred to either standard cell culture dishes, feeder- or Geltrex-coated dishes as indicated below in 5.2.2.5. *Reprogramming of primary fibroblasts*.

Table 5: Nucleofection reaction set up

	Optimization	Reprogramming
Number of cells/ reaction	100 000 cells	400 000 cells
Nucleofector solution (P2 for FBs, P3 for MEFs)	16.4 μ l	82 μ l
Supplement solution	3.6 μ l	18 μ l
<i>pmaxGFP</i> vector	1 μ g	
Transposase plasmid (<i>pCMV(CAT)T7-SB100X</i>)		0.1/ 0.2/ 0.5 μ g
Reprogramming factor plasmid		1/ 2/ 5 μ g

5.2.2.5. Reprogramming of primary murine fibroblasts

After delivery of the reprogramming factors via nucleofection, the fibroblasts were cultured in mouse iPSC medium and monitored daily for morphological changes indicating successful reprogramming. Medium was changed daily until picking of colonies was completed.

In order to optimize the reprogramming process, different culture conditions were tested. Therefore, after nucleofection the fibroblasts were either seeded onto standard cell culture dishes or feeder cells or Geltrex-coated cell culture dishes. When the cells became highly confluent, plates were trypsinized and passaged using the standard techniques described above in 5.2.1.3. *Passaging and counting of cells.*

5.2.2.6. Picking of colonies and establishment of clonal cell lines

To establish clonal IPS cell lines, colonies of *bona fide* iPSCs that showed the typical round, spheroid and compact morphology of mESCs, were chosen for picking between day 19 and day 27 after nucleofection with the reprogramming factor plasmids (Figure 19).

Therefore, the plates were placed under a 3D-Stereomicroscope (Stemi 2000-CS, Carl Zeiss) and the chosen colonies were mechanically dislodged from the surface with a 20 μ l pipet tip (1), carefully sucked into the pipet tip and transferred into one well of a 96-V-bottom non-

treated microplate filled with prewarmed trypsin (2). After 5 min incubation at 37°C (3) mouse IPSC medium was added and the breakdown of the colonies to a single cell suspension was achieved by pipetting up and down repeatedly (4). The single cell suspension was then transferred into one well of a 24-well plate previously seeded with feeder cells (5). This was counted as passage 0 of the thereby newly established clonal IPS cell line.

We named the established cell lines TAXX for MEF-derived iPSCs, ETAXX for EAR-FB-derived iPSCs, TTAXX for TAIL-FB-derived iPSCs reprogrammed with the *pT2OSKM/OSKML* vector; or ETACXX for EAR-FB-derived iPSCs reprogrammed with the *RMCE-OSKM/OSMKL-Cherry* vector.

Picked iPSCs were cultured under standard condition for up to one week. Cells that formed many round, spheroid and compact colonies were considered successfully reprogrammed iPSCs and frozen until further analysis. Cells that failed to maintain iPSC morphology, and therefore were probably not successfully reprogrammed, were discarded. Cells that only formed few, large colonies were passaged once and then either frozen or discarded.

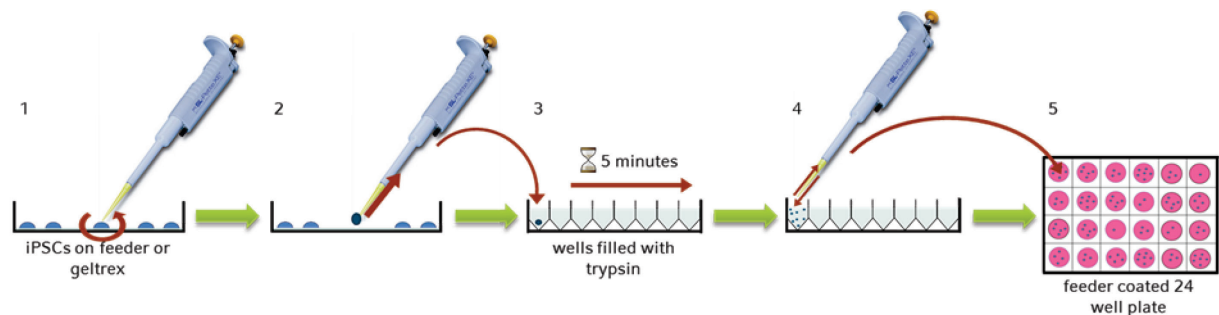


Figure 19: Schematic depiction of the picking of *bona fide* iPSC colonies (self-designed).

- (1) Colonies are mechanically dislodged from the cell culture dish.
- (2) Colonies are sucked into the pipet tip and transferred into trypsin.
- (3) Colonies are incubated for 5 min in trypsin.
- (4) Further dissociation of the colonies into a single cell suspension.
- (5) Transfer of the single cell suspension onto feeder-coated 24-well plates.

5.2.3. Differentiation of induced pluripotent stem cells

5.2.3.1. Formation of embryoid bodies in hanging drops

Feeder-free mIPSCs were harvested using standard techniques described in 5.2.1.2. *Culturing mouse ESCs and mouse iPSCs* and 5.2.1.3. *Passaging and counting of cells*, and resuspended in hanging drop medium consisting of DMEM with 20% FBS and 1% Penicillin-Streptomycin supplemented with 1% non-essential amino acids and 0.1 mM β -mercaptoethanol at a concentration of 40 000 cells/ml (Table 6).

Then 20 μ l drops of this suspension containing 800 cells each were placed on the lid of a 10 cm-Petri dish. The bottom of the plate was covered with sterile PBS to provide a humid atmosphere preventing the small drops from drying out. Then the lid was carefully inverted in order not to destroy the drops, and placed on the bottom (Figure 20). Under this culture condition, mIPSCs cluster together forming EBs [235]. EBs were cultured for five days in hanging drop culture before being used for downstream experiments.

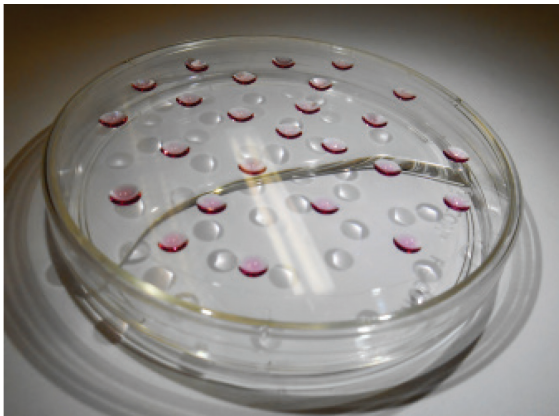


Figure 20: Hanging drop culture of mIPSCs.

20 μ l drops containing 800 cells on the lid of a 10 cm-Petri dish. The bottom of the dish is covered with sterile PBS to provide a humid atmosphere.

Table 6: Hanging drop medium

Supplement	Concentration	Volume	Distributor
Dulbecco's Modified Eagle's medium (DMEM) <i>modified with high glucose, sodium pyruvate, GlutaMAX™ and phenol red</i>	78%	400 ml	Invitrogen
Fetal Bovine Serum (FBS)	20%	100 ml	Invitrogen
Penicillin-Streptomycin (5000 U/ml)	1%	5 ml	Invitrogen
Non-essential amino acids (100x)	1%	5 ml	Invitrogen
β-mercaptoethanol	0.1 mM	3.2 μl	Sigma

5.2.3.2. Spontaneous differentiation of mIPSCs in embryoid bodies

To evaluate the potential of the generated iPSCs to differentiate into the three germ layers, cells were allowed to differentiate spontaneously in EBs.

Therefore, EBs generated by the hanging drop method described above in 5.2.3.1. *Formation of embryoid bodies in hanging drops* were transferred at day 5 into 96 V-shaped-bottom, non-treated microplates and maintained as spheroids for further 16 days in free floating medium (Table 7) consisting of DMEM supplemented with 10% FBS and 10% horse serum as well as 1% Penicillin-Streptomycin (Figure 21). Medium was changed twice a week. After a total of 21 days of differentiation, mRNA for qPCR analysis was isolated from EBs. Spontaneous differentiation of mIPSCs in EBs and subsequent mRNA analysis was performed in triplicates.



Figure 21: Spontaneous differentiation of mIPSCs in embryoid bodies (self-designed).

iPSCs were cultured under feeder-free standard conditions before embryoid body formation was achieved by hanging drop culture. Embryoid bodies were maintained in hanging drops for 5 days before they were transferred to 96 V-shaped-bottom non-treated microplates, and maintained in suspension for additional 16 days.

Table 7: Free floating medium

Supplement	Concentration	Volume	Distributor
Dulbeco's Modified Eagle's medium (DMEM) <i>modified with high glucose, sodium pyruvate, GlutaMAXTM and phenol red</i>	79%	500 ml	Invitrogen
Fetal Bovine Serum (FBS)	10%	50 ml	Invitrogen
Horse Serum	10%	50 ml	Invitrogen
Penicillin-Streptomycin (5000 U/ml)	1%	5 ml	Invitrogen

5.2.3.3. Chondrogenic differentiation of mIPSCs via chondrogenic colonies

Scaffoldless chondrogenic differentiation of mIPSC clone ETA04 was carried out by exposure of intact IPSC colonies to mesoendodermal pre-differentiation medium followed by chondrogenic medium and subsequent transfer of the formed chondrogenic nodules into free floating culture as described by *Yamashita et al.* [127].

IPSCs were cultured under feeder-free conditions on Geltrex-coated 6-well plates until colonies reached medium size. Then mesoendodermal predifferentiation was induced by changing the culture medium to mesoendodermal medium (Table 8) consisting of DMEM/F12 (Invitrogen) with 1% FBS, 1% Penicillin-Streptomycin and 1% Insulin Transferrin Selenite Plus3 Mix (ITS, Sigma-Aldrich) supplemented with the growth factors Wnt3a (R&D Systems) and Activin A (R&D Systems) at a concentration of 10 ng/ml each. After three days of mesoendodermal pre-differentiation chondrogenic differentiation was induced by changing the culture medium to chondrogenic colonies medium (Table 9) consisting of DMEM, 1% FBS and 1% Penicillin-Streptomycin supplemented with non-essential amino acids, sodium pyruvate (Sigma-Aldrich), Insulin Transferrin Selenite Plus3 Mix (Sigma-Aldrich) and L-ascorbic acid (Sigma-Aldrich). IPSCs were maintained as colonies on Geltrex for four days either in chondrogenic colonies medium (noGF) or in chondrogenic colonies medium supplemented with the chondrogenic growth factors bone morphogenetic protein 2 (BMP2, R&D Systems), transforming growth factor beta1 (TGF β 1, R&D Systems) and growth and differentiation factor 5 (GDF5, R&D Systems) at a concentration of 10 ng/ml each (BTG). After four days, most colonies had spontaneously detached from the plates and were transferred to free floating culture in 6 cm non-adherent Petri dishes. Chondrogenic nodules were maintained in free floating culture in

chondrogenic colonies medium with or without supplemented growth factors for up to 42 days (Figure 22). Medium was changed twice a week. At day 14, 31 and 42, nodules were either subjected to mRNA isolation for qPCR analysis or embedded for histological analysis.

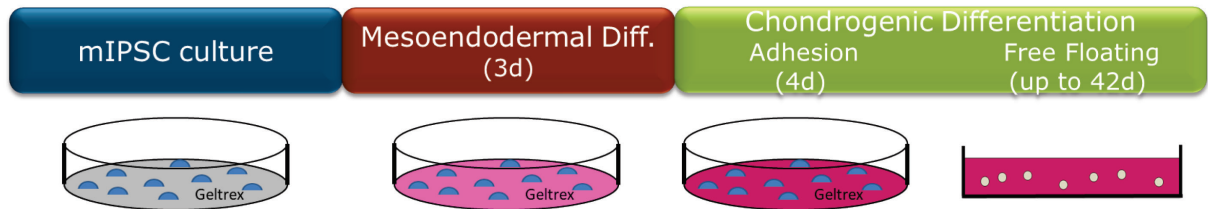


Figure 22: Chondrogenic differentiation of mIPSCs via chondrogenic colonies (self-designed)

IPSCs were cultured under feeder-free standard conditions before mesoendodermal pre-differentiation was induced in mesoendodermal medium supplemented with Wnt3a and Activin A for 3 days. Initial chondrogenic differentiation was induced by culturing the predifferentiated IPSC colonies in chondrogenic colonies medium (noGF) or in chondrogenic colonies medium supplemented with BMP2, TGFβ1 and GDF5 (BTG) for 4 days. After one week of differentiation the colonies started to detach from the plates and were transferred to free floating culture. The chondrogenic nodules were maintained up to 42 days in free floating culture.

Table 8: Mesoendodermal medium

Supplement	Concentration	Volume	Distributor
DMEM/F12	97%	48.5 ml	Invitrogen
Fetal Bovine Serum (FBS)	1%	0.5 ml	Invitrogen
Penicillin Streptomycin (5000U/ml)	1%	0.5 ml	Invitrogen
Insulin Transferrin Selenite Plus3 (ITS, 100X)	1%	0.5 ml	Sigma

Table 9: Chondrogenic colonies medium

Supplement	Concentration	Volume	Distributor
Dulbecco's Modified Eagle's medium (DMEM) <i>modified with high glucose, sodium pyruvate, GlutaMAXTM and phenol red</i>	95%	47.0 ml	Invitrogen
Fetal Bovine Serum (FBS)	1%	0.5 ml	Invitrogen
Penicillin-Streptomycin (5000 U/ml)	1%	0.5 ml	Invitrogen
Non-essential amino acids (100x)	1%	0.5 ml	Invitrogen
Sodium pyruvate (100 mM)	1% (1 mM)	0,5 ml	Sigma
Insulin Transferrin Selenite Plus3 (ITS, 100X)	1%	0.5 ml	Sigma
L-ascorbic acid (5 mg/ml)	1% (50 µg/ml)	0.5 ml	Sigma

5.2.3.4. Chondrogenic differentiation of mIPSCs via embryoid bodies

After spontaneous pre-differentiation of mIPSCs in EBs in hanging drop culture for 5 days, they were transferred into 96-V-bottom non treated microplates and maintained as spheroids for up to 42 days in chondrogenic medium (noGF) or chondrogenic medium supplemented with chondrogenic growth factors bone morphogenetic protein 2 (BMP2, R&D Systems, Minneapolis, Minnesota, USA) at a concentration of 100 ng/ml and transforming growth factor beta1 (TGFβ1, R&D Systems) at a concentration of 10 ng/ml (BT) (Figure 23). The serum-free chondrogenic medium (Table 10) consisted of DMEM and 1% Penicillin-Streptomycin supplemented with dexamethason (Sigma-Aldrich), sodium pyruvate (Sigma-Aldrich), L-ascorbic acid (Sigma-Aldrich) and Insulin Transferrin Selenite Plus3 Mix (Sigma-Aldrich), representing a standard medium for chondrogenic differentiation [211, 218]. Medium was changed twice a week. At day 14, 28 and 42, spheroids were either subjected to mRNA isolation for qPCR analysis or embedded for histological analysis. Formation of chondrogenic spheroids and subsequent mRNA and histological analyses were performed in triplicates.



Figure 23: Chondrogenic differentiation of mIPSCs via embryoid bodies (self-designed).

IPSCs were cultured under feeder-free standard conditions before embryoid body formation was achieved by hanging drop culture. Embryonic bodies were maintained in hanging drops for 5 days before they were transferred to 96 V-shaped-bottom non-treated microplates containing either chondrogenic medium (noGF) or chondrogenic medium supplemented with BMP2 and TGF β 1 (BT). The forming chondrogenic spheroids were maintained up to 42 days.

Table 10: Chondrogenic spheroid medium

Supplement	Concentration	Volume	Distributor
Dulbecco's Modified Eagle's medium (DMEM) modified with high glucose, sodium pyruvate, GlutaMAX TM and phenol red	94,4%	47.2 ml	Invitrogen
Penicillin-Streptomycin (5000 U/ml)	1%	0.5 ml	Invitrogen
Dexamethason (1 mM)	1% (10 μ M)	0.5 ml	Sigma
Natrium Pyruvate (100 mM)	1% (1 mM)	0.5 ml	Sigma
L-Ascorbic Acid (12.5 mM)	1.6% (0.195 mM)	0.78 ml	Sigma
Insulin Transferrin Selenite Plus3 (ITS, 100X)	1%	0.5 ml	Sigma

5.3. Cytological analysis

5.3.1. Alkaline phosphatase staining

ESCs and iPSCs were cultured in 6-well plates under standard culture conditions on feeder cells for 2 – 4 days. When the colonies reached medium size, the plates were washed with PBS before the cells were fixed with pre-cooled 4% paraformaldehyde (PFA, Merck) for 15 min at room temperature. Then the plates were washed twice with sterile PBS to remove all remaining PFA. The cells were equilibrated in DIG III Buffer (0.1 M Tris pH 9.5, 0.1 M NaCl, 0.05 M MgCl₂ in dH₂O, chemicals from Sigma-Aldrich and Merck) for 10 min before they were covered with the staining solution consisting of 200 µl nitro blue tetrazolium chloride/ 5-bromo-4-chloro-3-indolyl-phosphate (NTC/BCIP, Roche Diagnostics, Risch, Switzerland) in 10 ml DIG III Buffer. Cells were allowed to stain for up to 20 min protected from light at room temperature. Then the staining solution was removed and the plates were washed twice with PBS before photomicrographs were taken using an AxioCam 105 color camera (Carl Zeiss) mounted on an Axio Observer.Z1 microscope (Carl Zeiss).

AP Staining was repeated twice.

5.3.2. Immunocytochemistry

ESCs and iPSCs were cultured on 4-well glass slides (Nunc, ThermoFisher Scientific) coated with 500 µl human fibronectin (Merck) per well at a concentration of 0.1 mg/ml on feeder cells under standard culture conditions for 2 days. When the colonies reached medium size, the cells were fixed with pre-cooled 4% PFA for 5 min at room temperature. Then the plates were washed twice with PBS to remove all remaining PFA.

After blocking and permeabilization in PBS supplemented with 1% bovine serum albumin (BSA, Roth) and 0.1% Triton X (Sigma) for 1h at room temperature, cells were incubated overnight in a wet chamber at 4°C with primary antibodies listed in Table 11. Next day, the slides were washed twice in PBS for 5 min to remove any primary antibodies that did not bind. Then the cells were incubated for 1h at room temperature with corresponding secondary antibodies listed in Table 11. After washing the slides again with PBS, they were mounted with

Fluoroshield mounting medium (Sigma-Aldrich) containing 4', 6-diamidino-2-phenylindole (DAPI) as a nuclear counterstaining (Sigma-Aldrich), and covered with 20 x 60 mm cover slips (Menzel Gläser, ThermoFisher Scientific). Fluorescence was observed and representative photomicrographs were taken with an AxioCam MRm camera (Carl Zeiss) mounted on an Axio Observer.Z1 microscope (Carl Zeiss).

Immunocytochemistry (ICC) was repeated twice.

Table 11: Antibodies for immunocytochemistry

Target	Type	Company Catalogue number	Dilution in PBS with 1% BSA and 0.1% TritonX
Primary antibodies			
Anti-Nanog	Polyclonal Goat IgG	R&D Systems AF2729	1:400
Anti-Oct3/4	Monoclonal Rat IgG _{2B}	R&D Systems MAB 1759	1:400
Anti-Sox2	Monoclonal Mouse IgG _{2A}	R&D Systems MAB 2018	1:400
Anti-SSEA1	Monoclonal Mouse IgM	R&D Systems MAB 2155	1:400
Secondary antibodies			
Anti-Goat IgG (H+L)	Donkey Alexa Fluor 488	Life Technologies A-11055	1:1000
Anti-Mouse IgG (H+L)	Donkey Alexa Fluor 488	Life Technologies A-21202	1:1000
Anti-Mouse IgM	Goat NL493	R&D Systems NL020	1:1000
Anti-Rat IgG (H+L)	Goat Alexa Fluor 488	Life Technologies A-11006	1:1000

5.4. mRNA analysis

5.4.1. Total RNA isolation

5.4.1.1. Total RNA isolation from cells

Total RNA was isolated from cells using the RNeasy Mini or Midi Kit (Qiagen, Hilden, Germany) according to the number of cells. Cells were harvested following the standard procedure described in *5.2.1.3 Passaging and counting of cells* and lysed in RLT buffer supplemented with 1% β -mercaptoethanol (Sigma). The lysate was homogenized by passing through QIAshredder spin columns before 70% ethanol was added in a 1:1 ratio. Samples were loaded to the RNeasy Mini or Midi spin columns and washed once with washing solution before 10 U of DNase (Qiagen) were added to digest genomic DNA. The columns were washed three times according to the manufacturer's instructions and dried by centrifugation at maximum speed before total RNA was eluted in RNase-free water. RNA concentration and purity were determined spectrometrically at A_{260} and $A_{260/280}$, respectively, using a Nanodrop 2000 spectrophotometer (ThermoFisher Scientific). RNA samples were stored at -80°C .

5.4.1.2. RNA isolation from embryoid bodies, chondrogenic nodules and spheroids

Total RNA was isolated from EBs, chondrogenic nodules and chondrogenic spheroids using the RNeasy Mini Kit (Qiagen, Hilden, Germany). EBs, chondrogenic nodules or spheroids were collected in 1,5 ml DNA LoBind Tubes (Eppendorf, Hamburg, Germany) and shortly centrifuged in order to collect them at the bottom of the tubes. Then, the supernatant was removed and the probes were lysed in TRIzol (Life Technologies) for 5 min at room temperature before chloroform (Merck) was added in a 1 : 5 ratio. The samples were centrifuged at 12 000 g for 15 min in order to separate the mixture into three phases. The upper phase containing the total RNA was harvested and mixed with 70% ethanol (Merck) in a 1 : 1 ratio to purify the RNA. Samples were loaded to the RNeasy Mini spin columns and washed once with washing solution before 10 U of DNase (Qiagen) were added to digest genomic DNA. The columns were washed three times according to the manufacturer's instructions and dried by centrifugation at maximum speed, before total RNA was eluted in RNase-free water.

RNA concentration and purity were determined spectrometrically at A_{260} and $A_{260/280}$, respectively. RNA samples were stored at -80°C .

5.4.2. cDNA synthesis

cDNA (complementary DNA) was synthesized using the Transcriptor First Strand cDNA Synthesis Kit (Roche Diagnostics). First, the RNA denaturation mix (Table 12) consisting of 100 ng total RNA and random hexamer primers (600 pmol/ μl) filled up with RNase free water to 13 μl was incubated at 65°C for 10 min. Then PCR buffer, 10 mM dNTPs, 20 U of RNase inhibitor and 10 U of reverse transcriptase were added (Table 13). This cDNA synthesis mix was incubated for 1 hour at 60°C . To evaluate quality of the synthesis, the newly synthesized cDNA was tested for expression of the housekeeping gene *glyceraldehyde-3-phosphate dehydrogenase (GAPDH)*.

Table 12: RNA denaturation mix and program

Total RNA (100 ng)	x μl	<i>65°C for 5 min</i> <i>Keep on ice</i>
Random hexamer primers (600 μM)	2 μl	
RNase free H ₂ O	11 μl – x μl	
Total volume	13 μl	

Table 13: cDNA synthesis mix and program

RNA denaturation mix	13 μl	<i>25°C for 10 min</i>
Reaction buffer (5x)	4 μl	
RNase inhibitor (40 U/ μl)	0.5 μl	<i>50°C for 60 min</i>
dNTP mix (10 mM each)	2 μl	<i>80°C for 5 min</i>
Reverse transcriptase (20 U/ μl)	0.5 μl	<i>4°C forever</i>
Total volume	20 μl	

5.4.3. Semi-quantitative reverse transcription PCR

For semi-quantitative reverse transcription (RT)-PCRs (polymerase chain reactions), the Fast Start Taq DNA Polymerase Kit (Roche Diagnostics) was used. Shortly, 1 μl of cDNA synthesis mix (Table 13) was added to a master mix consisting of PCR buffer, 0.2 mM dNTPs each, 0.25 pmol gene-specific primers and 1 U Taq DNA Polymerase (Table 14). This mix was incubated in a Thermocycler (Peqstar 2x, Peqlabs, Erlangen, Germany) using a gene specific program as indicated below. The primer pairs and their annealing temperatures used in this study are listed in Table 15.

Amplified PCR products were separated via agarose gel electrophoresis on 2% agarose gels containing ethidium bromide (Sigma). As a reference for the size of the products, a 100 bp molecular weight standard (Invitrogen) was used. PCR bands were visualised by a gel imaging system (Vilber Lourmat, Eberhardzell, Germany) and densitometrically quantified by the Bio Capt Software (Vilber Lourmat).

Table 14: RT-PCR reaction set up and program

10x PCR reaction buffer with MgCl_2	2 μl	94°C	5 min	
Primer forward (10 pmol/ μl)	0.5 μl			
Primer reverse (10 pmol/ μl)	0.5 μl	$X \text{ cycles}$	94°C	30 s
dNTP Mix (10 mM each)	0.4 μl		$Y^\circ\text{C}$	30 s
Taq polymerase	0.2 μl		72°C	60 s
cDNA	1 μl	72°C	5 min	
dH ₂ O (PCR grade)	15.4 μl	4°C	forever	
Total volume	20 μl			

Annealing temperature (Y) and number of cycles (X) are specific for each gene and listed in Table 15

Table 15: Oligonucleotides used for RT-PCR

Target gene	Primer sequence (5' to 3') (f: forward, r: reverse)	Annealing temperature	Number of cycles	Product size (bp)	Reference
House-keeping gene					
<i>GAPDH</i>	f: <i>CAACTACATGGTTTACATGTTT</i> r: <i>GCCAGTGGACTCCACGAC</i>	50°C	30	181	[236]
Embryonic stem cell markers					
<i>Dax1</i>	f: <i>TGCTGCGGTCCAGGCCATCAAGAG</i> r: <i>GGGCACIGTTCAGTTCAGCGGATC</i>	56°C	35	233	[55]
<i>Ecat1</i>	f: <i>TGTGGGGCCCTGAAAGGCGAGCTGAGAT</i> r: <i>ATGGGCCGCCATACGACGACGCTCAACT</i>	60°C	40	164	[15]
<i>Eras*</i>	f: <i>GCCCCTCATCAGACTGCTAC</i> r: <i>GCAGCTCAAGGAGAGGTGT</i>	49°C	40	66	[55]
<i>Nanog</i>	f: <i>GAAATCCCTTCCCTCGCCATC</i> r: <i>CTCAGTAGCAGACCCCTTGTAAAGC</i>	58°C	30	161	[237]
<i>Rex1</i>	f: <i>ACGAGTGGCAGTTTCTTCTTGGGA</i> r: <i>TATGACTCACTTCCAGGGGGCACT</i>	56°C	35	287	[15]
<i>Zfp296</i>	f: <i>CCTATGCTTGTGCCAGAGTA</i> r: <i>CTAAAGTGCTGCCATTTC</i>	53°C	30	214	[55]
Reprogramming factors					
<i>c-Myc</i>	f: <i>TCAAGCAGACGAGCACAAAGC</i> r: <i>TACAGTCCCAAAGCCCCAGC</i>	53°C	30	242	[55]
<i>Klf4</i>	f: <i>GGCGAGAAACCTTACCACTGT</i> r: <i>TACTGAACTCTCTCTCCTGGCA</i>	53°C	30	226	[55]
<i>Oct3/4</i>	f: <i>TCAGGTTGGACTGGGCCTAGT</i> r: <i>GGAGGTTCCCTCTGAGTTGCTT</i>	58°C	30	100	[237]
<i>Sox2*</i>	f: <i>GAGGGCTGGACTGCGAACT</i> r: <i>TTTGACCCCTCCCAATTC</i>	58°C	30	72	[237]
Chondrogenic matrix proteins					
<i>Col II** A&B</i>	f(1): <i>GCCTCGCGGTGAGCCATGATC</i> r(1): <i>CTCCATCTCTGCCACGGGGT</i> f(2): <i>GGTTTGGAGAGACCATGAAC</i> r(2): <i>TGGGTTGCAATGGATTGTG</i>	60°C	30	IIA: 472 IIB: 268	[129]

*: Agarose-gel electrophoresis for PCR products was carried out on 3% agarose gel.

** : For simultaneous analysis of the expression of the two isoforms of procollagen II (*Col II A* and *Col II B*), two primer pairs were used within the same probe resulting in two bands during agarose gel electrophoresis.

5.4.4. Quantitative PCR

Quantitative PCR (qPCR) was performed with a Light Cycler 96 instrument (Roche Diagnostics) using either the LightCycler SYBR Green Master Kit (Roche Diagnostics) or Taq-Man probes. The crossing point (Ct) of each curve was determined by the second derivative maximum method. The comparative $2^{-\Delta\Delta Ct}$ method was used to determine the fold change of gene expression levels relative to *GAPDH* between experimental and control conditions.

Equation 5: $\Delta Ct_{\text{Experimental}} = Ct_{\text{Experimental}} (GOI) - Ct_{\text{Experimental}} (GAPDH)$
 $\Delta Ct_{\text{Control}} = Ct_{\text{Control}} (GOI) - Ct_{\text{Control}} (GAPDH)$
GOI: Gene of interest

Equation 6: $\Delta\Delta Ct = \Delta Ct_{\text{Experimental}} - \Delta Ct_{\text{Control}}$

Equation 7: Expression fold change = $2^{-\Delta\Delta Ct}$

5.4.4.1. LightCycler SYBR Green method

For qPCR with the LightCycler SYBR Green Master Kit (Roche Diagnostics), 0.5 μl of cDNA synthesis mix (Table 13) were added to the SYBR Green Master Mix supplemented with 0.5 pmol gene-specific primers (Table 16). The sequences of the primer pairs used are given in Table 17.

Amplification cycles and melting curve analysis were performed according to the manufacturer's instructions. Quantitative PCR runs with the LightCycler SYBR Green Master Kit were performed in triplicates.

Table 16: SYBR Green qPCR reaction set up

2x SYBR Green Master Mix	10 μl
Primer forward (10 pmol/ μl)	1 μl
Primer reverse (10 pmol/ μl)	1 μl
cDNA	0.5 μl
dH ₂ O (PCR grade)	7.5 μl
Total volume	20 μl

Table 17: Oligonucleotides used for qPCR (SYBR Green Kit)

Target gene	Primer sequence (5' to 3') (f: forward, r: reverse)	Product size (bp)	Reference
House keeping gene			
<i>GAPDH</i>	f: <i>CAACTACATGGTTTACATGTTT</i> r: <i>GCCAGTGGACTCCACGAC</i>	181	[236]
Pluripotency markers			
<i>Nanog</i>	f: <i>GAAATCCCTTCCCTCGCCATC</i> r: <i>CTCAGTAGCAGACCCCTTGTAAGC</i>	161	[237]
<i>Oct3/4</i>	f: <i>TCAGGTTGGACTGGGCCTAGT</i> r: <i>GGAGGTTCCCTCTGAGTTGCTT</i>	100	[237]
Endodermal markers			
<i>Sox17</i>	f: <i>GATGCGGGATACGCCAGTG</i> r: <i>CCACCACCTCGCCTTTCAC</i>	136	Harvard Primer Bank
<i>FoxA2</i>	f: <i>CATGGGACCTCACCTGAGTC</i> r: <i>CATCGAGTTCATGTTGGCGTA</i>	97	Harvard Primer Bank
Mesodermal markers			
<i>MyoD1</i>	f: <i>CCACTCCGGGACATAGACTTG</i> r: <i>AAAAGCGCAGGTCTGGTGAG</i>	109	[238]
<i>Brachyury</i>	f: <i>CAGCCCACCTACTGGCTCTA</i> r: <i>GAGCCTGGGGTGATGGTA</i>	72	[53]
Ectodermal markers			
<i>Pax6</i>	f: <i>GCGCAGACGGCATGTATGATA</i> r: <i>GGGTTGCCCTGGTACTGAAG</i>	104	Harvard Primer Bank
<i>Ncam1</i>	f: <i>CACTTTGTGTTTCAGGACCTCAG</i> r: <i>AAAAGCAATGAGACCAAGGTG</i>	92	[53]

5.4.4.2. Taq-Man probes

Taq-Man probes containing gene specific primer pairs and quenchers were purchased from IDT (Integrated DNA Technologies, Coralville, Iowa, USA). For qPCR, 1 μ l of cDNA synthesis mix (Table 13) was added to the Prime Time Gene Expression Master Mix (IDT) supplemented with 0.5 pmol gene-specific primers (Table 18). The sequences of the primer pairs and quenchers are given in Table 19.

Experimental set up was designed according to the manufacturer's instructions. Quantitative PCR runs with the Taq-Man probes were performed in duplicates.

Table 18: Taq-Man probes qPCR reaction set up

2x Prime Time Gene Expression Master Mix	10 μ l
Primer mix (5pmol/ μ l each)	2 μ l
cDNA (diluted 1:5 in dH ₂ O)	5 μ l
dH ₂ O (PCR grade)	3 μ l
Total volume	20 μl

Table 19: Oligonucleotides used for qPCR (Taq Man probes)

Target gene	Primer sequence (5' to 3') (P: probe f: forward, r: reverse)
House keeping gene	
<i>GAPDH</i>	P: 56-FAM/TGCAAATGG/ZEN/CAGCCCTGGTG/3IABkFQ f: GTGGAGTCATACTGGAACATGTAG r: AATGGTGAAGGTCGGTGTG
Pluripotency markers	
<i>Nanog</i>	P: 56-FAM/CCACCGCTT/ZEN/GCACTTCATCCTTTG/3IABkFQ f: TGCTGAGCCCTTCTGAATC r: CTCCATTCTGAACCTGAGCTAT
<i>Oct3/4</i>	P:56-FAM/TCGAACCAC/ZEN/ATCCTTCTCTAGCCCA f: GTAGCCTCATACTTCTCTCGTTG r: CCTACAGCAGATCACTCACAT
Matrix proteins	
<i>Acan</i>	P: 56-FAM/ACCAGACAG/ZEN/TCAGATACCCCATCCA/3IABkFQ f: CCTTGTCACCATAGCAACCT r: CTACAGAACAGCGCCATCA
<i>Col2a1 2-4</i>	P: 56-FAM/AGAGTGCTG/ZEN/TCCCATCTGCCC/3IABkFQ f: CTCCTTTCTGCCCCTTTGG r: TCCTCTGCGATGACATTATCTG
<i>Coll0a1</i>	P: 56-FAM/TAGCCCCAA/ZEN/GACACAATACTTCATCCC/3IABkFQ f: ATGCCTTGTTCTCCTCTTACTG r: TGCTGAACGGTACCAAACG
Integrins	
<i>Itga10</i>	P: 56-FAM/CATTGTGAA/ZEN/CCAGCCTCAGCAGC/3IABkFQ f: TGTCACAGACTTGAACCTGGC r: CGATGTCAGGTGGTAAGGTG
Transcription factors	
<i>Runx2</i>	P: 56-FAM/TTACTGAGA/ZEN/GAGGAAGGCCAGAGGC/3IABkFQ f: AGGGATGAAATGCTTGGGAA r: GATGATGACACTGCCACCTC
<i>Sox9</i>	P: 56-FAM/AGACCACTA/ZEN/CCCGCATCTGCAC/3IABkFQ f: GTCTCTTCTCGCTCTCGTTC r: CGACCCATGAACGCCTT

5.5. Splinkerette PCR

Splinkerette PCR is a PCR based method to determine the number of transposon integration sites in genomic DNA (gDNA) [53, 239]. It allows to amplify the gDNA sequence that lies between the transposon terminal inverted repeats (TIRs) and a nearby restriction site [240].

A schematic depiction of the Splinkerette PCR protocol is given in Figure 24. Shortly, the gDNA is subjected to digestion with a type II restriction enzyme (DpnII) leading to sticky ends (1, 2). Then specially designed Splinkerette adapters consisting of a long strand adaptor and a short strand adaptor are ligated to these ends. The short strand adaptor contains a hairpin loop preventing end-repair priming (3). Next the junction between the genome and the transposon TIR is amplified in two nested PCR steps. During the first amplification step one of the primers consists of part of the sequence of the long strand adaptor (Splink1), whereas the other primer (Tbal Rev3) is compatible to a transposon-specific sequence located on the same strand the long strand adaptor is ligated to. Therefore, during the first PCR amplification step only one strand starting from the Tbal Rev3 primer is synthesized (4,I). During the next amplification step the Splink1 primer can now bind to that newly synthesized strand, and the genomic DNA-transposon-junction between Tbal Rev3 and Splink1 is amplified during the following PCR amplification steps (4,II). Next, a second PCR step using the Splink2 primer, which sequence is part of the long strand adaptor, and the Tbal primer, which sequence is compatible to part of the transposon sequence, is carried out to enhance the specificity (5). These PCR steps result in PCR products of a different length for each integration site as the distance of the integration event from the next restriction site is variable (6) [53, 240]. Therefore, the number of PCR products seen on the gel after agarose gel electrophoresis represents the number of integration sites [53].

Figure 24: Splinkerette PCR (next page):

A. Overview of the Splinkerette PCR protocol (self-designed). (1). Genomic DNA isolated from mouse iPSCs containing the transposon sequence at an unknown location is subjected to enzymatic digestion with a type II restriction enzyme (DpnII). (2). The digestion leads to sticky ends, generating a GATC overhang. (3). Ligation of the Splinkerette adaptor consisting of a long strand adaptor (lsA) and a short strand adaptor (ssA) containing a hairpin loop to the sticky ends. (4) First PCR amplification step of the genomic DNA-transposon-junction. The primer Splink1 contains part of the sequence of the long strand adaptor. Therefore, this primer is compatible to the strand synthesized during the first PCR amplification starting from the second primer (Tbal Rev3) which is compatible to a known sequence of the transposon. This ensures that only the genomic DNA-transposon-junction is amplified. (5). Second PCR amplification step of the genomic DNA-transposon-junction.

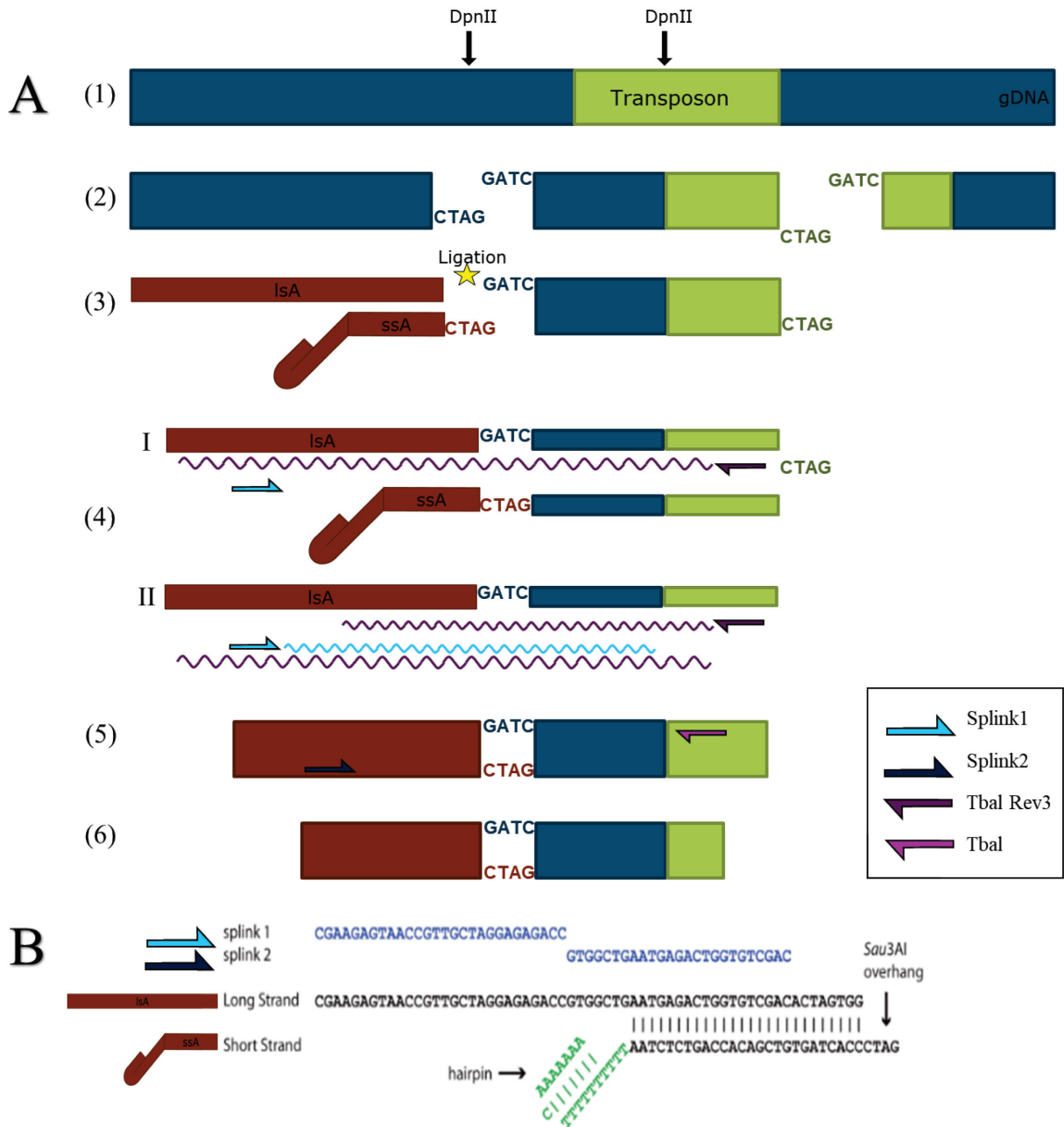


Figure 24: Splinkerette PCR (continued from previous page)

A (5, continued from previous page). To increase specificity a second nested PCR step is performed. The primers are identical to part of the sequence of the long strand adaptor (Splink) or compatible to the same strand of the transposon-sequence (Tbal). (6). The length of final PCR products is different for each integration site.

B. Primers and adaptors used for Splinkerette PCR, adapted from *Uren et al.* [240]. The sequences of the primers Splink1 and Splink2 are identical to parts of the long strand adaptor (IsA). The long strand adaptor and the short strand adaptor are partially compatible leading to formation of a CTAG-sticky end compatible to the GATC-overhang generated by the type II restriction enzyme during the first step of splinkerette PCR. The short strand adaptor contains a sequence that forms a hairpin-loop to prevent end-repair priming.

5.5.1. Isolation of genomic DNA

Total gDNA was isolated from mouse iPSCs by a phenol-chloroform extraction protocol. Cells were harvested and, when necessary, separated from feeder cells using standard procedures described in 5.2.1. *Standard cell culture conditions and procedures*, then lysed overnight in 250 – 500 μ l lysis buffer composed of 100 mM Tris-HCl pH 8.5, 5 mM EDTA, 0.2% SDS, 200 mM NaCl and 100 μ g/ml proteinase K (Merck, Darmstadt, Germany). After total lysis of the cells, 250 – 500 μ l of phenol-chloroform (1:1)-solution (Roth) was added to extract the gDNA. The samples were centrifuged for 5 min at 12 000 rpm resulting in two phases. The supernatant containing the gDNA was harvested and mixed with 250-500 μ l of chloroform (Merck). Then the samples were centrifuged again for 5 min at 12 000 rpm resulting in two phases. The supernatant containing the gDNA was harvested and mixed with 250 – 500 μ l of isopropanol (Merck) to precipitate the gDNA. The gDNA was pelleted by centrifugation and washed once with 70% ethanol. Finally, gDNA was resuspended in 50 – 100 μ l EB Buffer (10 mM Tris-HCl, pH 8.5). The gDNA concentration and purity was determined spectrometrically at A_{260} and $A_{260/280}$, respectively, using a Nanodrop 2000 spectrophotometer (ThermoFisher Scientific). gDNA Samples were stored at 4°C.

5.5.2. Digestion of gDNA

2 μ g of gDNA were digested with the restriction enzyme DpnII (New England Biolabs, Ipswich, Massachusetts, USA). The digestion mix consisting of 2 μ g gDNA, digestion buffer, and 10 U DpnII was incubated overnight at 37°C (Table 20). Then the restriction enzyme was heat inactivated at 65°C for 20 min. Agarose gel electrophoresis was performed to check for complete digestion of gDNA using a 0.8% agarose gel at 120V for 60 min.

Table 20: gDNA digestion set up and program

total gDNA	x μ l \cong 2 μ g	<i>37°C overnight</i> <i>Heat inactivation: 65°C for 20 min</i>
10x NEBuffer	3 μ l	
Dpn II (10 U/ml)	1 μ l	
dH ₂ O	30 μ l – x μ l	
Total volume	30 μl	

5.5.3. Ligation of digested gDNA with Splinkerette adapters

Splinkerette adapters were ligated to the sticky ends of the digested gDNA. Prior to ligation the Splinkerette adapter mix consisting of 25 μM long strand adapter and 25 μM short strand adapter in 5x NEB Buffer 2 (New England Biolabs) was denaturated at 95°C for 5 min, and annealing of the adapters to each other was allowed by slowly cooling the probe down to room temperature at a rate of 0.1°C/s. Then the gDNA ligation mix (Table 21) consisting of 1 μl Splinkerette adapter mix, 4.5 μl digested and heat inactivated gDNA digestion mix, 2 μl DNA ligase buffer and 40 U T4 DNA Ligase (Promega, Madison, USA) was incubated at 4°C overnight. The reaction was stopped by heat inactivation of the ligase at 65°C for 20 min.

Table 21: gDNA ligation set up and program

Digested gDNA	4.5 μl	<i>4°C overnight</i> <i>Heat inactivation: 65°C for 20 min</i>
Splinkerette adapter mix	1 μl	
T4 DNA ligase buffer	2 μl	
T4 DNA ligase (20U/ μl)	2 μl	
dH ₂ O	35.5 μl	
Total volume	40 μl	

5.5.4. PCR amplifications

Finally, the junction region between the genome and the transposon was amplified in two consecutive PCRs. To enhance the specificity, touch-down protocols were used.

Reaction set ups and PCR protocols are shown in Tables 22 and 23. The reagents are the same used in 5.4.3. *Semi-quantitative Reverse-Transcription (RT)-PCR*.

Table 22: Set up and program of the first PCR amplification

10x PCR reaction buffer	5.0 μ l	94°C	3 min
Primer Splink1	1.0 μ l	15 cycles	94°C 30 s
Primer Tbal Rev3	1.0 μ l		70°C 30 s
dNTP mix	1.0 μ l		72°C 30 s
Taq polymerase	0.5 μ l	5 cycles	94°C 30 s
Ligated digested DNA	5.0 μ l		63°C 30 s
dH ₂ O (PCR grade)	36.5 μ l		72°C 2 s (+2 s/cycle)
Total volume	50 μl	5 cycles	94°C 30 s
			62°C 30 s
			72°C 12 s (+2 s/cycle)
		5 cycles	94°C 30 s
			61°C 30 s
			72°C 22 s (+2 s/cycle)
		5 cycles	94°C 30 s
			60°C 30 s
			72°C 30 s
		72°C	5 min
		4°C	forever

Table 23: Set up and program of the second PCR amplification

10x PCR reaction buffer	2.0 μ l	94°C	3 min
Primer Splink2	0.5 μ l	10 cycles	94°C 30 s
Primer Tbal	0.5 μ l		65°C 30 s
dNTP mix	0.4 μ l		72°C 30 s
TAQ	0.2 μ l	25 cycles	94°C 30 s
First PCR amplification mix	1.0 μ l		58°C 30 s
dH ₂ O	15.4 μ l		72°C 30 s
Total volume	20μl	72°C	5 min
		4°C	forever

5.5.5. Oligonucleotides used for Splinkerette PCR

The sequences of the Splinkerette adapters and the PCR primers used for Splinkerette PCR are listed in Table 24 below.

Table 24: Oligonucleotides used for Splinkerette PCR

Name	Sequence (5' to 3')	Ref.
Splinkerette adaptors		
long strand adaptor (lsA)	<i>CGAAGAGTAACCGTTGCTAGGAGAGACCGTGGCTGAATGAGACTGGTGTCGACACTAGTGC</i>	[240]
short strand adaptor (ssA)	<i>GATCCCACTAGTGTCGACACCAGTCTCTAATTTTTTTTTTCAAAAAA</i>	[240]
Primers		
Splink1	<i>CGAAGAGTAACCGTTGCTAGGAGAGACC</i>	[240]
Splink2	<i>GTGGCTGAATGAGACTGGTGTCGAC</i>	[240]
Tbal Rev3	<i>CATGACATCATTCTGGAATT</i>	[53]
Tbal	<i>CTTGTGTCATGCACAAAGTAGATGTCC</i>	[53]

5.6. Histological analysis

5.6.1. Processing of samples

5.6.1.1. Fixation

For histological analysis, chondrogenic nodules and spheroids were washed twice with PBS before fixation in pre-cooled 4% paraformaldehyde (PFA, Merck) in PBS for 30 min at room temperature. Next, the fixed samples were washed twice with PBS to remove all remaining PFA.

5.6.1.2. Embedding

After fixation, samples were placed in ascending solutions of sucrose (Sigma) in PBS: 10% and 20% for 30 min at room temperature and 30% overnight at 4°C. The next day, samples were transferred to disposable vinyl specimen molds (Cryomolds, Tissue Tek Sakura Finetek, Torrance, California, USA) and embedded in cryomedium (OCT, Tissue Tek). Then samples were placed on the surface of a chilled chopper plate on dry ice until frozen completely. Samples were wrapped in Parafilm (Bemis, Oshkosh, Wisconsin, USA) and stored at -20°C until further processing.

5.6.1.3. Sectioning

Cryosectioning was performed with a cryotome Microm HM5000 (Fisher, Walldorf, Germany). Slices of 10 µm thickness were collected onto SuperFrost glass slides (ThermoScientific) and stored at -20°C until use.

5.6.2. Histochemical staining

5.6.2.1. Safranin Orange staining

Safranin Orange is a cationic dye showing high affinity to negatively charged GAG chains of proteoglycans in the extracellular matrix of cartilage [241]. The intensity of the resulting red-orange color is proportional to the proteoglycan content in the section [241].

For Safranin Orange staining cryosections of chondrogenic nodules and spheroids were washed 2 x 3 min with PBS to remove any remaining cryomedium. Then the samples were covered with 0.1% Safranin Orange (Sigma-Aldrich) solution in dH₂O for 5 min. Subsequently, excessive staining solution was removed by turning the slides on Wattman paper (Sigma) and the slides were mounted with Roti-Histokitt (Sigma).

5.6.2.2. Toluidine blue staining

Negatively charged GAG chains of proteoglycans in the ECM of cartilage are stained blue-violett by the cationic dye Toluidine blue [241].

For Toluidine blue staining cryosections of chondrogenic nodules and spheroids were washed 2 x 3 min with PBS to remove any remaining cryomedium. Then the samples were covered with 0.1% Toluidine Blue (Sigma) solution in toluidine blue buffer (0.05 M K₂HPO₄ and 0.04 M HCl pH 2,5) for 5 min. Subsequently excessive staining solution was removed by turning the slides on Wattman paper (Sigma) and the slides were mounted with Roti-Histokitt (Sigma).

5.6.3. Immunohistochemistry

To verify deposition of type II collagen and aggrecan in the ECM of the chondrogenic nodules and spheroids, we performed immunohistochemistry (IHC) on cryosections. The antibodies used are listed in Table 25.

The slides were washed twice in PBS to remove any remaining cryomedium. Endogenous peroxidase activity was blocked for 20 min at room temperature with 1% H₂O₂ (Carl Roth) in

absolute methanol (Merck). Then 0.2% bovine testicular hyaluronidase in PBS (pH 5, Sigma-Aldrich) was applied to the sections at 37°C for 30 min before blocking.

For aggrecan detection, blocking was performed with 1% BSA in PBS for 1h at room temperature followed by overnight incubation with the primary antibody at 4°C. The next day the slides were washed twice in PBS to remove any antibody that did not bind before incubation with biotinylated secondary antibody in 1% BSA for 1h.

Since the type II collagen primary antibody is a monoclonal, mouse antibody (II-II6B3, Developmental Studies Hybridoma Bank, University of Iowa, Iowa City, Iowa, USA) we used the MOM Kit (VectorLabs, Burlingame, California, USA) for reliable detection of the antigen on the mouse tissue. After blocking with the MOM Mouse Ig Blocking Reagent (4% in PBS) for 1h at room temperature, the sections were preincubated in MOM diluent (5% MOM Protein Concentrate in PBS) for 5 min at room temperature followed by overnight incubation with the primary antibody. After washing the sections twice in PBS, the next day biotinylated anti-mouse-IgG-Reagent (4% in PBS) was applied to the sections for 10 min at room temperature.

Antibody binding was detected by the Vectastain ABC Kit (VectorLabs) followed by diaminobenzidine (DAB) staining. Shortly, the Vectastain ABC reagent, prepared according to the manufacturer's instruction, was applied to the slides for 30 min (aggrecan) or 5 min (type II collagen) at room temperature. Then the slides were immersed in DAB staining solution (0.027% 3,3'-diaminobenzidine (Sigma) in 25 mM Tris-HCl, pH 7.6 + 120 μ l 5% H₂O₂ in dH₂O) for 7 min at room temperature in the dark. Then slides were washed with dH₂O and mounted with Roti-Mount Aqua (Carl Roth), and covered with 20 x 40 mm cover slips.

Table 25: Antibodies for immunohistochemistry

Target	Type	Company Catalogue number	Dilution
Primary Antibodies			
Anti-Aggrecan	polyclonal Rabbit IgG	Merck Millipore AB1031	1:400 in 1% BSA
Anti-Collagen II	monoclonal Mouse IgG ₁	DSHB II-II6B3	1:400 in MOM diluent
Secondary Antibodies			
Anti-Rabbit IgG	biotinylated	Vectastain ABC HRP Kit (Rabbit IgG) PK-4001	1:200 in 1% BSA
Anti-Mouse IgG	biotinylated	Vectastain MOM Kit	1:250 in PBS

5.7. Chemicals

Unless otherwise indicated, chemicals and reagents were obtained from one of the following distributors:

- Invitrogen, Thermo Fisher Scientific, Waltham, Massachusetts, USA
- Sigma-Aldrich/Merck, Darmstadt, Germany
- Carl Roth, Karlsruhe, Germany

5.8. Microscopy

To take representative phase contrast, bright field and fluorescent pictures, we either used the AxioCam Color 105 or the AxioCam MRm Camera (both Carl Zeiss) mounted on an AxioObserver.Z1 microscope (Carl Zeiss). For large specimen we used the AxioCam Color 105 camera mounted on a Stemi 2000-CS 3D microscope (Carl Zeiss).

5.9. Computer programs and statistics

In this thesis, quantitative data was evaluated and various graphs were created by Microsoft Office Excel 2010 (Microsoft, Redmond, USA), SPSS 25.0 (IBM SPSS Statistics, Ehningen, Germany) and Graph Pad Prism7 (GraphPad, La Jolla, USA). Data are shown as mean \pm standard deviation (SD) for normally distributed data or as median (interquartile range, IQR) for non-normally distributed data. For comparison of two groups, paired or unpaired t-tests or Mann-Whitney-U-tests were performed as applicable. For comparison of more than two groups ANOVA was used. A p-value < 0.05 was considered statistically significant and p-values were adapted for multiple testing where necessary.

Photomicrographs were processed with ZEN2012 – ZEISS Efficient Navigation software (Carl Zeiss) and arranged in figures with Adobe Photoshop CS26 (Adobe System, San Jose, USA). Morphometric analyses were performed with ImageJ 1.41 (<http://rsb.info.nih.gov/ij/>, USA).

The following link was used as major source of publications: <http://www.ncbi.nlm.nih.gov/sites/entrez> and references were managed by EndNote X8 (Thomson Reuters, New York City, USA).

6. Results

6.1. Isolation and culture of primary fibroblasts

Murine fibroblasts were the first cells to be successfully reprogrammed and have been widely used for the assessment of different reprogramming methods [15, 53].

Primary fibroblasts were isolated from mouse embryos at 12.5 – 13.5 dpc (MEFs) as well as from ear (EAR-FBs) and tail (TAIL-FBs) of adult wild-type mice.

The cell suspension gained from dissected mouse embryos contained a high number of cells from various types. However, after 24h in culture only few spindle shaped cells had adhered to the tissue culture plate. These were considered as murine embryonic fibroblasts (MEFs). These cells rapidly expanded and nearly covered the complete 10 cm-dish 72h after isolation. The cells maintained their typical morphology and high proliferation rate for many passages (up to P10) (Figure 25A). After Mitomycin C treatment, however, proliferation ceased. Otherwise, the cells appeared healthy and could be used as feeder cells for pluripotent stem cells.

After mincing and digesting the tissue chunks from ear and tail tip, cells started to spread out from the tissue chunks. EAR-FBs and TAIL-FBs both initially showed a spindle-shaped morphology but started to spread out during culture. EAR-FBs and TAIL-FBs were morphologically indistinguishable (Figure 25 B and C). EAR-FBs however, proliferated faster than TAIL-FBs as they could be passaged at a 1 : 2 ratio every 4 – 5 days whereas TAIL-FBs could only be passaged at a 1 : 2 ratio every 6 – 7 days.

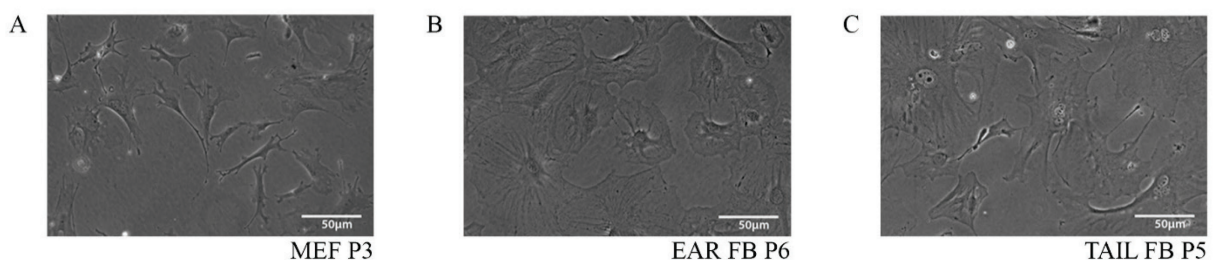


Figure 25: Morphology of primary murine fibroblasts.

(A) Murine embryonic fibroblasts (MEFs) at passage 3. (B) Murine fibroblasts isolated from ear (EAR-FBs) at passage 6. (C) Murine fibroblasts isolated from tail (TAIL-FBs) at passage 5. Scale bars represent 50 µm.

6.2. Nucleofection of primary fibroblasts

Nucleofection is an efficient, electroporation-based delivery method for plasmids that transfers nucleic acids directly to the nucleus [43]. Transposons are not equipped to cross cell membranes themselves, therefore delivery of the transposon plasmids into target-cells is a rate-limiting factor in transposition [42]. Nucleofection has been shown suitable for the delivery of Sleeping Beauty transposon-based reprogramming plasmids into fibroblasts [53].

However, efficiency and survival rates vary among cell types and depend upon the solutions and programs used. Therefore, the first step was to find the optimal program and solution for the primary fibroblasts used in the subsequent reprogramming experiments. Several nucleofections with the *pmaxGFP* vector using different programs and solutions were performed as recommended by the manufacturer to optimize efficiency and survival rates. The results of the optimization are summarized in Table 26 – 28. Figure 26 shows representative photomicrographs of nucleofected fibroblasts expressing GFP.

For primary mouse embryonic fibroblasts (MEFs) we achieved the best results with the solution P3 and the program EH-198. 86% ($\pm 3\%$) of the cells survived the nucleofection procedure. Of these about 87% ($\pm 9\%$) expressed GFP 24h after nucleofection. For primary fibroblasts derived from ear (EAR-FBs) or tail-tips (TAIL-FBs) of adult wild type mice the best results were achieved with the solution P2 and the program EH-198. EAR-FBs showed a survival rate of 73% ($\pm 6\%$) and an efficiency rate of 41% ($\pm 4\%$). 62% ($\pm 5\%$) of the TAIL-FBs survived nucleofection and of these about 53% ($\pm 7\%$) showed GFP expression the next day.

Table 26: Nucleofection of MEFs with the *pmaxGFP* vector (P3 Solution)

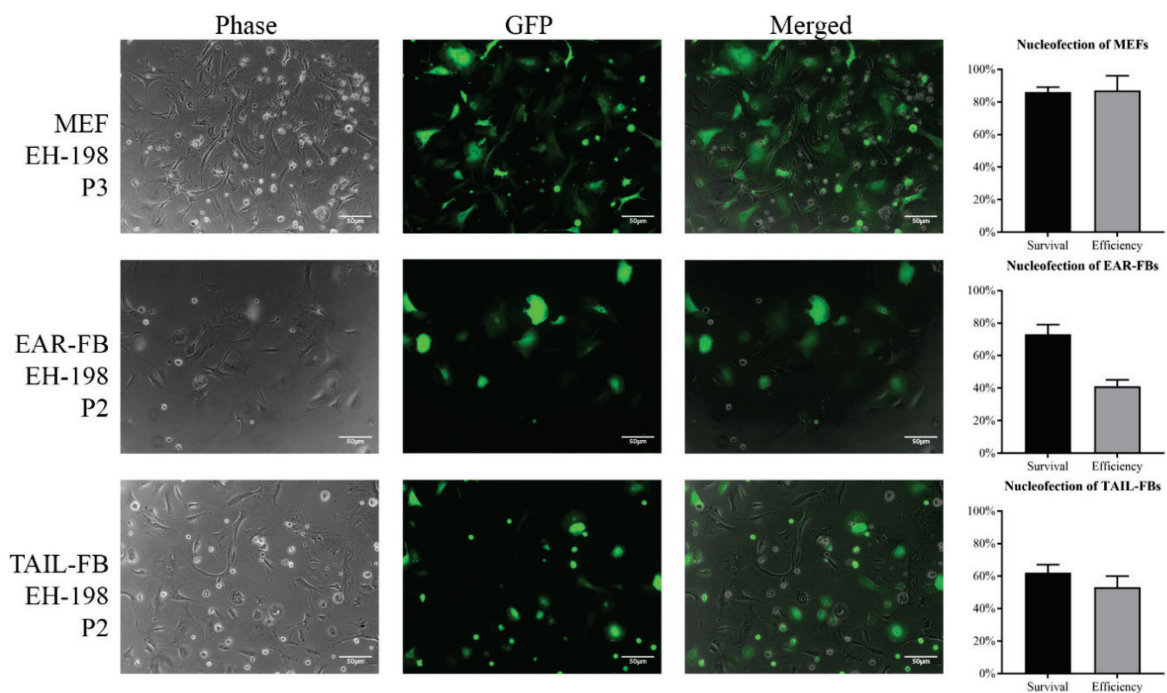
Program	Survival rate (\pm SD)	Efficiency (\pm SD)
EN-150	0.93 (\pm 0.05)	0.62 (\pm 0.10)
EH-198	0.86 (\pm 0.03)	0.87 (\pm 0.09)
EH-156	0.74 (\pm 0.04)	0.90 (\pm 0.05)
ER-150	0.56 (\pm 0.07)	0.54 (\pm 0.16)

Table 27: Nucleofection of EAR-FBs with the *pmaxGFP* vector (P2 Solution)

Program	Survival rate (\pm SD)	Efficiency (\pm SD)
EN-150	0.74 (\pm 0.04)	0.10 (\pm 0.02)
EH-198	0.73 (\pm 0.06)	0.41 (\pm 0.04)
EH-156	0.71 (\pm 0.02)	0.45 (\pm 0.03)
ER-150	0.66 (\pm 0.04)	0.47 (\pm 0.07)

Table 28: Nucleofection of TAIL-FBs with the *pmaxGFP* vector (P2 Solution)

Program	Survival rate (\pm SD)	Efficiency (\pm SD)
EN-150	0.70 (\pm 0.03)	0.19 (\pm 0.04)
EH-198	0.62 (\pm 0.05)	0.53 (\pm 0.07)
EH-156	0.58 (\pm 0.08)	0.23 (\pm 0.10)
ER-150	0.49 (\pm 0.16)	0.13 (\pm 0.08)

**Figure 26: Nucleofection of primary fibroblasts with the *pmaxGFP* vector.**

MEFs, EAR-FBs and TAIL-FBs were nucleofected using the *pmaxGFP* vector and different solutions and programs. Survival rate was estimated by counting the dead cells in the supernatant, whereas efficiency rate was estimated by the percentage of cells showing GFP expression 24h after nucleofection. Using program EH-198 and solution P3 86% (\pm 3%) of the MEFs expressed GFP 24h after nucleofection. EAR-FB showed an efficiency rate of 41% (\pm 4%), whereas 53% (\pm 7%) of the TAIL-FBs were positive for GFP. Bars indicate 50 μ m.

6.3. Reprogramming of primary fibroblasts

6.3.1. Reprogramming of MEFs, EAR-FBs and TAIL-FBs with the *pT2OSKM(L)* plasmid

6.3.1.1. Reprogramming of MEFs with the *pT2OSKM* or *pT2OSKML* plasmid

MEFs at passage 3 were nucleofected with the *SBI100X* and the *pT2OSKM* or the *pT2OSKML* plasmid in a ratio of 1 : 10 (0.5 µg and 5 µg or 0.2 µg and 2 µg), then transferred to Geltrex-coated 6-well plates, and maintained in ESC-medium. Around day 5, first clusters of small cells started to form, which still displayed a fibroblast-like morphology. At day 11, the cells were transferred to feeder cells, and by day 13 small IPSC-like colonies became visible in all wells.

By day 20, the colonies were big enough to be mechanically picked and transferred to feeder-coated 24-well plates. Picking was performed at days 20, 21 and 22 and altogether 96 colonies were picked. The thereby established clonal cell lines were named TAXX (TA01 – TA96). The cell lines were maintained in mouse IPSC medium on feeder cells for three to five days before they were either frozen for long term storage or discarded.

From the plate containing the colonies derived from transfection with 2 µg *pT2OSKM* 20 colonies could be picked. Seven from the thereby established cell lines consisted of many small colonies displaying the typical IPSC morphology (*bona fide* IPSC), whereas in one well no colonies were forming at all. The remnant wells contained either only few colonies that grew slowly or colonies that failed to maintain the typical IPSC morphology, and showed signs of dedifferentiation. From the colonies derived from MEFs nucleofected with 5 µg *pT2OSKM* 30 colonies were picked. Of these 9 *bona fide* IPS cell lines were emerging, whereas 7 wells completely failed to form colonies. From the nucleofection with 2 µg *pT2OSKML* 30 colonies were picked of which 9 gave rise to *bona fide* IPSC colonies and none failed to form colonies at all. 16 colonies were picked from the plate containing the colonies derived from nucleofection with 5 µg *pT2OSKML* and a single IPS cell line could be established, whereas in 7 wells no colonies formed at all.

These results are summarized in Table 29. From the 26 cell lines initially showing a typical IPSC morphology, 6 were chosen for further propagation and assessment.

Table 29: Cell lines established from MEFs reprogrammed with *pT2OSKM* or *pT2OSKML*

Plasmid	Colonies picked	<i>Bona fide</i> iPSC	no colonies
2 µg <i>pT2OSKM</i>	20	7 (35%)	1 (5%)
5 µg <i>pT2OSKM</i>	30	9 (33%)	7 (23%)
2 µg <i>pT2OSKML</i>	30	9 (33%)	0 (0%)
5 µg <i>pT2OSKML</i>	16	1 (6%)	7 (43%)
TOTAL	96	26 (27%)	15 (16%)

6.3.1.2. Reprogramming of EAR-FBs with the *pT2OSKM* or *pT2OSKML* plasmid

EAR-FBs at passage 6 were nucleofected with the *SB100X* and the *pT2OSKM* or the *pT2OSKML* plasmid in a ratio of 1 : 10 (0.5 µg and 5 µg or 0.2 µg and 2 µg). After nucleofection the cells were transferred to feeder-coated 6-well plates and maintained in mouse iPSC medium. However, by day 9 the cell layer became very dense with the cells forming a thin tissue-like sheet that started to lift off the plate at the borders. Therefore, the plates were trypsinized and the cell suspension was transferred to 6 cm-cell culture dishes at day 10. Around day 15, the first iPSC-like colonies emerged, and at day 17 all dishes contained many small iPSC-like colonies.

Colonies were picked at day 19, 21 and 23 and maintained on feeder-coated 24-well plates for 5 to 7 days. 12 colonies were picked for each reprogramming factor dosage and the established clonal cell lines were named ETAXX (ETA01 – ETA46). As 7 wells contained only a single big colony after picking, these cells were trypsinized to dissociate the colony, and reseeded into the same well to allow formation of multiple small colonies. 12 cell lines initially or after being passaged once formed many small colonies displaying the typical iPSC morphology and were considered *bona fide* iPSCs. From these, 5 clones were chosen for further propagation and assessment. In 11 wells however, no colonies were emerging at all. The remaining 25 wells contained either only few colonies that grew slower than the *bona fide* iPSCs or contained colonies that started to flatten and dedifferentiate. Table 30 summarizes these results.

Table 30: Cell lines established from EAR-FBs reprogrammed with *pT2OSKM* or *pT2OSKML*

Plasmid	Colonies picked	<i>Bona fide</i> iPSC	no colonies
2 µg <i>pT2OSKM</i>	12	7 (58%)	1 (8%)
5 µg <i>pT2OSKM</i>	12	2 (17%)	4 (33%)
2 µg <i>pT2OSKML</i>	12	1 (8%)	3 (25%)
5 µg <i>pT2OSKML</i>	12	2 (17%)	3 (25%)
TOTAL	46	12 (26%)	11 (24%)

6.3.1.3. Reprogramming of TAIL-FBs with the *pT2OSKM* or *pT2OSKML* plasmid

TAIL-FBs at passage 5 were nucleofected with the *SB100X* and the *pT2OSKM* or the *pT2OSKML* plasmid in a ratio of 1 : 10 (0.5 µg and 5 µg or 0.2 µg and 2 µg). After nucleofection the cells were transferred to feeder-coated 6-well plates and maintained in mouse iPSC medium. Around day 12, the first iPSC-like colonies became visible.

Picking of colonies was performed at days 19, 24 and 27. Altogether 44 colonies were picked and the established cell lines were named TTA XX (TTA01 – TTA44). Half of the wells initially contained only a single large colony. Therefore, after 4 to 7 days, these wells were trypsinized once to dissociate this colony into single cells and allow formation of multiple small iPSC colonies. After 4 to 11 days, 16 of the wells contained many small *bona fide* iPSC colonies, of which 4 were chosen for further propagation and assessment. However, one of these chosen cell lines (TTA19) failed to maintain iPSC-like morphology during propagation likely due to incomplete reprogramming, and was discarded. The remaining 3 clonal cell lines were assessed for pluripotency traits. Three clonal cell lines were discarded after picking as they did not contain any iPSC-like colonies. These results are summarized in Table 31.

Table 31: Cell lines established from TAIL-FBs reprogrammed with *pT2OSKM* or *pT2OSKML*

Plasmid	Colonies picked	<i>Bona fide</i> iPSC	no colonies
2 µg <i>pT2OSKM</i>	13	4 (31%)	0 (0%)
5 µg <i>pT2OSKM</i>	12	5 (42%)	1 (8%)
2 µg <i>pT2OSKML</i>	6	2 (33%)	1 (17%)
5 µg <i>pT2OSKML</i>	13	5 (38%)	1 (8%)
TOTAL	44	16 (36%)	3 (7%)

Figure 27 gives an overview of the strategies used to reprogram MEFs, EAR-FBs and TAIL-FBs with the *pT2OSKM* or *pT2OSKML* plasmid. In summary, all tested strategies led to successful establishment of several IPS cell lines. About $\frac{1}{3}$ (26 – 36%) of all initially picked colonies gave rise to *bona fide* iPSC cell lines. Colonies derived from *pT2OSKML* plasmids initially showed a flatter morphology with more roughened borders than colonies derived from the *pT2OSKM* plasmids. These differences, however, vanished after picking and subsequent passaging, and the colonies reprogrammed with the *pT2OSKM* or *pT2OSKML* plasmid became indistinguishable.

Notably, from TAIL-FBs less colonies that were harder to break down into a single cell suspension could be picked than from EAR-FBs and MEFs. This is likely due to the passaging step in the reprogramming protocols used for EAR-FBs and MEFs as emerging colonies by day 10 or 11 were disrupted by passaging and could give rise to several daughter colonies. But, although the overall number of colonies available for picking can be increased by the passaging step, it bears the risk that several cell lines originate from the same starting cell.

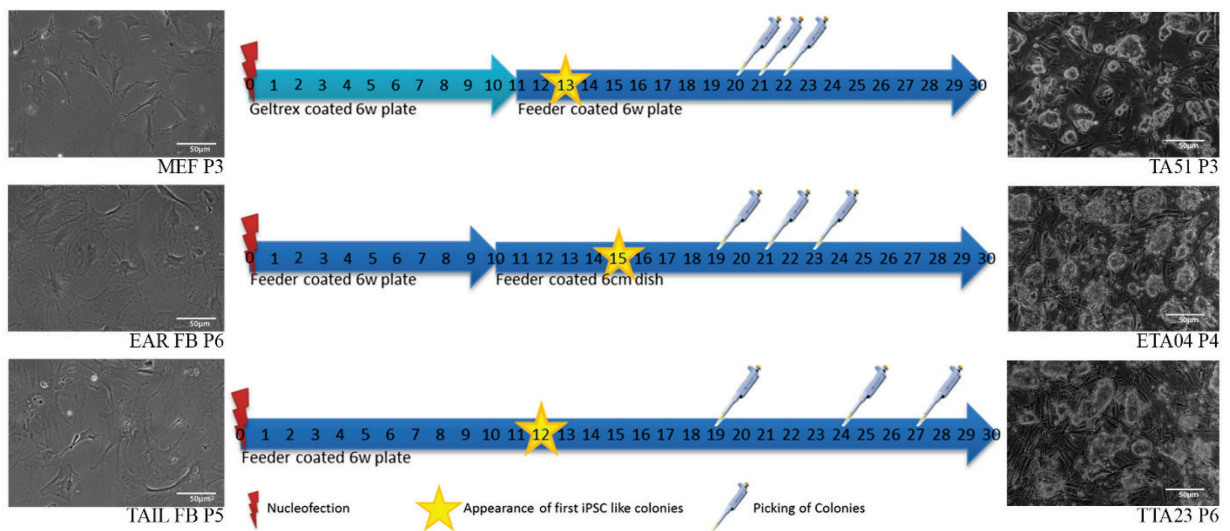


Figure 27: Reprogramming of MEFs, EAR-FBs and TAIL-FBs with the *pT2OSKM* and *pT2OSKML* plasmids.

Schematic depiction of the reprogramming strategies used for MEFs, EAR-FBs and TAIL-FBs. After nucleofection with the *pT2OSKM* or *pT2OSKML* plasmid, MEFs were initially seeded onto Geltrex-coated 6-well plates and transferred to feeder-coated 6-well plates on day 11. The first colonies were visible at day 13, and picking was performed on days 20, 21 and 22. EAR-FBs were seeded onto feeder-coated 6-well plates after nucleofection with the reprogramming factor plasmids and passaged onto feeder-coated 6 cm-cell culture dishes on day 10. The first small colonies became visible around day 15 and could be picked on days 19, 21 and 23. TAIL-FBs were cultured on a feeder-coated 6-well plate after nucleofection. The first iPSC-like colonies could be detected around day 12. Colonies were picked at days 19, 24 and 27. Scale bars represent 50 μm.

6.3.2. Reprogramming of EAR-FBs with the *RMCE-OSKM(L)-Cherry* plasmid

The *RMCE-OSKM(L)-Cherry* plasmids additionally to the reprogramming factor cassette contain an (*EOS3+*)*mCherry* pluripotency reporter cassette and the transgene is flanked by heterospecific *loxP* sites allowing modification by recombinase mediated cassette exchange (RMCE) [53].

After nucleofection of EAR-FBs at passage 8 with 0.1 μg or 0.2 μg of the *SBI00X* plasmid and 1 μg or 2 μg of the *RMCE-OSKM(L)-Cherry* plasmid (ratio 10:1), the cells were either seeded onto Geltrex-coated, feeder-coated or uncoated 10 cm-cell culture dishes and maintained under ESC conditions. The first colonies became visible around day 13 under all three conditions and were picked on days 20 and 24. Figure 28 summarizes the reprogramming strategy used for EAR-FBs and *RMCE-OSKM(L)-Cherry* plasmids.

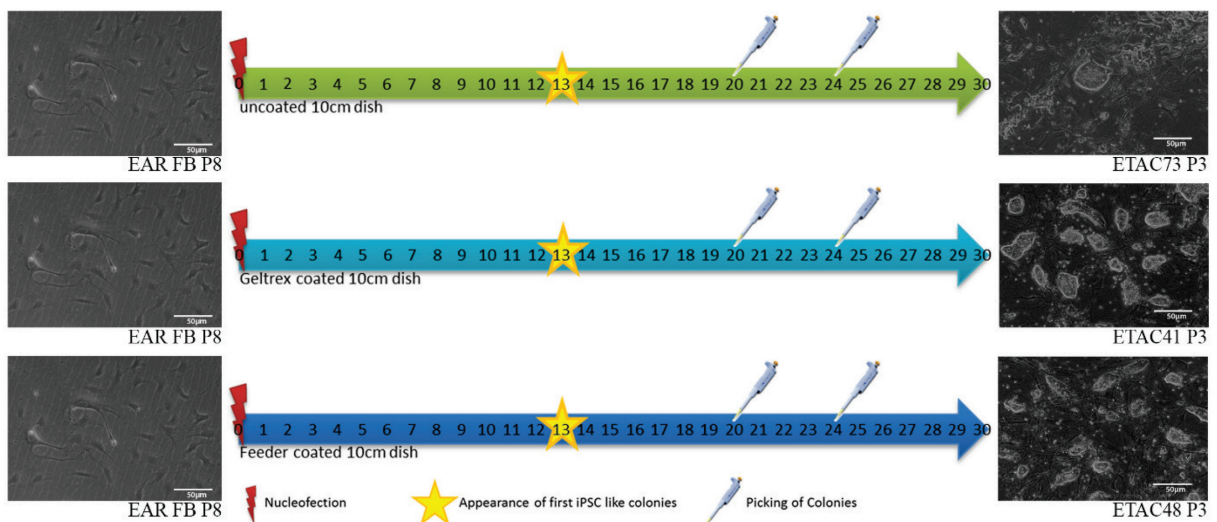


Figure 28: Reprogramming of EAR-FBs with the *RMCE-OSKM(L)-Cherry* plasmids.

Schematic depiction of the reprogramming strategies used for EAR-FBs with the *RMCE-OSKM(L)-Cherry* plasmids. After nucleofection, EAR-FBs were seeded either onto uncoated, Geltrex-coated or feeder-coated 10 cm-cell culture dishes and maintained under ESC conditions. The first small colonies became visible around day 13 and could be picked at day 20 and 24.

Altogether, 96 colonies were picked from the EAR-FBs reprogrammed with the *RMCE-OSKM(L)-Cherry* plasmids, and the established clonal cell lines were named ETACXX (ETAC01 - ETAC96). Of these, 41 *bona fide* IPS cell lines emerged whereas in 24 wells no colonies could be detected. Notably, from the EAR-FBs reprogrammed with only 1 μg of reprogramming factor plasmids less colonies could be picked than from the FBs reprogrammed with 2 μg of the reprogramming factor plasmids (21 colonies from 1 μg *RMCE-OSKM-Cherry* and *RMCE-OSKML-Cherry* each vs. 27 colonies from 2 μg *RMCE-OSKM-Cherry* and *RMCE-OSKML-Cherry* each). There was no difference in the number of colonies that could be picked from the different coatings. The exact results are listed in Table 32.

17 clonal cell lines were chosen for further analysis, however, 4 of these failed to maintain IPSC morphology during further propagation and were discarded.

Table 32: Cell lines established from EAR-FBs reprogrammed with *RMCE-OSKM(L)-Cherry*

Plasmid	Coating	Colonies picked	<i>Bona fide</i> IPSC	no colonies
1 μg <i>RMCE-OSKM</i>	no coating	8	4 (50%)	2 (25%)
1 μg <i>RMCE-OSKM</i>	Geltrex	7	1 (14%)	4 (57%)
1 μg <i>RMCE-OSKM</i>	Feeder	6	1 (17%)	2 (33%)
2 μg <i>RMCE-OSKM</i>	no coating	9	5 (56%)	1 (11%)
2 μg <i>RMCE-OSKM</i>	Geltrex	9	3 (33%)	2 (22%)
2 μg <i>RMCE-OSKM</i>	Feeder	9	3 (33%)	4 (44%)
1 μg <i>RMCE-OSKML</i>	no coating	7	3 (43%)	2 (29%)
1 μg <i>RMCE-OSKML</i>	Geltrex	7	3 (43%)	1 (14%)
1 μg <i>RMCE-OSKML</i>	Feeder	7	3 (43%)	2 (29%)
2 μg <i>RMCE-OSKML</i>	no coating	9	2 (22%)	4 (44%)
2 μg <i>RMCE-OSKML</i>	Geltrex	9	6 (67%)	0 (0%)
2 μg <i>RMCE-OSKML</i>	Feeder	9	7 (77%)	0 (0%)
TOTAL		96	41 (43%)	24 (25%)

6.3.3. Morphological changes during the reprogramming process

Cells of a mesenchymal origin like *for example* fibroblasts undergo a mesenchymal to epithelial transition (MET) during reprogramming [68, 73]. This includes changes of the gene expression pattern and cell morphology.

During the reprogramming process, fibroblasts were observed daily for signs of ongoing reprogramming. Representative photomicrographs taken during the reprogramming process of EAR-FBs with *RMCE-OSKM(L)-Cherry* are depicted in Figure 29.

By day 9, the fibroblasts cultured on uncoated or Geltrex-coated dishes had become highly confluent and the fibroblast and feeder cells had formed a dense cell layer in the feeder-coated dishes. Within these cell sheets, diffuse clusters of small round cells started to form, probably corresponding to fibroblasts undergoing MET and gaining ESC-like proliferation rate during the initiation phase of reprogramming [69, 70].

By day 13, these clusters had increased in size and spread out diffusely among the surrounding fibroblasts in the uncoated and Geltrex-coated dishes, whereas in the feeder-coated plates already small iPSC-like colonies became visible. By day, 19 iPSC-like colonies had formed in all plates, and the size was considered appropriate for picking which was performed the next day.

Notably, the colonies in the uncoated and Geltrex-coated dishes showed more roughened borders and were harder to dislodge from the surrounding cell sheet than the colonies in the feeder-coated dishes. Furthermore, colonies reprogrammed with the *RMCE-OSKML-Cherry* plasmid appeared more flattened than colonies resulting from nucleofection with *RMCE-OSKM-Cherry*. These differences, however, vanished after picking and subsequent passaging, and the established clonal cell lines became morphologically indistinguishable.

Conclusively, clonal IPS cell lines could be successfully established from EAR-FBs by nucleofection with the *RMCE-OSKM-Cherry* or the *RMCE-OSKML-Cherry* plasmid regardless of the coating (uncoated, Geltrex-coated or feeder coated 10 cm-cell culture dish) they were maintained on during the reprogramming process.

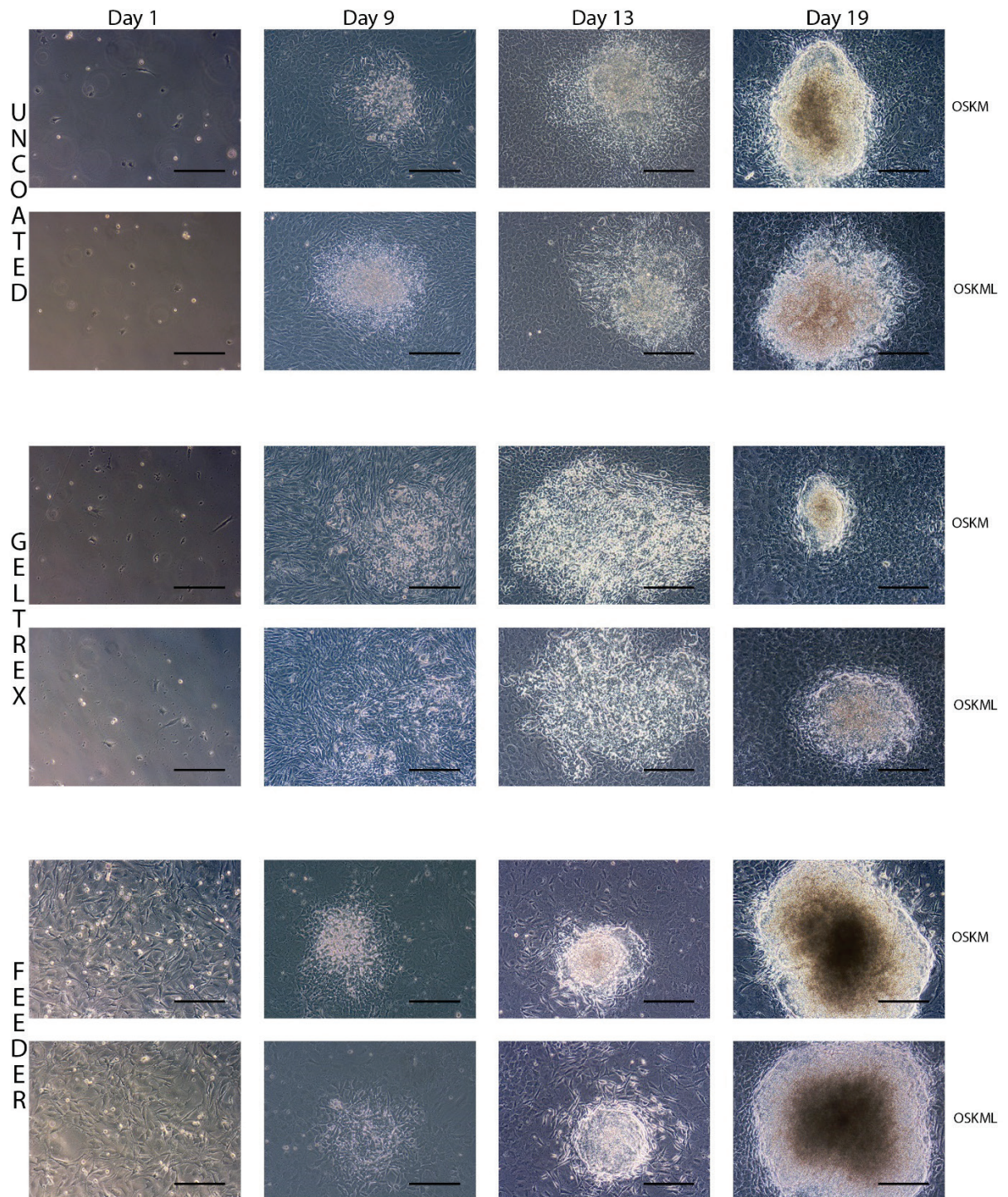


Figure 29: Morphological changes of EAR-FBs during reprogramming with *RMCE-OSKM(L)-Cherry* plasmids cultured on different coatings.

Morphological changes of EAR-FBs cultured either on uncoated, Geltrex-coated or feeder-coated 10 cm-cell culture dishes after nucleofection with the *RMCE-OSKM-Cherry* or *RMCE-OSKML-Cherry* plasmid. Scale bars represent 50 μm.

6.4. Analysis of induced pluripotent stem cells

6.4.1. Morphology and proliferation

Mouse embryonic stem cells (mESCs) grow in characteristic round, dome-shaped colonies composed of small cells with large nuclei and scant cytoplasm when maintained on feeder cells (Figure 30A) [15, 23]. The morphology of successfully reprogrammed iPSCs is highly similar to ESCs [15].

After picking, the newly established TA, ETA, TTA and ETAC murine IPS cell lines were cultured on feeder cells. They showed a mESC-like proliferation rate and could be splitted in a ratio of 1 : 5 – 1 : 10 every 2 – 4 days. Successfully reprogrammed iPSCs formed characteristic round, dome-shaped colonies with smooth and bright edges when cultured on feeder cells and maintained this morphology up to high passages (Figure 30B).

ETAC-iPSCs contain additionally to the reprogramming factor cassette an *(EOS3+)mCherry* pluripotency reporter cassette. Therefore, successfully reprogrammed colonies initially exhibited red fluorescence. At higher passages, however, this fluorescence partially declined probably indicating silencing of the transgene (Figure 30C).

For certain applications, like differentiation assays, feeder-free iPSCs are desirable. Therefore, iPSCs can be maintained on synthetic extracellular matrixes like Geltrex. When cultured on Geltrex, iPSCs maintain their characteristic growth pattern of round dome-shaped colonies (Figure 30D).

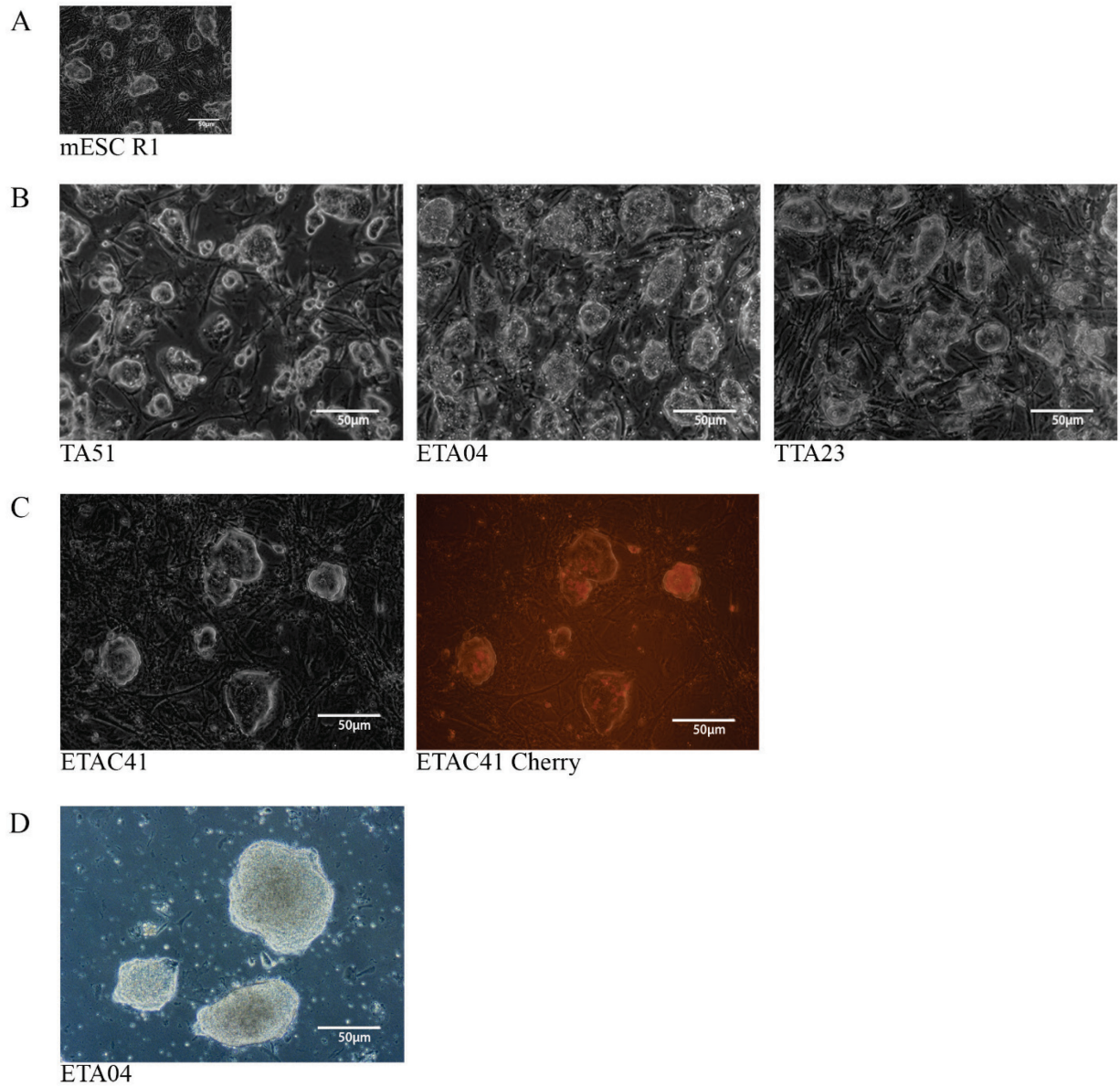


Figure 30: Morphology of ESCs and iPSCs.

(A) mESCs (R1) maintained on feeder cells grow in round, dome-shaped colonies consisting of many small cells. (B) mIPSCs (TA51, ETA04, TTA23) show a mESC-like morphology when cultured on feeder cells. (C) ETAC-IPSCs (ETAC41) additionally show a red fluorescence due to the presence of the *mCherry* pluripotency reporter cassette among the inserted transgenes. (D) iPSCs (ETA04) cultured on Geltrex form round dome-shaped colonies. Scale bars represent 50 μm.

6.4.2. Alkaline phosphatase staining

As cells gradually gain traits of pluripotent stem cells during the reprogramming process they start to express the membrane enzyme alkaline phosphatase (AP) [70]. Expression of AP can

easily be visualized by alkaline phosphatase staining as it reacts with nitro-blue-tetrazolium-chloride/ 5-bromo-4-chloro-3-indolyl-phosphate (NBT/BCIP) solution leading to an insoluble purple precipitation. Alkaline phosphatase staining is therefore a fast and easy screening for successful reprogramming.

We performed alkaline phosphatase staining on the original plates after picking enough colonies (Figure 31A). Here the remaining colonies showed a purple color, whereas the surrounding feeder cells and fibroblasts did not stain. This shows, that the emerging colonies during the reprogramming process passed at least the first steps of the reprogramming process and expressed first pluripotency-related genes.

Furthermore, we stained the established IPS cell lines for alkaline phosphatase using the murine ES cell line R1 as a positive control (Figure 31B). All ESC as well as all iPSC colonies gained a clear purple color when exposed to NBT/BCIP, whereas the feeder cells did not react with the substrate. This indicates successful induction of pluripotency in our established IPS cell lines.

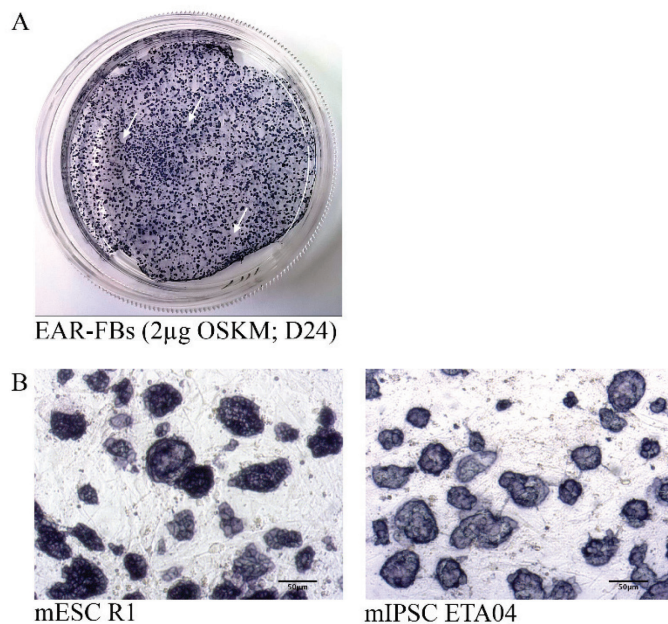


Figure 31: Alkaline phosphatase staining of IPSCs

(A) Alkaline phosphatase staining of EAR-FBs grown on feeder cells in a 6 cm-cell culture dish at day 24 after nucleofection with 2µg of the *pT2OSKM* plasmid. iPSC colonies stain purple whereas the surrounding feeders and fibroblasts do not stain. Arrows mark holes in the cell layer resulting from picking of colonies. (B) Alkaline phosphatase staining of mESCs R1 and IPSCs ETA04. ESC and IPSC colonies show a purple color indicating expression of AP. Scale bars represent 50 µm.

6.4.3. Number of transposon insertion sites

For successful subsequent differentiation of iPSCs, or excision or exchange of the reprogramming factor cassette, a low number of transposon integration sites or even only a single transgene insertion is favorable. Therefore, we performed Splinkerette PCR to analyze the number of transposons integrated into the genome of our established IPS cell lines.

Splinkertte PCR is a PCR-based method to specifically amplify the gDNA sequence that lies between the transposon terminal inverted repeats (TIRs) and a nearby restriction site [240]. Each integration sites results in a PCR product of a different length. Therefore, the number of PCR products seen on the gel after agarose gel electrophoresis represents the number of integration sites [53].

Splinkerette PCR (Figure 32) showed, that the number of integration sites for the tested clones was up to five (ETAC 75). Interestingly, the clones TA55 and TA81 showed an identical pattern of PCR products. These clones might therefore de facto represent only a single clonal cell line, that has either accidentally been picked twice as some remaining cells after the first picking formed a new colony, or they result from the same initial colony, that has been disrupted during passaging at day 10, which led to formation of at least two colonies on the second plate. To rule out the second possibility it seems favorable not to passage the cells during the reprogramming process.

We could identify two clones with only a single integration site: ETA04 and ETAC41. Of these ETA04 was chosen for chondrogenic differentiation.

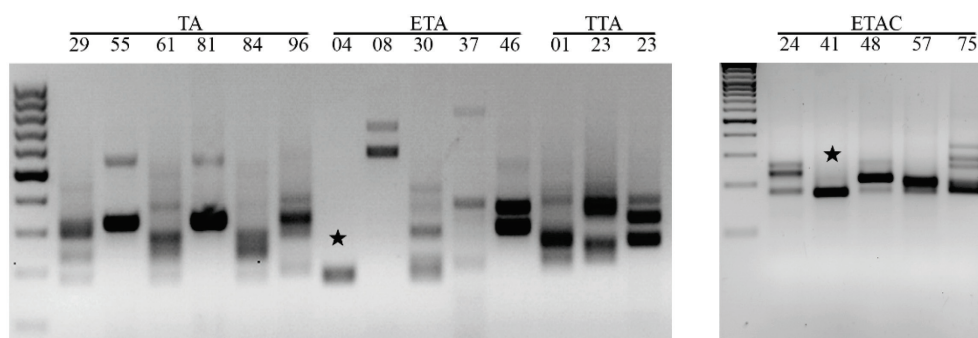


Figure 32: Splinkerette PCR

The number of PCR products seen on the gel corresponds to the number of transgene insertion sites. Stars mark the single integration clones ETA04 and ETAC41.

6.4.4. Expression of pluripotency markers

During the reprogramming process, the cells gradually reach pluripotency. To prove that pluripotency was successfully induced, we analyzed the gene expression profile of the newly established clonal IPS cell lines on mRNA and protein level.

6.4.4.1. mRNA analysis of pluripotent stem cell markers

We isolated RNA from feeder-free iPSCs as well as from feeder-free mESCs and parental MEFs or FBs as a positive or negative control, and performed semiquantitative RT-PCR for several stem cell markers. Representative pictures of agarose gel electrophoreses are shown in Figure 33 - 36. Quantification of three runs of PCRs is represented as mean + SD relative to expression of the housekeeping gene *GAPDH*.

The transcription factors *Dax1* [55, 242] and *Nanog* [15, 24] are part of the pluripotency network that is established during reprogramming. *Ecat1* [15], *Eras* [55, 243], *Rex1* [15, 68] and *Zfp296* [55, 244] are highly expressed in undifferentiated murine ESCs and well-known pluripotency markers. All established clonal IPS cell lines expressed these endogenous pluripotency markers at RNA levels comparable to ESCs, whereas the parental MEFs or FBs showed no or only marginal expression of these markers.

Results

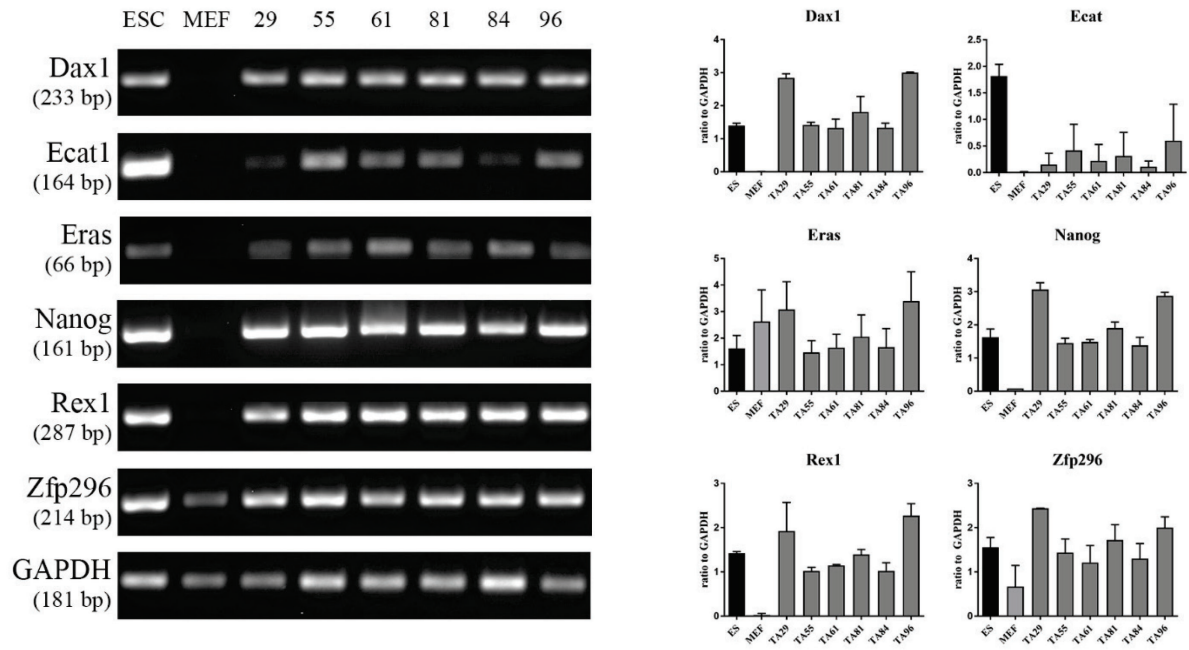


Figure 33: ET-PCR for ESC markers on TA clones.

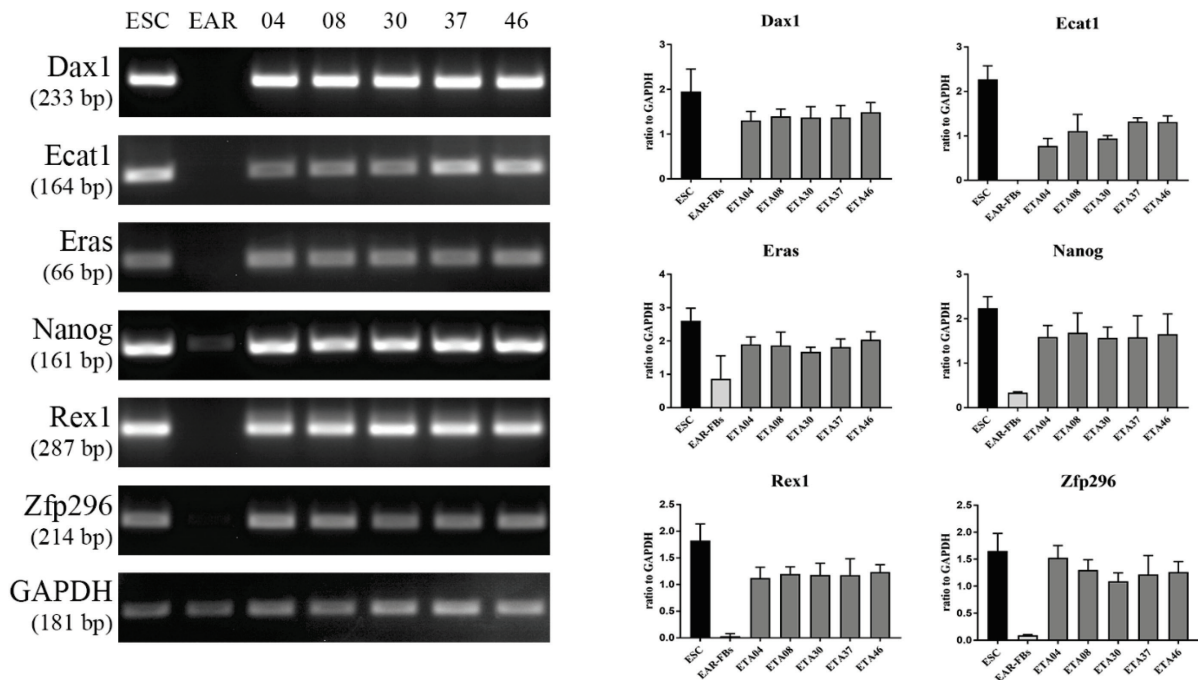


Figure 34: RT-PCR for ESC markers on ETA clones.

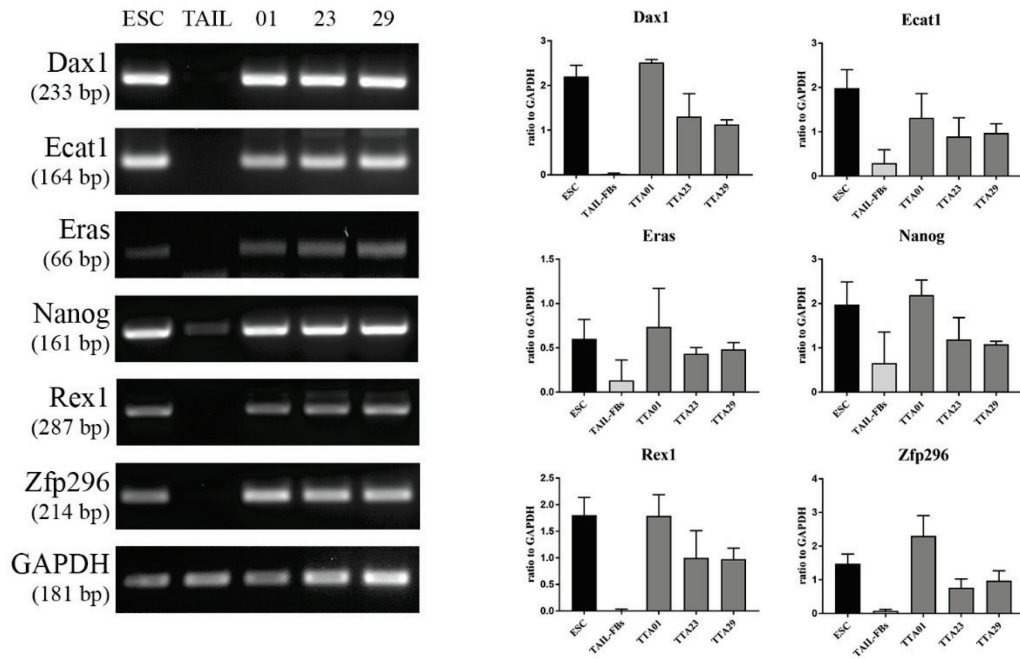


Figure 35: RT-PCR for ESC markers on TTA clones.

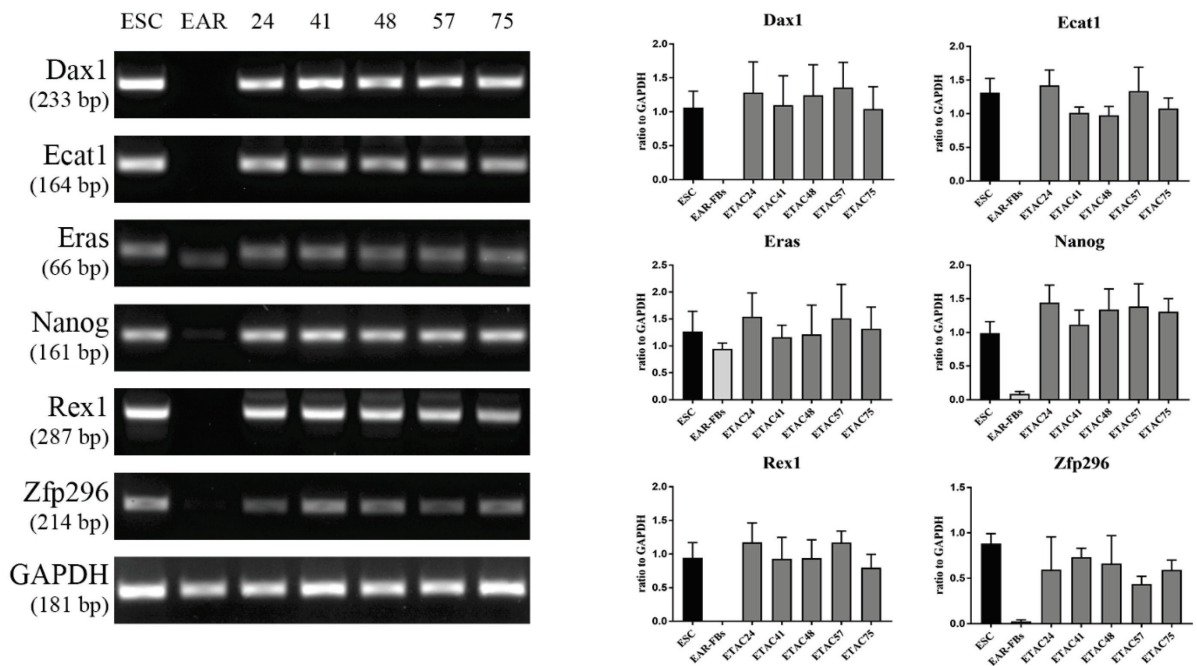


Figure 36: RT-PCR for ESC markers on ETAC clones.

6.4.4.2. mRNA analysis of reprogramming factors

Semiquantitative RT-PCR for reprogramming factors was performed on mRNA samples from feeder-free mIPSCs as well as on mRNA isolated from feeder-free mESCs, MEFs or adult fibroblasts. Representative pictures of agarose gel electrophoreses are shown in Figure 37 – 40. Quantification of three runs of PCRs is represented as mean + SD relative to expression of the housekeeping gene *GAPDH*.

For the reprogramming factors *c-Myc* and *Klf4* we used primers that could specifically detect endogenous expression of the reprogramming, whereas mRNA transcribed from the transgenes did not result in a PCR product [55].

All clones tested expressed *Klf4* at levels comparable to mESCs indicating successful induction of endogenous pluripotency genes during the reprogramming process. Expression of *c-Myc* however, was remarkably lower than in mESCs for all tested clones.

mRNA levels of *Oct3/4* and *Sox2* were also comparable between all tested IPSC clones and mESCs, although the primers used here could not distinguish between endogenous and exogenous transcripts.

Interestingly, MEFs as well as EAR-FBs and TAIL-FBs showed high endogenous levels of *c-Myc* and *Klf4* expression. Therefore, exogenous expression of *Oct3/4* and *Sox2* alone might be sufficient to reprogram these cell types reducing size of the introduced transgene and therefore potentially facilitating subsequent manipulation of the inserted transgene. Further research is needed to reveal the feasibility of this approach.

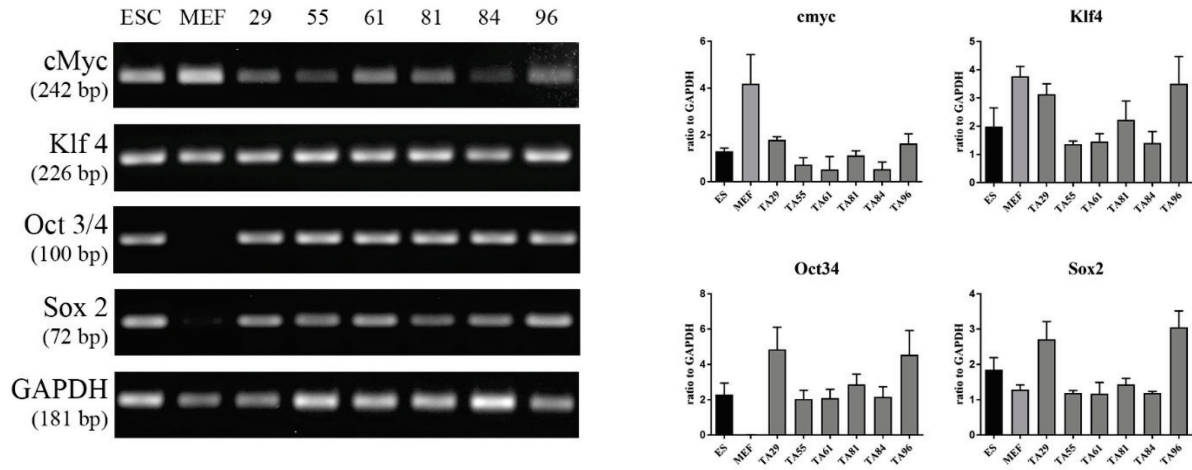


Figure 37: RT-PCR for reprogramming factors on TA clones.

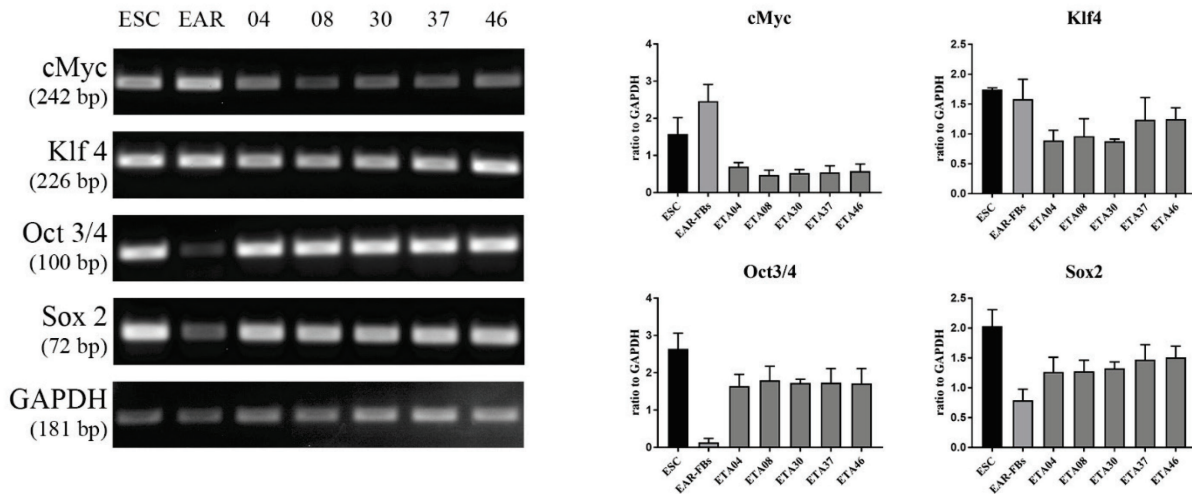


Figure 38: RT-PCR for reprogramming factors on ETA clones.

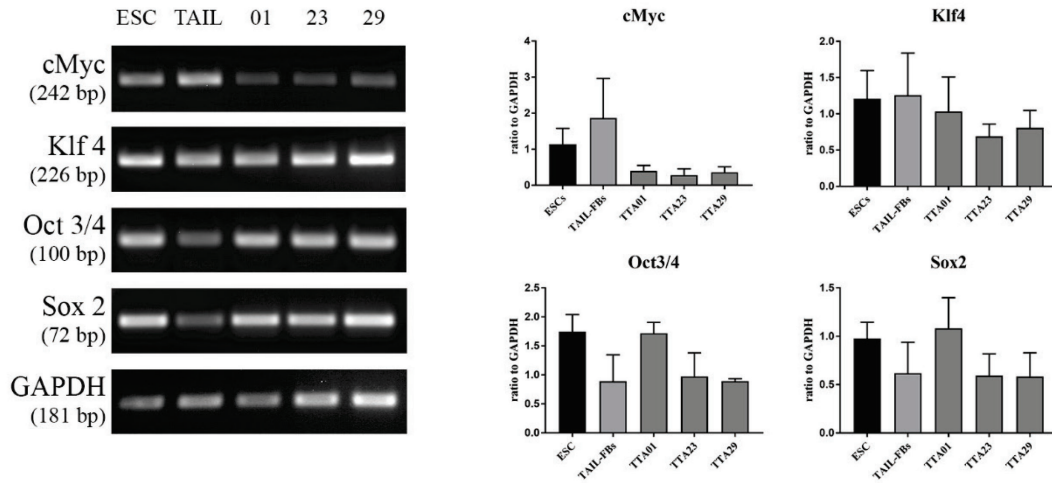


Figure 39: RT-PCR for reprogramming factors on TTA clones.

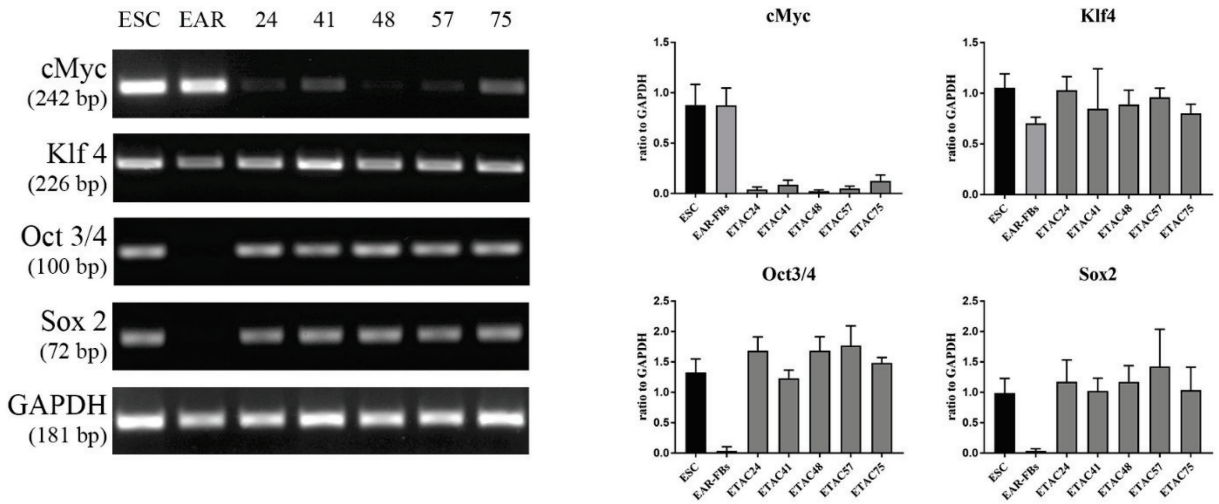


Figure 40: RT-PCR for reprogramming factors on ETAC clones.

6.4.4.3. Protein analysis of pluripotency markers by immunocytochemistry

Immunofluorescence staining was performed for the reprogramming factors Oct3/4 and Sox2 as well as for the endogenous pluripotency markers Nanog and SSEA1 on all established iPSC clones. Murine ESCs were used as a positive control, whereas the feeder cells, on which the iPSCs or ESCs were cultured, served as negative control. Representative photomicrographs of the immunofluorescence staining of the mES cell line R1 and the miPS cell lines ETA04 and ETAC41 are shown in Figure 41 and Figure 42.

All tested iPSC clones showed positive immunofluorescence staining for the transcription factors Oct3/4, Sox2 and Nanog. Comparison with the nuclear dye 4', 6-diamidino-2-phenylindole (DAPI) signals confirmed nuclear localization of the transcription factors. The fluorescence pattern of the iPSC clones was indistinguishable from the mESCs that served as positive control. The nuclei of the MEF-feeder cells, however, showed a clear DAPI signal but were negative for Oct3/4, Sox2 and Nanog.

Furthermore, the tested iPSC colonies showed positive fluorescence for the membrane marker SSEA1 that was comparable to the staining pattern of mESCs, whereas the feeder cells did not react.

Positive fluorescence for Oct3/4 and Sox2 could be due to transgene expression. However, positive fluorescence for Nanog and SSEA1 clearly confirmed expression of pluripotency markers at the protein level indicating successful reprogramming of the established IPS cell lines.

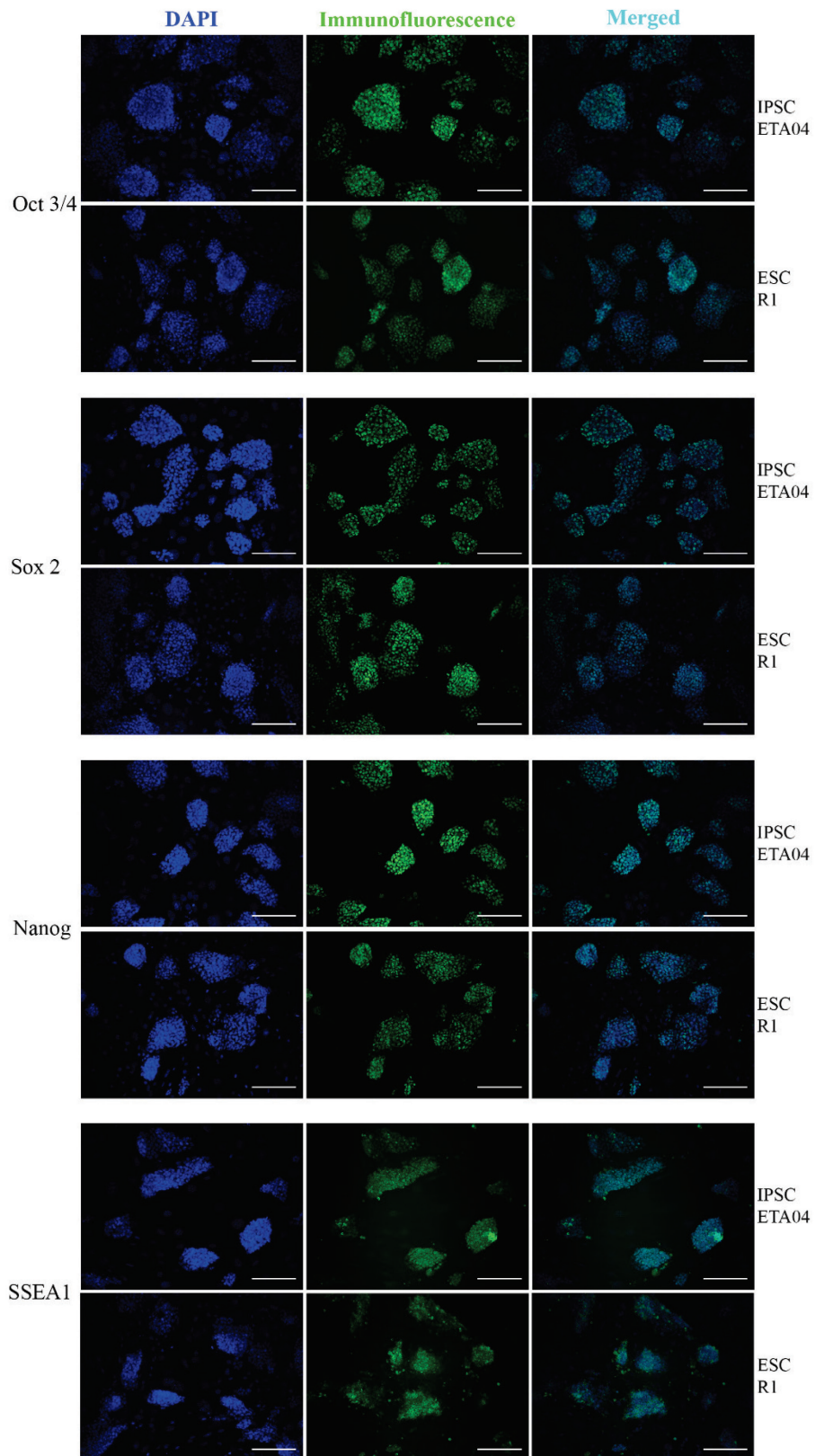


Figure 41: Immunofluorescence staining for pluripotency markers on mESCs (R1) and ETA04

Immunofluorescence staining for Oct3/4, Sox2, Nanog and SSEA1 on IPSCs (ETA04, upper rows) and ESCs (R1, lower rows).

Scale bars represent 50 μm.

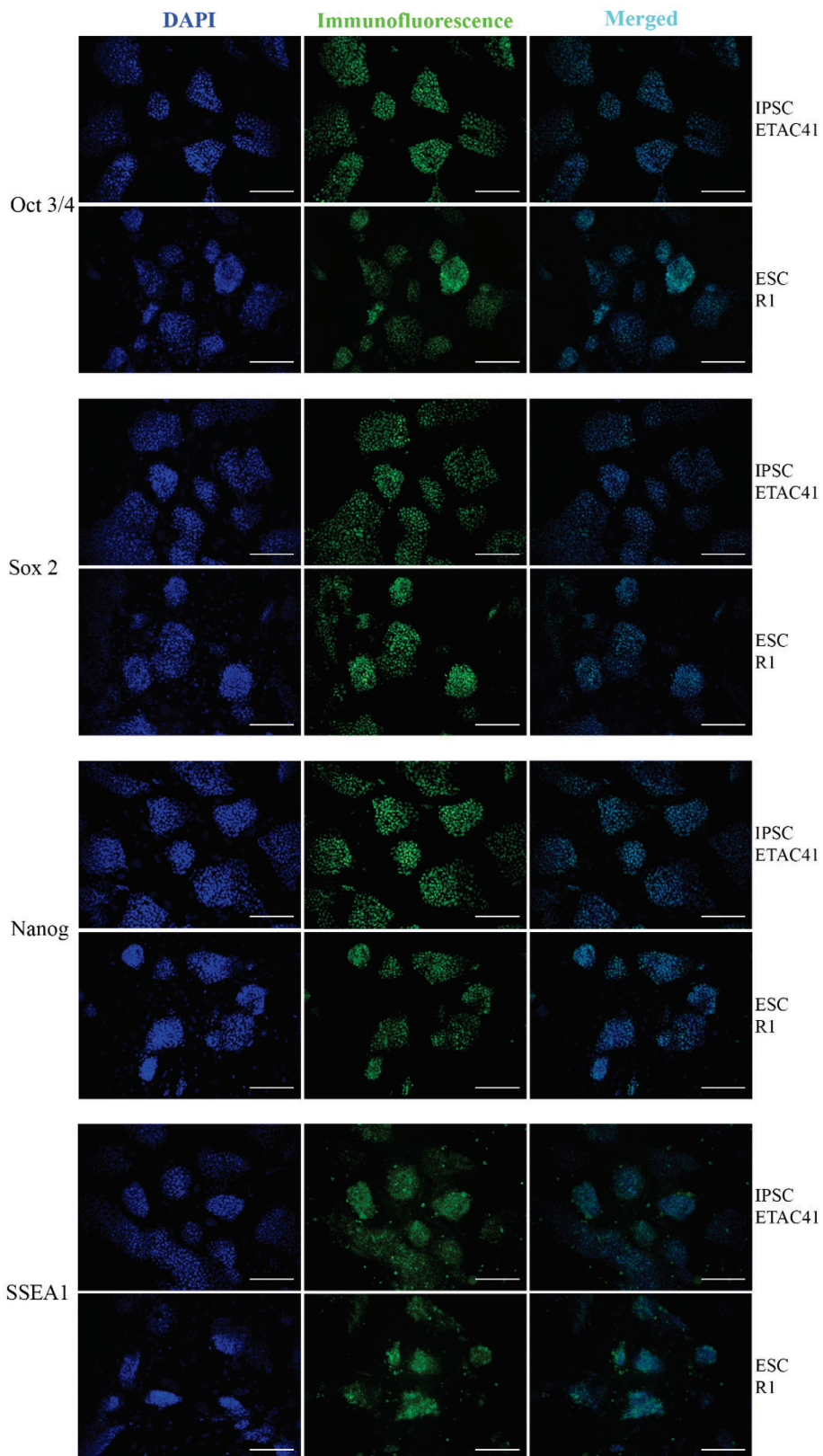


Figure 42: Immunofluorescence staining for pluripotency markers on mESCs (R1) and ETAC41

Immunofluorescence staining for Oct3/4, Sox2, Nanog and SSEA1 on iPSCs (ETAC41, upper rows) and ESCs (R1, lower rows). Scale bars represent 50 μm.

6.4.5. Trilineage differentiation potential during spontaneous differentiation in embryoid bodies

Pluripotent stem cells have the ability to differentiate into cell types from all three embryonic germ layers – ectoderm, mesoderm and endoderm [2]. Therefore, it is a crucial part of the assessment of recently established IPS cell lines to prove their three-lineage differentiation potential. For murine iPSCs, this is commonly carried out either by chimera formation [15, 17, 18] or teratoma formation [15, 17, 18] which both require laborious in vivo protocols. Spontaneous differentiation in embryoid bodies (EBs) is a feasible and reliable alternative in vitro to demonstrate the three-lineage differentiation potential of iPSCs [53]. EBs are small clusters of pluripotent stem cells that resemble early stages of embryonic development [4].

We cultured selected feeder-free clones from all established iPS cell lines as hanging drops without LIF leading to formation of small EBs. On day 5, they were transferred to free floating culture in non-adherent 96-well plates, and cultured, still without LIF, for additional 16 days (Figure 43). Feeder-free culture without LIF allows spontaneous differentiation to occur within the EBs. After 21 days in culture, gene expression for pluripotency and lineage-specific markers was analyzed by qPCR.

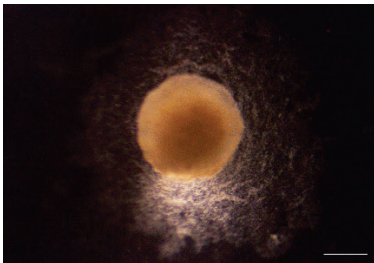


Figure 43: Embryoid body on day 21 of spontaneous differentiation in free floating culture.

Embryoid body derived by spontaneous differentiation of ETA04 in free floating culture on day 21. Scale bar represents 100 μm .

For the single-integration clone ETA04 both pluripotency markers tested were significantly downregulated after 21 days (*Oct3/4*, $p < 0.005$; *Nanog*, $p < 0.05$). The ectodermal marker *Pax6* was significantly upregulated ($p < 0.005$) and the ectodermal marker *Ncam1* showed a strong tendency of higher expression in EBs. Both endodermal markers tested (*Sox17* and *FoxA2*) were significantly upregulated in EBs at day 21 (*Sox17*, $p < 0.005$; *FoxA2*, $p < 0.05$). For the

mesodermal markers *MyoD1* and *Brachyury* higher expression levels were detected in EBs at day 21, which were, however, not statistically significant. Figure 44 shows the expression of these markers as fold change compared to parental IPS cell line ETA04.

Similar results were obtained for the other clones tested. Notably, there was high variability in gene expression between the replicates which correlates well with the results reported *e.g.* by *Mansergh et al.* for spontaneous differentiation of murine pluripotent stem cells [245]. However, our results clearly indicate, that our iPSCs have upregulated ectodermal, endodermal and mesodermal markers during spontaneous differentiation in EBs proving their three-lineage differentiation potential.

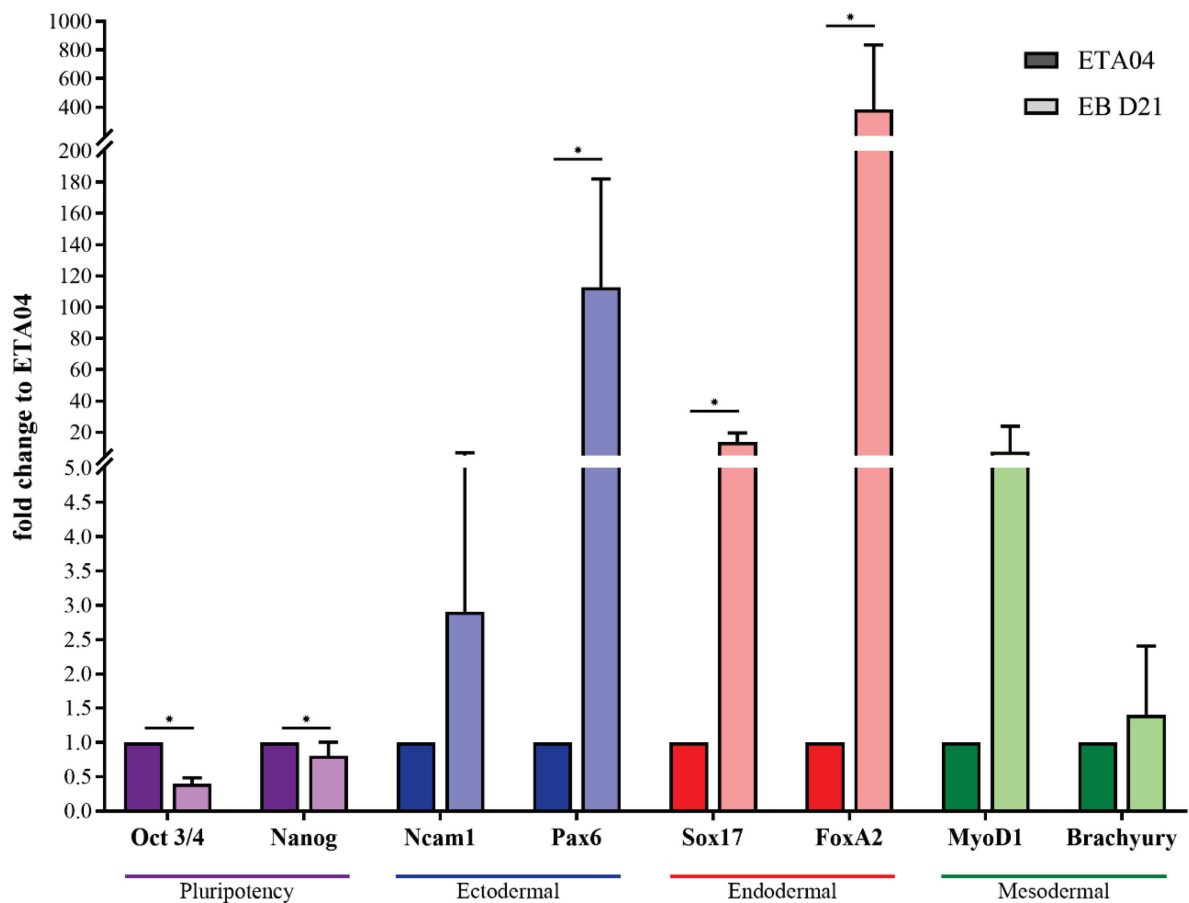


Figure 44: qPCR of pluripotency and lineage-specific markers of iPSCs (ETA04) and embryoid bodies at day 21 (EB D21).

Expression of pluripotency markers *Oct3/4* and *Nanog* was significantly downregulated in EBs at day 21, whereas expression of lineage specific markers *Ncam1*, *Pax6*, *Sox17*, *FoxA2*, *MyoD1* and *Brachyury* was upregulated. Bars represent fold change of gene expression compared to ETA04 and are plotted as mean + SD. Asterisks mark significant changes of gene expression levels.

6.5. Chondrogenic differentiation of iPSCs via chondrogenic colonies

As described in 3.3.2.2. *Chondrogenic differentiation of pluripotent stem cells*, there are different strategies to induce chondrogenic differentiation of pluripotent stem cells.

In 2015, *Yamashita et al.* described a scaffoldless method for chondrogenic differentiation of human iPSCs via chondrogenic nodules that are formed directly from iPSC colonies through exposure to different media supplemented with growth factors [127].

We attempted to transfer this method to our murine induced pluripotent stem cells generated by the Sleeping Beauty transposon system.

The single integration clone ETA04 was cultured under feeder-free conditions on Geltrex-coated 6-well plates. As soon as the colonies reached medium size, the culture medium was replaced by a mesoendodermal medium supplemented with the growth factors Wnt3a and Activin A as described by *Yamashita et al.* [127]. Colonies were maintained for three days in this medium. During that time the colonies did not gain significantly in size but otherwise appeared healthy. On day four, chondrogenic differentiation of the colonies was induced by changing the media to a chondrogenic medium consisting of DMEM, FBS, Penicillin-Streptomycin supplemented with non-essential amino acids, sodium pyruvate, insulin transferrin and selenite, and L-ascorbic acid [127]. The colonies were either grown in chondrogenic medium (noGF) or in chondrogenic medium supplemented with the growth factors BMP2, TGF β 1 and GDF5 (BTG), as *Yamashita et al.* had reported the best results for chondrogenic differentiation of human iPSCs using this combination [127]. Around day 6, the colonies started to lift off the plate which was about one week earlier than reported by *Yamashita et al.* [127]. The formed chondrogenic nodules were therefore transferred to a free-floating culture in 6 cm-Petri dishes on day 7. Here, the chondrogenic nodules were maintained under the conditions described above for up to 42 days. During that period the spheroids neither gained obviously in size nor changed their macroscopic appearance. As reported by *Yamashita et al.* we observed single cells that separated from the developing nodules and sank to the bottom of the dishes [127]. On days 14, 31 and 42, the chondrogenic nodules were harvested and subjected to histological and gene expression analysis.

6.5.1. Histological analysis of chondrogenic colonies

Figure 45 shows representative photomicrographs of chondrogenic nodules derived from chondrogenic colonies on day 42. Safranin Orange and Toluidine Blue staining showed no substantial deposition of sulfated GAGs in the ECM neither of unstimulated (noGF) nor of stimulated (BTG) nodules. Immunohistochemistry for aggrecan and type II collagen was negative both in unstimulated (noGF) and stimulated (BTG) nodules. So, no evidence for chondrogenic differentiation of iPSCs in chondrogenic nodules was seen in histological analysis.

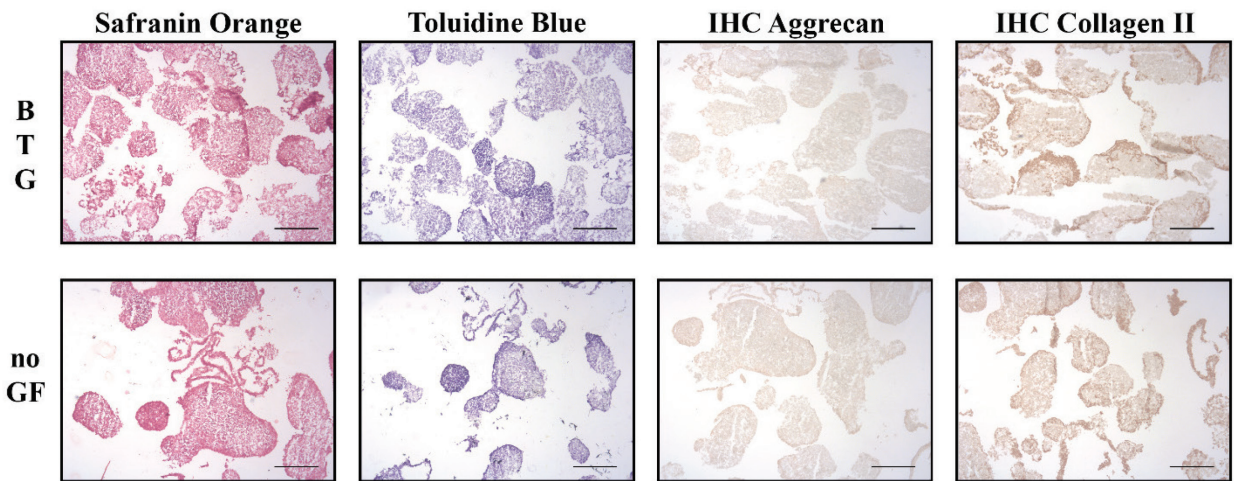


Figure 45: Histological analysis of chondrogenic nodules on day 42.

Chondrogenic nodules were stained with Safranin Orange and Toluidine Blue to detect deposition of GAGs in the ECM. Immunohistochemistry was performed for aggrecan and type II collagen. The upper row shows nodules stimulated with the chondrogenic growth factors BMP2, TGF β 1 and GDF5, while the lower row shows nodules grown in chondrogenic medium without additional growth factors. Scale bars represent 100 μ m.

6.5.2. Gene expression analysis of chondrogenic colonies

We performed qPCR on mRNA isolated from chondrogenic nodules on days 14, 31 and 42 to further assess their chondrogenic potential. RNA isolated from parental iPSCs and from rib cage cartilage of mice embryos served as controls.

6.5.2.1. Analysis of pluripotency markers in chondrogenic colonies

Analysis of the expression of the pluripotency markers *Oct3/4* and *Nanog* revealed significant downregulation of these markers as soon as day 14 (*Oct3/4*, $p < 0.0001$; *Nanog*, $p < 0.0001$). From thereon expression remained stable at low levels in stimulated and non-stimulated nodules. Figure 46 shows the result of qPCR on pluripotency markers as fold change compared to expression in parental IPSC (ETA04).

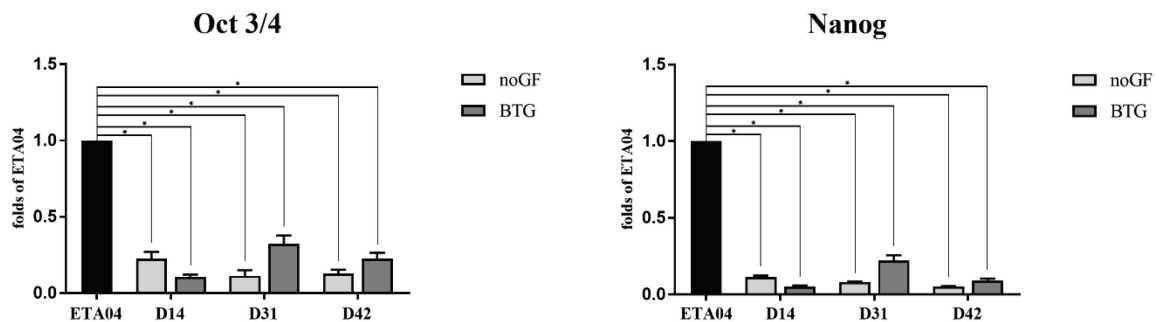


Figure 46: qPCR of pluripotency markers in stimulated (BTG) and non-stimulated (noGF) chondrogenic colonies.

Expression of pluripotency markers *Oct3/4* and *Nanog* was significantly downregulated in chondrogenic nodules derived from chondrogenic colonies as soon as day 14. Bars represent fold change of gene expression compared to ETA04 and are plotted as mean \pm SD. Asterisks mark significant changes of gene expression levels.

6.5.2.2. Analysis of chondrogenic markers in chondrogenic colonies

Figure 47 shows the results of qPCR on chondrogenic markers as fold change compared to rib cage cartilage. qPCR on the chondrogenic markers *aggrecan* (*Acan*), *Type II Collagen* (*Col2a1*), *Sox9* and *Integrin $\alpha 10$* (*Igta10*) confirmed the poor chondrogenic differentiation seen in histological analysis. No significant changes were seen for the expression of *aggrecan*. *Sox9* expression was significantly upregulated in non-stimulated nodules on day 14 ($p < 0.01$) and day 42 ($p < 0.001$), and *type II collagen* expression was significantly upregulated in non-stimulated nodules on day 42 ($p < 0.001$) compared to expression in parental IPSCs. No significant upregulation for these markers, however, was seen in stimulated nodules. Expression of *Integrin $\alpha 10$* was significantly downregulated in non-stimulated nodules on days 14 and 31 ($p < 0.001$) and in stimulated nodules throughout the complete differentiation

($p < 0.001$). Furthermore, expression of all markers was negligible compared to expression in rib cage cartilage tissue.

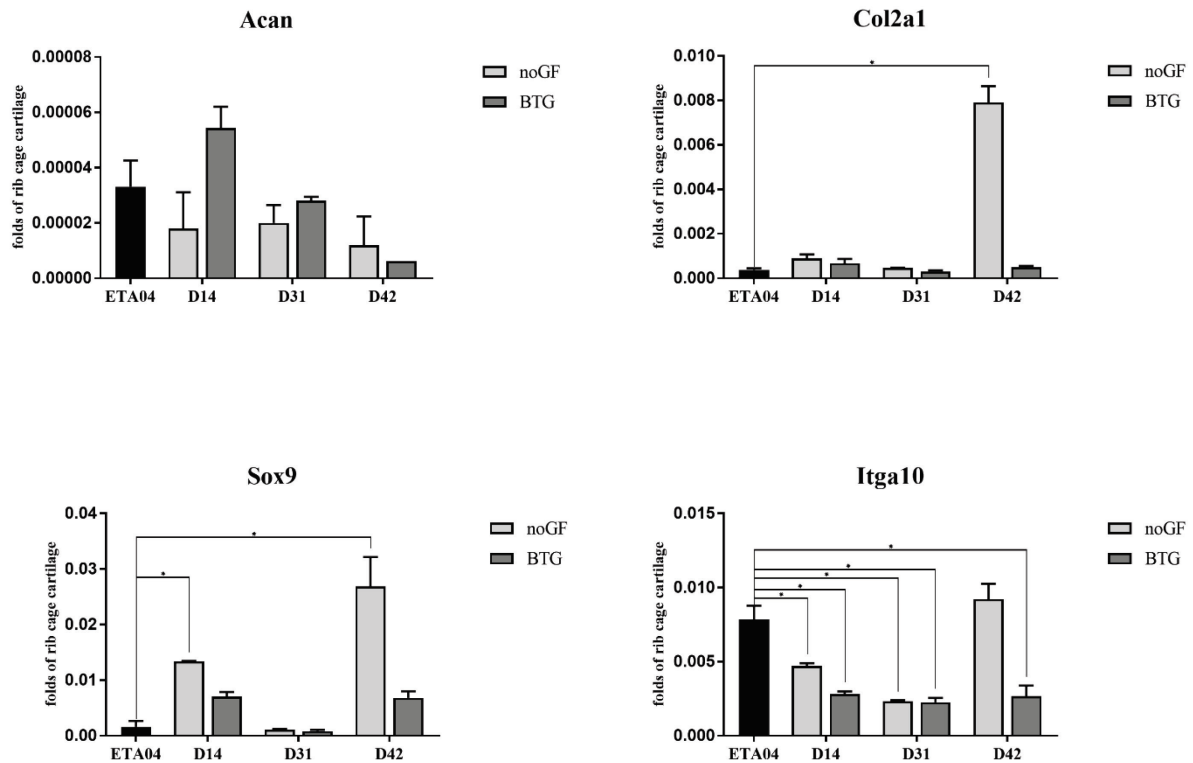


Figure 47: qPCR of chondrogenic markers in stimulated (BTG) and non-stimulated (noGF) chondrogenic nodules.

Expression of chondrogenic markers aggrecan (*Acan*), type II collagen (*Col2a1*), *Sox9* and integrin $\alpha 10$ (*Itga10*) compared to parental iPSCs. Bars represent fold change of gene expression compared to rib cage cartilage and are plotted as mean + SD. Asterisk mark significant changes of gene expression levels.

So, in conclusion, we were unable to induce chondrogenic differentiation of our murine iPSCs with the method described by *Yamashita et al.* [127]. Despite significant downregulation of pluripotency markers, our nodules failed to relevantly upregulate chondrogenic gene expression and correspondingly, no cartilage specific proteins were detectable in the ECM.

6.6. Chondrogenic differentiation of iPSCs via embryoid bodies

Therefore, we searched for other methods to efficiently induce chondrogenic differentiation of our iPSCs.

In protocols involving pre-differentiation of iPSCs or ESCs in embryoid bodies (EBs), these EBs are either disrupted or plated onto agarose coated plates. Cells directly from disrupted EBs or from their outgrowths are then submitted to high-speed centrifugation to generate high-density pellets similar to the standard protocol used for MSC [229, 230]. However, disruption of EBs and subsequent centrifugation are considered stressful for the cells and the outgrowth from the EBs usually contains a mixed cell population. It has been shown that chondrogenic differentiation of iPSCs can also be achieved by culturing iPSCs in a microcavity hydrogel, in which they form EB-like structures that directly undergo chondrogenic differentiation [223].

Therefore, we suggested, that disrupting the EBs into a single cell suspension is not necessary for chondrogenic differentiation. As EBs represent a high-density culture system resembling Yamashita's nodules and conventional centrifugation-derived pellets, we supposed that it might be sufficient to maintain EBs under chondrogenic conditions in a free-floating culture system to induce chondrogenic differentiation of the iPSCs.

We cultured feeder-free iPSCs from the single integration cell line ETA04 for five days in hanging drops without LIF allowing formation of embryoid bodies. These EBs were then directly transferred into a free-floating culture system and maintained in chondrogenic medium consisting of DMEM supplemented with dexamethason, natrium pyruvate, L-ascorbic acid and insulin transferrin selenite (ITS). The resulting pellet-like aggregates were termed chondrogenic spheroids.

These chondrogenic spheroids were maintained either without additional growth factors (noGF) or with the well-known chondrogenic growth factors bone morphogenetic protein 2 (BMP2) and transforming growth factor β 1 (TGF β 1) added to the medium (BT) for up to 42 days. During that period the EBs significantly increased in size (EBs vs. noGF, $p < 0.001$; EBs vs. BT, $p < 0.001$; Figure 48). EBs at day 5 had a median diameter of 181 μm (IQR 65 μm). EBs stimulated with BMP2 and TGF β 1 reached a mean diameter of $770 \pm 60 \mu\text{m}$ at day 42, and were significantly larger than non-stimulated spheroids that showed a mean diameter of 680

$\pm 50 \mu\text{m}$ ($p < 0.001$). Furthermore, the stimulated spheroids were more compact with smoother edges and showed a white color typical for cartilage particles.

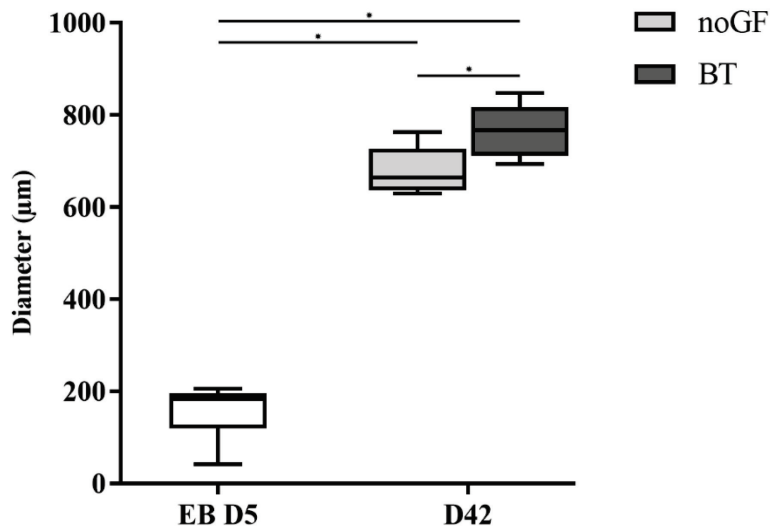


Figure 48: Size of EBs on day5 and CSs on day 42.

During chondrogenic differentiation the chondrogenic spheroids gained significantly in size and reached a mean size of $680 \pm 50 \mu\text{m}$ when maintained without growth factors or $770 \pm 60 \mu\text{m}$ when stimulated with growth factors BMP2 and TGF β 1.

Boxes represent Median \pm IQR, Whiskers show min/max-values. Significant differences are marked with asterisks.

6.6.1. Histological analysis of chondrogenic spheroids

Chondrogenic spheroids were harvested after 2, 4 and 6 weeks in free floating culture (Days 14, 28 and 42). Different histological analyses were performed on cryosections to evaluate chondrogenic differentiation of the spheroids.

6.6.1.1. Safranin Orange staining of chondrogenic spheroids

Safranin Orange staining confirmed deposition of sulfated proteoglycans (PGs) in the ECM of chondrogenic spheroids cultured with chondrogenic growth factors (BT) on day 28 and day 42. Spheroids at day 14 mostly consisted of densely packed cells for both conditions (no GF and BT). Spheroids cultured in chondrogenic medium alone (noGF) revealed only small areas with PG deposition on day 42 and were less compact than factor-supplemented spheroids.

Representative photomicrographs of the sections are shown in figure 49 (upper part).

6.6.1.2. Toluidine Blue staining of chondrogenic spheroids

Toluidine Blue staining confirmed the results of Safranin Orange staining showing deposition of negatively charged PGs in the ECM of chondrogenic spheroids maintained with BMP2 and TGF β 1 on day 28 and 42 (BT). Only small positive areas could be detected in the control spheroids (noGF). Spheroids at day 14 consisted of densely packed cells with no relevant PGs deposited in the ECM for both conditions.

Representative photomicrographs of the sections are shown in figure 49 (lower part).

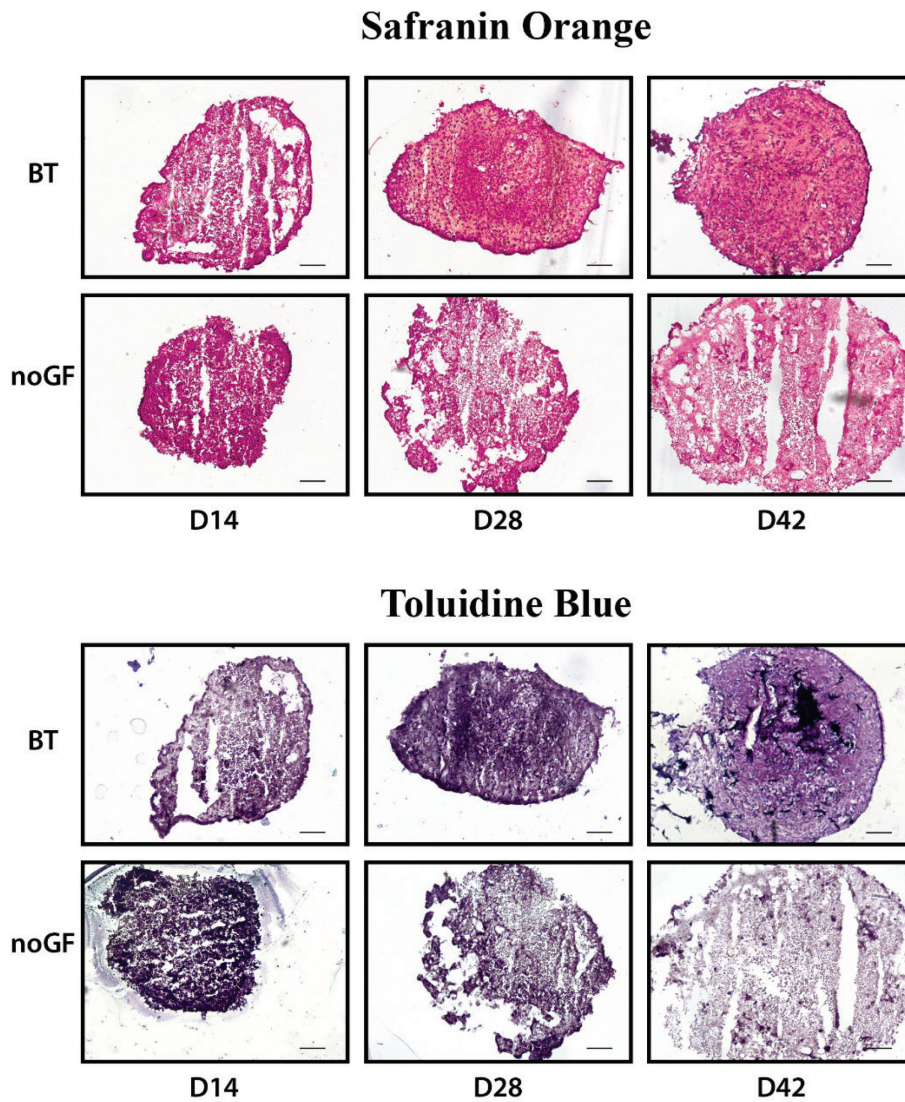


Figure 49. Safranin Orange and Toluidine Blue staining for chondrogenic spheroids.

The upper rows depict chondrogenic spheroids cultured with BMP2 and TGF β 1 (BT), the lower rows depict the corresponding control spheroids maintained in chondrogenic medium without growth factors (noGF) on days 14, 28 and 42. Proteoglycan deposition could be detected in the ECM of stimulated spheroids on days 28 and 42. Scale bars represent 100 μ m.

6.6.1.3. Immunohistochemistry for aggrecan and type II collagen

Immunohistochemistry (IHC) confirmed deposition of aggrecan and type II collagen in the ECM of chondrogenic spheroids treated with BMP2 and TGF β 1 on days 28 and 42. Aggrecan could be detected diffusely throughout the complete spheroid, whereas deposition of type II collagen seemed restricted to certain spots within the spheroid on day 42. No aggrecan or type II collagen could be detected in supplemented spheroids on day 14, or in control spheroids at any time. Figure 50 shows representative photomicrographs of the immunohistochemistry.

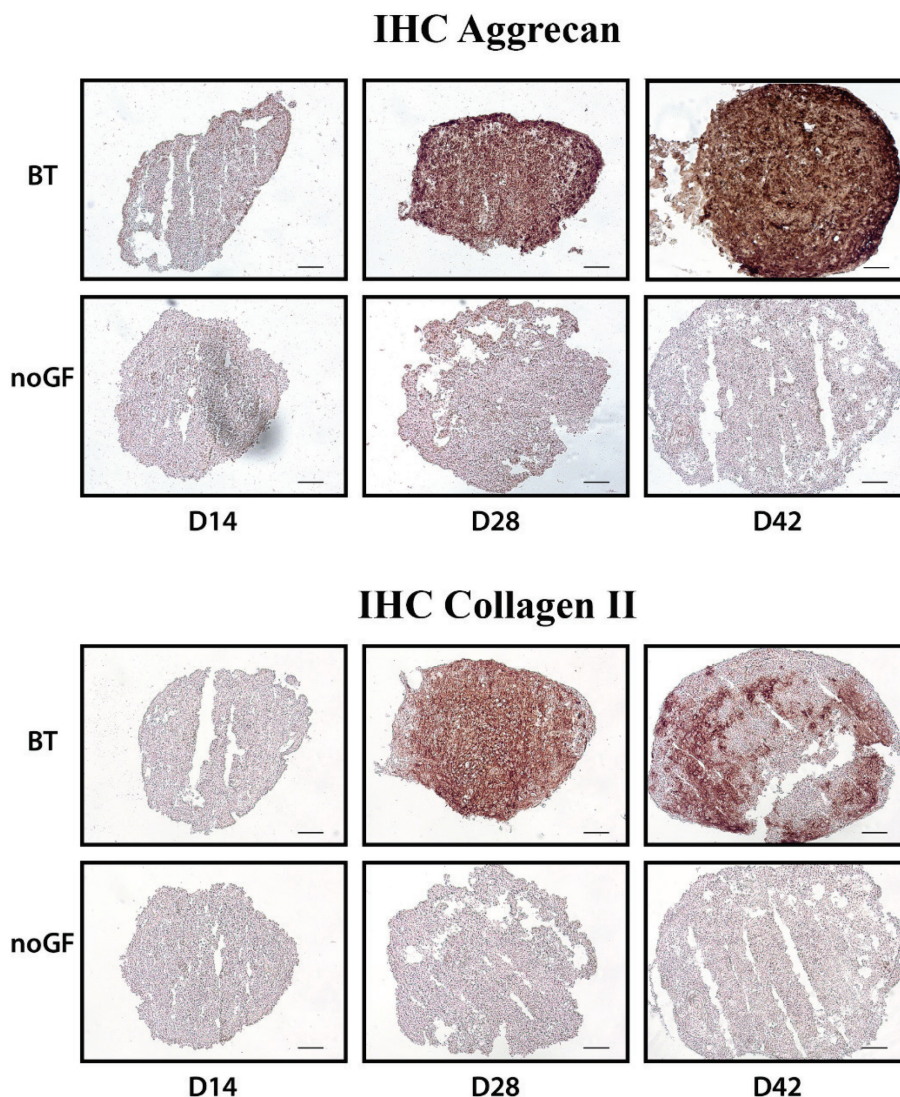


Figure 50: Immunohistochemistry for aggrecan and type II collagen on chondrogenic spheroids

The upper rows depict chondrogenic spheroids cultured with BMP2 and TGF β 1 (BT), the lower rows depict the corresponding control spheroids maintained in chondrogenic medium without growth factors (noGF) on days 14, 28 and 42. Deposition of aggrecan and type II collagen could be detected in the ECM of stimulated spheroids on days 28 and 42. Scale bars represent 100 μ m.

Taken together, histochemical analysis and immunohistochemistry revealed deposition of negatively charged proteoglycans as well as aggrecan and type II collagen in the ECM of chondrogenic spheroids derived from the IPS cell line ETA04 via EBs stimulated with chondrogenic growth factors BMP2 and TGF β 1 (BT). This clearly indicates that chondrogenic differentiation can be achieved by culturing EBs under chondrogenic conditions. Supplementation of chondrogenic growth factors, however, seems to be required as spheroids cultured in chondrogenic medium alone did not deposit PGs, aggrecan or type II collagen in their ECM.

6.6.2. Gene expression analysis of chondrogenic spheroids

To further assess chondrogenic differentiation of iPSCs in EB-derived chondrogenic spheroids, qPCR was performed on mRNA isolated from stimulated and non-stimulated chondrogenic spheroids (BT and noGF) on days 14, 28 and 42. RNA isolated from the parental iPSCs and from rib cage cartilage of mouse embryos served as controls.

6.6.2.1. Expression of pluripotency markers in chondrogenic spheroids

qPCR for the pluripotency markers *Oct3/4* and *Nanog* showed that both pluripotency markers were significantly downregulated compared to parental iPSCs as soon as day 14 (*Oct3/4*, $p < 0.05$; *Nanog*, $p < 0.001$). No significant changes between spheroids cultured with or without chondrogenic growth factors (BT vs noGF) could be detected at any timepoint. No significant changes of gene expression occurred after day 14 for both markers. Interestingly for *Oct3/4* a tendency of higher expression could be detected on days 28 and 42 in both stimulated and non-stimulated spheroids compared to day 14, whereas the expression of *Nanog* remained stable at low levels. This might be due to reactivation of exogenous *Oct3/4* from the genomically integrated reprogramming factor expression cassette that becomes reactivated during the differentiation process. To certainly rule out this possibility transgene-free iPSCs would be favorable.

Figure 51 shows the results of the qPCR of pluripotency markers as fold change compared to expression in parental IPSC (ETA04).

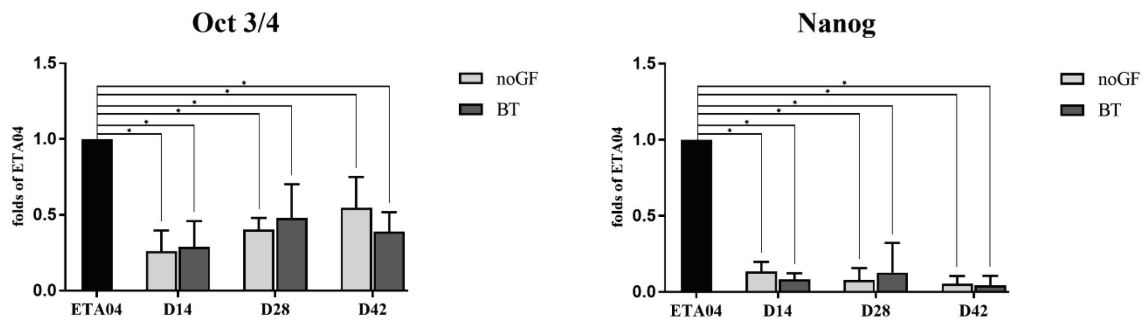


Figure 51: qPCR of pluripotency markers in stimulated (BT) and non-stimulated (noGF) chondrogenic spheroids.

Expression of pluripotency markers *Oct3/4* and *Nanog* was significantly downregulated in chondrogenic spheroids as soon as day 14. No significant differences could be detected between stimulated and non-stimulated spheroids. Bars represent fold change of gene expression compared to ETA04 and are plotted as mean + SD. Asterisks mark significant changes of gene expression levels.

6.6.2.2. Expression of chondrogenic markers in chondrogenic spheroids

We performed qPCR for the chondrogenic markers aggrecan (*Acan*), type II collagen (*Col2a1*), *Sox9* and α 10-integrin (*Itga10*).

In the stimulated spheroids *Acan* and *Col2a1* expression was significantly upregulated on day 28 compared to parental IPSCs and high expression levels were maintained until day 42 (*Acan*, day 28, $p < 0.05$; day 42, $p < 0.01$; *Col2a1*, day 28, $p < 0.05$; day 42, $p < 0.005$). This matches the results of the immunohistochemistry where deposition of aggrecan and type II collagen in the ECM could only be detected in stimulated spheroids on day 28 and 42. No relevant expression of *Acan* or *Col2a1* was induced by culturing EBs in chondrogenic medium without growth factor supplementation.

Interestingly, the chondrogenic transcription factor *Sox9* was significantly upregulated in both, stimulated and non-stimulated chondrogenic spheroids as soon as day 28 compared to parental IPSCs (noGF, $p < 0.05$; BT, $p < 0.001$ at days 28 and 42). There were no significant differences in the expression of *Sox9* between stimulated and non-stimulated spheroids, although a clear tendency for higher expression levels of *Sox9* could be seen for the spheroids maintained under the influence of BMP2 and TGF β 1 (BT) at all time points.

Similar results were seen for expression of $\alpha 10$ -integrin (*Itga10*). Its expression was significantly upregulated in control spheroids on day 42 ($p < 0.001$) and growth-factor stimulated spheroids starting from day 28 ($p < 0.01$ at day 28; $p < 0.001$ at day 42) compared to parental IPSCs. No significant differences could be detected between supplemented and non-supplemented spheroids at any time point, although a tendency for higher expression of *Itga10* could be seen in stimulated spheroids.

Taken together, culture of IPSC-derived EBs in chondrogenic medium alone induced significant upregulation of cartilage-specific transcription factor *Sox9* as well as of the cartilage-specific *integrin $\alpha 10$* . Stimulation of spheroids with the growth factors BMP2 and TGF β 1, however, was necessary to induce production of the cartilage-specific ECM proteins *aggrecan* and *type II collagen*.

Figure 52 shows the results of the qPCR of chondrogenic markers as fold change compared to expression in murine embryonic rib cage cartilage.

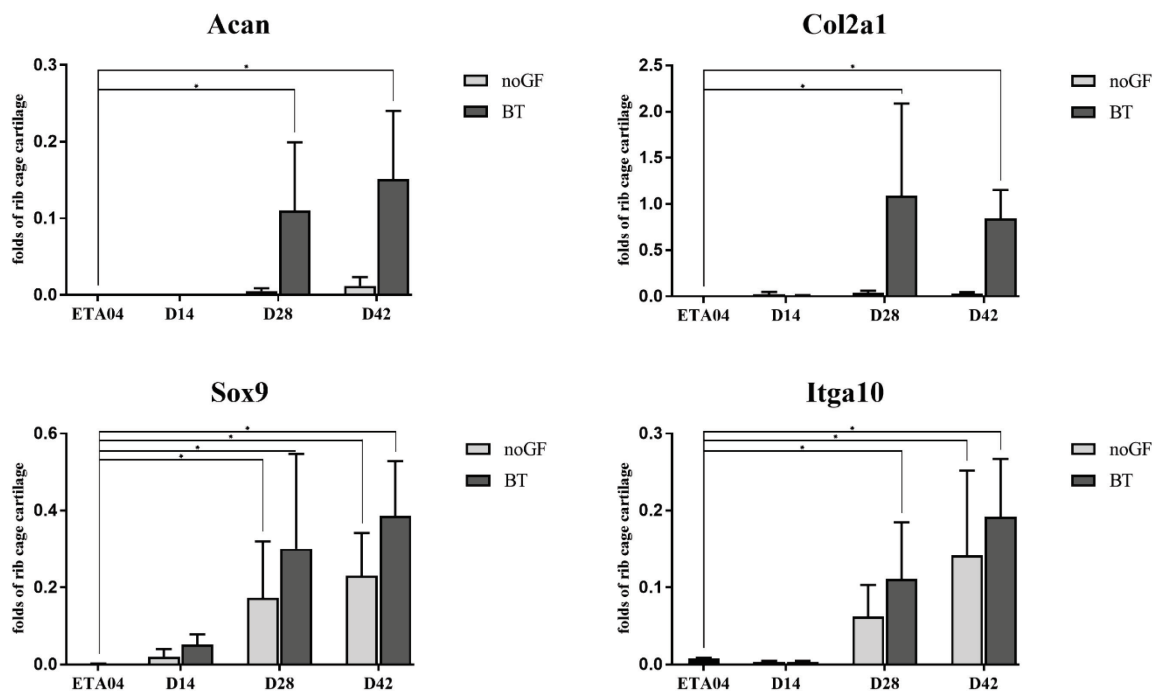


Figure 52: qPCR of chondrogenic markers in stimulated (BT) and non-stimulated (noGF) chondrogenic spheroids.

Expression of chondrogenic markers Aggrecan (*Acan*) and Collagen Type II (*Col2a1*) was significantly upregulated in stimulated chondrogenic spheroids as soon as day 28 compared to parental IPSCs (ETA04). *Sox9* and $\alpha 10$ -integrin (*Itga10*) expression was significantly upregulated compared to parental IPSCs (ETA04) in stimulated and non-stimulated spheroids on day 28 and 42. Bars represent fold change of gene expression compared to rib cage cartilage and are plotted as mean + SD. Asterisks mark significant changes of gene expression levels.

Furthermore, we analyzed expression of both isoforms of type II procollagen, procollagen IIA (*Col II A*) and procollagen IIB (*Col II B*), in stimulated and non-stimulated chondrogenic spheroids on day 42. We used a specially designed quadruple of primers that allow to simultaneously detect procollagen IIA and procollagen IIB during one run of PCR leading to two PCR products on agarose gel electrophoresis (Figure 53) [129].

In rib cage cartilage only the mature form *Col IIB* could be detected. Expression of both isotypes was seen in stimulated and non-stimulated spheroids indicating presence of chondroprogenitor cells as well as more mature chondrocytes. The stimulated spheroids, however, clearly showed higher expression levels of the mature isotype procollagen IIB.

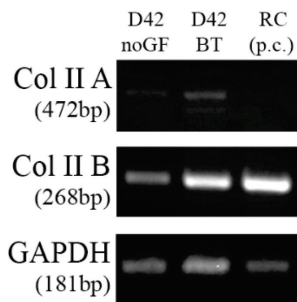


Figure 53: RT-PCR for procollagen II isoforms procollagen IIA (*Col II A*) and B (*Col IIB*)

For simultaneous analysis of the expression of the two isoforms of Procollagen II (*Col II A* and *Col II B*) in stimulated (BT) and non-stimulated (noGF) chondrogenic spheroids on day 42 two primer pairs were used within the same probe resulting in two bands after agarose gel electrophoresis. Rib cage Cartilage (RC) was used as a positive control.

These results further support our hypothesis that chondrogenic differentiation of induced pluripotent stem cells can be achieved by culturing EBs in chondrogenic medium. To achieve a hyaline cartilage phenotype with high expression of mature chondrogenic markers and deposition of cartilage specific ECM, however, these spheroids need to be stimulated by chondrogenic growth factors.

6.6.2.3. Expression of hypertrophy markers in chondrogenic spheroids

Finally, we analyzed expression of hypertrophy markers *Runx2* and type X Collagen (*Col10a1*).

Expression of *Runx2* was significantly upregulated in stimulated spheroids as soon as day 28, whereas expression of *Col X* was significantly upregulated in stimulated spheroids only on day 42 compared to parental iPSCs.

Figure 54 shows the results of the qPCR of chondrogenic markers as fold change compared to expression in murine embryonic rib cage cartilage.

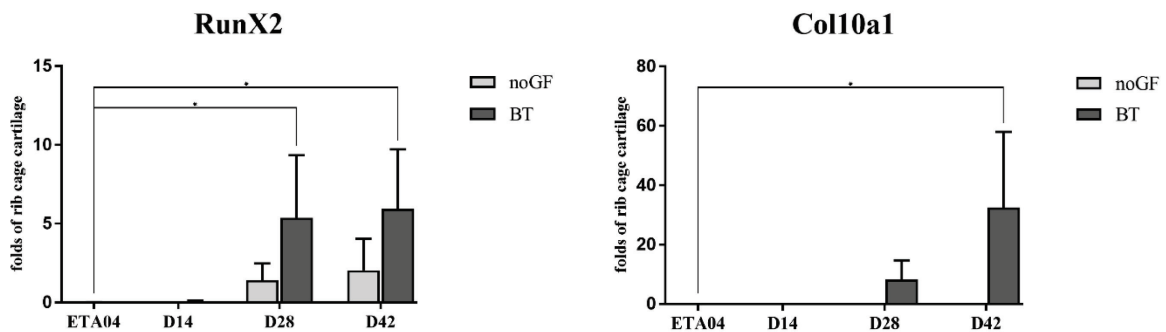


Figure 54: qPCR of hypertrophy markers in stimulated (BT) and non-stimulated (noGF) chondrogenic spheroids.

Expression of hypertrophy marker *Runx2* was significantly upregulated in stimulated chondrogenic spheroids as soon as day 28 compared to parental iPSCs (ETA04). Collagen Type X (*Col X*) expression was significantly upregulated compared to parental iPSCs (ETA04) in stimulated spheroids on day 42. Bars represent fold change of gene expression compared to rib cage cartilage and are plotted as mean + SD. Asterisks mark significant changes of gene expression levels.

These results indicate that despite successful chondrogenic differentiation also hypertrophy occurred within the stimulated spheroids. This might be due to prolonged exposure to BMP2 which is known to not only enhance chondrogenesis but also to play an important role in the induction of hypertrophy during endochondral ossification [156]. Further research is necessary to evaluate the effect of more elaborate growth factor supplementation on the quality of chondrogenic spheroids derived from culture of EBs under chondrogenic conditions.

7. **Discussion**

7.1. **Sleeping Beauty transposon system for reprogramming**

For the generation of the first iPSCs, *Takahashi et al.* screened 24 candidate genes for their ability to direct somatic cells back to a pluripotent state, and identified the four reprogramming factors Oct3/4, Sox2, Klf4 and c-Myc. Each gene was transfected by an individual retroviral vector. This approach led to high expression of the transfected genes and allowed reprogramming at a quite high efficiency [15]. However, multiple genomic insertion sites of the individual reprogramming factors were produced [15]. This imposes a high risk of insertional mutagenesis, and chances that one of the multiple insertion sites is inefficiently silenced or reactivated during differentiation are high [41].

Since then, multiple gene delivery methods have been used for induction of pluripotency each with their own inherent advantages and disadvantages that are summarized in Table 33.

Viral vectors offer high efficiency for delivery of transgenes into cells as viruses are natural gene transfer vehicles that have evolved to cross cellular membranes [43]. However, viruses are potentially immunogenic and are therefore generally considered less suitable for generation of clinical grade iPSCs. Non-viral methods contrarily suffer from low efficiency rates, but provide easier handling and are less immunogenic [51].

Integrating methods provide stable transgene expression over a prolonged time allowing high reprogramming efficiencies, but they bear the risk of insertional mutagenesis [42]. Integration of a transgene into a gene or its regulatory elements might not only disrupt transcriptional units, but can lead to transcriptional activation or inactivation of nearby genes [42, 246]. Such genotoxic effects can have devastating consequences for the cell [42]. Non-integrating methods, are considered safer, but suffer from low reprogramming efficiencies due to limited duration of transgene-expression rendering repeated transfections necessary [43].

In polycistronic vectors, the cDNA sequences of the reprogramming factors are separated by self-cleaving 2A peptide sequences [247]. This allows expression of all reprogramming factors from a single expression cassette, therefore minimizing the number of integration sites required and ensuring expression of the reprogramming factors in a 1:1 stoichiometry [51, 247]. Furthermore, all reprogramming factors can be expressed from a single promoter reducing

interference of the exogenous promoter with nearby endogenous promoters [51]. Therefore, the reprogramming factors should be provided as polycistronic vectors for both research and clinical purposes.

Table 33: Methods for the generation of induced pluripotent stem cells

		Delivery method	Advantages	Disadvantages
Integrating methods	Viral	Retroviral vectors [15, 17]	<ul style="list-style-type: none"> Efficient 	<ul style="list-style-type: none"> Insertional mutagenesis Transgene reactivation Integration preferentially into transcriptional start sites
		Lentiviral vectors [19, 66, 247, 248]	<ul style="list-style-type: none"> Highly efficient 	<ul style="list-style-type: none"> Insertional mutagenesis Transgene reactivation Integration preferentially into actively transcribed genes
	Non-viral	Transposons [53-55]	<ul style="list-style-type: none"> Efficient Safe integration profile Possibility of removal 	<ul style="list-style-type: none"> Insertional mutagenesis Transgene reactivation
Non-integrating methods	Viral	Adenoviral vectors [44]	<ul style="list-style-type: none"> No genomic integration 	<ul style="list-style-type: none"> Inefficient Repeated transfections required High workload
		Sendai virus [45]	<ul style="list-style-type: none"> Efficient No genomic integration 	<ul style="list-style-type: none"> Difficult handling No GMP-grade reagent available
	Non-viral	Plasmids Minicircles [46, 47]	<ul style="list-style-type: none"> No genomic integration Easy handling 	<ul style="list-style-type: none"> Highly inefficient Repeated transfections required Spontaneous integration possible
		Episomal plasmids [48]	<ul style="list-style-type: none"> No genomic integration Autonomous replication 	<ul style="list-style-type: none"> Inefficient
		mRNA [50]	<ul style="list-style-type: none"> Efficient No genomic integration 	<ul style="list-style-type: none"> Difficult handling Repeated transfections required High workload
		Protein [49]	<ul style="list-style-type: none"> No genomic integration 	<ul style="list-style-type: none"> Inefficient Difficult production Repeated transfections required

7.1.1. Integrating viral vectors

Retroviral vectors have been used by *Takahashi et al.* for the generation of the first iPSCs [15]. They are easy to use and provide stable expression of transgenes facilitating high reprogramming efficiency [15, 41]. Lentiviruses do not rely on cell division to integrate their cargo into the host's genome, and thus are able to infect a broader range of cell types [41]. Lentiviral vectors have been widely applied for reprogramming of murine and human somatic cells [19, 66, 247, 248].

Retroviral vectors are commonly based on the murine leukemia virus (MLV) and preferentially integrate their genetic cargo into transcriptional start sites of active genes [249]. Lentiviral vectors are often derived from the human immune deficiency virus (HIV-1) and show a strong tendency to integrate their cargo into actively transcribed genes [250]. Therefore, both gene vectors impose a high risk of insertional mutagenesis [59, 65]. Virally induced transgenes regularly are silenced during the reprogramming process, however, reactivation of potential oncogenes like *c-Myc* can occur upon differentiation and imposes a high risk of tumor formation [17, 41].

Doxycycline-inducible lentiviral vectors have been used to generate secondary, inducible reprogramming systems, that are powerful tools in understanding the molecular mechanism of reprogramming [66, 67]. Differentiated cells carrying the inactive transgene (*e.g.* fibroblasts or lymphocytes) are isolated from chimeras generated by injection of “primary” iPSCs into blastocysts. Upon exposure to doxycycline, the reprogramming factors are re-expressed and the somatic cells are reprogrammed into “secondary” iPSCs in a controllable and synchronous manner [67, 71].

But, despite being valuable tools for basic research on the reprogramming process, retroviral and lentiviral vectors are less suitable for clinical applications.

7.1.2. Non-integrating viral vectors

Replication-defective adenoviral vectors have been used to generate iPSCs [44]. As they do not integrate into the host genome, they are gradually lost due to cell division so that multiple viral

infections are required [41, 44]. Also, production of adenoviral vectors is labor-intensive and reprogramming efficiency is low [41]. Therefore, adenoviruses seem less suitable for the generation of iPSCs for research or cell therapy purposes.

Recently the non-integrating RNA Sendai virus has been used successfully to generate iPSCs [45]. This method is effective and does not bear the risk of insertional mutagenesis [3]. Furthermore, after successful reprogramming, remaining virus containing cells can be easily removed by antibody mediated negative selection [41, 45]. However, Sendai viruses are difficult to handle, and no good manufacturing practice (GMP)-grade reagents are available so far [3, 41]. Although Sendai-virus based vectors are promising, more research is required before they can be used to generate clinical-grade iPSCs.

7.1.3. Non-integrating non-viral vectors

Delivery of the reprogramming factors as plasmids or minicircles is a simple method for generation of induced pluripotent stem cells [46, 47]. These DNA-based vectors are easy to produce and can be delivered using standard transfection techniques [41, 42]. But, since the vectors do not integrate into the genome, they are diluted upon cell division so that multiple transfections are required [42]. The overall reprogramming efficiency of these methods remains very low [41]. Furthermore, spontaneous genomic integration of these DNA molecules can occur requiring labor-intensive screening for integration-free clones [41, 251]. Therefore, these plasmid-based vectors are not optimal to generate clinical-grade iPSCs.

Episomal plasmids are based on the Epstein-Barr Nuclear Antigen-1 (oriP-EBNA1) [41]. Although these plasmids do not integrate, they attach to the host chromatin and replicate synchronously with the host genome during cell division [41]. Even though the generation of induced pluripotent stem cells using episomal vectors has been reported, the reprogramming efficiency remains very low hampering widespread application of this method [3, 48].

The transcription factors can also be provided as mRNA or proteins [49, 50]. Reprogramming with mRNA is an effective and safe method, as there is no risk of genomic integration [3]. However, mRNA is difficult to handle and suffers from a relatively short half-life, so that repeated transfections are required [3]. Furthermore, naked mRNA is highly immunogenic [41].

Delivering the reprogramming factors as synthetic proteins also requires multiple transfections and shows only very low reprogramming efficiency [41]. Furthermore, it is difficult to synthesize proteins in the required quantities [3]. Therefore, neither mRNA- nor protein-based delivery of the reprogramming factors are optimal approaches for reprogramming.

7.1.4. Integrating non-viral vectors

Transposon-based gene delivery vectors consist of a donor plasmid that contains the gene of interest flanked by terminal inverted repeats (TIRs) and a source of the transposase enzyme that is mostly provided by a second plasmid. After transfection, the transposase enzyme catalyzes excision and genomic integration of the gene of interest in a cut-and-paste mechanism [43, 57].

There are many transposon systems available for gene transfer in murine and human cells. The Sleeping Beauty (SB) and PiggyBac (PB) systems belong to the most well-established systems, and have been successfully used for the generation of induced pluripotent stem cells from murine and human somatic cells [53-55].

Transposons combine the advantages of integrating viral vectors with the advantages of non-viral delivery systems [42, 51]. Development of hyperactive variants of the transposases (*e.g.* SB100x for Sleeping Beauty) allowed gene delivery at efficiency levels comparable to viral vectors overcoming one of the main barriers of non-viral delivery methods [58]. As integrating vectors, they provide stable expression of the induced transgenes during the reprogramming process facilitating successful reprogramming [51, 53]. On the other hand, transposons are less immunogenic than viral vectors [51]. Furthermore, as plasmid-based systems, they can be easily and cost-effectively produced at high quality and do not require a biohazard facility [51, 54]. They offer high DNA cargo capacity and can accommodate a polycistronic construct containing all reprogramming factors and additional genes like *for example* selection markers [53, 54].

However, as integrating vectors, transposons still impose a risk for insertional mutagenesis. Comparison of the integration preferences of several gene transfer vectors including the transposons Sleeping Beauty, PiggyBac and Tol2, the retroviral murine leukemia virus (MLV) and the lentiviral human immune deficiency virus (HIV) showed a highly favorable integration

profile for the SB transposon system (Figure 55) [59, 65]. On the primary DNA level, Sleeping Beauty is highly specific and integrates strictly only into TA-dinucleotides [56, 64]. On a genome-wide basis, however, it shows a nearly random distribution with no bias for integration into genes or transcriptional regulatory regions [65, 252]. Therefore, the majority of SB integrations occurs in intergenic regions causing no relevant insertional mutagenesis [43]. Bioinformatical analysis of the integration sites regarding proximity to genes, cancer-related genes and microRNAs further confirmed the favorable integration profile of Sleeping Beauty [42].

The PiggyBac system shows a slight bias for integration into promoters and exonic regions which resembles the integration pattern of the retroviral MLV [65, 252].

Although the Sleeping Beauty transposon integrates its cargo into the host genome, its favorable integration profile makes it less prone to cause insertional mutagenesis. Therefore, it might represent a good compromise between efficient reprogramming, that requires stable transgene expression, and safety concerns, that fear insertional mutagenesis.

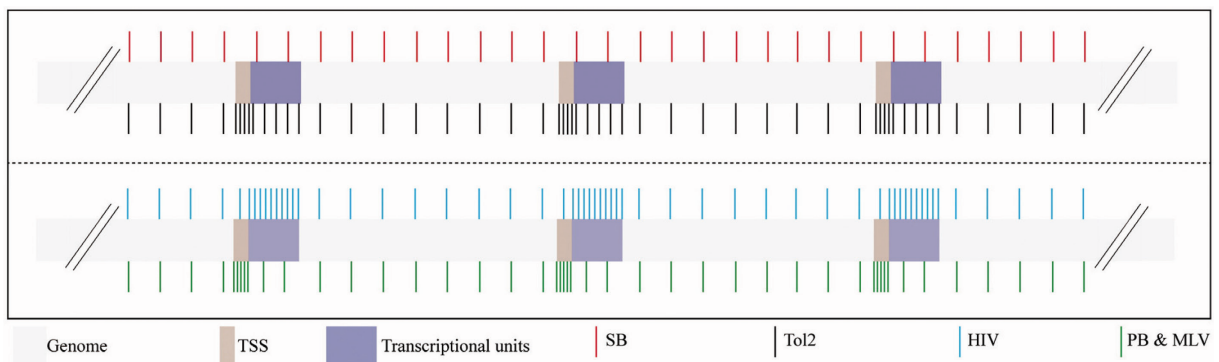


Figure 55: Integration profile of commonly used gene vectors. From Narayanavari et al. [59].

Whereas the Sleeping Beauty (SB) transposon system shows a nearly random integration profile on a genome wide basis, other integrating vectors like the PiggyBac (PB) and Tol2 transposon system as well as the retroviral murine leukemia virus (MLV) and the lentiviral human immune deficiency virus (HIV) show a clear bias for integration into genes or transcriptional start sites (TSS).

Furthermore, the TIRs of Sleeping Beauty – in contrary to the PiggyBac system – have no endogenous enhancer or promoter activity [253, 254]. Also, there are no SB-related elements within mammalian genomes that could be cross-mobilized by the introduced transposons as it has been reported for the PiggyBac system [41, 53].

The Sleeping Beauty system is in fact considered safe enough to be applied in clinical trials. It has been widely used as a gene delivery vector for gene therapy in several animal models [42]. This includes *e.g.* the delivery of coagulation factor IX to mouse liver cells that led to long term stable expression of the factor in a mouse model of hemophilia B [255], or delivery of FAH (fumarylacetoacetate hydrolase) to mouse livers that led to correction of murine tyrosinemia type I [256]. Recently two clinical trials using SB transposons in humans have been launched. One includes the delivery of PDEF (pigment epithelium-derived factor) into retinal pigment epithelial or iris pigment epithelial cells, that are harvested and transplanted back into the patient after transfection during a single surgical session (TargetAMD) [42, 257]. Furthermore, SB is used to deliver chimeric antigen receptors (CAR) into tumor reactive T-cells that are used in the treatment of B-cell malignancies [42, 258].

Taken together, the Sleeping Beauty transposon system has been used successfully for the generation of iPSCs in mouse and human. It is an easy to use gene vector, and due to its favorable integration profile, considered safe-enough for clinical applications. Therefore, it might be applicable to use iPSCs generated with the Sleeping Beauty system not only for research purposes but also for iPSC-based therapies in a clinical setting.

For clinical applications, possible reactivation of the genomically integrated reprogramming factors, especially the known oncogenes *Klf4* and *c-Myc*, raises safety concerns [41]. Therefore, removal of the reprogramming factor cassette after successful reprogramming would be desirable. This could be achieved by re-expressing the transposase enzyme that now catalyzes excision of the transposon from its genomic location. This approach has been successfully used to produce integration free iPSCs from the PiggyBac transposon [259, 260]. The PiggyBac transposon can be removed seamlessly and leaves no footprint in the genome [261]. For the Sleeping Beauty system however, excision rates are quite low, and a footprint is left behind that imposes a remnant risk for insertional mutagenesis [262, 263]. Excision of the reprogramming factor cassette furthermore requires labor-intensive screening for clones with few or only a single integration site, mapping of the integration site, excision of the reprogramming factor cassette and validation of the factor-free clone [51]. Additionally, there is still a risk of reintegration of the excised transposon by the transposase at a new genomic location.

Exchange of the reprogramming factor cassette by recombinase mediated cassette exchange (RMCE) would therefore be an appealing alternative to complete removal of the

reprogramming factor cassette. By flanking the reprogramming factor expression cassette with heterospecific *loxP* sites, it is possible to exchange the transgene for another gene of interest by exposure to the Cre recombinase [53]. The genomically integrated reprogramming factor cassette could serve as a “safe harbor site” for other transgenes that would *e.g.* correct genetic diseases. It would be furthermore possible to generate iPSCs “primed” for a certain differentiation lineage *e.g.* by overexpression of lineage-specific key transcription factors. More research is required to enlighten the impact of RMCE-introduced genes of interest on iPSC’s differentiation potential and safety.

7.1.5. Conclusion

Since the generation of the first iPSCs more than ten years ago, many advances have been made in optimizing the reprogramming process. However, there is still no ideal vector to deliver the reprogramming factors, instead the right vector must be carefully chosen for the right application.

For the generation of iPSCs for cell therapy purposes, the vector must be safe, *i.e.* non-oncogenic, with no off-target effects even if that involves high work load or rather inefficient reprogramming. To generate iPSCs for basic research purposes however, a high reprogramming efficiency along with a low work-load is desirable to facilitate *e.g.* high-throughput screenings or enable generation of iPSCs from scarce starting cell populations [41].

There is a broad consent, that avoiding viral insertions is a strict requirement for clinical translation of iPSCs. To dissect the reprogramming process itself however, inducible lentiviral vectors allow the generation of secondary iPSCs and play a fundamental role in basic iPSC research [67, 71]. Non-integrating methods, however, suffer from low reprogramming efficiencies. Transposons combine the high reprogramming efficiency of integrating vectors with the superior safety profile of non-viral vectors and might therefore be suitable to generate iPSCs for basic research and cell therapy.

7.1.6. Reprogramming of murine fibroblasts with a Sleeping Beauty transposon-based reprogramming system

In this thesis, we used a Sleeping Beauty transposon-based reprogramming system consisting of two plasmids. One plasmid carried the transposon TIRs flanking the reprogramming factors and additional selection markers, whereas the second plasmid served as a source of the hyperactive transposase SB100X.

Four different reprogramming factor plasmids were used. All carried the reprogramming factor cassette consisting of a polycistronic vector carrying the cDNAs of *Oct3/4*, *Sox2*, *Klf4* and *c-Myc* plus/minus *Lin28* separated by self-cleaving 2A-peptides [247]. On the *pT2OSKM* and *pT2OSKML* plasmids the reprogramming factor cassette and a *Puro Δ TK* selection marker was inserted between the transposon TIRs. The *RMCE-OSKM-Cherry* and *RMCE-OSKML-Cherry* plasmids additionally contained a *mCherry* pluripotency reporting cassette and heterospecific *loxP* sites that would allow for modification of the genomically integrated transposon by RMCE [53].

These plasmids were delivered into primary mouse embryonic and adult fibroblasts by nucleofection, which has been shown to be a suitable delivery method for plasmid-based transposon systems [53]. Efficiency rates for the delivery of plasmids into our primary cell populations by nucleofection were determined by transfection with a *GFP*-plasmid and ranged between 40% for EAR-FBs and 87% for MEFs. Nucleofection efficiencies for the Sleeping Beauty transposon system were supposedly lower, due to the larger size of the reprogramming factor plasmids and the need for co-transfection of two plasmids. However, since a single genomic integration of the transposon is sufficient for successful reprogramming, delivery of the transposon system by nucleofection was still considered suitable.

The optimal transposase : transposon ratio for the Sleeping Beauty transposon system is about 1:10 [63]. Therefore, we co-transfected 0.1 μ g, 0.2 μ g or 0.5 μ g of the SB100x-transposase plasmid with 1 μ g, 2 μ g or 5 μ g of the respective reprogramming factor plasmid.

With this approach we succeeded at reprogramming primary murine embryonic fibroblasts and primary murine adult fibroblasts isolated from ear or tail of adult wild-type mice. More than 250 iPSC colonies were picked, and assessment of 22 selected IPS cell lines for morphological traits and expression of pluripotency markers confirmed their successful reprogramming.

Splinkerette PCR is an established method to determine the number of genomically integrated transposon copies [53]. Two of the 22 analyzed cell lines were confirmed to contain only a single transposon integration site, and were therefore considered especially suitable for subsequent differentiation assays. There was no evident correlation found between the number of transposon integration sites and the amount of transposase and transposon used to transfect the respective cells, likely due to the limited number of analyzed cell lines.

In conclusion, we have established a reliable and effective reprogramming protocol for primary murine cells using the Sleeping Beauty transposon based reprogramming system. Since the reprogramming plasmids used in this thesis have also been successfully used to reprogram human cells, transfer of our reprogramming system to primary cells isolated from patients would likely be possible [53].

7.2. Significance of IPSCs for cartilage regeneration

7.2.1. State of the art of cartilage repair

Focal cartilage lesions and osteoarthritis dramatically impair quality of life of affected patients and impose a large socioeconomic burden on society [168, 171]. Although modern MRI imaging allows detection of early osteoarthritis-associated changes, there is still no causative treatment [170, 171]. In early stages treatment of osteoarthritis is limited to reduction of risk factors like obesity or surgical correction of joint malalignment [171, 174]. Pharmaceutical treatment of symptomatic osteoarthritis by analgesic and anti-inflammatory drugs is hardly effective and does not stop progression of cartilage degradation [170, 171]. Definitive treatment of osteoarthritis can only be achieved by total joint replacement [174]. Despite good to excellent results of total joint replacement for hip and knee osteoarthritis, it remains a maximally invasive procedure with non-negligible operative and perioperative risks [174]. The perioperative risks include *e.g.* bleeding with need for transfusion (6-12%), wound infections (1%), deep vein thrombosis (0,2 – 0,7%) and pulmonary embolism (0,2 – 0,5%) [264]. The 15-year survival rate of the prosthesis is about 86% for total hip replacement and 80% for total knee replacement with aseptic loosening being the most common cause for revision [174, 265, 266].

The poor intrinsic regeneration capacity of articular cartilage as well as the propensity of focal cartilage lesions to progress into osteoarthritis are well-known facts [169]. There is broad consent that, especially in younger patients, sufficient treatment of focal cartilage lesions to prevent progression into osteoarthritis, and delay need for total joint replacement is desirable.

Current therapeutic options for focal cartilage lesions include microfracture, osteochondral autograft transfer and autologous chondrocyte injection.

The microfracture technique mimics natural repair of osteochondral defects. Small holes are made arthroscopically in the subchondral bone through which bone-marrow mesenchymal stem cells (BM-MSCs) along with blood and fat emerge [181, 182]. These stem cells differentiate over time into chondrocytes and fill the defect with fibrocartilaginous tissue [181, 183]. Initially significant clinical improvement is seen with about 67% of patients reporting good to excellent knee function two years after microfracture procedure due to symptomatic focal cartilage lesions [181]. The most common complications of microfracture are subchondral bone edema,

osteophytes and subchondral cysts [183, 186]. Currently, microfracture represents the gold standard for the initial treatment of small lesions ($< 2\text{cm}^2$) [186]. It is especially suitable as a first line treatment in low demanding patients, as it is a minimally invasive, single stage procedure with minimal morbidity [181, 185]. However, due to formation of biomechanically inferior fibrocartilage many patients report secondary deterioration of symptoms after two to four years [181, 184, 267]. Therefore, microfracture does not represent an optimal method for cartilage regeneration.

The AMIC (autologous matrix induced chondrogenesis) procedure represents an advanced modification of microfracture. Here a collagen I/III membrane (e.g. *Chondro-Gide*®, Geistlich Pharma AG, Wolhusen, Switzerland) is applied to stabilize the clot formed by microfracture [187]. Patients treated with AMIC reported significant reduction of pain and significant improvement of Lysholme score two years after treatment [188, 268]. Even after five years, patients treated with AMIC showed stable improvement in the modified Cincinnati score and reported very low pain, whereas in patients treated with microfracture alone, both parameters had already deteriorated [189]. Histological results, however, showed that the defect areas are mostly filled with fibrocartilaginous repair tissue after two years [189]. Therefore, it is likely that in a long term follow up with an adequate number of patients the clinical improvement by AMIC is not durable, too.

During osteochondral autograft transfer (OAT) the defect is filled with osteochondral cylinders harvested from low weight-bearing areas of the joint [193]. Today, transfer of multiple small osteochondral grafts – also known as mosaicplasty – represents the state of art since it results in smaller donor site defects and allows better contouring at the recipient site compared to transfer of a single large graft [195]. Besides for cartilage lesions in the knee joint, OAT has been used successfully for focal cartilage defects of the talar dome, the capitulum humeri, the humeral head and the femoral head [196]. Analysis of a prospective database with more than 1000 patients undergoing mosaicplasty showed good-to excellent results in 74% - 92% of the patients after 10 years depending on the location of the recipient site [196]. However, 3% of patients reported moderate to severe symptoms at the donor site [196]. Biopsies taken after up to 3.5 years after OAT showed fibrocartilage filling at the donor sites and a good survival of the transplanted hyaline cartilage at the recipient sites [193]. Despite good clinical and

functional results application of OAT is restricted to small defects due to the limited availability of donor sites [186, 193, 196].

Autologous chondrocyte injection (ACI) is indicated for full-thickness osteochondral defects with a size of 2 cm² to 12 cm² [177, 186], or in patients where microfracture has failed [115, 177]. Articular cartilage is harvested from a non-weight bearing area of the joint, then chondrocytes are isolated and expanded in vitro before they are injected into the defect area during a second surgery [200]. During expansion in monolayer culture, dedifferentiation of chondrocytes occurs. The morphology gradually changes from small polygonal cells to a flattened, spindle-shaped, fibroblast-like morphology [202, 216]. Furthermore, expression of chondrocyte markers like *Sox9*, *aggrecan* and type II collagen (*Col2a1*) decreases whereas expression of type I collagen (*Colla1*) increases [202]. Injection of these dedifferentiated cells leads to biomechanically inferior fibrocartilage as repair tissue [201]. In first generation ACI, the cell suspension was injected under a periosteal flap [200]. Although the reported clinical outcome was good to excellent after two years, this method not only requires harvesting of a periosteal flap, leading to longer operating times and harvesting site morbidity, but over the years, often symptomatic hypertrophy of the periosteal flap occurred [176, 177, 200, 269]. Therefore, the periosteal flap was replaced by synthetic membranes consisting *e.g.* of collagen I/III (*Bio-Gide*®, Geistlich Biomaterials, Wolhusen, Switzerland) [203]. *Gomoll et al.* showed that reoperation rate due to patch-related issues was significantly lower in the synthetic membrane group (26% vs. 5%) [203]. Furthermore, ACI requires at least two surgeries and a long recovering period imposing high costs on the health system as well as pain and discomfort on the patient [115, 177, 206].

In conclusion, currently available repair strategies for focal chondral lesions suffer from formation of biomechanically inferior fibrocartilage, destruction of healthy articular cartilage leading to donor-site morbidity, and need for invasive surgical procedures [176, 186].

During matrix assisted ACI (MACI), the harvested chondrocytes are cultured in hydrogels like *CaReS*® from ArthroKinetics, Esslingen, Germany [204] or *BioSeed-C*® from BioTissue, Zürich, Switzerland [205]. This not only ensures a more even distribution of the implanted chondrocytes within the defect and provides easier surgical handling, but also helps to prevent chondrocyte dedifferentiation [186, 205]. Both matrixes resulted in significant clinical improvement after two or three years [204, 205]. Similar products could be generated with

chondrogenically differentiated MSCs or iPSCs providing ready-to-use off-the-shelf products for cartilage repair [176, 206].

7.2.2. Mesenchymal stem cells for cartilage repair

Due to their well-described chondrogenic potential, mesenchymal stem cells (MSCs) are an intensively studied cell population for cartilage repair. Autologous and allogenic MSCs have been used in clinical trials for the treatment of cartilage defects [211, 212]. Compared to autologous chondrocytes, MSCs have a superior proliferation capacity and can be harvested in higher numbers *e.g.* from the iliac crest under local anesthesia without need for general anesthesia or destruction of healthy cartilage [211]. Comparison of autologous bone marrow derived MSCs (BM-MSCs) and autologous chondrocytes for injection into cartilage defects showed significant improvement of quality of life as well as knee function two years after treatment for both cell types with no significant difference between these approaches [211].

However, the most commonly used and best-studied BM-MSCs do not only require invasive and painful harvesting but are also known to occur only in very limited numbers in bone marrow [213]. MSCs make up only about 0.0001% of all mononuclear cells in a bone marrow aspirate [270]. Furthermore, BM-MSCs have an inherent propensity to display a hypertrophic phenotype during chondrogenic differentiation, probably due to the role of cartilage as a bone-template during endochondral ossification [133, 172]. Deposition of type I and type X collagen in the extracellular matrix results in a tissue that is not adapted to the pressure and shear forces articular cartilage is subjected to and is therefore an inferior replacement for hyaline cartilage [217].

Adipose tissue derived stem cells (ADSCs) can be harvested from liposuction aspirates and are more abundant than BM-MSCs, making up about 0.05% of all mononuclear cells within a liposuction sample [270]. However, proliferative capacity and chondrogenic potential of ADSCs are lower than of BM-MSCs [133]. ADSCs showed less upregulation of chondrogenic markers (*ACAN*, *COL2A1*) as well as lower GAG-content in the ECM during chondrogenic differentiation [133]. Therefore, ADSCs do not represent an optimal cell source for cartilage regeneration, too.

Furthermore, there is an age-related decline in in vivo frequency and in vitro proliferation rate of MSCs [271, 272]. MSCs isolated from older donors can undergo only a limited number of population doublings before senescence, so it might be challenging to retrieve enough cells for tissue engineering applications [271]. Additionally, the chondrogenic differentiation capacity is reduced in MSCs from older donors [271, 272]. It has also been shown that BM-MSCs isolated from patients with severe osteoarthritis have a significant lower proliferation rate as well as a significant reduced chondrogenic activity compared to healthy age-matched controls [273]. Therefore, especially for patients most in need of articular cartilage repair, autologous MSCs might not be the optimal cell source for tissue engineering applications [213].

Use of allogeneic MSCs would allow for a single-stage cartilage repair procedure [206]. In a first-in-human clinical trial *Park et al* used allogeneic human umbilical cord blood derived MSCs (hUCB-MSCs) embedded in a hyaluronic acid hydrogel (*Cartistem*) to treat osteoarthritis or focal cartilage defects in seven patients [212]. During the seven year follow up period, all patients reported clinical improvement and no serious adverse events (SAEs) occurred [212]. Importantly, no rejection of the allogeneic stem cell derived product occurred, which is likely due to the hypoimmunogenic and immunomodulatory properties of MSCs [212]. Umbilical cord blood-derived MSCs can be harvested non-invasively after delivery, but can be only isolated from around 30% of the samples. Furthermore, risk of immune reactions and infectious disease transmission hampers their clinical applicability [115, 206].

Taken together, despite successful clinical application of MSCs for cartilage repair, MSCs suffer from invasive harvesting, the propensity to form hypertrophic cartilage as well as an age-related decline in in vivo frequency and in vitro proliferation potential [172, 213]. Induced pluripotent stem cells might overcome the limitations of current cartilage repair strategies and become a valuable alternative for treatment of focal cartilage lesions.

7.2.3. Induced pluripotent stem cells for cartilage regeneration

Due to their somatic origin, their unlimited proliferation potential and their ability to differentiate into every desired cell type, induced pluripotent stem cells offer promising possibilities for regenerative medicine and tissue engineering.

Patient-derived autologous iPSCs would theoretically facilitate transplantation of patient-specific tissues or organs without risk of immune-rejection and therefore without need for immunosuppressive medication [274, 275]. However, it has been shown, that transplantation of undifferentiated iPSCs into syngeneic hosts led to T-cell infiltration and necrosis suggesting that these autologous iPSCs are immunogenic [276]. Differentiated derivatives of iPSCs though showed less propensity of provoking an immune rejection response [277, 278]. Additionally, it has been shown that the immunogenicity of iPSC-derivatives varies among cell types and recipient sites [279]. Due to its avascular structure and dense ECM, cartilage is considered an immune-privileged tissue, and even transplantation of unrelated donors hardly induces a relevant immune response [16]. Immunogenicity of autologous iPSC-derived chondrocytes or cartilage matrix might therefore be less clinically relevant. However, more research needs to be conducted on determining the underlying mechanisms of iPSC-immunogenicity in general and its implications on the utility of iPSCs for cartilage regeneration.

Autologous iPSCs can be successfully reprogrammed from various cell sources like fibroblast [19], keratinocytes [37], blood cells [36] or urinary tract epithelium [280] that can be accessed minimally or even non-invasively. Generating autologous iPSCs for each individual patient, however, would require time- and labor-intensive isolation and propagation of cells, reprogramming, picking and expansion of IPS cell lines, testing for complete reprogramming and screening for potentially harmful mutations through the reprogramming process. Performing all these procedures under GMP guidelines is extremely laborious and costly [16, 113].

As producing autologous iPSCs for every single patient – at least at the moment – seems not feasible and still bears a small risk of immune rejection, HLA-matched allogenic iPSCs might represent a valuable alternative [16, 274]. Large database-analyses suggested that about 50 homozygous IPS cell lines would allow a haplotype match of over 90% in Japan, whereas in the UK about 150 homozygous IPS cell lines would be needed [274, 281, 282]. It was estimated that a bank of 100 homozygous IPS cell lines would offer a haplotype match to 78% of Europeans, 63% of Asians, 52% of Hispanics and 45% of African Americans [283].

For allogenic iPSCs to be used for cartilage repair, probably no ideal HLA match would be required due to the immune-privileged nature of articular cartilage. Therefore, such iPSC banks could provide stem-cell based cartilage repair for even a higher percentage of patients.

However, efficient differentiation of iPSCs into hyaline cartilage tissue remains challenging and hampers development of an allogenic iPSC-based off-the shelf product for cartilage repair [206]. Reliable and scalable chondrogenic differentiation protocols are needed before iPSC-based cartilage repair can be considered for clinical applications.

7.3. Chondrogenic differentiation of pluripotent stem cells

In order to apply iPSCs for cartilage repair in patients, safe and reliable differentiation protocols that are scalable to produce implantable grafts in sufficient size are needed. Currently four different strategies for the differentiation of pluripotent stem cells (PSCs) into cartilage have been described: first, co-culture of PSCs with mature chondrocytes [134, 217, 218]; second, culture of PSCs under the influence of growth factors mimicking physiological chondrogenic development during embryogenesis [127, 135, 219]; third, two-step differentiation via mesenchymal stem cell (MSC)-like cells as an intermediate [220-222]; and finally, formation of embryoid bodies (EBs) allowing spontaneous differentiation of PSCs and subsequent selection of a chondrogenically primed subpopulation and its direction towards the chondrogenic lineage [126, 223, 224]. Upregulation of chondrogenic markers as well as formation of implantable grafts can be achieved by all these methods, however, none of these methods is already applicable for cartilage repair in patients due to safety concerns or laborious and expensive differentiation protocols.

7.3.1. Chondrogenic differentiation of iPSCs via chondrogenic colonies

Chondrogenic differentiation of PSCs can be achieved by exposure to defined chondrogenic growth factors.

Oldershaw et al. established a protocol for the stepwise differentiation of ESCs towards chondrocytes mimicking embryonic development via mesendodermal and mesodermal intermediates. ESCs were grown for 14 days in monolayer culture and a sequence of growth factors including Wnt3a, Activin A, FGF2, BMP4, follistatin, neurotrophin4 and GDF5 was added to the culture medium at defined concentrations for each time point. During the differentiation, the cells showed a temporary upregulation of mesoendodermal and mesodermal markers. After 14 days, the ESC-derived chondrocyte-like cells expressed chondrogenic markers like *Sox9*, *Col2a1* and *Acan* and showed sGAG and type II collagen deposition in their surrounding ECM [219].

Saito et al adapted this protocol for the differentiation of iPSCs. After 14 days the iPSC-derived chondrocytes were seeded into a cylindrical culture vessel to form a chondrogenic disk. This

scaffold was subsequently implanted into cartilage defect in the distal femur of NOD/SCID-mice. Histological analysis after 8 and 16 weeks revealed that the defects treated with the chondrogenic disks were filled with hyaline cartilage-like tissue. However, in one mouse, a large tumor containing various tissues was observed indicating the persistence of undifferentiated pluripotent stem cells inside the chondrogenic disk. Therefore, it is crucial to improve the differentiation method and carefully assess the formed scaffolds for remaining undifferentiated cell populations before application in patients might be considered [135].

Taken together, exposure of PSCs to growth factors is effective at inducing chondrogenic differentiation. But the need for laborious cell culture protocols hampers their application for large-scale production of clinical grade cartilage scaffolds. Furthermore, these protocols should include a definite separation step to prevent contamination of the final product with an undifferentiated cell population to increase the safety profile before their use in patients is considered.

Yamashita et al. induced mesoendodermal differentiation of human iPSCs by culturing iPSC-colonies on Matrigel-coated dishes in a medium supplemented with the growth factors Wnt3a and Activin A. After three days, medium was changed to chondrogenic medium supplemented with BMP2, TGF β 1, GDF5 and FGF2. After 14 days, the colonies formed compact spheroid nodules that were then maintained in suspension culture for up to 42 days. Successful chondrogenic differentiation was confirmed histologically as well as by RT-PCR. Implantation of the nodules into in vivo cartilage defect models in rats and mini-pigs showed good integration and maturation of the tissue without any hint for teratoma formation. Compared to the Oldershaw-Protocol, this method is simpler since only two different sets of growth factors at steady concentrations were used during differentiation. Furthermore, the suspension culture reduces risk of teratoma formation since non-chondrogenic cells detached from the particles and collected at the bottom of the culture dishes. When the particles were implanted subcutaneously into SCID mice, no teratoma formation was observed even after 12 months [127]. However, when we applied this protocol to our murine iPSCs no evident chondrogenesis was induced. Although small nodules were formed from the iPSC colonies, we observed neither an upregulation of chondrogenic gene expression nor significant deposition of GAGs, aggrecan or type II collagen in the ECM.

Whereas *Yamashita et al.* differentiated their iPSCs for 14 days in adherent culture, our particles started to lift off the plates already on day 6. This might be due to the different coatings the iPSCs were cultured on, as *Yamashita et al.* used Matrigel coating, whereas we cultured our iPSCs on Geltrex-coated plates. It could also result from the different structure of the colonies formed by human and murine iPSCs. Whereas colonies formed by human iPSCs are flatter and proliferate slower, the colonies formed by murine iPSCs are usually dome shaped and contain fast proliferating cells [23]. Therefore, differentiation of murine iPSCs in colony-derived particles might not be suitable.

We exposed our cells to a combination of the chondrogenic growth factors BMP2, TGF β 1 and GDF5 at a concentration of 10 ng/ml each in a chondrogenic medium consisting of DMEM supplemented with FBS, non-essential amino acids, sodium pyruvate, insulin transferrin selenite mix and L-ascorbic acid (chondrogenic colonies medium). However, neither through the medium alone (noGF) nor through the growth-factor supplemented medium (BTG), chondrogenesis could be successfully induced. However, when we exposed EB-derived chondrogenic spheroids to a chondrogenic medium consisting of DMEM supplemented with sodium pyruvate, insulin transferrin selenite mix, L-ascorbic acid and dexamethasone (chondrogenic spheroids medium) and supplemented BMP2 at a concentration of 100 ng/ml and TGF β 1 at a concentration of 10 ng/ml chondrogenic differentiation could be observed in unstimulated and stimulated spheroids. Therefore, it could be possible that the medium and growth factor scheme applied by *Yamashita et al.* might not be suitable for murine iPSCs. More research is required to elucidate whether chondrogenic nodules maintained *for example* in our chondrogenic spheroids medium or under a different growth factor regime show signs of chondrogenesis.

7.3.2. Chondrogenic differentiation of iPSCs via embryoid body derived chondrogenic spheroids

One of the simplest and most straight-forward protocols to differentiate PSCs into the chondrogenic lineage is to expose outgrowth cultures of embryoid bodies to chondrogenic media supplemented with chondrogenic growth factors. Cells that spontaneously differentiated towards the mesoendodermal or mesodermal lineage and therefore are primed for chondrogenesis, start to proliferate under these conditions and form chondrogenic nodules.

Deposition of sGAGs in the ECM of these nodules could be confirmed by Alcian Blue staining. Additionally, upregulation of chondrogenic markers like *Col2a1* and *Sox9* was described [126, 160]. However, no implantable graft can be derived from this method hampering its applicability to clinical cartilage repair.

In order to form an implantable graft, it is possible to isolate cells from the EB outgrowth or directly from dissociated EBs to form chondrogenic pellets by a standard high-speed centrifugation method. These pellets are not only comparable to MSC-derived pellets but could also successfully fill an osteochondral defect in vivo [230, 231]. Furthermore, it is possible to isolate MSC-like cells from embryoid bodies that can be differentiated into the chondrogenic lineage by standard micromass and pellet culture protocols [213, 224].

Pre-differentiation of PSCs in embryoid bodies induces formation of a chondrogenically primed subpopulation that has the propensity to differentiate into the chondrogenic lineage. However, most of the protocols described in literature require disruption of formed embryoid bodies or trypsinization of outgrowth cultures to form a cell suspension that is then transferred to high density culture methods like micromass or pellets. These manipulations are laborious and potentially damage the cells. *He et al.* cultured iPSCs for 14 days in an alginate-based microcavity hydrogel which allowed formation of EBs inside the microcavities. Subsequently the EBs were exposed to a series of growth factors inducing chondrogenic differentiation via mesodermal intermediates similar to the protocol described by *Oldershaw et al.* [219]. Gene expression analysis revealed upregulation of chondrogenic markers *Sox9*, *Col2a1* and *Acan*, while Safranin O staining confirmed deposition of sGAGs and IHC staining demonstrated deposition of type II collagen in the ECM. Finally, the alginate matrix could be removed by sodium citrate leading to a scaffold free chondrogenic graft [223].

Since, on the one hand, chondrogenic differentiation of iPSCs could be achieved by exposing intact embryoid bodies to chondrogenic differentiation in a hydrogel and, on the other hand, *Yamashita et al.* had shown that suspension culture of chondrogenic nodules is – in principle – feasible, we hypothesized that chondrogenic differentiation of iPSC can be easily and effectively induced by maintaining EBs in chondrogenic medium [127, 223].

EBs are three-dimensional aggregates formed by pluripotent stem cells in the absence of LIF and feeder cells. PSCs spontaneously differentiate into derivatives from all three germ layers in

EBs mimicking some aspects of early embryogenesis. Therefore, formation of EBs is widely used as a trigger for in vitro differentiation of PSCs. There are many methods of producing EBs, however suspension culture in liquid media and hanging drop culture are the most commonly used protocols [284, 285].

PSCs can be cultured in suspension culture in bacterial grade Petri dishes. Under these conditions, PSCs cannot adhere to the culture vessel and spontaneously aggregate into EBs [286]. Although this approach is easy and effective, very heterogenous EBs are formed, because the number of cells per aggregate is not determined. The derived EBs show great variation in shape and size, and do not differentiate synchronously [284]. Therefore, this method seems not suitable to form EBs for chondrogenic differentiation.

For hanging drop culture, small drops containing a defined number of cells (400 – 1000) are placed on the lid of a Petri dish. The lid is inverted, and the cells sediment to the bottom of the drop, where they form an aggregate [287]. Here, the size of the formed bodies can be controlled by choosing an appropriate concentration of the cell suspension resulting in more homogenous EBs. This method seemed suitable to generate EBs for chondrogenic differentiation as it effectively forms an appropriate number of relatively homogenous EBs [284]. It remains to be elucidated, if embryoid bodies formed by other methods like *e.g.* stirred suspension culture in spinner flasks or rotary cell culture systems are susceptible for chondrogenic differentiation as well. These methods are scalable to produce EBs in large quantities, and would therefore facilitate production of implantable chondrogenic grafts [285].

Duration of pre-differentiation of PSCs in EBs varies between 4 [288] to 12 days [230] with most authors culturing EBs for 5 [126, 160] to 7 days [162, 165, 231]. A shorter incubation period bears the risk for incomplete pre-differentiation resulting in many undifferentiated cells that are not susceptible for subsequent differentiation signals, whereas during a longer incubation method, especially in non-chondrogenic medium, spontaneous differentiation into non-chondrogenic lineages will occur imposing a high risk of contamination of the final product with non-cartilaginous tissues. We choose a pre-differentiation period of 5 days in hanging drops. After that time, the formed EBs had a medium size of $160 \pm 60 \mu\text{m}$ and were stable enough to be transferred from the hanging drops to a 96-well plate for further culture. The EBs showed a compact spheroid morphology with no signs of cystic structures indicating formation of cystic embryoid bodies visible yet. It is suggested that large cystic structures formed by EBs

resemble the visceral yolk sac of postimplantation embryos, and are therefore indicative of advanced differentiation stages in EBs [285]. We observed homogenous chondrogenic differentiation in our chondrogenic spheroids derived from EBs maintained in HD culture for 5 days. The impact of a shorter or longer pre-differentiation time in EBs on chondrogenesis needs to be further evaluated.

During hanging drop culture, the EBs were maintained in our standard iPSC medium without LIF to allow spontaneous differentiation. There were no specific growth factors added and proliferation was stimulated only by the serum present in the medium. However, it has been described that a mesoendodermal pre-differentiation of iPSCs can be achieved by growth factors Wnt3a and Activin A [127, 219]. This intermediate step mimics the differentiation pathway of cartilage during embryonic development [219]. It remains to be elucidated, whether supplementation of Wnt3a and Activin A would improve chondrogenesis also in EBs.

During subsequent free-floating culture, we used a very simple scheme of growth factor stimulation with BMP2 and TGF β 1 added over the whole course of the differentiation at constant concentrations. Both factors are well known to enhance chondrogenic differentiation of PSCs [126, 127, 159-161]. By stimulation of embryoid bodies with these growth factors upregulation of chondrogenic markers *Sox9*, *Itga10*, *Acan* and *Col2a1* was induced and deposition of GAGs, aggrecan and type II collagen could be detected in the ECM. However, we found that the hypertrophy markers *Runx2* and *Col10* were upregulated as well. Hypertrophy was significantly stronger induced in growth factor-stimulated spheroids than in control spheroids. Since especially BMP2 is known to induce hypertrophy during chondrogenic differentiation of stem cells, a more elaborated growth factor supplementation scheme could help to prevent or reduce occurrence of hypertrophy [156]. Many other growth factors like *for example* FGF2 [127, 135, 219, 223, 288], GDF5 [127, 135, 219, 223, 288] or BMP4 [135, 219, 224, 288, 289] have been shown to enhance chondrogenesis. Their effect on chondrogenic differentiation of iPSCs via suspension culture of embryoid bodies needs yet to be determined.

However, it should be noted that we conducted the experiment using murine iPSCs. Although murine iPSCs share many features with human iPSCs, there are certain differences. They are known to represent different developmental states regarding embryonic development. Murine iPSCs represent naïve iPSCs resembling ESCs from preimplantation blastocysts, whereas human iPSCs are more equivalent to murine EpiSCs that resemble ESCs from postimplantation

blastocysts and are therefore termed primed iPSCs [22]. However, the methods to induce chondrogenesis in murine and human PSCs are comparable. Chondrogenic differentiation via pre-differentiation in embryoid bodies has been described for murine iPSCs [126, 160] as well as for human iPSCs [230, 288]. But it still remains to be elucidated, whether by the method described here, chondrogenic differentiation can also be induced in human induced pluripotent stem cells.

On the other hand, efficient and reliable methods for chondrogenic differentiation of murine iPSCs are needed, nevertheless. To study multifactorial diseases like osteoarthritis, mouse models still play an important role in musculoskeletal research [290]. Furthermore, knock-out mouse models allow to dissect the role of growth factors, cellular receptors or ECM-components in articular cartilage development and degradation [141, 291, 292]. Since chondrocytes are difficult to isolate in sufficient number and undergo dedifferentiation when maintained in culture, iPSCs generated from transgenic mice would be an additional tool to reveal molecular consequences of the genetic aberration during chondrogenic differentiation and in iPSC-derived chondrocytes [202].

Taken together, we demonstrated as a proof of principle, that chondrogenic differentiation of iPSCs via chondrogenic spheroids derived directly from embryoid bodies is possible and effective. Optimization of the differentiation time-table and growth factor supplementation scheme is needed to improve chondrogenesis and reduce hypertrophy.

7.3.3. Generation of chondrogenically primed iPSCs by RMCE

Besides the significant upregulation of chondrogenic markers *Sox9*, *ItgA10*, *Acan* and *Col2a1*, our qPCR results showed, that expression of pluripotency markers *Oct3/4* and *Nanog* was significantly downregulated in EB-derived chondrogenic spheroids compared to parental iPSCs. However, even at day 42 of chondrogenic differentiation, expression of *Oct3/4* and *Nanog* was still detectable. This could be due to the presence of undifferentiated cells within the spheroids, or it could result from reactivation of the genomically integrated reprogramming factor cassette. To rule out the second possibility, removal of the reprogramming factor cassette would be desirable.

Although removal of the Sleeping Beauty transposon carrying the reprogramming factor cassette by re-expression of the transposase is possible in theory, the efficiency of this method is very low [262]. Therefore, exchange of the reprogramming factor cassette for other genes of interest *e.g.* by recombinase mediated cassette exchange (RMCE) is an appealing alternative as discussed in 7.1.4. *Integrating Non-Viral Vectors*.

In terms of cartilage regeneration, these genes of interest could be chondrogenic transcription factors like *for example Sox9* or cartilage specific genes like *for example integrin $\alpha 10$* . The transposon could act as a genomic “safe harbor site” for the integration of these transgenes. Exchange of the reprogramming factors for these chondrogenic factors would lead to chondrogenically-primed iPSCs that might show improved chondrogenesis when exposed to chondrogenic conditions, and an enhanced safety profile due to the absence of genomically integrated oncogenes after removal of the reprogramming factor cassette (Figure 56). Our method would offer an ideal platform to explore the possibilities of these chondrogenically primed iPSCs since it offers an efficient and reliable differentiation method to induce chondrogenesis.

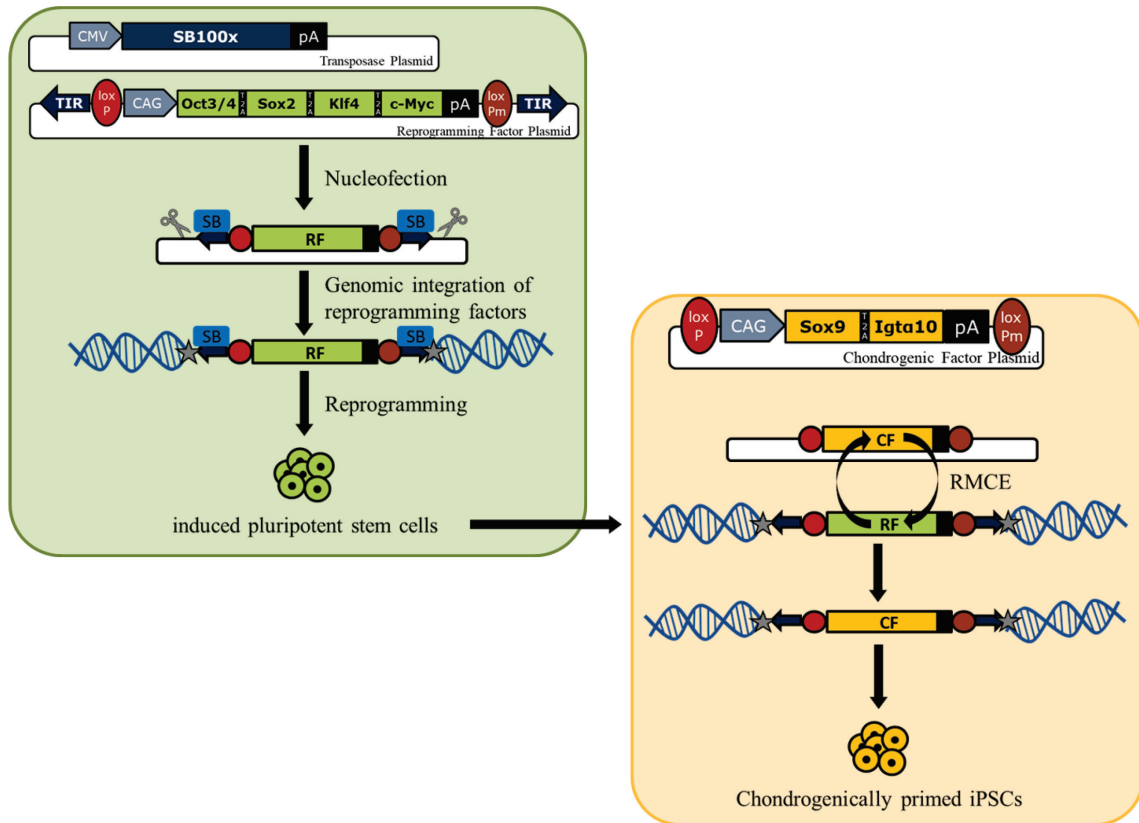


Figure 56: Generation of chondrogenically primed iPSCs by recombinase mediated cassette exchange (self-designed)
 First, iPSCs are generated with a transposon-based reprogramming system consisting *e.g.* of a transposase plasmid providing the hyperactive transposase SB100X and a reprogramming factor plasmid which contains heterospecific *loxP* sites flanking the reprogramming factors (RF). When these plasmids are delivered into the cell by nucleofection, the transposase mediates genomic integration of the reprogramming factor cassette and the heterospecific *loxP* sites, and the cells are subsequently reprogrammed to induced pluripotent stem cells (green box). Then the reprogramming factors are exchanged for chondrogenic factors (CF) *e.g.* provided on a second plasmid by recombinase mediated cassette exchange (RMCE). Thereby chondrogenically primed iPSCs can be generated (yellow box).

8. Literature

1. Fortier, L.A., *Stem cells: classifications, controversies, and clinical applications*. Vet Surg, 2005. **34**(5): p. 415-23.
2. Kolios, G. and Y. Moodley, *Introduction to stem cells and regenerative medicine*. Respiration, 2013. **85**(1): p. 3-10.
3. Menon, S., et al., *An Overview of Direct Somatic Reprogramming: The Ins and Outs of iPSCs*. Int J Mol Sci, 2016. **17**(1).
4. Singh, V.K., et al., *Describing the Stem Cell Potency: The Various Methods of Functional Assessment and In silico Diagnostics*. Front Cell Dev Biol, 2016. **4**: p. 134.
5. Stevens, L.C., *Studies on transplantable testicular teratomas of strain 129 mice*. J Natl Cancer Inst, 1958. **20**(6): p. 1257-75.
6. Evans, M.J. and M.H. Kaufman, *Establishment in culture of pluripotential cells from mouse embryos*. Nature, 1981. **292**(5819): p. 154-6.
7. Thomson, J.A., et al., *Embryonic stem cell lines derived from human blastocysts*. Science, 1998. **282**(5391): p. 1145-7.
8. Denker, H.W., *Potentiality of embryonic stem cells: an ethical problem even with alternative stem cell sources*. J Med Ethics, 2006. **32**(11): p. 665-71.
9. Brons, I.G., et al., *Derivation of pluripotent epiblast stem cells from mammalian embryos*. Nature, 2007. **448**(7150): p. 191-5.
10. Campbell, K.H., et al., *Somatic cell nuclear transfer: Past, present and future perspectives*. Theriogenology, 2007. **68 Suppl 1**: p. S214-31.
11. Rodriguez-Osorio, N., et al., *Reprogramming mammalian somatic cells*. Theriogenology, 2012. **78**(9): p. 1869-86.
12. Wilmut, I., et al., *Viable offspring derived from fetal and adult mammalian cells*. Nature, 1997. **385**(6619): p. 810-3.
13. Brambrink, T., et al., *ES cells derived from cloned and fertilized blastocysts are transcriptionally and functionally indistinguishable*. Proc Natl Acad Sci U S A, 2006. **103**(4): p. 933-8.
14. Munsie, M.J., et al., *Isolation of pluripotent embryonic stem cells from reprogrammed adult mouse somatic cell nuclei*. Curr Biol, 2000. **10**(16): p. 989-92.
15. Takahashi, K. and S. Yamanaka, *Induction of pluripotent stem cells from mouse embryonic and adult fibroblast cultures by defined factors*. Cell, 2006. **126**(4): p. 663-76.
16. Tsumaki, N., M. Okada, and A. Yamashita, *iPS cell technologies and cartilage regeneration*. Bone, 2015. **70**: p. 48-54.
17. Okita, K., T. Ichisaka, and S. Yamanaka, *Generation of germline-competent induced pluripotent stem cells*. Nature, 2007. **448**(7151): p. 313-7.
18. Wernig, M., et al., *In vitro reprogramming of fibroblasts into a pluripotent ES-cell-like state*. Nature, 2007. **448**(7151): p. 318-24.
19. Takahashi, K., et al., *Induction of pluripotent stem cells from adult human fibroblasts by defined factors*. Cell, 2007. **131**(5): p. 861-72.
20. Yu, J., et al., *Induced pluripotent stem cell lines derived from human somatic cells*. Science, 2007. **318**(5858): p. 1917-20.
21. NobelMediaAB. *Shinya Yamanaka – Facts*. . 2019 [cited 2019 March 16, 2019]; Available from: <https://www.nobelprize.org/prizes/medicine/2012/yamanaka/facts/>.
22. Nichols, J. and A. Smith, *Naive and primed pluripotent states*. Cell Stem Cell, 2009. **4**(6): p. 487-92.

23. Rawat, N. and M.K. Singh, *Induced pluripotent stem cell: A headway in reprogramming with promising approach in regenerative biology*. Vet World, 2017. **10**(6): p. 640-649.
24. Plath, K. and W.E. Lowry, *Progress in understanding reprogramming to the induced pluripotent state*. Nat Rev Genet, 2011. **12**(4): p. 253-65.
25. Teshigawara, R., et al., *Mechanism of human somatic reprogramming to iPS cell*. Lab Invest, 2017. **97**(10): p. 1152-1157.
26. Hamanaka, S., et al., *Generation of germline-competent rat induced pluripotent stem cells*. PLoS One, 2011. **6**(7): p. e22008.
27. Takenaka-Ninagawa, N., et al., *Generation of rat-induced pluripotent stem cells from a new model of metabolic syndrome*. PLoS One, 2014. **9**(8): p. e104462.
28. Honda, A., et al., *Naive-like conversion overcomes the limited differentiation capacity of induced pluripotent stem cells*. J Biol Chem, 2013. **288**(36): p. 26157-66.
29. Esteban, M.A., et al., *Generation of induced pluripotent stem cell lines from Tibetan miniature pig*. J Biol Chem, 2009. **284**(26): p. 17634-40.
30. Kues, W.A., et al., *Derivation and characterization of sleeping beauty transposon-mediated porcine induced pluripotent stem cells*. Stem Cells Dev, 2013. **22**(1): p. 124-35.
31. Nagy, K., et al., *Induced pluripotent stem cell lines derived from equine fibroblasts*. Stem Cell Rev, 2011. **7**(3): p. 693-702.
32. Talluri, T.R., et al., *Derivation and characterization of bovine induced pluripotent stem cells by transposon-mediated reprogramming*. Cell Reprogram, 2015. **17**(2): p. 131-40.
33. Debowski, K., et al., *Non-viral generation of marmoset monkey iPS cells by a six-factor-in-one-vector approach*. PLoS One, 2015. **10**(3): p. e0118424.
34. Fujie, Y., et al., *New type of Sendai virus vector provides transgene-free iPS cells derived from chimpanzee blood*. PLoS One, 2014. **9**(12): p. e113052.
35. Qu, X., et al., *Induced pluripotent stem cells generated from human adipose-derived stem cells using a non-viral polycistronic plasmid in feeder-free conditions*. PLoS One, 2012. **7**(10): p. e48161.
36. Loh, Y.H., et al., *Generation of induced pluripotent stem cells from human blood*. Blood, 2009. **113**(22): p. 5476-9.
37. Li, W., et al., *Generation of human-induced pluripotent stem cells in the absence of exogenous Sox2*. Stem Cells, 2009. **27**(12): p. 2992-3000.
38. Kim, J.B., et al., *Oct4-induced pluripotency in adult neural stem cells*. Cell, 2009. **136**(3): p. 411-9.
39. Liu, H., et al., *Generation of endoderm-derived human induced pluripotent stem cells from primary hepatocytes*. Hepatology, 2010. **51**(5): p. 1810-9.
40. Bar-Nur, O., et al., *Epigenetic memory and preferential lineage-specific differentiation in induced pluripotent stem cells derived from human pancreatic islet beta cells*. Cell Stem Cell, 2011. **9**(1): p. 17-23.
41. Brouwer, M., H. Zhou, and N. Nadif Kasri, *Choices for Induction of Pluripotency: Recent Developments in Human Induced Pluripotent Stem Cell Reprogramming Strategies*. Stem Cell Rev, 2016. **12**(1): p. 54-72.
42. Hudecek, M., et al., *Going non-viral: the Sleeping Beauty transposon system breaks on through to the clinical side*. Crit Rev Biochem Mol Biol, 2017. **52**(4): p. 355-380.
43. Ivics, Z. and Z. Izsvak, *Nonviral gene delivery with the sleeping beauty transposon system*. Hum Gene Ther, 2011. **22**(9): p. 1043-51.
44. Zhou, W. and C.R. Freed, *Adenoviral gene delivery can reprogram human fibroblasts to induced pluripotent stem cells*. Stem Cells, 2009. **27**(11): p. 2667-74.

45. Fusaki, N., et al., *Efficient induction of transgene-free human pluripotent stem cells using a vector based on Sendai virus, an RNA virus that does not integrate into the host genome*. Proc Jpn Acad Ser B Phys Biol Sci, 2009. **85**(8): p. 348-62.
46. Narsinh, K.H., et al., *Generation of adult human induced pluripotent stem cells using nonviral minicircle DNA vectors*. Nat Protoc, 2011. **6**(1): p. 78-88.
47. Si-Tayeb, K., et al., *Generation of human induced pluripotent stem cells by simple transient transfection of plasmid DNA encoding reprogramming factors*. BMC Dev Biol, 2010. **10**: p. 81.
48. Yu, J., et al., *Human induced pluripotent stem cells free of vector and transgene sequences*. Science, 2009. **324**(5928): p. 797-801.
49. Kim, D., et al., *Generation of human induced pluripotent stem cells by direct delivery of reprogramming proteins*. Cell Stem Cell, 2009. **4**(6): p. 472-6.
50. Warren, L., et al., *Feeder-free derivation of human induced pluripotent stem cells with messenger RNA*. Sci Rep, 2012. **2**: p. 657.
51. Kumar, D., et al., *Transposon-based reprogramming to induced pluripotency*. Histol Histopathol, 2015. **30**(12): p. 1397-409.
52. Skipper, K.A., et al., *DNA transposon-based gene vehicles - scenes from an evolutionary drive*. J Biomed Sci, 2013. **20**: p. 92.
53. Grabundzija, I., et al., *Sleeping Beauty transposon-based system for cellular reprogramming and targeted gene insertion in induced pluripotent stem cells*. Nucleic Acids Res, 2013. **41**(3): p. 1829-47.
54. Muenthaisong, S., et al., *Generation of mouse induced pluripotent stem cells from different genetic backgrounds using Sleeping beauty transposon mediated gene transfer*. Exp Cell Res, 2012. **318**(19): p. 2482-9.
55. Woltjen, K., et al., *piggyBac transposition reprograms fibroblasts to induced pluripotent stem cells*. Nature, 2009. **458**(7239): p. 766-70.
56. Ivics, Z., et al., *Molecular reconstruction of Sleeping Beauty, a Tc1-like transposon from fish, and its transposition in human cells*. Cell, 1997. **91**(4): p. 501-10.
57. Liu, H. and G.A. Visner, *Applications of Sleeping Beauty transposons for nonviral gene therapy*. IUBMB Life, 2007. **59**(6): p. 374-9.
58. Mates, L., et al., *Molecular evolution of a novel hyperactive Sleeping Beauty transposase enables robust stable gene transfer in vertebrates*. Nat Genet, 2009. **41**(6): p. 753-61.
59. Narayanavari, S.A., et al., *Sleeping Beauty transposition: from biology to applications*. Crit Rev Biochem Mol Biol, 2017. **52**(1): p. 18-44.
60. Ivics, Z. and Z. Izsvak, *Sleeping Beauty Transposition*. Microbiol Spectr, 2015. **3**(2): p. MDNA3-0042-2014.
61. Richardson, P.D., et al., *Gene repair and transposon-mediated gene therapy*. Stem Cells, 2002. **20**(2): p. 105-18.
62. Geurts, A.M., et al., *Gene transfer into genomes of human cells by the sleeping beauty transposon system*. Mol Ther, 2003. **8**(1): p. 108-17.
63. Grabundzija, I., et al., *Comparative analysis of transposable element vector systems in human cells*. Mol Ther, 2010. **18**(6): p. 1200-9.
64. Vigdal, T.J., et al., *Common physical properties of DNA affecting target site selection of sleeping beauty and other Tc1/mariner transposable elements*. J Mol Biol, 2002. **323**(3): p. 441-52.
65. Gogol-Doring, A., et al., *Genome-wide Profiling Reveals Remarkable Parallels Between Insertion Site Selection Properties of the MLV Retrovirus and the piggyBac Transposon in Primary Human CD4(+) T Cells*. Mol Ther, 2016. **24**(3): p. 592-606.

66. Buganim, Y., et al., *Single-cell expression analyses during cellular reprogramming reveal an early stochastic and a late hierarchic phase*. Cell, 2012. **150**(6): p. 1209-22.
67. Polo, J.M., et al., *A molecular roadmap of reprogramming somatic cells into iPS cells*. Cell, 2012. **151**(7): p. 1617-32.
68. Samavarchi-Tehrani, P., et al., *Functional genomics reveals a BMP-driven mesenchymal-to-epithelial transition in the initiation of somatic cell reprogramming*. Cell Stem Cell, 2010. **7**(1): p. 64-77.
69. Smith, Z.D., et al., *Dynamic single-cell imaging of direct reprogramming reveals an early specifying event*. Nat Biotechnol, 2010. **28**(5): p. 521-6.
70. David, L. and J.M. Polo, *Phases of reprogramming*. Stem Cell Res, 2014. **12**(3): p. 754-61.
71. Hanna, J., et al., *Direct cell reprogramming is a stochastic process amenable to acceleration*. Nature, 2009. **462**(7273): p. 595-601.
72. Krause, M.N., I. Sancho-Martinez, and J.C. Izpisua Belmonte, *Understanding the molecular mechanisms of reprogramming*. Biochem Biophys Res Commun, 2016. **473**(3): p. 693-7.
73. Li, R., et al., *A mesenchymal-to-epithelial transition initiates and is required for the nuclear reprogramming of mouse fibroblasts*. Cell Stem Cell, 2010. **7**(1): p. 51-63.
74. Aasen, T., et al., *Efficient and rapid generation of induced pluripotent stem cells from human keratinocytes*. Nat Biotechnol, 2008. **26**(11): p. 1276-84.
75. Aoi, T., et al., *Generation of pluripotent stem cells from adult mouse liver and stomach cells*. Science, 2008. **321**(5889): p. 699-702.
76. Koche, R.P., et al., *Reprogramming factor expression initiates widespread targeted chromatin remodeling*. Cell Stem Cell, 2011. **8**(1): p. 96-105.
77. Mikkelsen, T.S., et al., *Dissecting direct reprogramming through integrative genomic analysis*. Nature, 2008. **454**(7200): p. 49-55.
78. Stadtfeld, M., et al., *Defining molecular cornerstones during fibroblast to iPS cell reprogramming in mouse*. Cell Stem Cell, 2008. **2**(3): p. 230-40.
79. Kim, K., et al., *Epigenetic memory in induced pluripotent stem cells*. Nature, 2010. **467**(7313): p. 285-90.
80. Polo, J.M., et al., *Cell type of origin influences the molecular and functional properties of mouse induced pluripotent stem cells*. Nat Biotechnol, 2010. **28**(8): p. 848-55.
81. Wang, P. and J. Na, *Mechanism and methods to induce pluripotency*. Protein Cell, 2011. **2**(10): p. 792-9.
82. Niwa, H., J. Miyazaki, and A.G. Smith, *Quantitative expression of Oct-3/4 defines differentiation, dedifferentiation or self-renewal of ES cells*. Nat Genet, 2000. **24**(4): p. 372-6.
83. Adachi, K. and H.R. Scholer, *Directing reprogramming to pluripotency by transcription factors*. Curr Opin Genet Dev, 2012. **22**(5): p. 416-22.
84. Sanges, D. and M.P. Cosma, *Reprogramming cell fate to pluripotency: the decision-making signalling pathways*. Int J Dev Biol, 2010. **54**(11-12): p. 1575-87.
85. Sridharan, R., et al., *Role of the murine reprogramming factors in the induction of pluripotency*. Cell, 2009. **136**(2): p. 364-77.
86. Niwa, H., *The pluripotency transcription factor network at work in reprogramming*. Curr Opin Genet Dev, 2014. **28**: p. 25-31.
87. Nandan, M.O. and V.W. Yang, *The role of Kruppel-like factors in the reprogramming of somatic cells to induced pluripotent stem cells*. Histol Histopathol, 2009. **24**(10): p. 1343-55.

88. Finver, S.N., et al., *Sequence analysis of the MYC oncogene involved in the t(8;14)(q24;q11) chromosome translocation in a human leukemia T-cell line indicates that putative regulatory regions are not altered*. Proc Natl Acad Sci U S A, 1988. **85**(9): p. 3052-6.
89. Nakagawa, M., et al., *Generation of induced pluripotent stem cells without Myc from mouse and human fibroblasts*. Nat Biotechnol, 2008. **26**(1): p. 101-6.
90. Boyer, L.A., et al., *Core transcriptional regulatory circuitry in human embryonic stem cells*. Cell, 2005. **122**(6): p. 947-56.
91. Kim, J., et al., *An extended transcriptional network for pluripotency of embryonic stem cells*. Cell, 2008. **132**(6): p. 1049-61.
92. Iwafuchi-Doi, M. and K.S. Zaret, *Pioneer transcription factors in cell reprogramming*. Genes Dev, 2014. **28**(24): p. 2679-92.
93. Soufi, A., G. Donahue, and K.S. Zaret, *Facilitators and impediments of the pluripotency reprogramming factors' initial engagement with the genome*. Cell, 2012. **151**(5): p. 994-1004.
94. Czerwinska, P., S. Mazurek, and M. Wiznerowicz, *Application of induced pluripotency in cancer studies*. Rep Pract Oncol Radiother, 2018. **23**(3): p. 207-214.
95. Sayed, N., C. Liu, and J.C. Wu, *Translation of Human-Induced Pluripotent Stem Cells: From Clinical Trial in a Dish to Precision Medicine*. J Am Coll Cardiol, 2016. **67**(18): p. 2161-2176.
96. Elitt, M.S., L. Barbar, and P.J. Tesar, *Drug screening for human genetic diseases using iPSC models*. Hum Mol Genet, 2018. **27**(R2): p. R89-R98.
97. Wu, S.M. and K. Hochedlinger, *Harnessing the potential of induced pluripotent stem cells for regenerative medicine*. Nat Cell Biol, 2011. **13**(5): p. 497-505.
98. Dimos, J.T., et al., *Induced pluripotent stem cells generated from patients with ALS can be differentiated into motor neurons*. Science, 2008. **321**(5893): p. 1218-21.
99. Sanchez-Danes, A., et al., *Disease-specific phenotypes in dopamine neurons from human iPS-based models of genetic and sporadic Parkinson's disease*. EMBO Mol Med, 2012. **4**(5): p. 380-95.
100. Han, L., et al., *Study familial hypertrophic cardiomyopathy using patient-specific induced pluripotent stem cells*. Cardiovasc Res, 2014. **104**(2): p. 258-69.
101. Sun, N., et al., *Patient-specific induced pluripotent stem cells as a model for familial dilated cardiomyopathy*. Sci Transl Med, 2012. **4**(130): p. 130ra47.
102. Cayo, M.A., et al., *JD induced pluripotent stem cell-derived hepatocytes faithfully recapitulate the pathophysiology of familial hypercholesterolemia*. Hepatology, 2012. **56**(6): p. 2163-71.
103. Jang, J., et al., *Disease-specific induced pluripotent stem cells: a platform for human disease modeling and drug discovery*. Exp Mol Med, 2012. **44**(3): p. 202-13.
104. Chamberlain, S.J., *Disease modelling using human iPSCs*. Hum Mol Genet, 2016. **25**(R2): p. R173-R181.
105. Lee, G., et al., *Large-scale screening using familial dysautonomia induced pluripotent stem cells identifies compounds that rescue IKBKAP expression*. Nat Biotechnol, 2012. **30**(12): p. 1244-8.
106. McNeish, J., et al., *From Dish to Bedside: Lessons Learned While Translating Findings from a Stem Cell Model of Disease to a Clinical Trial*. Cell Stem Cell, 2015. **17**(1): p. 8-10.
107. Liu, H., et al., *In vivo liver regeneration potential of human induced pluripotent stem cells from diverse origins*. Sci Transl Med, 2011. **3**(82): p. 82ra39.

108. Takebe, T., et al., *Vascularized and functional human liver from an iPSC-derived organ bud transplant*. Nature, 2013. **499**(7459): p. 481-4.
109. Nori, S., et al., *Grafted human-induced pluripotent stem-cell-derived neurospheres promote motor functional recovery after spinal cord injury in mice*. Proc Natl Acad Sci U S A, 2011. **108**(40): p. 16825-30.
110. Suzuki, N., et al., *Generation of engraftable hematopoietic stem cells from induced pluripotent stem cells by way of teratoma formation*. Mol Ther, 2013. **21**(7): p. 1424-31.
111. Xie, F., et al., *Seamless gene correction of beta-thalassemia mutations in patient-specific iPSCs using CRISPR/Cas9 and piggyBac*. Genome Res, 2014. **24**(9): p. 1526-33.
112. Kimbrel, E.A. and R. Lanza, *Current status of pluripotent stem cells: moving the first therapies to the clinic*. Nat Rev Drug Discov, 2015. **14**(10): p. 681-92.
113. Solomon, S., F. Pitossi, and M.S. Rao, *Banking on iPSC--is it doable and is it worthwhile*. Stem Cell Rev, 2015. **11**(1): p. 1-10.
114. Turner, M., et al., *Toward the development of a global induced pluripotent stem cell library*. Cell Stem Cell, 2013. **13**(4): p. 382-4.
115. Zhang, L., J. Hu, and K.A. Athanasiou, *The role of tissue engineering in articular cartilage repair and regeneration*. Crit Rev Biomed Eng, 2009. **37**(1-2): p. 1-57.
116. Temenoff, J.S. and A.G. Mikos, *Review: tissue engineering for regeneration of articular cartilage*. Biomaterials, 2000. **21**(5): p. 431-40.
117. Brody, L.T., *Knee osteoarthritis: Clinical connections to articular cartilage structure and function*. Phys Ther Sport, 2015. **16**(4): p. 301-16.
118. Poole, A.R., et al., *Composition and structure of articular cartilage: a template for tissue repair*. Clin Orthop Relat Res, 2001(391 Suppl): p. S26-33.
119. Lach, M., et al., *Directed differentiation of induced pluripotent stem cells into chondrogenic lineages for articular cartilage treatment*. J Tissue Eng, 2014. **5**: p. 2041731414552701.
120. Hunziker, E.B., T.M. Quinn, and H.J. Hauselmann, *Quantitative structural organization of normal adult human articular cartilage*. Osteoarthritis Cartilage, 2002. **10**(7): p. 564-72.
121. Foster, N.C., et al., *Dynamic 3D culture: models of chondrogenesis and endochondral ossification*. Birth Defects Res C Embryo Today, 2015. **105**(1): p. 19-33.
122. Hulmes, D.J., *Building collagen molecules, fibrils, and suprafibrillar structures*. J Struct Biol, 2002. **137**(1-2): p. 2-10.
123. Ricard-Blum, S., *The collagen family*. Cold Spring Harb Perspect Biol, 2011. **3**(1): p. a004978.
124. Mackay, A.M., et al., *Chondrogenic differentiation of cultured human mesenchymal stem cells from marrow*. Tissue Eng, 1998. **4**(4): p. 415-28.
125. Pittenger, M.F., et al., *Multilineage potential of adult human mesenchymal stem cells*. Science, 1999. **284**(5411): p. 143-7.
126. Saito, T., et al., *Generation of Col2a1-EGFP iPS cells for monitoring chondrogenic differentiation*. PLoS One, 2013. **8**(9): p. e74137.
127. Yamashita, A., et al., *Generation of scaffoldless hyaline cartilaginous tissue from human iPSCs*. Stem Cell Reports, 2015. **4**(3): p. 404-18.
128. McAlinden, A., *Alternative splicing of type II procollagen: IIB or not IIB?* Connect Tissue Res, 2014. **55**(3): p. 165-76.

129. Gouttenoire, J., et al., *BMP-2 and TGF-beta1 differentially control expression of type II procollagen and alpha 10 and alpha 11 integrins in mouse chondrocytes*. Eur J Cell Biol, 2010. **89**(4): p. 307-14.
130. Zhang, L., et al., *Chondrogenic differentiation of human mesenchymal stem cells: a comparison between micromass and pellet culture systems*. Biotechnol Lett, 2010. **32**(9): p. 1339-46.
131. Heinegard, D., *Fell-Muir Lecture: Proteoglycans and more--from molecules to biology*. Int J Exp Pathol, 2009. **90**(6): p. 575-86.
132. Roughley, P.J., *The structure and function of cartilage proteoglycans*. Eur Cell Mater, 2006. **12**: p. 92-101.
133. Diekman, B.O., et al., *Chondrogenesis of adult stem cells from adipose tissue and bone marrow: induction by growth factors and cartilage-derived matrix*. Tissue Eng Part A, 2010. **16**(2): p. 523-33.
134. Qu, C., et al., *Chondrogenic differentiation of human pluripotent stem cells in chondrocyte co-culture*. Int J Biochem Cell Biol, 2013. **45**(8): p. 1802-12.
135. Saito, T., et al., *Hyaline cartilage formation and tumorigenesis of implanted tissues derived from human induced pluripotent stem cells*. Biomed Res, 2015. **36**(3): p. 179-86.
136. Lüllmann-Rauch, R., *Taschenlehrbuch Histologie*. 3., vollst. überarb. Aufl. ed. 2009, Stuttgart, Germany: Georg-Thieme Verlag KG. 137-143.
137. Loeser, R.F., *Integrins and chondrocyte-matrix interactions in articular cartilage*. Matrix Biol, 2014. **39**: p. 11-6.
138. Zeltz, C. and D. Gullberg, *The integrin-collagen connection - a glue for tissue repair?* J Cell Sci, 2016. **129**(6): p. 1284.
139. Lundgren-Akerlund, E. and A. Aszodi, *Integrin alpha10beta1: a collagen receptor critical in skeletal development*. Adv Exp Med Biol, 2014. **819**: p. 61-71.
140. Camper, L., U. Hellman, and E. Lundgren-Akerlund, *Isolation, cloning, and sequence analysis of the integrin subunit alpha10, a beta1-associated collagen binding integrin expressed on chondrocytes*. J Biol Chem, 1998. **273**(32): p. 20383-9.
141. Bengtsson, T., et al., *Loss of alpha10beta1 integrin expression leads to moderate dysfunction of growth plate chondrocytes*. J Cell Sci, 2005. **118**(Pt 5): p. 929-36.
142. Varas, L., et al., *Alpha10 integrin expression is up-regulated on fibroblast growth factor-2-treated mesenchymal stem cells with improved chondrogenic differentiation potential*. Stem Cells Dev, 2007. **16**(6): p. 965-78.
143. Long, F. and D.M. Ornitz, *Development of the endochondral skeleton*. Cold Spring Harb Perspect Biol, 2013. **5**(1): p. a008334.
144. Wuelling, M. and A. Vortkamp, *Chondrocyte proliferation and differentiation*. Endocr Dev, 2011. **21**: p. 1-11.
145. Wang, L. and Y.G. Chen, *Signaling Control of Differentiation of Embryonic Stem Cells toward Mesendoderm*. J Mol Biol, 2016. **428**(7): p. 1409-22.
146. Tickle, C., *How the embryo makes a limb: determination, polarity and identity*. J Anat, 2015. **227**(4): p. 418-30.
147. Fang, J., et al., *Roles of TGF-beta 1 signaling in the development of osteoarthritis*. Histol Histopathol, 2016. **31**(11): p. 1161-7.
148. Derynck, R. and Y.E. Zhang, *Smad-dependent and Smad-independent pathways in TGF-beta family signalling*. Nature, 2003. **425**(6958): p. 577-84.
149. Song, B., K.D. Estrada, and K.M. Lyons, *Smad signaling in skeletal development and regeneration*. Cytokine Growth Factor Rev, 2009. **20**(5-6): p. 379-88.

150. Massague, J., *TGFbeta signaling: receptors, transducers, and Mad proteins*. Cell, 1996. **85**(7): p. 947-50.
151. Augustyniak, E., et al., *The role of growth factors in stem cell-directed chondrogenesis: a real hope for damaged cartilage regeneration*. Int Orthop, 2015. **39**(5): p. 995-1003.
152. Kim, Y.I., et al., *Overexpression of TGF-beta1 enhances chondrogenic differentiation and proliferation of human synovium-derived stem cells*. Biochem Biophys Res Commun, 2014. **450**(4): p. 1593-9.
153. Noth, U., et al., *Chondrogenic differentiation of human mesenchymal stem cells in collagen type I hydrogels*. J Biomed Mater Res A, 2007. **83**(3): p. 626-35.
154. Yoo, J.U., et al., *The chondrogenic potential of human bone-marrow-derived mesenchymal progenitor cells*. J Bone Joint Surg Am, 1998. **80**(12): p. 1745-57.
155. Chen, D., M. Zhao, and G.R. Mundy, *Bone morphogenetic proteins*. Growth Factors, 2004. **22**(4): p. 233-41.
156. Zhou, N., et al., *BMP2 induces chondrogenic differentiation, osteogenic differentiation and endochondral ossification in stem cells*. Cell Tissue Res, 2016. **366**(1): p. 101-11.
157. Liao, J., et al., *Sox9 potentiates BMP2-induced chondrogenic differentiation and inhibits BMP2-induced osteogenic differentiation*. PLoS One, 2014. **9**(2): p. e89025.
158. Sakaguchi, Y., et al., *Comparison of human stem cells derived from various mesenchymal tissues: superiority of synovium as a cell source*. Arthritis Rheum, 2005. **52**(8): p. 2521-9.
159. Koay, E.J., G.M. Hoben, and K.A. Athanasiou, *Tissue engineering with chondrogenically differentiated human embryonic stem cells*. Stem Cells, 2007. **25**(9): p. 2183-90.
160. Kuboth, S., J. Kramer, and J. Rohwedel, *Chondrogenic differentiation in vitro of murine two-factor induced pluripotent stem cells is comparable to murine embryonic stem cells*. Cells Tissues Organs, 2012. **196**(6): p. 481-9.
161. Toh, W.S., et al., *Cartilage repair using hyaluronan hydrogel-encapsulated human embryonic stem cell-derived chondrogenic cells*. Biomaterials, 2010. **31**(27): p. 6968-80.
162. Suchorska, W.M., et al., *Gene expression profile in human induced pluripotent stem cells: Chondrogenic differentiation in vitro, part A*. Mol Med Rep, 2017. **15**(5): p. 2387-2401.
163. Akiyama, H., et al., *The transcription factor Sox9 has essential roles in successive steps of the chondrocyte differentiation pathway and is required for expression of Sox5 and Sox6*. Genes Dev, 2002. **16**(21): p. 2813-28.
164. Nishimura, R., et al., *Regulation of bone and cartilage development by network between BMP signalling and transcription factors*. J Biochem, 2012. **151**(3): p. 247-54.
165. Augustyniak, E., et al., *Gene expression profile in human induced pluripotent stem cells: Chondrogenic differentiation in vitro, part B*. Mol Med Rep, 2017. **15**(5): p. 2402-2414.
166. Aroen, A., et al., *Articular cartilage lesions in 993 consecutive knee arthroscopies*. Am J Sports Med, 2004. **32**(1): p. 211-5.
167. Solheim, E., et al., *Symptoms and function in patients with articular cartilage lesions in 1,000 knee arthroscopies*. Knee Surg Sports Traumatol Arthrosc, 2016. **24**(5): p. 1610-6.
168. Heir, S., et al., *Focal cartilage defects in the knee impair quality of life as much as severe osteoarthritis: a comparison of knee injury and osteoarthritis outcome score in 4 patient categories scheduled for knee surgery*. Am J Sports Med, 2010. **38**(2): p. 231-7.

169. Lohmander, L.S., et al., *The long-term consequence of anterior cruciate ligament and meniscus injuries: osteoarthritis*. Am J Sports Med, 2007. **35**(10): p. 1756-69.
170. Felson, D.T. and R. Hodgson, *Identifying and treating preclinical and early osteoarthritis*. Rheum Dis Clin North Am, 2014. **40**(4): p. 699-710.
171. Glyn-Jones, S., et al., *Osteoarthritis*. Lancet, 2015. **386**(9991): p. 376-87.
172. Oldershaw, R.A., *Cell sources for the regeneration of articular cartilage: the past, the horizon and the future*. Int J Exp Pathol, 2012. **93**(6): p. 389-400.
173. Braun, H.J. and G.E. Gold, *Diagnosis of osteoarthritis: imaging*. Bone, 2012. **51**(2): p. 278-88.
174. de l'Escalopier, N., P. Anract, and D. Biau, *Surgical treatments for osteoarthritis*. Ann Phys Rehabil Med, 2016. **59**(3): p. 227-33.
175. Braun, S., et al., *The 5.5-year results of MegaOATS--autologous transfer of the posterior femoral condyle: a case-series study*. Arthritis Res Ther, 2008. **10**(3): p. R68.
176. Dewan, A.K., et al., *Evolution of autologous chondrocyte repair and comparison to other cartilage repair techniques*. Biomed Res Int, 2014. **2014**: p. 272481.
177. Batty, L., et al., *Autologous chondrocyte implantation: an overview of technique and outcomes*. ANZ J Surg, 2011. **81**(1-2): p. 18-25.
178. Oehler, N., T. Schmidt, and A. Niemeier, *[Total Joint Replacement and Return to Sports]*. Sportverletz Sportschaden, 2016. **30**(4): p. 195-203.
179. Wengler, A., U. Nimptsch, and T. Mansky, *Hip and knee replacement in Germany and the USA: analysis of individual inpatient data from German and US hospitals for the years 2005 to 2011*. Dtsch Arztebl Int, 2014. **111**(23-24): p. 407-16.
180. Steadman, J.R., W.G. Rodkey, and J.J. Rodrigo, *Microfracture: surgical technique and rehabilitation to treat chondral defects*. Clin Orthop Relat Res, 2001(391 Suppl): p. S362-9.
181. Mithoefer, K., et al., *The microfracture technique for the treatment of articular cartilage lesions in the knee. A prospective cohort study*. J Bone Joint Surg Am, 2005. **87**(9): p. 1911-20.
182. Shapiro, F., S. Koide, and M.J. Glimcher, *Cell origin and differentiation in the repair of full-thickness defects of articular cartilage*. J Bone Joint Surg Am, 1993. **75**(4): p. 532-53.
183. Gudas, R., et al., *A prospective randomized clinical study of mosaic osteochondral autologous transplantation versus microfracture for the treatment of osteochondral defects in the knee joint in young athletes*. Arthroscopy, 2005. **21**(9): p. 1066-75.
184. Erggelet, C. and P. Vavken, *Microfracture for the treatment of cartilage defects in the knee joint - A golden standard?* J Clin Orthop Trauma, 2016. **7**(3): p. 145-52.
185. Devitt, B.M., et al., *Surgical treatments of cartilage defects of the knee: Systematic review of randomised controlled trials*. Knee, 2017. **24**(3): p. 508-517.
186. Schenker, H., et al., *[Current overview of cartilage regeneration procedures]*. Orthopade, 2017. **46**(11): p. 907-913.
187. Benthien, J.P. and P. Behrens, *Autologous Matrix-Induced Chondrogenesis (AMIC): Combining Microfracturing and a Collagen I/III Matrix for Articular Cartilage Resurfacing*. Cartilage, 2010. **1**(1): p. 65-8.
188. Schagemann, J., et al., *Mid-term outcome of arthroscopic AMIC for the treatment of articular cartilage defects in the knee joint is equivalent to mini-open procedures*. Arch Orthop Trauma Surg, 2018. **138**(6): p. 819-825.
189. Volz, M., et al., *A randomized controlled trial demonstrating sustained benefit of Autologous Matrix-Induced Chondrogenesis over microfracture at five years*. Int Orthop, 2017. **41**(4): p. 797-804.

190. Mithoefer, K., et al., *Chondral resurfacing of articular cartilage defects in the knee with the microfracture technique. Surgical technique.* J Bone Joint Surg Am, 2006. **88 Suppl 1 Pt 2**: p. 294-304.
191. Outerbridge, H.K., R.E. Outerbridge, and D.E. Smith, *Osteochondral defects in the knee. A treatment using lateral patella autografts.* Clin Orthop Relat Res, 2000(377): p. 145-51.
192. Richter, D.L., et al., *Knee Articular Cartilage Repair and Restoration Techniques: A Review of the Literature.* Sports Health, 2016. **8(2)**: p. 153-60.
193. Hangody, L. and P. Fules, *Autologous osteochondral mosaicplasty for the treatment of full-thickness defects of weight-bearing joints: ten years of experimental and clinical experience.* J Bone Joint Surg Am, 2003. **85-A Suppl 2**: p. 25-32.
194. Hangody, L., et al., *Arthroscopic autogenous osteochondral mosaicplasty for the treatment of femoral condylar articular defects. A preliminary report.* Knee Surg Sports Traumatol Arthrosc, 1997. **5(4)**: p. 262-7.
195. Matsusue, Y., T. Yamamuro, and H. Hama, *Arthroscopic multiple osteochondral transplantation to the chondral defect in the knee associated with anterior cruciate ligament disruption.* Arthroscopy, 1993. **9(3)**: p. 318-21.
196. Hangody, L., et al., *Autologous osteochondral grafting--technique and long-term results.* Injury, 2008. **39 Suppl 1**: p. S32-9.
197. Brucker, P.U., S. Braun, and A.B. Imhoff, *[Mega-OATS technique--autologous osteochondral transplantation as a salvage procedure for large osteochondral defects of the femoral condyle].* Oper Orthop Traumatol, 2008. **20(3)**: p. 188-98.
198. Sherman, S.L., et al., *Fresh osteochondral allograft transplantation for the knee: current concepts.* J Am Acad Orthop Surg, 2014. **22(2)**: p. 121-33.
199. Winthrop, Z., G. Pinkowsky, and W. Hennrikus, *Surgical treatment for osteochondritis dessicans of the knee.* Curr Rev Musculoskelet Med, 2015. **8(4)**: p. 467-75.
200. Brittberg, M., et al., *Treatment of deep cartilage defects in the knee with autologous chondrocyte transplantation.* N Engl J Med, 1994. **331(14)**: p. 889-95.
201. Roberts, S., et al., *Immunohistochemical study of collagen types I and II and procollagen IIA in human cartilage repair tissue following autologous chondrocyte implantation.* Knee, 2009. **16(5)**: p. 398-404.
202. Minegishi, Y., K. Hosokawa, and N. Tsumaki, *Time-lapse observation of the dedifferentiation process in mouse chondrocytes using chondrocyte-specific reporters.* Osteoarthritis Cartilage, 2013. **21(12)**: p. 1968-75.
203. Gomoll, A.H., et al., *Use of a type I/III bilayer collagen membrane decreases reoperation rates for symptomatic hypertrophy after autologous chondrocyte implantation.* Am J Sports Med, 2009. **37 Suppl 1**: p. 20S-23S.
204. Maus, U., et al., *[Clinical results after three years use of matrix-associated ACT for the treatment of osteochondral defects of the knee].* Z Orthop Unfall, 2008. **146(1)**: p. 31-7.
205. Ossendorf, C., et al., *Treatment of posttraumatic and focal osteoarthritic cartilage defects of the knee with autologous polymer-based three-dimensional chondrocyte grafts: 2-year clinical results.* Arthritis Res Ther, 2007. **9(2)**: p. R41.
206. Vonk, L.A., et al., *Autologous, allogeneic, induced pluripotent stem cell or a combination stem cell therapy? Where are we headed in cartilage repair and why: a concise review.* Stem Cell Res Ther, 2015. **6**: p. 94.
207. Docheva, D., et al., *Human mesenchymal stem cells in contact with their environment: surface characteristics and the integrin system.* J Cell Mol Med, 2007. **11(1)**: p. 21-38.

208. Friedenstein, A.J., et al., *Heterotopic of bone marrow. Analysis of precursor cells for osteogenic and hematopoietic tissues*. Transplantation, 1968. **6**(2): p. 230-47.
209. Dominici, M., et al., *Minimal criteria for defining multipotent mesenchymal stromal cells. The International Society for Cellular Therapy position statement*. Cytotherapy, 2006. **8**(4): p. 315-7.
210. Ando, W., et al., *In vitro generation of a scaffold-free tissue-engineered construct (TEC) derived from human synovial mesenchymal stem cells: biological and mechanical properties and further chondrogenic potential*. Tissue Eng Part A, 2008. **14**(12): p. 2041-9.
211. Nejadnik, H., et al., *Autologous bone marrow-derived mesenchymal stem cells versus autologous chondrocyte implantation: an observational cohort study*. Am J Sports Med, 2010. **38**(6): p. 1110-6.
212. Park, Y.B., et al., *Cartilage Regeneration in Osteoarthritic Patients by a Composite of Allogeneic Umbilical Cord Blood-Derived Mesenchymal Stem Cells and Hyaluronate Hydrogel: Results from a Clinical Trial for Safety and Proof-of-Concept with 7 Years of Extended Follow-Up*. Stem Cells Transl Med, 2017. **6**(2): p. 613-621.
213. Chen, Y.S., et al., *Small molecule mesengenic induction of human induced pluripotent stem cells to generate mesenchymal stem/stromal cells*. Stem Cells Transl Med, 2012. **1**(2): p. 83-95.
214. Lee, J., et al., *Generation of disease-specific induced pluripotent stem cells from patients with rheumatoid arthritis and osteoarthritis*. Arthritis Res Ther, 2014. **16**(1): p. R41.
215. Xu, M., et al., *Chondrocytes Derived From Mesenchymal Stromal Cells and Induced Pluripotent Cells of Patients With Familial Osteochondritis Dissecans Exhibit an Endoplasmic Reticulum Stress Response and Defective Matrix Assembly*. Stem Cells Transl Med, 2016. **5**(9): p. 1171-81.
216. Ma, B., et al., *Gene expression profiling of dedifferentiated human articular chondrocytes in monolayer culture*. Osteoarthritis Cartilage, 2013. **21**(4): p. 599-603.
217. Bigdeli, N., et al., *Coculture of human embryonic stem cells and human articular chondrocytes results in significantly altered phenotype and improved chondrogenic differentiation*. Stem Cells, 2009. **27**(8): p. 1812-21.
218. Hwang, N.S., S. Varghese, and J. Elisseeff, *Derivation of chondrogenically-committed cells from human embryonic cells for cartilage tissue regeneration*. PLoS One, 2008. **3**(6): p. e2498.
219. Oldershaw, R.A., et al., *Directed differentiation of human embryonic stem cells toward chondrocytes*. Nat Biotechnol, 2010. **28**(11): p. 1187-94.
220. Chijimatsu, R., et al., *Characterization of Mesenchymal Stem Cell-Like Cells Derived From Human iPSCs via Neural Crest Development and Their Application for Osteochondral Repair*. Stem Cells Int, 2017. **2017**: p. 1960965.
221. Guzzo, R.M., et al., *Efficient differentiation of human iPSC-derived mesenchymal stem cells to chondroprogenitor cells*. J Cell Biochem, 2013. **114**(2): p. 480-90.
222. Hynes, K., et al., *Generation of functional mesenchymal stem cells from different induced pluripotent stem cell lines*. Stem Cells Dev, 2014. **23**(10): p. 1084-96.
223. He, P., J. Fu, and D.A. Wang, *Murine pluripotent stem cells derived scaffold-free cartilage grafts from a micro-cavitary hydrogel platform*. Acta Biomater, 2016. **35**: p. 87-97.
224. Umeda, K., et al., *Human chondrogenic paraxial mesoderm, directed specification and prospective isolation from pluripotent stem cells*. Sci Rep, 2012. **2**: p. 455.

225. Driessen, B.J.H., C. Logie, and L.A. Vonk, *Cellular reprogramming for clinical cartilage repair*. Cell Biol Toxicol, 2017. **33**(4): p. 329-349.
226. Kang, R., et al., *Mesenchymal stem cells derived from human induced pluripotent stem cells retain adequate osteogenicity and chondrogenicity but less adipogenicity*. Stem Cell Res Ther, 2015. **6**: p. 144.
227. Nejadnik, H., et al., *Improved approach for chondrogenic differentiation of human induced pluripotent stem cells*. Stem Cell Rev, 2015. **11**(2): p. 242-53.
228. Fukuta, M., et al., *Derivation of mesenchymal stromal cells from pluripotent stem cells through a neural crest lineage using small molecule compounds with defined media*. PLoS One, 2014. **9**(12): p. e112291.
229. Pettinato, G., X. Wen, and N. Zhang, *Engineering Strategies for the Formation of Embryoid Bodies from Human Pluripotent Stem Cells*. Stem Cells Dev, 2015. **24**(14): p. 1595-609.
230. Ko, J.Y., et al., *In vitro chondrogenesis and in vivo repair of osteochondral defect with human induced pluripotent stem cells*. Biomaterials, 2014. **35**(11): p. 3571-81.
231. Nam, Y., et al., *Cord blood cell-derived iPSCs as a new candidate for chondrogenic differentiation and cartilage regeneration*. Stem Cell Res Ther, 2017. **8**(1): p. 16.
232. Chen, Y.T. and A. Bradley, *A new positive/negative selectable marker, puDeltatk, for use in embryonic stem cells*. Genesis, 2000. **28**(1): p. 31-5.
233. Szymczak, A.L., et al., *Correction of multi-gene deficiency in vivo using a single 'self-cleaving' 2A peptide-based retroviral vector*. Nat Biotechnol, 2004. **22**(5): p. 589-94.
234. Hirai, H., P. Karian, and N. Kikyo, *Regulation of embryonic stem cell self-renewal and pluripotency by leukaemia inhibitory factor*. Biochem J, 2011. **438**(1): p. 11-23.
235. Rohwedel, J., et al., *Muscle cell differentiation of embryonic stem cells reflects myogenesis in vivo: developmentally regulated expression of myogenic determination genes and functional expression of ionic currents*. Dev Biol, 1994. **164**(1): p. 87-101.
236. Bocker, W., et al., *IKK-2 is required for TNF-alpha-induced invasion and proliferation of human mesenchymal stem cells*. J Mol Med (Berl), 2008. **86**(10): p. 1183-92.
237. Darini, C.Y., et al., *Self-renewal gene tracking to identify tumour-initiating cells associated with metastatic potential*. Oncogene, 2012. **31**(19): p. 2438-49.
238. Gupta, R.K., et al., *Transcriptional control of preadipocyte determination by Zfp423*. Nature, 2010. **464**(7288): p. 619-23.
239. Potter, C.J. and L. Luo, *Splinkerette PCR for mapping transposable elements in Drosophila*. PLoS One, 2010. **5**(4): p. e10168.
240. Uren, A.G., et al., *A high-throughput splinkerette-PCR method for the isolation and sequencing of retroviral insertion sites*. Nat Protoc, 2009. **4**(5): p. 789-98.
241. Kiraly, K., et al., *Application of selected cationic dyes for the semiquantitative estimation of glycosaminoglycans in histological sections of articular cartilage by microspectrophotometry*. Histochem J, 1996. **28**(8): p. 577-90.
242. Niakan, K.K. and E.R. McCabe, *DAX1 origin, function, and novel role*. Mol Genet Metab, 2005. **86**(1-2): p. 70-83.
243. Takahashi, K., K. Mitsui, and S. Yamanaka, *Role of ERas in promoting tumour-like properties in mouse embryonic stem cells*. Nature, 2003. **423**(6939): p. 541-5.
244. Fujii, Y., et al., *Zfp296 is a novel Klf4-interacting protein and functions as a negative regulator*. Biochem Biophys Res Commun, 2013. **441**(2): p. 411-7.
245. Mansergh, F.C., et al., *Gene expression profiles during early differentiation of mouse embryonic stem cells*. BMC Dev Biol, 2009. **9**: p. 5.
246. Baum, C., et al., *Chance or necessity? Insertional mutagenesis in gene therapy and its consequences*. Mol Ther, 2004. **9**(1): p. 5-13.

247. Carey, B.W., et al., *Reprogramming of murine and human somatic cells using a single polycistronic vector*. Proc Natl Acad Sci U S A, 2009. **106**(1): p. 157-62.
248. Sommer, C.A., et al., *Excision of reprogramming transgenes improves the differentiation potential of iPS cells generated with a single excisable vector*. Stem Cells, 2010. **28**(1): p. 64-74.
249. Wu, X., et al., *Transcription start regions in the human genome are favored targets for MLV integration*. Science, 2003. **300**(5626): p. 1749-51.
250. Schroder, A.R., et al., *HIV-1 integration in the human genome favors active genes and local hotspots*. Cell, 2002. **110**(4): p. 521-9.
251. Zhang, Y., et al., *A poor imitation of a natural process: a call to reconsider the iPSC engineering technique*. Cell Cycle, 2012. **11**(24): p. 4536-44.
252. Yant, S.R., et al., *High-resolution genome-wide mapping of transposon integration in mammals*. Mol Cell Biol, 2005. **25**(6): p. 2085-94.
253. Moldt, B., et al., *Cis-acting gene regulatory activities in the terminal regions of sleeping beauty DNA transposon-based vectors*. Hum Gene Ther, 2007. **18**(12): p. 1193-204.
254. Walisko, O., et al., *Transcriptional activities of the Sleeping Beauty transposon and shielding its genetic cargo with insulators*. Mol Ther, 2008. **16**(2): p. 359-69.
255. Yant, S.R., et al., *Somatic integration and long-term transgene expression in normal and haemophilic mice using a DNA transposon system*. Nat Genet, 2000. **25**(1): p. 35-41.
256. Montini, E., et al., *In vivo correction of murine tyrosinemia type I by DNA-mediated transposition*. Mol Ther, 2002. **6**(6): p. 759-69.
257. *Transposon-Based, Targeted Ex Vivo Gene Therapy to Treat Age-Related Macular Degeneration (TargetAMD)*. Hum Gene Ther Clin Dev, 2015. **26**(2): p. 97-100.
258. Kebriaei, P., et al., *Phase I trials using Sleeping Beauty to generate CD19-specific CAR T cells*. J Clin Invest, 2016. **126**(9): p. 3363-76.
259. Woltjen, K., et al., *Transgene-free production of pluripotent stem cells using piggyBac transposons*. Methods Mol Biol, 2011. **767**: p. 87-103.
260. Igawa, K., et al., *Removal of reprogramming transgenes improves the tissue reconstitution potential of keratinocytes generated from human induced pluripotent stem cells*. Stem Cells Transl Med, 2014. **3**(9): p. 992-1001.
261. Fraser, M.J., et al., *Precise excision of TTAA-specific lepidopteran transposons piggyBac (IFP2) and tagalong (TFP3) from the baculovirus genome in cell lines from two species of Lepidoptera*. Insect Mol Biol, 1996. **5**(2): p. 141-51.
262. Davis, R.P., et al., *Generation of induced pluripotent stem cells from human foetal fibroblasts using the Sleeping Beauty transposon gene delivery system*. Differentiation, 2013. **86**(1-2): p. 30-7.
263. Luo, G., et al., *Chromosomal transposition of a Tc1/mariner-like element in mouse embryonic stem cells*. Proc Natl Acad Sci U S A, 1998. **95**(18): p. 10769-73.
264. Courtney, P.M., A.J. Boniello, and R.A. Berger, *Complications Following Outpatient Total Joint Arthroplasty: An Analysis of a National Database*. J Arthroplasty, 2017. **32**(5): p. 1426-1430.
265. Hopley, C.D., L.S. Crossett, and A.F. Chen, *Long-term clinical outcomes and survivorship after total knee arthroplasty using a rotating platform knee prosthesis: a meta-analysis*. J Arthroplasty, 2013. **28**(1): p. 68-77 e1-3.
266. Makela, K.T., et al., *Countrywise results of total hip replacement. An analysis of 438,733 hips based on the Nordic Arthroplasty Register Association database*. Acta Orthop, 2014. **85**(2): p. 107-16.

267. Kreuz, P.C., et al., *Is microfracture of chondral defects in the knee associated with different results in patients aged 40 years or younger?* Arthroscopy, 2006. **22**(11): p. 1180-6.
268. Gille, J., et al., *Outcome of Autologous Matrix Induced Chondrogenesis (AMIC) in cartilage knee surgery: data of the AMIC Registry.* Arch Orthop Trauma Surg, 2013. **133**(1): p. 87-93.
269. Harris, J.D., et al., *Failures, re-operations, and complications after autologous chondrocyte implantation--a systematic review.* Osteoarthritis Cartilage, 2011. **19**(7): p. 779-91.
270. Kern, S., et al., *Comparative analysis of mesenchymal stem cells from bone marrow, umbilical cord blood, or adipose tissue.* Stem Cells, 2006. **24**(5): p. 1294-301.
271. Baxter, M.A., et al., *Study of telomere length reveals rapid aging of human marrow stromal cells following in vitro expansion.* Stem Cells, 2004. **22**(5): p. 675-82.
272. Stolzing, A., et al., *Age-related changes in human bone marrow-derived mesenchymal stem cells: consequences for cell therapies.* Mech Ageing Dev, 2008. **129**(3): p. 163-73.
273. Murphy, J.M., et al., *Reduced chondrogenic and adipogenic activity of mesenchymal stem cells from patients with advanced osteoarthritis.* Arthritis Rheum, 2002. **46**(3): p. 704-13.
274. Garreta, E., et al., *Roadblocks in the Path of iPSC to the Clinic.* Curr Transplant Rep, 2018. **5**(1): p. 14-18.
275. Tapia, N. and H.R. Scholer, *Molecular Obstacles to Clinical Translation of iPSCs.* Cell Stem Cell, 2016. **19**(3): p. 298-309.
276. Zhao, T., et al., *Immunogenicity of induced pluripotent stem cells.* Nature, 2011. **474**(7350): p. 212-5.
277. Guha, P., et al., *Lack of immune response to differentiated cells derived from syngeneic induced pluripotent stem cells.* Cell Stem Cell, 2013. **12**(4): p. 407-12.
278. de Almeida, P.E., et al., *Transplanted terminally differentiated induced pluripotent stem cells are accepted by immune mechanisms similar to self-tolerance.* Nat Commun, 2014. **5**: p. 3903.
279. Zhao, T., et al., *Humanized Mice Reveal Differential Immunogenicity of Cells Derived from Autologous Induced Pluripotent Stem Cells.* Cell Stem Cell, 2015. **17**(3): p. 353-9.
280. Sun, H., et al., *Generation of induced pluripotent stem cell line (ZZUi011-A) from urine sample of a normal human.* Stem Cell Res, 2018. **29**: p. 28-31.
281. Nakatsuji, N., F. Nakajima, and K. Tokunaga, *HLA-haplotype banking and iPS cells.* Nat Biotechnol, 2008. **26**(7): p. 739-40.
282. Taylor, C.J., et al., *Generating an iPSC bank for HLA-matched tissue transplantation based on known donor and recipient HLA types.* Cell Stem Cell, 2012. **11**(2): p. 147-52.
283. Gourraud, P.A., et al., *The role of human leukocyte antigen matching in the development of multiethnic "haplobank" of induced pluripotent stem cell lines.* Stem Cells, 2012. **30**(2): p. 180-6.
284. Brickman, J.M. and P. Serup, *Properties of embryoid bodies.* Wiley Interdiscip Rev Dev Biol, 2017. **6**(2).
285. Kurosawa, H., *Methods for inducing embryoid body formation: in vitro differentiation system of embryonic stem cells.* J Biosci Bioeng, 2007. **103**(5): p. 389-98.

286. Doetschman, T.C., et al., *The in vitro development of blastocyst-derived embryonic stem cell lines: formation of visceral yolk sac, blood islands and myocardium*. J Embryol Exp Morphol, 1985. **87**: p. 27-45.
287. Hopfl, G., M. Gassmann, and I. Desbaillets, *Differentiating embryonic stem cells into embryoid bodies*. Methods Mol Biol, 2004. **254**: p. 79-98.
288. Lee, J., et al., *Early induction of a prechondrogenic population allows efficient generation of stable chondrocytes from human induced pluripotent stem cells*. FASEB J, 2015. **29**(8): p. 3399-410.
289. Diekman, B.O., et al., *Cartilage tissue engineering using differentiated and purified induced pluripotent stem cells*. Proc Natl Acad Sci U S A, 2012. **109**(47): p. 19172-7.
290. Bapat, S., et al., *Pros and cons of mouse models for studying osteoarthritis*. Clin Transl Med, 2018. **7**(1): p. 36.
291. Lauing, K.L., et al., *Aggrecan is required for growth plate cytoarchitecture and differentiation*. Dev Biol, 2014. **396**(2): p. 224-36.
292. Usami, Y., et al., *Wnt signaling in cartilage development and diseases: lessons from animal studies*. Lab Invest, 2016. **96**(2): p. 186-96.

9. List of Figures

Figure 1: Potency of stem cells (self-designed).....	18
Figure 2: Types of pluripotent stem cells (self-designed).	21
Figure 3: Transposons. Modified from <i>Ivics et al.</i> [43].....	24
Figure 4: Sleeping Beauty transposition. Modified from <i>Liu et al</i> [57].....	25
Figure 5: Phases of the reprogramming process. Adapted from <i>David et al.</i> [70] and <i>Plath et al.</i> [24].	29
Figure 6: Applications of induced pluripotent stem cells (self-designed).....	35
Figure 7: Structure of aggrecan. Adapted from <i>Brody et al.</i> [117].	39
Figure 8: Extracellular matrix of articular cartilage. Adapted from <i>Brody et al</i> [117] and <i>Poole et al.</i> [118].	41
Figure 9: Endochondral ossification. Adapted from <i>Long et al.</i> [143].....	45
Figure 10: TGF β signaling pathway.....	47
Figure 11: BMP signaling pathway.....	49
Figure 12: X-Ray Image of an osteoarthritic knee joint. Modified from <i>Braun et al.</i> [173]....	52
Figure 13: Total joint replacement of the knee with an endoprosthesis. From <i>de l'Escalopier et al.</i> [174]	53
Figure 14: Microfracture. Modified from <i>Mithoefer et al.</i> [190].	54
Figure 15: Osteochondral autograft transfer (OAT). From <i>Winthrop et al.</i> [199].	56
Figure 16: Autologous chondrocyte injection (ACI). From <i>Brittberg et al.</i> [200].....	57
Figure 17: Methods for the chondrogenic differentiation of pluripotent stem cells. Adapted from <i>Driessen et al.</i> [225].	61
Figure 18: Plasmids of the Sleeping Beauty reprogramming system. Modified from <i>Grabundjiza et al.</i> [53].	67
Figure 19: Schematic depiction of the picking of <i>bona fide</i> iPSC colonies (self-designed)....	78
Figure 20: Hanging drop culture of mIPSCs.....	79
Figure 21: Spontaneous differentiation of mIPSCs in embryoid bodies (self-designed).	80
Figure 22: Chondrogenic differentiation of mIPSCs via chondrogenic colonies (self-designed)	82
Figure 23: Chondrogenic differentiation of mIPSCs via embryoid bodies (self-designed).	84
Figure 24: Splinkerette PCR (next page):	94
Figure 25: Morphology of primary murine fibroblasts.	105

Figure 26: Nucleofection of primary fibroblasts with the <i>pmaxGFP</i> vector.....	107
Figure 27: Reprogramming of MEFs, EAR-FBs and TAIL-FBs with the <i>pT2OSKM</i> and <i>pT2OSKML</i> plasmids.....	111
Figure 28: Reprogramming of EAR-FBs with the <i>RMCE-OSKM(L)-Cherry</i> plasmids.	112
Figure 29: Morphological changes of EAR-FBs during reprogramming with <i>RMCE-OSKM(L)-Cherry</i> plasmids cultured on different coatings.	115
Figure 30: Morphology of ESCs and iPSCs.....	117
Figure 31: Alkaline phosphatase staining of iPSCs	118
Figure 32: Splinkerette PCR.....	119
Figure 33: ET-PCR for ESC markers on TA clones.	121
Figure 34: RT-PCR for ESC markers on ETA clones.....	121
Figure 35: RT-PCR for ESC markers on TTA clones.....	122
Figure 36: RT-PCR for ESC markers on ETAC clones.....	122
Figure 37: RT-PCR for reprogramming factors on TA clones.....	124
Figure 38: RT-PCR for reprogramming factors on ETA clones.	124
Figure 39: RT-PCR for reprogramming factors on TTA clones.	125
Figure 40: RT-PCR for reprogramming factors on ETAC clones.	125
Figure 41: Immunofluorescence staining for pluripotency markers on mESCs (R1) and ETA04	127
Figure 42: Immunofluorescence staining for pluripotency markers on mESCs (R1) and ETAC41.....	128
Figure 43: Embryoid body on day 21 of spontaneous differentiation in free floating culture.	129
Figure 44: qPCR of pluripotency and lineage-specific markers of iPSCs (ETA04) and embryoid bodies at day 21 (EB D21).	130
Figure 45: Histological analysis of chondrogenic nodules on day 42.....	132
Figure 46: qPCR of pluripotency markers in stimulated (BTG) and non-stimulated (noGF) chondrogenic colonies.	133
Figure 47: qPCR of chondrogenic markers in stimulated (BTG) and non-stimulated (noGF) chondrogenic nodules.	134
Figure 48: Size of EBs on day5 and CSs on day 42.....	136
Figure 49. Safranin Orange and Toluidine Blue staining for chondrogenic spheroids.	138

Figure 50: Immunohistochemistry for aggrecan and type II collagen on chondrogenic spheroids 139

Figure 51: qPCR of pluripotency markers in stimulated (BT) and non-stimulated (noGF) chondrogenic spheroids. 141

Figure 52: qPCR of chondrogenic markers in stimulated (BT) and non-stimulated (noGF) chondrogenic spheroids. 142

Figure 53: RT-PCR for procollagen II isoforms procollagen IIA (*Col II A*) and B (*Col II B*) 143

Figure 54: qPCR of hypertrophy markers in stimulated (BT) and non-stimulated (noGF) chondrogenic spheroids. 144

Figure 55: Integration profile of commonly used gene vectors. From Narayanavari et al. [59]. 150

Figure 56: Generation of chondrogenically primed iPSCs by recombinase mediated cassette exchange (self-designed) 170

10. List of Tables

Table 1: Mouse EF medium 69

Table 2: Mouse iPSC medium 71

Table 3: Freezing medium 73

Table 4: Collagenase-Dispase medium 74

Table 5: Nucleofection reaction set up 77

Table 6: Hanging drop medium 80

Table 7: Free floating medium 81

Table 8: Mesoendodermal medium 82

Table 9: Chondrogenic colonies medium 83

Table 10: Chondrogenic spheroid medium 84

Table 11: Antibodies for immunocytochemistry 86

Table 12: RNA denaturation mix and program 88

Table 13: cDNA synthesis mix and program 88

Table 14: RT-PCR reaction set up and program 89

Table 15: Oligonucleotides used for RT-PCR 90

Table 16: SYBR Green qPCR reaction set up 91

Table 17: Oligonucleotides used for qPCR (SYBR Green Kit) 92

Table 18: Taq-Man probes qPCR reaction set up 92

Table 19: Oligonucleotides used for qPCR (Taq Man probes) 93

Table 20: gDNA digestion set up and program 96

Table 21: gDNA ligation set up and program 97

Table 22: Set up and program of the first PCR amplification 98

Table 23: Set up and program of the second PCR amplification 98

Table 24: Oligonucleotides used for Splinkerette PCR 99

Table 25: Antibodies for immunohistochemistry 103

Table 26: Nucleofection of MEFs with the pmaxGFP vector (P3 Solution) 106

Table 27: Nucleofection of EAR-FBs with the pmaxGFP vector (P2 Solution) 107

Table 28: Nucleofection of TAIL-FBs with the pmaxGFP vector (P2 Solution) 107

Table 29: Cell lines established from MEFs reprogrammed with *pT2OSKM* or *pT2OSKML* 109

Table 30: Cell lines established from EAR-FBs reprogrammed with *pT2OSKM* or 110

Table 31: Cell lines established from TAIL-FBs reprogrammed with *pT2OSKM* or 110
Table 32: Cell lines established from EAR-FBs reprogrammed with..... 113
Table 34: Methods for the generation of induced pluripotent stem cells 146

11. List of Equations

Equation 1: number of cells/ml (CC) = [(A+B+C+D)/4] x 10⁴ 72

Equation 2: total cell count (n) = number of cells/ml (CC) x total cell suspension volume (V)
..... 72

Equation 3: Survival rate (%) = (1 – mean dead cell count/100 000) x 100..... 76

Equation 4: Efficiency rate (%) = (fluorescent cells pvf/ total cell number pvf) x 100..... 76

Equation 5: $\Delta Ct_{\text{Experimental}} = Ct_{\text{Experimental}} (GOI) - Ct_{\text{Experimental}} (GAPDH)$
 $\Delta Ct_{\text{Control}} = Ct_{\text{Control}} (GOI) - Ct_{\text{Control}} (GAPDH)$ 91

Equation 6: $\Delta\Delta Ct = \Delta Ct_{\text{Experimental}} - \Delta Ct_{\text{Control}}$ 91

Equation 7: Expression fold change = $2^{-\Delta\Delta Ct}$ 91

12. List of abbreviations

Acan	Aggrecan
ACI	Autologous chondrocyte injection
ADAMTS	A disintegrin and metalloproteinase with thrombospondin-like motifs
ADSC	Adipose tissue derived stem cell
AMIC	Autologous matrix-induced chondrogenesis
AP	Alkaline phosphatase
BCIP	5-bromo-4-chloro-3-indolyl-phosphate
BM-MSC	Bone marrow mesenchymal stem cell
BMP	Bone morphogenetic protein
BMPR	BMP receptor
BSA	Bovine serum albumin
CAR	Chimeric antigen receptor
cDNA	Complementary DNA
CF	Chondrogenic factor
CMV	Cytomegalovirus
c-Myc	Avian myelocytomatosis viral oncogene homolog
Col2a1	Collagen type II alpha 1 chain
COMP	Cartilage oligomeric matrix protein
Co-SMAD	Common-mediator Smad
CP chondrocytes	Columnar proliferating chondrocytes
CS	Chondroitin sulfate
DAB	Diaminobenzidine
DAPI	4',6-diamino-2-phenylindole
DeltaTK	Truncated version of herpes simplex virus typ I thymidine kinase
DMEM	Dulbecco's modified Eagle's medium
DMSO	Dimethylsulfoxid
DR	Direct repeat
EAR FB	Ear fibroblast
EB	Embryoid body
EBNA1	Epstein-Barr Nuclear Antigen-1
ECC	Embryonic carcinoma cells
ECM	Extracellular matrix
EF	Embryonic feeder
EGC	Embryonic germ cell
EOS(3+)	ETn LTR coupled with a trimer of the Oct4 enhancer motif
EpiSC	Epiblast stem cells
Erk	Extracellular signal regulated kinase
ESC	Embryonic stem cell
Etn	Early Transposon
FACS	Fluorescence activated cell sorting

List of abbreviations

FAH	Fumarylacetoacetate hydrolase
FB	Fibroblast
FBS	Fetal bovine serum
FGF	Fibroblast growth factor
FIAU	1-(2-desoxy-fluoro-1-beta-darabino-furanosyl)-5-ioduracil
GAG	Glycosaminoglycan
GAPDH	Glyceraldehyde-3-phosphate dehydrogenase
GDF	Growth and differentiation factors
gDNA	Genomic DNA
GFP	Green fluorescent protein
GMP	Good manufacturing practice
GOI	Gene of interest
GSC	Germ stem cell
HAS	Hyaluronan-synthase
HIV	Human immune deficiency virus
HLA	Human leucocyte antigen
ICC	Immunocytochemistry
ICM	Inner cell mass
ICSC	Induced cancer stem cell
IGF	Insulin-like growth factor
IHC	Immunohistochemistry
Ihh	Indian hedgehog
IL-6	Interleukin 6
IPSC	Induced pluripotent stem cell
IQR	Interquartile range
ISCT	International Society for Cellular Therapy
Itga10	Alpha 10 integrin
ITS	Insulin-Transferrin-Selenite
JNK	C-Jun-N-terminal kinase
Klf4	Kruppel-like factor 4
KS	Keratan sulfate
LP	Link protein
lsA	Long strand adaptor
LTR	Long terminal repeat
MACI	Matrix assisted autologous chondrocyte injection
MAPK	Mitogen activated protein kinase
MEF	Mouse embryonic fibroblast
mESC	Mouse embryonic stem cell
MET	Mesenchymal to epithelial transition
MIF	Mullerian inhibitory factor
mIPSC	Mouse induced pluripotent stem cell
MLV	Murine leukemia virus

List of abbreviations

MMP	Matrix-metalloprotease
MSC	Mesenchymal stem cell
NCC	Neural crest cell
NTC	Nitro blue tetrazolium chloride
NT-SC	Nuclear transfer-derived stem cell
OAT	Osteochondral autograft transfer
OCAT	Osteochondral allograft transplantation
Oct3/4	Octamer-binding transcription factor 3/4
OSKM	Oct3/4, Sox2, Klf4 and c-Myc
OSKML	Oct3/4, Sox2, Klf4, c-Myc and Lin28
PB	PiggyBac
PBS	Phosphate Buffered Saline
PCR	Polymerase chain reaction
PDEF	Pigment epithelium-derived factor
PFA	Paraformaldehyde
PG	Proteoglycan
PGC	Primary germ cell
PI3K	Phosphatidylinositol-3-kinase
PP2A	Proteinphosphatase2A
PSCs	Pluripotent stem cell
Puro	Puromycin N-actetyltransferase
pvf	Per viewing field
qPCR	Quantitative PCR
RC	Rib cage cartilage
RF	Reprogramming factor
RMCE	Recombinase mediated cassette exchange
RP chondrocytes	Round proliferating chondrocytes
R-SMAD	Receptor regulated Smad
RT-PCR	Reverse transcription PCR
Runx2	Runt-related transcription factor 2
SAE	Serious adverse event
SB	Sleeping Beauty
SCNT	Somatic cell nuclear transfer
SD	Standard deviation
SLRP	Small leucin rich protein
Sox2	Sex determining region of Y box 2
Sox9	Sex determining region of Y box 9
SRY	Sex determining region of Y
ssA	Short strand adaptor
SSEA1	Stage specific embryonic antigen 1
TAIL FB	Tail fibroblast
TGFBR	TGF β receptor

List of abbreviations

TGF β	Transforming growth factor β
TIR	Terminal inverted repeat
TNF α	Tumor necrosis factor α
UCB-MSC	Umbilical cord blood derived mesenchymal stem cell
VEGF	Vascular endothelial growth factor
Wnt	Wingless-related integration site

13. Acknowledgement

This thesis would have never been completed successfully without the help of many people.

First of all, I would like to express my sincerest gratitude to my doctor father, PD Dr. rer. nat. Attila Aszodi, head of the cartilage research unit of the ExperiMed laboratory for Experimental Surgery and Regenerative Medicine. He provided me the opportunity to conduct this ambitious research project and helped me with his knowledge and guidance to finish my work successfully. I would especially like to thank him for keeping believing in me and this thesis through all challenges and failed experiments on the way.

Furthermore, I would like to thank Dr. Paolo Alberton, for showing all important methods to me and providing helpful advice with many experiments. Moreover, I would like to thank Zsuzsanna (“Zsusza”) Farkas, for her assistance and good mood. Without their experience and encouragement this work would have never been possible.

I would like to express my gratitude to all current and former members of the ExperiMed group, particularly Heidrun Grondiger, Martina Burggraf, Dr. Maximilian Saller, Dr. Veronika Schönitzer, Dr. Riham Flifel, Dr. Chi-Fen Hsieh, Dr. Tsvetan Popov and Prof. Dr. Denitsa Docheva. It was an invaluable experience for me to become a part of this international research group and a great pleasure to work with every single member of the ExperiMed lab. Especially I would like to thank the lovely Dr. Sarah Dex for providing food during hangry moments, awesome riding lessons, unforgettable trips to Barcelona and becoming a good friend.

I would like to thank Markus Moser (Max Plank Institute for Biochemistry, Martinsried, Germany) for supplying us with LIF and Dr. Zoltán Ivics (Paul Ehrlich Institute, Federal Institute for Vaccines and Biomedicines, Langen, Germany) for providing the Sleeping Beauty transposon based reprogramming system used in this thesis. Moreover, I would like to thank Prof. Dr. med. Wolfgang Böcker, director of the “Klinik für Allgemeine, Unfall- und Wiederherstellungschirurgie“ – LMU Munich for giving me the opportunity to work in the ExperiMed Laboratory.

Last but not least I would like to thank my family and friends for their support and encouragement throughout the work on this thesis.

14. Publikationen

Talks

Februar 2015 „iPS Cells for Cartilage Regeneration“
Experimed Mini-Symposium “Cross-roads in Musculoskeletal Regeneration”, Klinik für
Allgemeine, Unfall- und Wiederherstellungschirurgie, Munich, Germany

Posters

Juli 2017 „Chondrogenic differentiation of murine induced pluripotent stem cells generated by a
transposon based reprogramming system via embryoid bodies”
VII. Münchner Symposium für experimentelle Orthopädie, Unfallchirurgie und
muskuloskelettale Forschung, Munich, Germany

Oktober 2017 „Chondrogenic differentiation of murine induced pluripotent stem cells
generated by a transposon based reprogramming system via embryoid bodies”
25th annual and anniversary meeting of the European orthopaedic research
society (EORS), Munich, Germany

15. Eidesstattliche Versicherung

Ich, Nicole Trebesius, geboren in Rosenheim

erkläre hiermit an Eides statt, dass ich die vorliegende Dissertation mit dem Titel

Chondrogenic differentiation of murine induced pluripotent stem cells generated by a transposon based reprogramming system via embryoid bodies

selbständig verfasst, mich außer der angegebenen keiner weiteren Hilfsmittel bedient und alle Erkenntnisse, die aus dem Schrifttum ganz oder annähernd übernommen sind, als solche kenntlich gemacht und nach ihrer Herkunft unter Bezeichnung der Fundstelle einzeln nachgewiesen habe.

Ich erkläre des Weiteren, dass die hier vorgelegte Dissertation nicht in gleicher oder in ähnlicher Form bei einer anderen Stelle zur Erlangung eines akademischen Grades eingereicht wurde.

München, 31.01.2020

Trebesius

Nicole Trebesius